Development of genome editing method for metabolic engineering of *Clostridium pasteurianum* reveals new features of metabolism

Vom Promotionsausschuss der

Technischen Universität Hamburg

zur Erlangung des akademischen Grades

Doktor der Naturwissenschaften (Dr. rer. nat.)

genehmigte Dissertation (Monografie)

von

Tom Nguyen, M.Sc.

aus

Hamburg

2024

1. Gutachter:	Prof. Dr. rer. nat. An-Ping Zeng
2. Gutachter:	Prof. Dr. rer. nat. Johannes Gescher
Tag der mündlichen Prüfung:	27. November 2024

DOI: https://doi.org/10.15480/882.13897

 https://orcid.org/0000-0002-8004-0816

Abstract

Clostridium pasteurianum is an important industrial microorganism with several unique advantages for production of 1,3-propanediol (PDO) and butanol, but suffers from lacking genetic tools for synthetic biology to expand its further applications. Previous synthetic biology studies of *C. pasteurianum* merely focused on single genomic modification. However, stable integration of foreign pathways on the genome of *C. pasteurianum*, such as for the formation of PDO from renewable resources like glucose, often requires deletion of multiple genes of competing pathways. To this end, the endogenous CRISPR-Cas method was further developed in this work to enable introduction of multiple genome modifications in the same mutant of *C. pasteurianum* for production of PDO from glucose. Previous development of an industrial PDO production process with very high productivity proved the unique advantages for production of PDO from glycerol in *C. pasteurianum* C8 (C8). These advantages make *C. pasteurianum* an attractive host for the production of PDO from glucose and only a glycerol synthesis pathway from *Saccharomyces cerevisiae* with genes glycerol-3-phosphate dehydrogenase (*GPD1*) and glycerol-1-phosphatase (*GPP2*) needs to be introduced. Studies of created mutants led to discovery of several unexpected phenotypes, including the formation of 2,3-butanediol. Another objective of this work was to create a *C. pasteurianum* R525 (R525) mutant which is similar to the C8 strain to verify if certain differences between these two strains could lead to increased PDO production from glycerol in C8. Three genes which are not present in C8 are deleted in a single mutant of R525 and an additional copy of PDO dehydrogenase from C8 (*dhaTC8*) was overexpressed. A final mutant with three genome modifications in total was successfully isolated and a significant increase in PDO yield by 94% and decrease in butanol yield by 54% was observed compared to R525. However, C8 still has a 181% higher PDO yield compared to R525 and almost no butanol was produced under the same conditions. The results verify that the examined differences contribute to higher PDO and lower butanol production, but it is evident that there are still other factors that lead to the high PDO production in C8. It is the first time that the endogenous CRISPR-Cas method was applied to delete multiple genes in *C. pasteurianum* and these deletions showed a direct impact on the metabolism which was observed in the form of reduced glycerol consumption or increased PDO to butanol ratio. The developed consecutive genome editing method enables the introduction of multiple genome modifications that show the effect of combined changes on the genome and is expected to expand the knowledge and understanding of the metabolism in *C. pasteurianum*.

Acknowledgements

I would like to express my immense gratitude to my supervisor Prof. Dr. rer. nat. An-Ping Zeng, former head of the Institute of Bioprocess and Biosystems Engineering (IBB), Hamburg University of Technology, for granting me the opportunity to work on an exciting PhD topic and for the guidance, advice and motivation during the time of my research work.

I would like to thank Prof. Dr. rer. nat. Johannes Gescher, head of the Institute for Technical Microbiology, Hamburg University of Technology, for reviewing my thesis and I am very thankful to Prof. Dr. Anna-Lena Heins, head of the Institute of Bioprocess and Biosystems Engineering, Hamburg University of Technology, for being the Chair of the committee.

I thank my master students Minu Paramesh Belavatta, Sivasubramanian Gurumoorthi and Tayyab Saeed for the assistance with the plasmid constructions, mutant verifications and fermentations and I especially thank Luca Meleski for the continuous support in the lab during his consecutive project work and master thesis.

I appreciate my previous supervisors, Dr.-Ing. Ludwig Selder and Dr.-Ing. Yaeseong Hong, and the members of COLIPI GmbH, Maximilian, Tyll, Philipp, Jan and Jonas, for their ongoing support in the institute. I want to thank Petar Keković from MicroHarvest GmbH for providing fermentation equipment for a certain time and Andrea Simon from the Zentrallabor Chemische Analytik (TUHH) as well as Dr. Wei Wang (IBB) for the assistance with GC-MS and GC-FID measurements. I would like to acknowledge Jan Sens, Olaf Schmidt and Christiane Schaffer for their help with ordering procedures and technical support. Last but not least, I express my gratitude to the IBB members and colleagues Prof. Pörtner, Chijian, Jingchun, Giovanni, Mojtaba, Nikolai, Cornelius, Lukas, Beshr, Yongfei, Timo and Janek for sharing their experiences with me.

Above all, I am very grateful to my friends and family, especially my mother, sister and late father for the loving and continuous support throughout the years.

Table of contents

List of figures

List of tables

Abbreviations

Abbreviation	Definition
PDO	1,3-propanediol
dhaTR, *dhaTC8*	Genes encoding 1,3-propanediol dehydrogenase from R525 and C8, respectively
2,3-BDO	2,3-Butanediol
3-HPA	3-Hydroxypropionaldehyde
AcAc	Acetate
ATP	Adenosine triphosphate
bp	Base pairs
BDM	Bio dry mass
BES	Bioelectrochemical system
BLAST	Basic Local Alignment Search Tool
BuOH	Butanol
adh2, *bdhA2*	Genes encoding butanol dehydrogenase
BuAc	Butyrate
bcd1, bcd2	Genes encoding butyryl-CoA dehydrogenase
C8	*C. pasteurianum* C8
R525	*C. pasteurianum* R525
Cm	Chloramphenicol
catP	Gene encoding chloramphenicol resistance
Cl	Clarithromycin
CRISPR	Clustered regularly interspaced short palindromic repeats
crRNAs	CRISPR RNAs
CFU	Colony forming units
CGE	Consecutive genome editing
DNA	Deoxyribonucleic acid
dhaK	Gene encoding dihydroxyacetone kinase
DHA	Dihydroxyacetone
DHAP	Dihydroxyacetone phosphate
Dam	DNA adenine methylase
ELU	Elution buffer for midiprep
EQU	Equilibration buffer for midiprep
Erm	Erythromycin
EtOH	Ethanol
EMS	Ethyl methanesulfonate
FoAc	Formate
GC-MS	Gas chromatography-Mass spectrometry
GPP2	Genes encoding glycerol-1-phosphatase

Abbreviation	Definition
GPD1	Genes encoding glycerol-3-phosphate dehydrogenase
dhaD1, *dhaD2*	Gene encoding glycerol dehydrogenase
HPLC	High performance liquid chromatography
IS	Insertion sequence
Kn	Kanamycin
LaAc	Lactate
mgsA	Gene encoding methylglyoxal synthase
NCBI	National center for biotechnology information
OD_{600}	Optical density
PCR	Polymerase chain reaction
PAM	Protospacer adjacent motif
RAST	Rapid annotation using subsystem technology
NADH	Reduced nicotinamide adenine dinucleotide
RI/UV	Refractive index/ Ultra-violet detector
RM	Restriction modification
RES	Resuspension buffer for midiprep
rpm	Revolutions per minute
Sp	Spectinomycin
SOB/SOC	Super optimal broth/ Super optimal broth with catabolite repression
Tc	Tetracyclin
Tm	Thiamphenicol
tpiA	Gene encoding triose phosphate isomerase
TAE	Tris, Acetic acid, EDTA buffer

1. Introduction

The anaerobic, gram-positive and spore-forming microorganism *Clostridium pasteurianum* is known for its efficient production of metabolic products such as butanol and 1,3-propanediol (PDO) from fermentations with glycerol [1–5]. PDO is an organic compound that can be used in adhesives, detergents and cosmetics and as a monomer for the production of polytrimethylene terephthalate (PTT) which is a polyester with optimal properties for fibers, carpets and textiles [6, 7]. Due to the many applications, the global PDO market was projected to reach $789.17 million in 2023 and $860.43 million in 2024 while a compound annual growth rate (CAGR) of 10.98% was estimated from 2024 to 2030 [8]. The recent market report shows the importance of a sustainable production of PDO from renewable substrates. The pathway of PDO production from renewable resources like glucose was established and commercialized by development of recombinant *E. coli* strains [9, 10] by the company DuPont (Wilmington, DE, USA) and the former company Genencor International, Inc. (Palo Alto, CA, USA). However, the introduction of a large set of genes was necessary, because PDO is not natively produced by *E. coli*. As a result of broad patenting of the DuPont strains, which prevented research studies on the characteristic details, other microorganisms including *Klebsiella pneumoniae* [11, 12] or *Corynebacterium glutamicum* [13] were engineered to produce PDO from glucose.

Development of an industrial PDO production process with very high productivity under unsterile conditions and with utilization of simplified medium without using costly vitamin B12 and yeast extract has proven the unique advantages for the production of PDO from glycerol in *C. pasteurianum* C8 (C8) [2, 14–17]. Because of these advantages, *C. pasteurianum* represents another attractive host for the production of PDO from glucose and only a glycerol synthesis pathway needs to be introduced. Such a pathway exists in *Saccharomyces cerevisiae* which contains the two enzymes glycerol-3-phosphate dehydrogenase (*GPD1*) and glycerol-1-phosphatase (*GPP2*) [18, 19]. *GPD1* catalyzes the conversion of the glycolysis intermediate dihydroxyacetone phosphate (DHAP) to glycerol-3-phosphate, which is then converted to glycerol by *GPP2*. Another reason why *C. pasteurianum* could be a suitable host strain is that PDO can then be produced by the native pathway from which the reaction steps are catalyzed by the glycerol dehydratase and PDO dehydrogenase (Figure 2-1). However, stable integration of foreign pathways, requires deletion of multiple gene targets of competing pathways.

In order to carry out the metabolic engineering of *C. pasteurianum*, attempts were tried in previous works to improve the genetic accessibility to create a genetically modified strain. An electrotransformation protocol with the accompanying in-vivo methylation of constructed plasmids was developed by Pyne et al. (2013) and different parameters and conditions were tested, which showed a positive impact on the transformation efficiency [20]. Schmitz et al. (2018) used a similar protocol to isolate *C. pasteurianum* R525 (R525) which showed an increased transformation efficiency compared to the *C. pasteurianum* DSM525 wildtype [21]. After isolation of strain R525, it was further transformed with a plasmid for conversion of the C1 components formate and CO_2 by Hong et al. (2020) with the introduction of a glycine synthase system from *Gottschalka acidurici* [22]. This triggered the formation of 2-oxobutryate which is an unexpected product and it indicates that previously unknown metabolic pathways of *C. pasteurianum* can be uncovered through synthetic biology work and thus improving our knowledge about this microorganism.

Additionally, the improved transformation procedure made it possible to introduce more complex plasmids with genome editing tools and previous synthetic biology studies of *C. pasteurianum* applied different methods such as the utilization of the endogenous CRISPR-Cas machineries [23], CRISPR-Cas9-nickase [21] and Allele-Coupled Exchange [24, 25], but they focused only on single genomic modification. Therefore, the endogenous CRISPR-Cas method was further developed to enable multiple modifications in this work.

1.1 Objectives and approaches

The strain C8 was studied extensively in our group because it can produce PDO from glycerol in fed-batch fermentations efficiently [2, 16, 17] and it is attempted to improve the overall PDO production in mutants of this work, by utilizing differences between the R525 and C8 strains. The objective of the first part of the results (chapter 4) is to find a method for transformation of C8 as the electrotransformation protocol was previously only optimized for *C. pasteurianum* DSM525. The first approach is protection of plasmids against restriction modification systems in C8 by construction of new methylation plasmids. Random mutagenesis by ethyl methane sulfonate (EMS) treatment of cells is also conducted to try the isolation of a transformable C8 mutant. In the third approach, plasmids are first introduced into R525 with the established method, then again extracted and purified and finally transformed into C8. The second part of chapter 4 focuses on the

development of a stable tool for metabolic engineering in order to enable consecutive genome editing of *C. pasteurianum*. With current methods, only one genome editing step can be realized in the same mutant and only gene deletions or replacements are possible. This is an important obstacle to overcome for introduction of multiple genome modifications.

The objective of the second part of the results (chapter 5) is to create a R525 mutant which is similar to C8 to verify if the differences between these two strains lead to an increased PDO production from glycerol in C8. Specifically, R525 carries four butanol dehydrogenase genes (*adh1*, *adh2*, *bdhA1*, *bdhA2*) and two butyryl-CoA dehydrogenase genes (*bcd1*, *bcd2*) compared to only two butanol dehydrogenase genes (*adh1*, *bdhA1*) and one butyryl-CoA dehydrogenase gene (*bcd2*) in strain C8. Overexpression by the presence of two additional butanol dehydrogenase genes and one butyryl-CoA dehydrogenase gene might be the reason of the high butanol production with R525. Another gene that has a different copy number on the genome of both strains is the 1,3-PDO dehydrogenase (*dhaT*). The strain C8 carries two genes (*dhaTR*, *dhaTC8*) that encode for this enzyme compared to one gene in R525 (*dhaTR*) [16]. The second copy of this gene (*dhaTC8*) may lead to a higher production of PDO with the accompanying NADH consumption through the reductive pathway. Therefore, targets include modification of the genome of R525 using plasmids for deletion of genes encoding *adh2*, *bdhA2* and *bcd1* along with the insertion of the gene *dhaTC8*.

The aim of the third part of the results (chapter 6) is to test the application of the developed consecutive genome editing system and create a mutant which carries three modifications in total. A third genome modification in the same mutant, namely the replacement of the genes glycerol dehydrogenase (*dhaD1*) and dihydroxyacetone kinase (*dhaK*) with the genes *GPD1* and *GPP2* is carried out and verified. In addition, mutants are created for overexpression of genes *GPD1* and GPP2 and characterization is conducted by analyzing results from batch fermentations with glucose to determine if PDO production occurred. The introduction of multiple genome modifications should show the effect of combined changes to the genome and is expected to expand the understanding of the metabolism in *C. pasteurianum*.

2 Theoretical background

2.1 *Clostridium pasteurianum*

2.1.1 Metabolic pathways of *Clostridium pasteurianum*

C. pasteurianum is an anaerobic, gram-positive and spore-forming microorganism which, in addition to nitrogen fixation, produces metabolic products such as ethanol, butanol and 1,3-propanediol from fermentations with glycerol [1–5]. Due to the highly reduced product profile in its metabolism, *C. pasteurianum* has an immense industrial potential in producing butanol during growth on glycerol [26]. In comparison, fermentation of *C. pasteurianum* with glucose as the main carbon source produces mainly acetate and butyrate [4]. The whole genome of the strain *C. pasteurianum* DSM525 (ATCC 6013) was sequenced in 2013 using high-throughput Illumina sequencing technology and is reported to have 4,285,687 bases [27]. Another genome sequencing took place in 2014 where 4,351,673 bases were reported [28] and this complete genome sequence was used in this work. Figure 2-1 shows the central metabolism with the metabolic products and additionally revealed pathways from this work and previous studies. *C. pasteurianum* is able to use the substrates glycerol and glucose together in mixed substrate fermentations which can lead to enhanced growth when a limitation of either substrate is avoided [1, 29].

When glucose limitation occurs in mixed substrate fermentations, growth cessation can be observed and it was found that the growth can be resumed by addition of glucose [30]. The medium composition and the fermentation conditions greatly influence the production of metabolites and as an example, Groeger et al. (2017) reported that lactate production increases significantly under iron limited conditions [31]. The All-in-One electrode developed by Utesch et al. (2018) was tested by glycerol fermentations with *C. pasteurianum* and an increase of butanol production and decrease of 1,3-propanediol (PDO) production were observed [32]. Further fermentations of C. *pasteurianum* in the bioelectrochemical system (BES) were carried out by Utesch et al. (2019) with the addition of redox mediators Brillant Blue (BB) or Neutral Red (NR) [33]. Furthermore, *C. pasteurianum* can be cultivated in defined media, which makes it a promising organism for industrial processes because by avoiding complex nutrients such as yeast extract, potential problems in downstream processing can be prevented. This can be further improved by a minimum salt fermentation medium which was shown to be important to overcome precipitation of desired products in the downstream process [15].

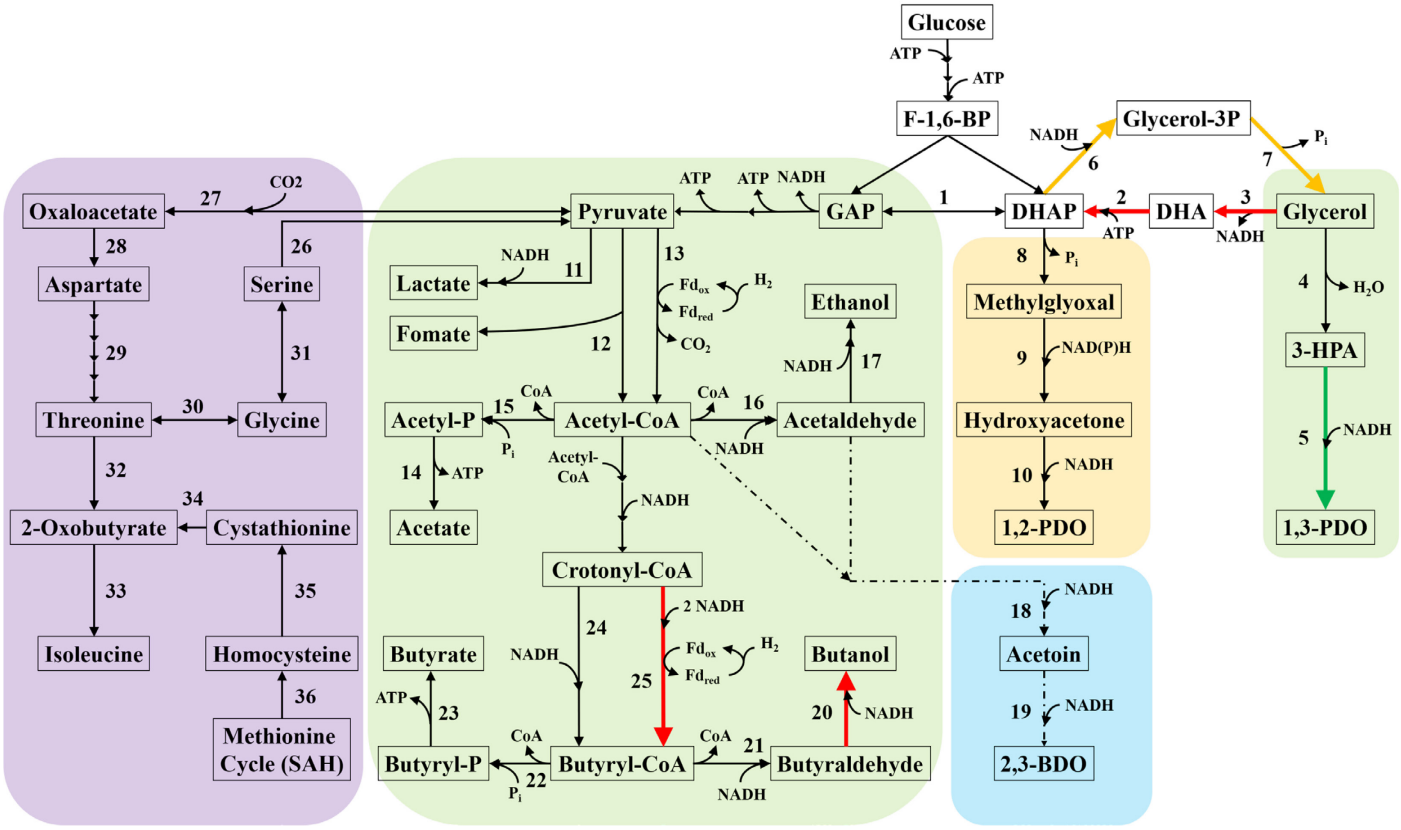

Figure 2-1: Metabolism of *C. pasteurianum* with additionally revealed pathways. Yellow arrows: introduced genes *GPD1* and *GPP2*, **red arrows**: targeted genes in this work, **green arrow**: introduced PDO dehydrogenase from *C. pasteurianum* C8 (*dhaTC8*). The central metabolism [25, 31] (**green area**) is expanded by previously revealed pathways towards 2-oxobutyrate [22] (**purple area**) and 1,2-PDO [34] (**orange area**). An assumed pathway for 2,3-BDO (**blue area**) from this work is depicted with dashed dotted arrows. Genes encoding enzymes involved in metabolic pathways are numbered as follows: 1, triose-phosphate isomerase (*tpiA*); 2, dihydroxyacetone kinase (*dhaK*); 3, glycerol dehydrogenase (*dhaD1*, *dhaD2*); 4, glycerol dehydratase (*dhaBCE*); 5, PDO dehydrogenase (*dhaT*); 6, glycerol-3-phosphate dehydrogenase (*GPD1*); 7, glycerol-1-phosphatase (*GPP2*); 8, methylglyoxal synthase (*mgsA*); 9, putative aldo-keto reductase; 10, type II glycerol dehydrogenase (*glyDH-II*); 11, lactate dehydrogenase; 12, pyruvate formate-lyase; 13, pyruvate:ferredoxin oxidoreductase; 14, acetate kinase; 15, phosphate acetyltransferase; 16, acetaldehyde dehydrogenase; 17, ethanol dehydrogenase; 18, acetoin oxidoreductase; 19, acetoin reductase; 20, butanol dehydrogenase (*adh1*, *adh2*, *bdhA1*, *bdhA2*); 21, butyraldehyde dehydrogenase; 22, phosphate butyryltransferase; 23, butyrate kinase; 24, butyryl-CoA dehydrogenase; 25, ferredoxin-dependent butyryl-CoA dehydrogenase/electron transferring flavoprotein complex (*BCdH-ETF*); 26, serine deaminase; 27, pyruvate carboxylase; 28, aspartate aminotransferase; 29, aspartate kinase, aspartic acid semialdehyde dehydrogenase, homoserine dehydrogenase, homoserine kinase, threonine synthase; 30, threonine aldolase; 31, serine hydroxymethyltransferase; 32, threonine deaminase; 33, acetohydroxyacid synthase; 34, cystathionine betalyase; 35, cystathionine synthase; 36, S-adenosylhomocysteine hydrolase. GAP: glyceraldehyde-3-phosphate, DHA:

dihydroxyacetone, DHAP: dihydroxyacetone phosphate, F-1,6-BP: Fructose 1,6-bisphosphate, 3P: 3-phosphate, 3-HPA: 3-hydroxypropionic aldehyde. The figure is adapted from [25, 31, 35].

Glycerol is a greatly reduced substrate and results in twice the amount of reduction equivalents in the form of NADH compared to using glucose as a fermentation substrate [25]. A portion of the glycerol is oxidized to dihydroxyacetone by glycerol dehydrogenase and phosphorylated by dihydroxyacetone kinase for subsequent transition to glycolysis. The remaining part of the glycerol is first dehydrated to 3-hydroxypropionaldehyde (3-HPA) and next reduced to PDO [4]. When using glucose as a substrate, two glyceraldehyde-3-phosphate molecules are formed from one glucose molecule via glycolysis, which are then converted to pyruvate. Two ATP molecules are required for this, so that two phosphate groups can be transferred to the glucose molecule and the breakdown into the two intermediates dihydroxyacetone phosphate (DHAP) and glyceraldehyde-3-phosphate takes place, whereby DHAP is converted to glyceraldehyde-3-phosphate by triose-phosphate isomerase *tpiA*. 1,2-PDO can be formed via methylglyoxal which is formed from DHAP by methylglyoxal synthase *mgsA* [34]. When a glyceraldehyde-3-phosphate molecule is converted to pyruvate, two molecules ATP and one NADH are formed.

In anaerobic microorganisms, pyruvate can be further processed in various ways, however, it is mostly converted to acetyl-CoA and CO_2 with the help of the enzyme pyruvate ferredoxin oxidoreductase (PFOR) with the concomitant reduction of a redox protein such as ferredoxin or flavodoxin, which serve as electron transmitters. Acetyl-CoA can also be formed from pyruvate via the pyruvate formate lyase (PFL) with simultaneous production of formate [31]. A crotonyl-CoA molecule is formed from two acetyl-CoA molecules, which can be converted to butyryl-CoA in the next step. Two different possibilities for the conversion of crotonyl-CoA to butyryl-CoA are shown and from past studies the metabolic flux analysis showed the importance of a newly identified so-called "electron bifurcation" pathway for the conversion of crotonyl-CoA to butyryl-CoA to regulate the redox balance [21]. Butyryl-CoA dehydrogenase *bcd* forms a BCdH-ETF complex with the electron transferring flavoprotein (ETF) and the accompanying reduction of a redox protein such as ferredoxin or flavodoxin takes place while the bifurcation pathway requires two NADH molecules [16, 36]. Production of acetate or butyrate releases an ATP molecule via substrate level phosphorylation while production of ethanol or butanol consumes two NADH

molecules [25]. The production of PDO is one of the main aspects examined in this work and organisms that produce PDO biotechnologically from glycerol or glucose are summarized in Table 2-1.

Table 2-1: Production of PDO in fermentations with various strains. FB: Fed-batch, C6: glucose, CG: crude glycerol, PG: pure glycerol, XY: xylose, B: batch fermentation.

Strain	Fermentation type + Substrate	PDO Titer [g L^{-1}]	PDO Yield [g g^{-1}]	PDO Productivity [g L^{-1} h^{-1}]	Ref.
(Recombinant) *E. coli*	FB + C6	135	0.51	3.50	[37]
C. glutamicum MBP14	FB + C6	110.4	0.42	2.30	[13]
C. glutamicum MBP15	FB + C6, XY	98.2	0.38	2.05	
K. pneumoniae J2B	FB + C6	62.0	0.54	0.94	[12]
C. pasteurianum K1	FB + CG	74.6	0.52	5.02	[17]
		55.0	0.52	2.30	[15]
C. pasteurianum C8	FB + PG	74.7	0.54	5.33	[2]
	FB + CG	58.4	0.46	3.43	
C. pasteurianum G8	FB + CG	74.2	0.52	5.30	
	B + PG	38.5	0.52	4.81	[16]
C. pasteurianum DSM525	FB + CG	53.7	/	0.81	[30]
	B + PG	5.3	0.1	0.26	[29]
Mixed cultures from sludge samples	FB + CG	70.0	0.46	2.60	[14]
C. butyricum AKR102a	FB + PG	93.7	0.52	3.30	[38]
	FB + CG	76.2	0.51	2.30	
C. butyricum VPI 1718	FB + CG	67.9	0.55	0.78	[39]
K. oxytoca FMCC-197	FB + CG	50.1	0.40	0.57	[40]
K. oxytoca NRCC3006	B + PG	16.9	0.34	0.68	[41]
C. freundii FMCC-B 294 (VK-19)	FB + CG	68.1	0.40	0.79	[42]
C. pasteurianum BC-I	B + PG	23.5	0.31	0.96	This study
C. pasteurianum BC-III		20.1	0.31	0.32	

According to Hong et al. (2020) [22], 2-oxobutyrate is formed in the amino acid metabolism. It can be produced via cystathionine from the methionine cycle [43] or as an intermediate in the

conversion of threonine to isoleucine [44]. Threonine is linked via threonine aldolase to glycine which is produced by serine hydroxymethyltransferase [45] from serine. Pyruvate can again be produced from serine via serine deaminase [46] and oxaloacetate, a precursor for aspartate, is produced from pyruvate via pyruvate carboxylase. Threonine is formed from aspartate via a reaction sequence consisting of aspartate kinase, aspartic semialdehyde dehydrogenase, homoserine dehydrogenase, homoserine kinase and threonine synthase with homoserine as an intermediate [35]. Afterwards, 2-oxobutyrate is formed via threonine deaminase and isoleucine is produced via acetohydroxyacid synthase [44]. The other pathway, where 2-oxobutyrate is produced via cystathionine betalyase from cystathionine, starts from the methionine cycle where S-adenosylhomocysteine (SAH) is converted to homocysteine via S-adenosylhomocysteine hydrolase. At the end, cystathionine γ-synthase converts homocysteine to cystathionine [43]. Overall, *C. pasteurianum* shows widely different product patterns when cultivations are carried out under different conditions and a novel approach for the analysis was presented in Hong et al. (2021) using sample data, collected from numerous *C. pasteurianum* cultivations [47].

2.1.2 Restriction modification systems

The first aim of this work (chapter 4.1.1) was to test different approaches to enable transformation of *C. pasteurianum* C8 and restriction modification (RM) systems are the main barrier for transformation with foreign DNA. There are different methods to avoid these RM systems and according to Bao et al. (2019), the chance of successful transformation is higher with decreasing number of unmethylated restriction sites [48]. Therefore, it's possible to design shuttle plasmids which are free of host restriction sites to improve the transformation. As an example, Johnston et al. (2019) provides a systematic approach to evade RM system by screening RM target sequences on their plasmid. In the next step, the sequence is adapted to create a RM-silent plasmid by changing single nucleotides (single-nucleotide polymorphisms) while keeping synonymous codons (codon substitution) [49]. Methylation recognition sites (motifs) can be detected by genome sequencing with single molecule real-time (SMRT) sequencing, which can differentiate between modified and unmodified nucleotides via fluorescence measurements [50, 51]. Various kinds of methylations exist including N^6-methyladenosine (m6A), N^4-methylcytosine (m4C) and 5-methylcytosine (m5C) [52, 53].

The genome of *C. pasteurianum* G8, which originates from strain C8, was sequenced by Zhang et al. (2023) [16] and it was found that there are different numbers of type I, type II and type III RM systems which were identified by Rapid Annotation using Subsystem Technology (RAST) [54]. This is reflected in the different numbers of restriction, methylation and specificity subunits as shown in Table 2-2. The recognition sites 5'-GATC-3' (CpaI) and 5'-CGCG-3' (CpaAI) are methylated in *C. pasteurianum* DSM525 via methylation in *E. coli* 10-beta and methylation plasmid pFnuDMIIKn [55]. Protection of plasmids with in vivo methylation was not only carried out in *C. pasteurianum* [20], but also for other clostridia strains such as *Clostridium cellulovorans* [56]. However, these are not specific sequences recognized by the RM systems of *C. pasteurianum* C8.

Table 2-2: Restriction modification systems in *C. pasteurianum* C8. The mentioned positions are from the sequenced genome of *C. pasteurianum* G8, which originates from strain C8 [16]. The methylation subunits with positions in bold were used in new methylation plasmids in this work. R: restriction subunit, M: methylation subunit, S: specificity subunit.

Type	Subunit	C8	Positions on the genome of C8
I	R	4	p1135, p1223, p3529, p3986
	M	3	p1136, p3532, p3741
	S	5	p1137, p1141, p3531, p3534, p3985
II	R	3	p482, p3375, p3733
	M	2	**p1384**, **p3734**
III	R	1	p477
	M	2	**p478 - p479**

2.1.3 EMS-induced random mutagenesis of *C. pasteurianum* C8

Ethyl methanesulfonate (EMS)-induced mutagenesis is frequently applied to isolate variant strains with improved product formation or transformation efficiency and examples of EMS treated microorganism are *Saccharomyces cerevisiae* [57], *Clostridium carboxidivorans* [58], *Clostridium acetobutylicum* [59, 60] and *Clostridium pasteurianum* [61]. Lakhssassi et al. (2020) [58] previously used serial EMS concentrations of 0.2% (20 mM) to 2.0% (200 mM) (w/v) to

mutagenize cultures of the *Clostridium carboxidivorans* P7 wild type strain in their exponential growth phase. However, it was found that EMS concentrations above 140 mM or 1.4% (w/v) are lethal for the P7 strain. Lemmel (1985) [59] performed mutagenesis of *Clostridium acetobutylicum* with 0.5% and 1.0% (v/v) EMS and noted that dilution by 1:100 of mutagenized cultures is necessary to recover the cells after the exposure to EMS, while dilution by 1:10 resulted in no growth. In this work, cultures of *C. pasteurianum* C8 are exposed to EMS to try the isolation of a mutant which can efficiently take up plasmids.

2.1.4 Comparison of genes in *C. pasteurianum* DSM525 and *C. pasteurianum* C8

The next aim of this work (chapter 5) was to create a *C. pasteurianum* R525 mutant which is similar to *C. pasteurianum* C8 to verify if the below mentioned differences could lead to enhanced PDO production in C8. In this work, the strain *C. pasteurianum* R525 is mainly used and it originates from the strain *C. pasteurianum* DSM525 and therefore they are treated as the same for the genes compared below (Table 2-3). For comparison, the genome sequence of *Clostridium pasteurianum* DSM525 was acquired from the National Centre for Biotechnology Information (NCBI, Reference Sequence: NZ_CP009267.1). According to Zhang et al. (2023) [16], a weakened butanol production pathway is present in *C. pasteurianum* C8 and *C. pasteurianum* DSM525 carries four butanol dehydrogenase genes compared to two genes in *C. pasteurianum* C8. The two genes *adh2* and *bdhA2* marked in red in Table 2-3 are the genes that are not present on the genome of *C. pasteurianum* C8.

The genes *adh1* and *bdhA1* from *C. pasteurianum* DSM525 share almost the same sequence with the genes from *C. pasteurianum* C8 with percent identities of 100% and 99.91%, respectively. The overexpression by the presence of two additional butanol dehydrogenase genes might be the reason of the high butanol production with *C. pasteurianum* DSM525. Another gene that has a different copy number on the genome of both strains is the PDO dehydrogenase and *C. pasteurianum* C8 carries two genes that encode for this enzyme compared to one gene in *C. pasteurianum* DSM525. This *dhaT* gene, which is present in both strains, will be called *dhaTR* in the following. When comparing the sequence of the second PDO dehydrogenase from *C. pasteurianum* C8 with the gene in *C. pasteurianum* DSM525, they differ by around 9.15% (Table 2-4). This second *dhaT* gene will be called *dhaTC8* in the following and it is present on the glycerol uptake operon (Figure 2-2).

Table 2-3: Genes encoding butanol dehydrogenases and butyryl-CoA dehydrogenases in *C. pasteurianum* DSM525. The position shows the number of base pairs on the genome of *Clostridium pasteurianum* DSM525 (NCBI Reference Sequence: NZ_CP009267.1). Each genes has an assigned locus tag and protein ID and the genes marked in red are the ones that are not present on the genome of *C. pasteurianum* C8.

Gene and protein name	Locus tag	Protein ID	Position on the genome	Size [bp]
adh1 NADPH-dependent butanol dehydrogenase	CPAST_c23980	WP_003441277.1	2,571,316 – 2,572,482	1167
adh2 NADPH-dependent butanol dehydrogenase	CPAST_c33950	WP_003446425.1	3,667,273 – 3,668,439	1167
bdhA1 NADH-dependent butanol dehydrogenase A	CPAST_c04370	WP_004455109.1	466,476 – 476,639	1164
bdhA2 NADH-dependent butanol dehydrogenase A	CPAST_c15980	WP_003443436.1	1,703,652 – 1,704,827	1176
bcd1 butyryl-CoA dehydrogenase	CPAST_c11000	WP_003444507.1	1,185,608 – 1,186,747	1140
bcd2 butyryl-CoA dehydrogenase	CPAST_c28620	WP_003443104.1	3,065,269 – 3,066,408	1140

On the genome of R525, this operon has a length of 5200 bp between the genes encoding *glpF* and transcriptional regulator and 12200 bp on the genome of C8. Zhang et al. (2022) [2] reported a high production of PDO with a total titer, yield and productivity of 74 g L^{-1}, 0.52 g g^{-1} and 5.3 g L^{-1} h^{-1}, respectively, in a adapted strain which was called *C. pasteurianum* G8. The second copy of this gene may lead to a higher NADH consumption through the reductive pathway for the production of PDO. The produced PDO from such efficient fed-batch fermentations can be purified with a novel downstream process for highly pure PDO as reported by Zhang et al. (2021) [17]. Both strains have lactate dehydrogenase genes, but there are large deletions on the L-lactate dehydrogenase genes *ldh1* and *ldh2* of *C. pasteurianum* C8 and lactate production was negligible [16].

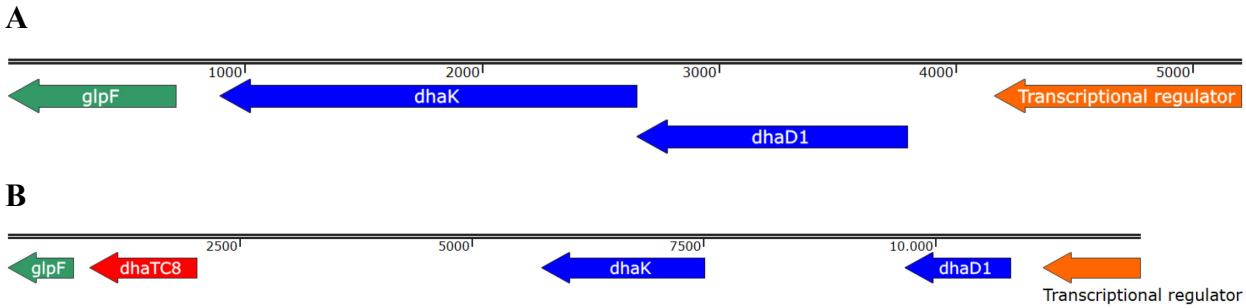

Figure 2-2: Glycerol uptake operons. A: glycerol uptake facilitator protein (*glpF*), *dhaK*, *dhaD1* and transcriptional regulator on the genome of *C. pasteurianum* R525 (5200 bp). **B**: *glpF*, *dhaTC8*, *dhaK*, *dhaD1* and transcriptional regulator on the genome of *C. pasteurianum* C8 (12200 bp). Three genes encoding pyruvate formate-lyase activating enzyme, pyruvate formate-lyase and phosphoenolpyruvate-dihydroxyacetone phosphotransferase are hidden so that only the relevant genes are shown.

Table 2-4: Comparison of number of genes encoding butanol dehydrogenases, PDO dehydrogenases and butyryl-CoA dehydrogenases in *C. pasteurianum* C8 and *C. pasteurianum* DSM525. The genes *adh1*, *bdhA1*, *dhaTR* and *bcd2* are present on the genome of both strains and the genes marked in red are the ones that are not present on the genome of *C. pasteurianum* C8. The percent identity describes the percentage of same nucleotides when comparing the genes from *C. pasteurianum* C8 to the corresponding gene in *C. pasteurianum* DSM525.

Enzyme	Genes		Percent identity [%]
	DSM525	C8	
NADPH dependent Butanol dehydrogenase	*adh1*		100
	adh2	/	/
NADH dependent Butanol dehydrogenase A	*bdhA1*		99.91
	bdhA2	/	/
1,3-propanediol dehydrogenase	*dhaTR*		99.91
	/	*dhaTC8*	90.85
Butyryl-CoA dehydrogenase	***bcd1***	/	/
	bcd2		99.82

2.1.5 Biosynthesis of glycerol and 1,3-propanediol from glucose

In contrast to conventional chemical methods, the biological production of PDO involves the use of microbes that convert renewable substrates, such as glucose into PDO. Various patents were registered regarding efficient conversion of glucose to PDO by a single recombinant microorganism [9, 10, 62–64]. The recombinant strains and production processes were established

and commercialized by the company DuPont (Wilmington, DE, USA) and the former Genencor International, Inc. (Palo Alto, CA, USA). A target of this work (chapter 6) was the synthesis of 1,3-propanediol from glucose in *C. pasteurianum* and study of the introduction of genes *GPD1* and *GPP2*, which are not naturally present in *C. pasteurianum*. As shown in Figure 2-1, *C. pasteurianum* is able to produce 1,3-propanediol from glycerol. When using glucose as substrate, a glycerol synthesis pathway can be introduced into the organism. Such a pathway exists in *Saccharomyces cerevisiae* in which two enzymes – *GPD1* (glycerol-3-phosphate dehydrogenase) and *GPP2* (glycerol-1-phosphatase) – convert the glycolysis intermediate DHAP to glycerol. *GPD1* catalyzes the conversion of DHAP to glycerol-3-phosphate, which is then converted to glycerol by *GPP2* [18, 19].

The genes for *GPD1* and *GPP2* can either be integrated into *C. pasteurianum* as single (separate) proteins or as a fusion protein. A fusion protein is one polypeptide consisting of two different proteins, both containing their original function. The fusion proteins are connected by a linker [65] and this is important because a direct protein connection can result in misfolding and reduced activity. Linkers from naturally-occurring fusion proteins most often contain proline, threonine and glutamine as amino acids and are templates for artificially designed empirical linkers. The latter can be subdivided in two main types: the first one consists of flexible linkers, which permit movement of the attached proteins. The second type consists of rigid linkers, which are less flexible and hold the proteins at a constant distance to each other. This reduces the interference of one protein with the other and can enhance the activity of each protein [66]. This was demonstrated in a publication about *E. coli* in which a *GPD1-GPP2* fusion protein exhibited a higher efficiency compared to the single genes [65].

2.2 Genome engineering and CRISPR-Cas

2.2.1 Genome modification methods for *C. pasteurianum*

The here reported metabolic engineering of *C. pasteurianum* would not be possible without the accomplishments from previous works including the isolation of R525 and the development of an electrotransformation protocol. There are reported works about overexpression of homologous genes such as hydrogenase (*hydA*), *dhaD1* and *dhaK* to enhance the hydrogen yield [67], but the focus here lies on modifications on the genome level. A summary of reported genome

modifications and editing methods for *C. pasteurianum* can be found in Table 2-5. Genetic engineering was already carried out successfully in other *Clostridia* strains before [68–71], but the first group-II-intron-mediated chromosomal gene disruption mutant of *C. pasteurianum* with deleted *cpaAIR* gene was isolated in Pyne et al. (2014) [72]. The same *cpaAIR* gene was later completely deleted in Pyne et al. (2016) [23] with the utilization of endogenous CRISPR-Cas machineries.

Table 2-5: Reported genome modifications and editing methods for *C. pasteurianum*. Genes were either deleted or disrupted in the mentioned studies and information is given for the respective method used for the conducted genome modification. Abbreviations for genes encoding: *spoIIE*: sporulation protein E, *cpaAIR*: CpaAI Type II restriction endonuclease, *Spo0A*: sporulation transcription factor, *dhaT*: PDO dehydrogenase, *hydA*: hydrogenase, *rex*: redox response regulator, *dhaBCE*: glycerol dehydratase, *dhaB*: glycerol dehydratase large subunit, *CpaAII* (I) and *CpaAIP* (II): Type I and Type II host restriction modification (RM) systems.

Genome modification	Description and editing method	Source
Disruption of *cpaAIR*	Applying group-II-intron for transformation of M.FnuDII-unmethylated plasmid DNA	[72]
Deletion of *Spo0A*	Gene knockout by a double-crossover editing method for increased butanol production	[73]
Deletion of *cpaAIR*	Harnessing native CRISPR-Cas machinery for selection against unmodified host cells	[23]
Disruption of *dhaT*	Chromosomal gene disruption by L1.ltrB group-II-intron for enhanced butanol production	[34]
Deletion of *hydA*, *rex* or *dhaBCE*	Allele-coupled exchange (ACE) to eliminate PDO synthesis	[25]
Deletion of *dhaB*	Utilization of Type II CRISPR/Cas9 nickase system inhibited PDO production	[21]
Deletion of *spoIIE*	Implementation of synthetic riboswitches to regulate Cas9 expression for CRISPR mediated modification	[74]
Successive deletion of *CpaAII* (I), *CpaAIP* (II)	Multiple genome modifications in a single mutant with ACE to improve transformation efficiency	[24]

The group II intron was again used to disrupt the *dhaT* gene in Pyne et al. (2016) [34] and transcriptional regulation was achieved via antisense-RNA [75]. The sporulation transcription factor Spo0A was knocked out by Sandoval et al. (2015) [73] by applying the method reported by Al-Hinai et al. (2012) [76] which uses an *E. coli*-based mazF gene as a counter-selection marker. In later studies, a sporulation protein E was deleted in Cañadas et al. (2019) [74] to prove the functionality of a CRISPR-mediated modification by application of riboswitches to regulate Cas9 expression. Schwarz et al. (2017) [25] utilized the so called Allelic Coupled Exchange (ACE) method, which was developed in Heap et al. (2012) [77] and Ng et al. (2013) [78], to delete the genes *hydA*, *rex* or *dhaBCE*. Schmitz et al. (2018) [21] deletes the *dhaB* gene with a method based on a Cas9 nickase which introduces a DNA single strand break instead of a double strand break.

Ortega (2020) shows that multiple genome modifications can be successfully introduced into *C. pasteurianum* with the ACE method of cargo integration without a counter-selection marker by restoring the *pyrE* allele [24], but in contrast the utilization of the endogenous CRISPR-Cas machineries is the focus of this work. A Cas12a-based CRISPR tool was presented by Joseph et al. (2023) [79] and it shows that gene expression can be repressed in *C. pasteurianum* by the binding of catalytically dead Cas enzymes (dCas9 or dCas12a) to a single target region or even multiple genes at once. The repression of the targeted genes in that study (*hydA*, *dhaB*, *dhaT*) resulted in no significant change in produced metabolites which indicates the importance of genetic modifications with the complete deletion of genes to achieve the desired change in metabolic behavior.

2.2.2 CRISPR-Cas types

CRISPR (clustered regularly interspaced short palindromic repeats) sequences together with Cas enzymes (CRISPR-associated proteins) are found in bacteria and archaea, provide protection against invading, foreign DNA and play an important role in the defense against bacteriophages [80–82]. Acquisition of specific nucleotide sequences from the invading DNA and incorporation into the CRISPR array on the genome is the first step for building a resistance against foreign DNA elements. The incorporated sequences are called spacers and are flanked with direct repeat sequences. The CRISPR array, that can contain up to a few hundred spacers, is transcribed into a large precursor CRISPR RNA (pre-crRNA) and then it will be processed into individual mature crRNAs by the Cas6 endonuclease (type I systems) [23, 83]. Type II CRISPR-Cas systems

additionally require transcription of trans-activating crRNA (tracrRNA) and the dual-RNA guided Cas9 originating from *Streptococcus pyogenes* forms a complex with crRNA and tracrRNA to introduce double-stranded breaks in target DNA [84, 85]. The crRNA and tracrRNA can be fused and transcribed together into a guide RNA (gRNA) to simplify the procedure [84, 86]. The type V CRISPR-Cas system utilizes Cas12a from *Francisella novicida*, previously known as Cpf1, for cleavage of target DNA without the need for a tracrRNA, although staggered double-stranded DNA breaks are introduced instead of blunt ends with Cas9 [87].

Single genomic modifications are enabled by repair mechanisms such as homology-directed repair (HDR) which requires a repair DNA fragment and non-homologous end joining (NHEJ) which does not require a homologous repair template [80, 88]. While the targeting of multiple genes at the same time is limited with Cas9 because multiple or large expression constructs are necessary, a single CRISPR array with multiple spacers, which is processed to multiple gRNAs, can be used for the editing of several genes with Cas12a simultaneously [89]. Multiplex genome editing with CRISPR-Cas systems was demonstrated in *Streptomyces lividans* [84] with short deletions, gene knockouts in *Streptomyces coelicolor* M145 [90], knockouts in *E. coli* MG1655 [91] and deletion of complete genes in *Streptococcus pneumoniae* crR6Rc [92]. It would be beneficial to transfer these CRISPR-Cas systems for multiplex genome editing to *C. pasteurianum*, but there are limitations that could hinder the application. The expression of Cas9 in *C. pasteurianum* can be toxic to the cells and significantly lowers transformation efficiency [21, 23]. The plasmid size would increase notably with multiple spacers and homologous repair templates and this would impede the transformation and isolation of a mutant with correct modifications because transformation efficiency was observed to decrease with increasing plasmid size [93].

2.2.3 Utilization of endogenous CRISPR-Cas machineries for genome editing

The presence of an endogenous CRISPR-Cas system in *C. pasteurianum* was used by Pyne et al. (2016) [23, 94] to develop a method for selecting mutants that were modified by genome editing methods. Homology between crRNA and the corresponding spacer sequence on the invading DNA results in DNA strand degradation by the Cas3 nuclease (type I systems). Sequencing of the genome of *C. pasteurianum* revealed that it contains a CRISPR-Cas system with a CRISPR array that contains 37 spacers in total [23]. Following steps are necessary for the application of this

method. The constructed plasmids contain the mentioned CRISPR array with a leader sequence containing a putative promoter, but with only a single 36 bp spacer that is flanked with direct repeats. The 3' end of the endogenous chromosomal CRISPR array is also included (Figure 2-3). Homology between the crRNA (from the expression of the CRISPR array) and the spacer sequence on the host genome results in DNA strand degradation by the Cas3 nuclease [23]. The same tool was used to construct plasmids in this work for gene deletion. By targeting a gene on the host genome that would be deleted, selection can take place where only cells survive that don't contain that certain gene anymore.

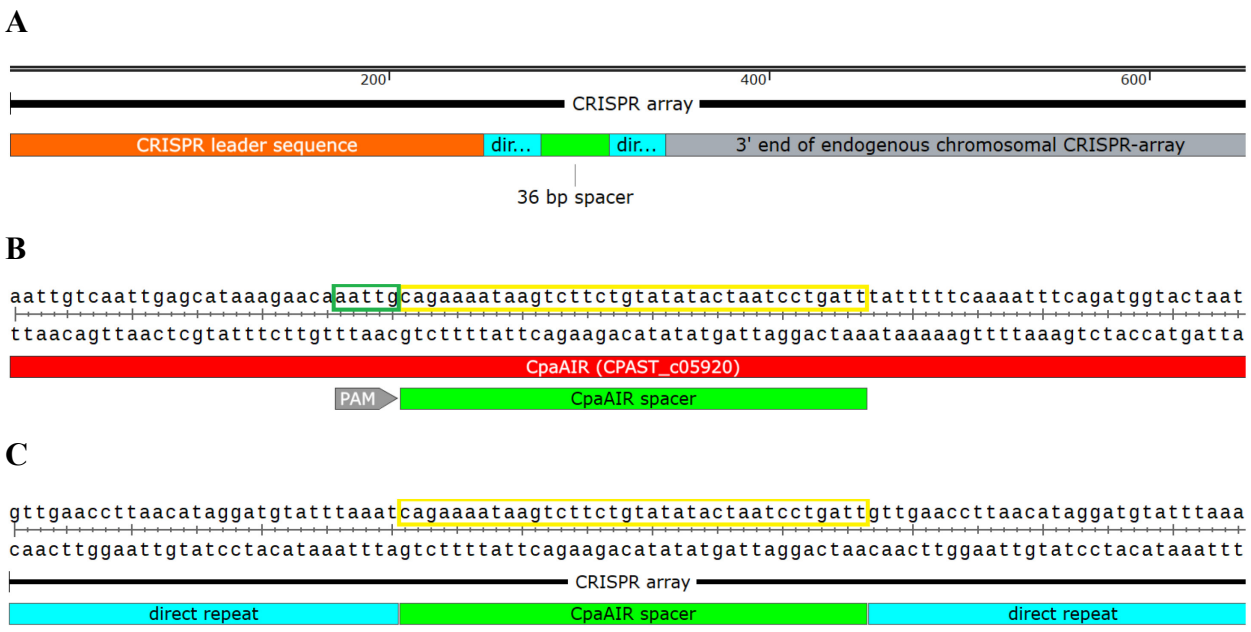

Figure 2-3: Template for selection of a spacer for deletion of gene *CpaAIR*. A: Components of the CRISPR array, **B**: Selection of spacer sequence on the *CpaAIR* gene, **C**: Insertion of that spacer sequence between the direct repeats on the CRISPR array. Part of the *CpaAIR* gene (CPAST_c05920) is shown in red (B) and the PAM and spacer sequences are marked in dark green and yellow boxes, respectively. The plasmid for the deletion of the gene *CpaAIR* can be designed by inserting the spacer between both direct repeats of the CRISPR array as can be seen in the lower part of the figure (C). The CpaAIR gene was the first gene to be deleted by the endogenous CRISPR-Cas method in the study by Pyne et al. (2016) [23] and is only shown here as an example.

A gene deletion on the genome requires two homologous recombination events. The region of 1000 bp upstream of the gene to be deleted are used for the first homologous region (H1) and again 1000 bp downstream are used for the second homologous region (H2). The editing template which

is cloned on the genome editing plasmids contains the H1 and H2 regions next to each other without the gene in between, similarly to how it was designed by Pyne et al. (2016) [23]. In the first homologous recombination event, the plasmid is incorporated into the genome and in the second event two possibilities can occur. If the second recombination occurs in the second homologous region, then the desired gene deletion is completed. If this occurs in the first homologous region again, then there will be no gene deletion because the initial state of separate plasmid and genome will be restored [77, 95]. When a simultaneous insertion is desired, the genes to be inserted need to be placed between the two homologous regions on the genome editing plasmid and the gene to be deleted will be replaced by the new gene. By using the endogenous CRISPR-Cas machineries, only cells with two different completed homologous recombination events can survive because they will not contain the spacer sequence anymore [23].

The gene deletion by the utilization of the endogenous CRISPR-Cas machineries was first applied for the deletion of the gene *CpaAIR* (CPAST_c05920) on the genome of *C. pasteurianum* and the following describes how the CRISPR array was designed for the deletion [23]. The same principle will then be used for all further genome editing plasmids. It was found that a possible PAM (Protospacer adjacent motif) sequence is 5'-AATTG-3' in *C. pasteurianum* and therefore, first a PAM sequence need to be found on the *CpaAIR* gene on the genomic DNA (Figure 2-3). The sequences 5'-TTTCA-3' or 5'-TATCT-3' were also found to be possible PAM sequences in *C. pasteurianum*, but the deletion of *CpaAIR* was tested with 5'-AATTG-3' by Pyne et al. (2016) [23]. The 36 base pairs following a PAM sequence can be used as a spacer and can be inserted into the CRISPR array between the two direct repeats. This can be done via PCR by amplifying the spacer region with primers or by designing the CRISPR array with the already inserted spacer as synthetic DNA. The PAM sequence won't be inserted because the CRISPR-associated nuclease Cas3 won't cleave the spacer sequence unless there is an adjacent PAM sequence.

The spacer regions for the CRISPR array were found with the help of the "Cas-Designer" tool (http://www.rgenome.net/cas-designer/) which requires to choose a PAM type and target genome. One protospacer adjacent motif (PAM) of *C. pasteurianum* R525 is 5'-AATTG-3' so the given option "BhCas12b v4 from Bacillus hisashii: 5'-ATTN-3'" was chosen for the PAM type and the target genome was chosen as the given option "*Clostridium pasteurianum* (ASM80725v1)". The

specified base N can be any base and PAM sequences need to be chosen with the base guanine (G) at the end. If a sequence with 5'-ATTG-3' was found on the target gene, it also needs to be checked if the base before is adenine to result in the full PAM sequence of 5'-AATTG-3'. The "Cas-Designer" tool will show all possible spacer regions on a gene and always two of them with the highest out of frame scores will be picked and used in the plasmid construction. For the targeting of any gene, various possible spacer sequences are available, because one of the three PAM sequences in *C. pasteurianum* should be present every 74 bp within the genome [23]. Not all of them are guaranteed to work so the testing of spacer sequences is essential, but this would result in many combinations to test, if several genes are targeted with various possible spacer sequences each and due to the mentioned limitations, multiple spacers on one plasmid were not attempted.

2.3 Plasmid construction

2.3.1 Polymerase chain reaction (PCR) and In-Fusion cloning

The expression of heterologous genes and the introduction of these genes into an organism can be achieved by incorporation of extrachromosomal DNA called plasmids. They can replicate independently of the chromosomal DNA because they have their own origin of replication and especially shuttle plasmids are used in this work. Shuttle plasmids can replicate in different organisms and plasmids that are transferred between *E. coli* and *C. pasteurianum* need an origin of replication for gram-negative and gram-positive organisms and one antibiotic marker for selection for both [96]. This is necessary when a potential host organism is difficult to work with in terms of general plasmid construction procedures. Plasmids can be designed individually according to the desired plasmid components.

A modular system for *Clostridium* shuttle plasmids was developed by Heap et al. (2009) [96] and it contains several components that were also used for constructed plasmids in this work. Necessary fragments such as the backbone, consisting of an antibiotic marker and the two replication origins, and genes can be amplified by polymerase chain reaction (PCR) and combined by In-Fusion cloning (Takara Bio). PCR is used to amplify a specific region of DNA and has three main steps which are repeated in 30 cycles: denaturation, annealing and elongation. During the first step of denaturation, the double stranded DNA is denatured at 98°C, yielding two single strands. This way, the forward and reverse primers can anneal at the single strands during the annealing step of PCR.

Where the primers anneal depends on their sequence, which is homologous to each end of the specific sequence of the DNA to be amplified. The annealing temperature is usually set 5°C lower than the melting temperature of the primers. During the elongation step, a polymerase attaches the bases in 5‘-3‘-direction at 72°C to synthesize a complementary DNA strand. The first two main steps of PCR can be completed in a few seconds while the time of elongation depends on the length of the fragment that is amplified and the type of polymerase used.

In-Fusion cloning (Takara Bio) can be used to fuse the desired plasmid components and this is done by adding the In-Fusion enzyme mix and the fragments that were amplified by PCR in a single tube. A 15-bp or 20-bp overlap for the fusion of multiple fragments is required between each fragment to be fused and this has to be considered in the design of forward and reverse primers. The sequence of the overlap is homologous to the respective end of the fragment where the fusing should take place. Depending on the length of the primers (without the overlap), it can be chosen on which of two fragments the overlap will be placed so that both primers still have the recommended primer length. The 3’-ends of the fragments to be fused are digested and overlapping ends are created, which anneal to one another. Thus, a recombinant vector is synthesized, which can be transformed into an organism such as *E. coli* for plasmid propagation. The sequence of the plasmid has to be confirmed by Sanger sequencing to make sure that no bases have been changed, deleted or inserted in the fusion or PCR process. A single changed base, which leads to one wrong amino acid (missense mutation) or a frame shift, which causes an overall wrong polypeptide chain (frame shift mutation), could cause unintended problems so that the constructed plasmid can’t be used for what it was designed for.

2.3.2 Electrotransformation of gram-positive bacteria

The uptake of foreign DNA in *C. pasteurianum* was challenging for some time, but starting from the laboratory strain, *C. pasteurianum* DSM525 could be isolated with an increased transformation rate using optimized methods. The result of the isolation was a cell strain with the property of taking up heterologous DNA with increased efficiency and this strain was called *C. pasteurianum* R525 [21]. During electroporation, the cells are exposed to an electrical pulse of high voltage of about 1,800 V just for milliseconds, which makes the membrane temporarily more permeable for substances such as plasmids [20]. If the voltage is too high or applied for too long, this can cause

permanent cell damage, which is not desired. The efficiency of electroporation depends on several factors, some of them are the applied plasmid concentration and the recovery time after electroporation. The thicker layer of gram-positive bacteria leads to a poorer transformation success compared to gram-negative bacteria because it keeps the genetic material from entering the cell. To counteract this problem, the cell wall needs to be pretreated with specific substances including glycine, which is able to weaken it [20].

The strains that were used in this work were made competent for the transformation with the synthesized recombinant vectors and this improves the uptake of genetic materials such as plasmids into the organism. Another barrier of transformation are restriction modification systems that function as a defense mechanism to protect the organism and it degrades foreign DNA that enter the cells. To prevent this, the DNA needs to be methylated so that the endonucleases won't cut at specific recognition sites. This can be seen in *C. pasteurianum*, which expresses the restriction enzymes *CpaAI* and *CpaI* which cut at the recognition sites 5'-CGCG-3' and 5'-GATC-3', respectively [55]. The native DNA of the host is protected by methylation of these recognition sites and plasmids that were introduced into *C. pasteurianum* were protected against digestion by in-vivo methylation with the plasmid pFnuDIIMKn [20] and Dam+ methylation by *E. coli*. This was found to be essential for successful transformations. The transformation efficiency in CFU μg^{-1} can be calculated according to the following equation and it describes how many colonies would have grown when plating the whole recovery medium, related to the added amount of plasmid DNA:

$$E_T = \frac{CFU \cdot V_{recovery}}{V_{streaked} \cdot m_{DNA}} \quad (1)$$

Colony forming unit (CFU): represents a colony grown from a single cell on the agar plate, $V_{recovery}$: volume of recovery medium into which cells are transferred after the electroporation step of the transformation, $V_{streaked}$: describes the volume that is used for streaking the transformed cells onto an agar plate (1 mL was centrifuged and plated), because not all of the recovery medium can be plated, m_{DNA}: amount of plasmid DNA (5.8 µg for pMTL85141) that was added for transformation.

2.4 Fermentation analysis

2.4.1 Fermentation types and general equations

When a mutant was successfully created, batch fermentations were carried out for characterization and the typical growth phases in a batch fermentation with bacterial cultures are shown in Figure 2-4. At the beginning in the lag phase (I), the cells are adapting to their new environment directly after inoculation into fresh cultivation medium. There is no growth yet and therefore growth rate μ is approximately zero. The duration of the lag phase depends on pre-culture conditions including growth phase and OD_{600} of the pre-culture, medium composition or antibiotic supplementation. The growth slowly starts in the first transition phase (acceleration phase) between growth phases I and II which initiates the exponential growth phase (II) where maximum growth rate μ_{max} is reached.

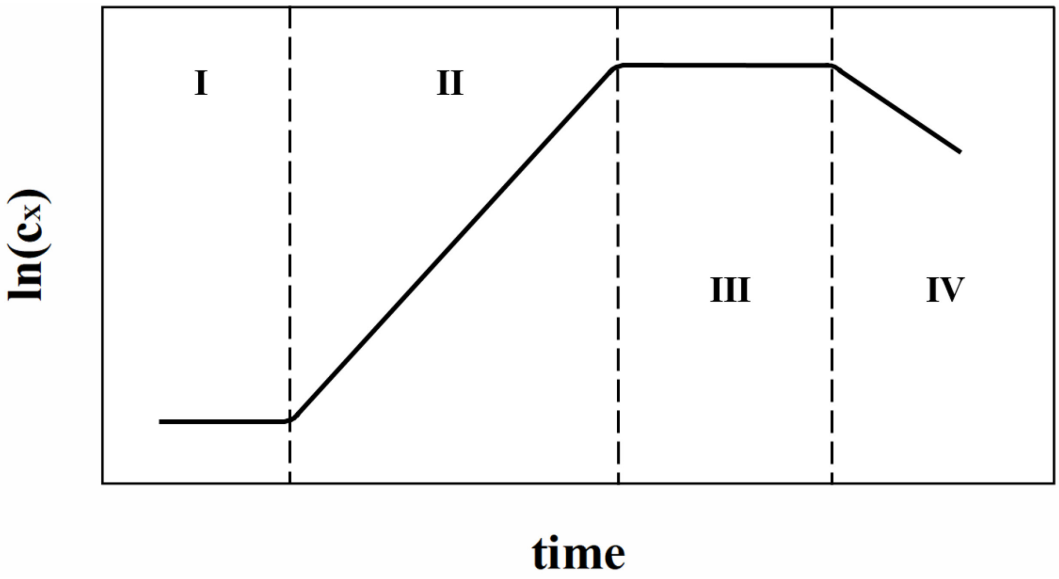

Figure 2-4: Growth phases in a batch fermentation. I: lag phase (μ = 0), **II**: exponential growth phase (μ = μ_{max}), **III**: stationary phase (μ = 0), **IV**: death phase (μ < 0). There is a first transition phase between growth phases I and II and the second transition phase is between growth phases III and IV. The figure was adapted from [97].

The maximum growth rate μ_{max} is characteristic for each microorganism and can vary between aerobic and anaerobic microorganisms or wildtype and genetically modified strains. As soon as biomass formation is slowed down by accumulation of inhibiting products or substrate limitation, the growth rate declines in the second transition phase which starts between growth phases II and

III. This takes place because the substrate is only added at the beginning of a batch fermentation. In the following stationary phase (III), the growth rate reaches zero while cell growth and lysis are in balance. Subsequently, cell lysis predominates in the death phase (IV) were the growth rate becomes negative. The volume in the bioreactor remains the same since no medium is added during the course of the fermentation procedure. [97]

During a batch cultivation, no fresh medium is added into the bioreactor as in the case with fed-batch fermentations, which starts with a batch phase with lower starting substrate concentration. After depletion of the initially added substrate in the fed-batch fermentation, a feeding phase with fresh medium starts and high cell densities can be reached, although the medium volume in the bioreactor increases over time. It's important to adjust the feeding rate to the growth of the cells (linear, exponential or pulse feeding) as too high substrate concentration can lead to substrate inhibition while low substrate concentrations leads to starvation of the cells. At the same time, no product is removed from the bioreactor as in the case with continuous fermentations. In this fermentation type, fresh medium is feeded into the bioreactor while medium (containing dead cells and metabolites) is simultaneously removed at a constant rate. Therefore, consumed nutrients are renewed while inhibiting metabolites are removed so that medium volume stays the same in continuous fermentation [97, 98].

The change of mass of a component i over time can be described with equation (2) and the mass balance within a closed system can be described with equation (3). The mass flux leaving the system is subtracted from the mass flux coming into the system and a reaction rate describes the produced or consumed amount of a component i [97]. There are no fluxes entering or leaving the system and there is no volume change in a batch fermentation. Therefore, specific production rates q_p in g $g_{biomass}^{-1}$ h^{-1} (positives values) and consumption rates q_s (negative values) can be calculated with equation (4).

$$\frac{dm_i}{dt} = \frac{d(c_i V_l)}{dt} = c_i \cdot \frac{dV_l}{dt} + V_l \cdot \frac{dc_i}{dt} \tag{2}$$

$$\frac{dm_i}{dt} = \dot{m}_{i,in} - \dot{m}_{i,out} \pm q_i \cdot c_X \cdot V_l \tag{3}$$

$$q_i = \frac{1}{c_X} \cdot \frac{dc_i}{dt} \tag{4}$$

The volumetric production or consumption rate Q_i in g L^{-1} h^{-1} can be calculated using equation (5) for the formed product or consumed substrate of a component i, while the overall volumetric rate was calculated for the time between t = 0 h and the end of fermentation.

$$Q_i = \frac{c_i(t_2) - c_i(t_1)}{t_2 - t_1} = \frac{\Delta c_i}{\Delta t} \tag{5}$$

Samples were taken regularly throughout the batch fermentations in this work and the concentration of dry biomass c_X in g L^{-1} can be determined turbidometrically with the optical density OD_{600} at a wavelength of 600 nm using equation (6) [31].

$$c_X = OD_{600} \cdot 0.336 \tag{6}$$

In order to determine the influence of genomic modifications on cell growth, the specific growth rate μ in h^{-1} can be calculated using equation (7) with the biomass concentrations $c_{X,2}$ and $c_{X,1}$ at time points t_2 and t_1, respectively.

$$\mu = \frac{lnc_{X,2} - lnc_{X,1}}{t_2 - t_1} \tag{7}$$

Concentrations of metabolites c_i in g L^{-1} were measured using HPLC and the amount of consumed substrate is different for each batch fermentation. In order to compare fermentations under the same conditions, the substrate specific yield $Y_{P/S}$ in g g^{-1} can be calculated according to equation (8).

$$Y_{P/S} = \frac{c_p(t) - c_p(t_0)}{c_s(t_0) - c_s(t)} = \frac{\Delta c_p}{\Delta c_s} \tag{8}$$

With $c_p(t)$, $c_p(t_0)$, $c_s(t)$, $c_s(t_0)$: concentration of a product p or substrate s in g L^{-1} at time point t or t = 0 h. The theoretical carbon molar concentration of carbon dioxide c_{C,CO_2} in $mmol_C$ L^{-1} can be calculated according to the metabolism of *C. pasteurianum* (Figure 1) with the following equation (9) [33].

$$c_{CO_2} = \frac{c_{ethanol}}{M_{ethanol}} + \frac{c_{acetate}}{M_{acetate}} + 2 \cdot \left(\frac{c_{butanol}}{M_{butanol}} + \frac{c_{butyrate}}{M_{butyrate}} \right) - \frac{c_{formate}}{M_{formate}} \tag{9}$$

To determine how much PDO production is higher compared to butanol production, it can be useful to calculate the molar $ratio_{PDO/BuOH}$ in mol mol^{-1} with equation (10) with M_{PDO} and M_{BuOH} as molar masses of PDO or butanol.

$$ratio_{PDO/BuOH} = \frac{\frac{\Delta c_{PDO}}{M_{PDO}}}{\frac{\Delta c_{BuOH}}{M_{BuOH}}} \quad (10)$$

2.4.2 Carbon and electron balance

Carbon distributions of produced metabolites can be used to evaluate the impact of genomic modifications on the metabolism. First, the molar concentration of each measured metabolite needs to be calculated and multiplied with the respective number of carbons. This is how the molar concentration of carbons $c_{C,i}$ of a formed product or consumed substrate of a component i in $mmol_C$ L^{-1} can be calculated with equation (11).

$$c_{C,i} = \frac{c_i \cdot N_{C,i}}{M_i} \quad (11)$$

With c_i: concentration of a component i in g L^{-1}; M_i: molar mass of a component i in g mol^{-1}; $N_{C,i}$: number of carbons of a component i. In order to determine the amount of produced product in carbons $\Delta c_{C,p}(t)$ in $mmol_C$ L^{-1}, the product concentration of carbons at t_0 (t = 0) was subtracted from the product concentration of carbons at a certain time point t as in equation (12). In order to determine the amount of consumed substrate for carbons $\Delta c_{C,s}(t)$ in $mmol_C$ L^{-1}, the concentration at a certain time point t was subtracted from the initial substrate concentration at t_0 (t = 0) as shown in equation (13).

$$\Delta c_{C,p}(t) = c_{C,p}(t) - c_{C,p}(t_0) \quad (12)$$

$$\Delta c_{C,s}(t) = c_{C,s}(t_0) - c_{C,s}(t) \quad (13)$$

The value for the carbon distribution $C_{distribution,p}$ of a product p in % can be determined by forming the ratio between the respective produced metabolite and the sum of all products as shown in equation (14).

$$C_{distribution,p} = \frac{\Delta c_{C,p}(t)}{\sum \Delta c_{C,p}(t)} \quad (14)$$

The following equation (15) determines the recovery of carbons C_R in % via the ratio between all produced products and consumed substrates [32, 99, 100]. With $\Delta c_{C,Gly}$, $\Delta c_{C,Glu}$: consumed glycerol or glucose, respectively, over the course of fermentation, BDM: bio dry mass. The terms $\Delta c_{C,Glu}$ or $\Delta c_{C,Gly}$ equal zero in fermentations with glycerol or glucose as sole carbon source, respectively.

$$C_R = \frac{c_{C,PDO} + c_{C,BuOH} + c_{C,BuAc} + c_{C,EtOH} + c_{C,LaAc} + c_{C,AcAc} + c_{C,BDM} + c_{C,FoAc} + c_{C,CO_2}}{\Delta c_{C,Gly} + \Delta c_{C,Glu}} \quad (15)$$

The electron balance was calculated analogously to the determination of the carbon balance. The respective degree of reduction γ_i was calculated for all products formed and substrates, and then the molar concentrations $c_{e,i}$ in $mmol_{electrons}\ L^{-1}$ can be determined using the equation (16):

$$c_{e,i} = \frac{c_i \cdot \gamma_i}{M_i} \quad (16)$$

The degree of reduction γ_i of a component i is calculated using the total number of electrons that can be gained or released by the atoms within a respective molecule. Carbon (C) can release four electrons, hydrogen (H) one electron, oxygen (O) can gain two and nitrogen (N) can gain three electrons. The degrees of reduction used for the calculation and the respective molar masses of the metabolites are summarized in Table 8-3. The following equation (17) determines the recovery of electrons e_R in % via the ratio between produced products and consumed substrates [101]:

$$e_R = \frac{c_{e,PDO} + c_{e,BuOH} + c_{e,BuAc} + c_{e,EtOH} + c_{e,LaAc} + c_{e,AcAc} + c_{e,BDM} + c_{e,FoAc} + c_{e,H_2}}{\Delta c_{e,Gly} + \Delta c_{e,Glu}} \quad (17)$$

3 Materials and methods

3.1 Bacterial strains and templates for plasmid construction

Microorganisms and templates (plasmids and synthetic DNA) used in this work for plasmid construction, in-vivo methylation and expression of genes are listed in Table 3-1 and Table 3-2. The first two strains are *Escherichia coli* 10-beta that were used for the construction of plasmids. The needed plasmid components were amplified by PCR and fused together with the In-Fusion cloning protocol (Takara Bio). The resulting plasmids were transformed into *E. coli* 10-beta for plasmid propagation and transformants were selected which carry the plasmid with the right sequence without mutations or random insertions. This was done with verification of the constructed plasmids by Sanger sequencing and the plasmids were then transformed into *E. coli* 10-beta+pFnuDIIMKn in order to methylate the constructed plasmids in vivo.

Subsequently, the plasmids were introduced into *C. pasteurianum* R525. All *E. coli* and *C. pasteurianum* strains were stored at -80°C in ROTI®Store cryo vials or in 1.8 mL cryogenic vials, respectively (Carl Roth GmbH + Co. KG, Karlsruhe, Germany). The cryo-stocks for *E. coli* contained porous beads and cryo-stocks of *C. pasteurianum* contained grown cultures with 20% glycerol. Synthetic DNA was ordered from Thermo Fisher Scientific (Waltham, MA, USA) and these contained the CRISPR array with the respective spacer sequence. For the construction of the plasmids, primers from Integrated DNA Technologies (Coralville, IA, USA) were used to amplify target sequences and to determine the plasmid sequence by Sanger sequencing. They were stored at -20°C as stock solutions (100 µM) and as working solutions (10 µM).

3.2 Design and construction of plasmids

3.2.1 PCR, DpnI digestion and agarose-gel electrophoresis

Plasmids were designed by using the SnapGene software and they were made to be shuttle vectors in order to be able to be transformed into *E. coli* and *C. pasteurianum*. This was done by including a replication origin for gram-positive and for gram-negative bacteria. Different plasmid components were used e.g., promoters, terminators and single genes were considered for the vectors. Plasmid components were amplified by polymerase chain reaction (PCR) according to the Takara Bio protocol using CloneAmp HiFi PCR Premix (Takara Bio). A PCR reaction with a total volume of 20 µL was prepared as follows: 10 µL CloneAmp HiFi PCR Premix (1x), 1 µL of each

primer (10 µM), 0.5 µL of template and 7.5 µL milli-Q water. The template concentration was variable because extracted plasmids that were used as a template showed variable concentrations below 100 ng μL^{-1}. After preparation of the PCR mix, the PCR tubes were shortly centrifuged in a microcentrifuge (Biozym, Hessisch Oldendorf, Germany) and placed in a thermal cycler (MiniAmp™ Plus, Thermo Fisher Scientific).

Table 3-1: Microorganisms used in this work for plasmid construction, in-vivo methylation and gene expression. Abbreviations: *adh2*$^{-}$: *adh2* deleted; *dhaTC8*$^{+}$: replaced by *dhaTC8*; *bdhA2*$^{-}$: *bdhA2* deleted; *dhaD1_dhaK*$^{-}$: *dhaD1* and *dhaK* deleted; *GPD1_GPP2*$^{+}$: replaced by *GPD1* and *GPP2*; *bcd1*$^{-}$: *bcd1* deleted.

Strain	Abbreviation	Characteristics	Reference
E. coli			
10-beta		Dam+ methylation	New England Biolabs (Ipswich, MA, USA)
10-beta + pFnuDIIMKn		Dam+ and *CpaAI* methylation	[22] [20]
C. pasteurianum			
R525		Originates from *C. pasteurianum* DSM525, Improved transformation efficiency	[21]
C8		Efficient PDO production	[2, 16]
R525+pGG6	GG6	Overexpression of *GPD1, GPP2*	This study
R525+pGG8	GG8	Overexpression of *GPD1-GPP2*-fusion	This study
R525+pAR	AR-I	$adh2^{dhaTC8+}$	This study
R525+pDX	DX	Overexpression of *dhaTC8*	This study
R525+pDY	DY	Overexpression of *dhaTR*	This study
R525+pBC	BC-I	$bcd1^{-}$	This study
R525+pDR	DR-I	$dhaD1\_dhaK^{GPD1\_GPP2+}$	This study
R525+pAR+pBD	BD-II	$adh2^{dhaTC8+}$, $bdhA2^{-}$	
R525+pAR+pBD+pBC	BC-III	$adh2^{dhaTC8+}$, $bdhA2^{-}$, $bcd1^{-}$	This study
R525+pAR+pBD+pDR	DR-III	$adh2^{dhaTC8+}$, $bdhA2^{-}$, $dhaD1\_dhaK^{GPD1\_GPP2+}$	This study

Table 3-2: Plasmids and synthetic DNA used in this work. pIM13, pBP1, pCD6 and pCB102: gram-positive replicons; ColE1 and p15a: gram-negative replicons; *catP*, *ermB*, *tetA*, *aad9*: antibiotic resistance markers against chloramphenicol/thiamphenicol, erythromycin, tetracycline and spectinomycin, respectively.

DNA	Abbreviation	Characteristics	Reference
Plasmids			
pMTL85141		pIM13, *catP*, ColE1	[96]
pMTL82254		pBP1, *ermB*, ColE1	[96]
pMTL84422		pCD6, *tetA*, p15a	[96]
pMTL83353		pCB102, *aad9*, ColE1	[96]
pMTL-GCSY1		pIM13, *catP*, ColE1, glycine synthase from *Gottschalkia acidurici*	[22]
pMTL007-PC		pCB102, *catP*, pyruvate carboxylase from *C. pasteurianum*	[21]
pGG2		pIM13, *catP*, ColE1, *GPD1*, *GPP2*	This study
pGG4		pIM13, *catP*, ColE1, *GPD1-GPP2*-fusion	This study
pGG6		pCB102, *catP*, ColE1, *GPD1*, *GPP2*	
pGG8		pCB102, *catP*, ColE1, *GPD1-GPP2*-fusion	This study
permB		pIM13, *ermB*, ColE1	This study
p_adh2-rpl	pAR	pCB102, *catP*, ColE1, repair template for *adh2* replacement with *dhaTC8*	This study
p_bdhA2-del	pBD	pIM13, *ermB*, ColE1, repair template for *bdhA2* deletion	This study
p_bcd1-del	pBC	pCB102, *catP*, ColE, repair template for *bcd1* deletion	This study
p_dhaD1-rpl	pDR	pCB102, *catP*, ColE1 repair template for *dhaD1* and *dhaK* replacement with *GPD1* and *GPP2*	This study
p_dhaTC8-ovex	pDX	pCB102, *catP*, ColE1, *dhaTC8*	This study
p_dhaTR-ovex	pDY	pCB102, *catP*, ColE1, *dhaTR*	This study
Synthetic DNA			
Pthl_1200-9-9_gpd1		*GPD1*, promoter	Thermo Fisher Scientific (Waltham, MA, USA)
Pfdx_gpp2_fdx_term		*GPP2*, promoter and terminator	
adh2_spacer_array		CRISPR array for targeting *adh2*	
bdhA2_spacer_array		CRISPR array for targeting *bdhA2*	
bcd1_spacer_array		CRISPR array for targeting *bcd1*	
dhaD1_spacer_array		CRISPR array for targeting *dhaD1*	

One PCR cycle was performed for a total of 30 times and each cycle contained following steps: denaturation (98°C for 10 s), annealing (T_m - 5°C for 10 s) and Elongation (72°C for 30 s kb^{-1}). The annealing temperature depends on the primer melting temperature (T_m) of the used primers and elongation time was adjusted according to the length of the sequence to be amplified. Plasmid components that were amplified from templates extracted from *E. coli* 10-beta were digested with the restriction enzyme FastDigest DpnI (Thermo Fisher Scientific). This was done to remove remaining Dam-methylated templates that could result in false positive colonies later on. 2 µL of 10x FastDigest Green Buffer (stain for agarose-gel electrophoresis) (Thermo Fisher Scientific)and 2 µL of the FastDigest Enzyme (Thermo Fisher Scientific) were pipetted into the tubes after the PCR reaction and incubated for at least 30 min at 37°C (no shaking).

In agarose-gel electrophoresis, the agarose gel was prepared by mixing agarose and TAE buffer (40 mM Tris, 20 mM acetic acid, 1 mM EDTA) to a concentration of 1% (w/v) and heating it in a microwave for around 2 minutes until it was a clear solution without particles. This was poured into a gel mold in a gel caster to solidify for around 40 minutes. Afterwards, the gel was placed in a DNA electrophoresis cell (Bio-Rad Laboratories, Hercules, CA, USA) where it was covered with TAE Buffer. 6 µL of samples (with 10x FastDigest Green Buffer) and the Gene Ruler DNA Ladder Mix (SM0333, Thermo Fisher Scientific) were pipetted in the gel wells. The electrophoresis was run for 40 min at 120 V or 160 V for small or large electrophoresis cell, respectively, by using a PowerPac HC high current power supply (Bio-Rad Laboratories, Hercules, CA, USA). To examine the result of the electrophoresis, the gel was placed in a metal container and covered with a solution containing 6 µL of SYBR™ Gold Nucleic Acid Gel Stain (Thermo Fisher Scientific) and 6 mL of TAE Buffer.

This was incubated for 30 min in the dark by covering the container with a lid and subsequently transferred to an Invitrogen Safe Imager Blue Light Transilluminator (Thermo Fisher Scientific). The visible DNA fragments were assigned to a specific base pair length by comparing them with the Gene Ruler DNA Ladder Mix. After examination of the gel, the PCR products with the target DNA were cut out with a scalpel and placed in a 2 mL eppendorf tube. The DNA extraction protocol for agarose gels (Takara Bio) was used to extract the amplified products. All steps were followed through according to this protocol, except for the following changes: in step 4, the

centrifugation time was raised to 2 min. In step 5, after pre-warming the elution buffer to 70°C in a thermomixer, the NucleoSpin® Gel and PCR Clean-up Column was placed in a 1.5 mL eppendorf tube after the washing step and also incubated at 70°C for 1 min. After 1 min, 30 µL Elution Buffer was pipetted into the column and the column in the 1.5 mL eppendorf tube was kept at room temperature for 1 min before being centrifuged for another minute. In the end, the column was discarded and the eppendorf tube with the purified DNA was stored at -20°C.

3.2.2 In-Fusion cloning and Sanger sequencing

The In-Fusion cloning of the amplified plasmid components was carried out according to the In-Fusion Snap Assembly Multiple-Insert Cloning Protocol (Takara Bio) and the protocol states that a total DNA amount of 200 ng for vector and all inserts to be fused is optimal for a 10 µL In-Fusion cloning reaction. The mentioned vector corresponds to the largest fragment to be fused, consisting of replication of origin and resistance marker. Samples for In-Fusion cloning were prepared accordingly as shown in the Table 3-3 below and only 5 µL In-Fusion reactions were prepared to save resources and this volume is sufficient for subsequent transformation into *E. coli*. A molar ratio of 2:1 for each insert to the vector is recommended by the protocol and it can be calculated with the equation (18) given below:

$$Molar\ ratio\ = \frac{\frac{m_{insert}}{l_{insert}\ \cdot M_{DNA}}}{\frac{m_{vector}}{l_{vector}\ \cdot M_{DNA}}} \tag{18}$$

With m_{insert}: mass of the respective insert in ng, $l_{insert:}$ length of the respective insert in basepairs, m_{vector} mass of the respective vector in ng, $l_{vector:}$ length of the respective vector in basepairs. The required mass for inserts and vector was determined with the help of the In-Fusion molar ratio calculator provided by Takara Bio and by assuming an average molar mass of DNA M_{DNA}, the equation (18) can be simplified as shown below in equation (19):

$$Molar\ ratio\ = \frac{\frac{m_{insert}}{l_{insert}}}{\frac{m_{vector}}{l_{vector}}} \tag{19}$$

Table 3-3: Recipe for In-Fusion cloning samples.

Reagent	Volume [µL]	Volume variable	Molar ratio to vector
5x In-Fusion® Snap Assembly Master Mix	1	V_{master_mix}	/
Linearized vector	$\frac{m_{vector}}{c_{vector}}$	V_{vector}	1
Purified inserts	$\frac{m_{insert}}{c_{insert}}$	$V_{inserts}$	2
Milli-Q water	$V_{total} - (V_{vector} + V_{inserts} + V_{master\_mix})$	$V_{Milli-Q}$	/
Total volume	5 µL	V_{total}	/

Samples were sequenced at Microsynth Seqlab GmbH (Göttingen, Germany) and the service for multiple sequencing reactions from one single tube was used. For each plasmid to be sequenced, a total volume of 30 µL was transferred to a 1.5 mL screw cap tube as a minimum sample volume of 12 µL is needed and 3 µL are consumed for each of up to six additional sequencing reactions. The highly automated sequencing process requires the use of 1.5 mL tubes and screw cap tubes were used because these are the most robust and no accidental lid opening can occur during the transport of samples to the sequencing facility. The Sanger Sequencing Service was used by assigning Economy Run Prepaid labels to each sample to be sequenced and sequencing orders were placed on the Microsynth Seqlab website. The opportunity was given to use sequencing primers with a working concentration of 10 µM that were prepared and send to the sequencing facility for storage and reuse for up to 4 months. The sequencing facility achieves the optimal primer concentration of 5 µM by mixing 3 µL sample with 3 µL primers for the sequencing reaction and the sequencing results were evaluated using the SnapGene Software. The "PRIO" service (Deutsche Post DHL Group, Bonn, Germany) was used to get samples shipped to the sequencing company until the next day. This was essential to quickly continue the work steps as sequencing results could be analyzed after one day.

3.2.3 Plasmid DNA purification

In order to verify the correct assembly with Sanger Sequencing, the constructed plasmids were isolated from *E. coli* 10-beta and *E. coli* 10-beta+pFnuDIIMKn using the plasmid DNA purification

protocol NucleoSpin® Plasmid (miniprep) for low copy plasmids (Macherey Nagel). The protocol was followed except for the DNA elution step where the column with the 1.5 mL eppendorf tube was incubated at 70°C for 1 min to evaporate the remaining washing solution. Afterwards 50 µL elution buffer (AE buffer or Milli-Q water), which was preheated to 70°C, was added on the column and incubated at room temperature for 1 min before being centrifuged for 1 min at 11,000 rpm. A high plasmid amount of up to 5 µg is needed for the transformation of *C. pasteurianum* R525 and for this the plasmid purification protocol NucleoBond® Xtra Midi (midiprep) was applied (Macherey Nagel). The protocol was followed for low copy plasmids from step 1 to 7 and then continued with the high copy protocol from step 7 to 15 but some adjustments were made.

For each plasmid, 5 mL of SOC medium with the appropriate antibiotics was inoculated with the cryo-stock containing the *E. coli* 10-beta+pFnuDIIMKn strain carrying the plasmid to purify. This culture was grown for 16 h at 37°C in a 50 mL centrifuge tube at 200 rpm. Then it was used as inoculum for 800 mL of SOC medium with the same antibiotic concentrations. The 800 mL medium was distributed equally to two 2 L shaking flasks and placed at 37°C and 200 rpm for 16 h. The cells were cooled on ice for 30 minutes and harvested by centrifugation at 5000 rpm for 20 min at 4°C. To remove the precipitate in step 8 (clarification and loading), centrifugation at 5000 rpm for 15 min at 4°C was performed before the column was loaded. The eluate in step 12 was transferred back to the column and eluted again and after precipitation, the 50 mL centrifuge tubes containing the solution was centrifuged at 8500 rpm for 60 min at 4°C. The precipitated pellet was transferred to a fresh 1.5 mL eppendorf tube and centrifuged at 13000 rpm for 30 min at 4°C after adding 70% ethanol. When the supernatant was discarded, the pellet was dried at 55°C for 30 min and reconstituted in 100 µL of elution buffer (ELU buffer from miniprep) by shaking for up to 60 min.

C. pasteurianum is a gram-positive bacterium and therefore a pretreatment step to remove the cell wall with lysozyme (≥45 000 FIP U mg^{-1}) (Carl Roth GmbH + Co. KG, Karlsruhe, Germany) was carried out before the plasmid isolation protocols, which were only intended for the use with the gram-negative *E. coli*. The pretreatment step was followed according to the supplementary NucleoSpin® Plasmid protocol for the purification of plasmid DNA from Agrobacterium tumefaciens (Macherey-Nagel).

3.3 Transformations and mutagenesis

3.3.1 Cultivation of *E. coli* 10-beta and heat-shock transformation

Super Optimal broth with Catabolite repression (SOC) medium was used for the cultivation of *E. coli* 10-beta and also as recovery medium after chemical transformation and the cultures were grown aerobically at 37°C and 200 rpm in a benchtop orbital shaker (Thermo Fisher Scientific Waltham, MA, USA). The medium was prepared by supplementing 26.64 g L^{-1} SOB medium which was bought readily mixed (20 g L^{-1} Tryptone, 5 g L^{-1} Yeast extract, 0.96 g L^{-1} $MgCl_2$, 0.5 g L^{-1} NaCl, 0.186 g L^{-1} KCl) with 20 mM glucose. 15 g L^{-1} of agar agar (Carl Roth GmbH + Co. KG, Karlsruhe, Germany) was supplemented to the SOC medium when agar plates were prepared and the plates were placed in the incubator at 37°C after plating transformed cells. Chemically competent *E. coli* 10-beta cells transformed with constructed plasmids were selected with chloramphenicol (34 µg ml^{-1} for agar plates, 25 µg ml^{-1} for liquid medium). Chemically competent *E. coli* 10-beta+pFnuDIIMKn additionally harbored an antibiotic resistance to kanamycin (50 µg ml^{-1} for agar plates, 35 µg ml^{-1} for liquid medium) from the methylation plasmid. Antibiotic concentrations of 30 µg mL^{-1} tetracycline (Tc30), 250 µg mL^{-1} spectinomycin (Sp250) and 300 µg mL^{-1} erythromycin (Em300) were used for additional antibiotic markers. All prepared media were homogenously mixed, autoclaved and glucose and antibiotics were added afterwards. After autoclaving, the bottles with SOB medium and agar were heated to 60°C in a shaking water bath (Julabo GmbH, Seelbach, Germany) for the preparation of agar plates. This was followed by heating in the microwave to dissolve the agar and before adding glucose and antibiotics, the bottles were cooled to 60°C again. Subsequently, the final mixture was poured into labelled, sterilized petri dishes and stored at 4°C.

Chemically competent *E. coli* 10-beta cells were prepared via chemical treatment with calcium chloride ($CaCl_2$) and stored at -80°C. For the preparation, a pre-culture was made by pouring 5 mL of SOC-Medium in a 50 mL centrifuge tube and inoculation from a cryo-stock. During this procedure, the cryo-stock was kept cold at all times and the culture was incubated at 37°C for 16 h. Afterwards, 100 mL of SOC-Medium in a shaking flask was inoculated with 1 mL of the pre-culture. This was incubated for 1-4 h until an OD_{600} of 0.5 was reached. To harvest the cells, the broth was equally divided into two 50 mL centrifuge tubes and cooled for 15 min on ice before being centrifuged at 5,000 rpm and 4°C for 10 min. Subsequently, the supernatant was discarded

and both pellets resuspended in 15 mL of 0.1 M $CaCl_2$ each. This suspension was placed on ice for 30 min and then centrifuged at 5,000 rpm and 4°C for 10 min.

Again, the supernatant was discarded and the pellets were resuspended in 2 mL of 0.1 M $CaCl_2$ + 15 % w/v glycerol each. This suspension was distributed into sterile 2 mL eppendorf tubes (100 µL each) and stored at -80°C. A sterile environment was always assured by working under the clean bench. With this method, chemically competent *E. coli* 10-beta cells and *E. coli* 10-beta cells containing the pFnuDIIMKn plasmid were generated. To transform *E. coli* 10-beta with the constructed plasmids, 100 µL of the prepared competent cells were thawed and subsequently 1 µL of plasmid-solution was added (5 µL for In-Fusion mixtures). This mixture was then incubated on ice for 30 min and for the introduction of DNA into the organism, the suspension was heat shocked by incubating it at 42°C for 35 s followed by 5 min on ice. Before shaking of the eppendorf tube for 1 h at 37°C, 700 µL of pre-warmed (37°C) SOC medium was added. 100 µL of the suspension could then be spread on an agar plate. The rest was concentrated by centrifugation for 1 min at 11,000 rpm and spread on a second agar plate for incubation at 37°C.

3.3.2 Cultivation of *C. pasteurianum* R525 and electrotransformation

2x YTG medium was used for the anaerobic cultivation of *C. pasteurianum* R525 and it contains 31 g L^{-1} 2xYT medium, 5 g L^{-1} glucose, 200 µL L^{-1} of 0.01% (w w^{-1}) resazurin and 0.5 g L^{-1} Cystein*HCL*H_2O. The readily mixed 2xYT medium contains 16 g L^{-1} Tryptone, 10 g L^{-1} Yeast extract, 5 g L NaCl. 15 g L^{-1} agar was supplemented when agar plates were used for the selection of transformants. The cells were incubated at 35°C in serum bottles with 50 mL or 100 mL liquid medium. The pH was adjusted to 6.5 and 7 µg ml^{-1} thiamphenicol or 300 µg mL^{-1} erythromycin was added for selection if needed. The liquid medium was prepared by heating up to 90°C in a 2 L bioreactor (Bioengineering AG, Wald, Switzerland) while sparging with nitrogen and after keeping the temperature for 20 min, the Cystein*HCL*H_2O was added. When the liquid cooled down, it was filled into serum bottles which were sparged with nitrogen for 1 min and then the bottles were sealed and autoclaved. Used antibiotic concentrations for the cultivation of *E. coli* and *C. pasteurianum* are summarized in Table 3-4, exemplary for the three mutants AR-I, BD-II and BC-III of this work (chapter 4 and 5).

Table 3-4: Applied antibiotic concentrations for cultivation of *E. coli* and *C. pasteurianum*. Higher antibiotic concentrations on agar plates are necessary for efficient selection of mutants. After verification of the mutants, inoculations into medium with lower antibiotic concentrations support fast growth. The exception is erythromycin with the same concentration for liquid and agar medium. The mentioned numbers after the abbreviations for the antibiotics are the respective concentrations in µg mL^{-1}. Cm: Chloramphenicol, Tm: thiamphenicol, Kn: kanamycin, Em: erythromycin, pFnuDIIMKn: methylation plasmid.

Medium type	Strain	AR-I	BD-II	BC-III
Liquid medium	*E. coli* 10-beta	Cm25	Tc30	Cm25
	E. coli 10-beta + pFnuDIIMKn	Cm25 Kn35	Tc30 Kn35	Cm25 Kn35
	C. pasteurianum	Tm7	Em300	Tm7
Agar medium	*E. coli* 10-beta	Cm34	Tc50	Cm34
	E. coli 10-beta + pFnuDMIIKn	Cm34 Kn50	Tc50 Kn50	Cm34 Kn50
	C. pasteurianum	Tm10	Em300	Tm10

The adapted transformation protocol [93] for *C. pasteurianum* took place over three days. First, a cryo-stock of *C. pasteurianum* was inoculated into a 50 mL 2xYTG serum bottle and incubated at 35°C (pre-culture). After approximately 15 h, a new 100 mL 2xYTG serum bottle (pre-warmed to 35°C) was inoculated with 5 mL of the pre-culture and also incubated at 35°C for about 3 hours until an OD_{600} of 0.4 was reached. Subsequently, 20 mL of 2 M sucrose and 6.6 mL of 18.78 % glycine were added and the culture incubated at 35°C for another 4 h until an OD_{600} of 0.6 was reached before placing the bottles on ice for 30 min and transferring the ice box into an anaerobic chamber (Coy Laboratory Products Inc., Grass Lake, MI, USA). The anaerobic chamber was filled with 5% hydrogen and 95% (v/v) N_2 and excess moisture was removed by a renkforce dehumidifier (Conrad Electronic, Hirschau, Germany). Two 50 mL centrifuge tubes for each serum bottle were also placed on ice. Afterwards, 30 mL of broth was transferred into each tube before centrifuging the tubes at 4°C and 5,000 rpm for 10 min. The supernatant was discarded and 10 mL of precooled SMP buffer was added.

The centrifuge tubes were then carefully vortexed until the suspension was homogenous. This suspension was collected in one of the two centrifuge tubes so that there was about 20 mL of suspension in it. This centrifuge tube was then centrifuged at 4°C and 5,000 rpm for 10 min. Again, the supernatant was discarded and 3.6 mL of precooled SMP buffer added. After careful vortexing, 600 µL of the suspension was transferred to each electroporation cuvette. Electroporation cuvettes (0.4 cm) were prepared by placing them on ice and adding plasmid DNA (≥ 5 µg, up to 100 µg, but max. 50 µL) and 30 µL of 99.99 % ethanol. After the suspension was added to the electroporation cuvettes (Bio-Rad Laboratories, Hercules, CA, USA), they were incubated for 10 min on ice. Subsequently to wiping them dry and flicking them, the cuvettes were placed in the shockpod of an Xcell electroporation system (Bio-Rad Laboratories, Hercules, CA, USA).

While holding a pipette with 1 mL of recovery medium, which was prepared beforehand by adding 10 mL 2xYTG medium with 0.2 M sucrose to 30 mL centrifuge tubes and incubating them until needed at 35°C, an exponential pulse (1.8 kV, 25 µF, ∞ Ω) was delivered. Immediately after the pulse, the cuvettes were flushed with the recovery medium. The whole content of the cuvette was then transferred to the recovery medium tubes and incubated at 35°C for 16 h. Afterwards, 1 mL of each recovery medium was centrifuged for 1 min in a microcentrifuge (Biozym, Hessisch Oldendorf, Germany) and then spread separately on agar plates with 2xYTG medium and 10 µg mL^{-1} of thiamphenicol or 300 µg mL^{-1} erythromycin. Those were incubated at 35°C for up to seven days until colonies appeared. Colonies of the agar plates were picked, inoculated in 20 mL 2x YTG medium and incubated at 35°C for 16 h. Subsequently, the broth was mixed with 10 ml of 50 % w/v glycerol, aliquoted into cryo-tubes and stored at -80°C. The Figure 3-1 shows all necessary steps for the construction of genome editing plasmids and introduction into *C. pasteurianum* R525.

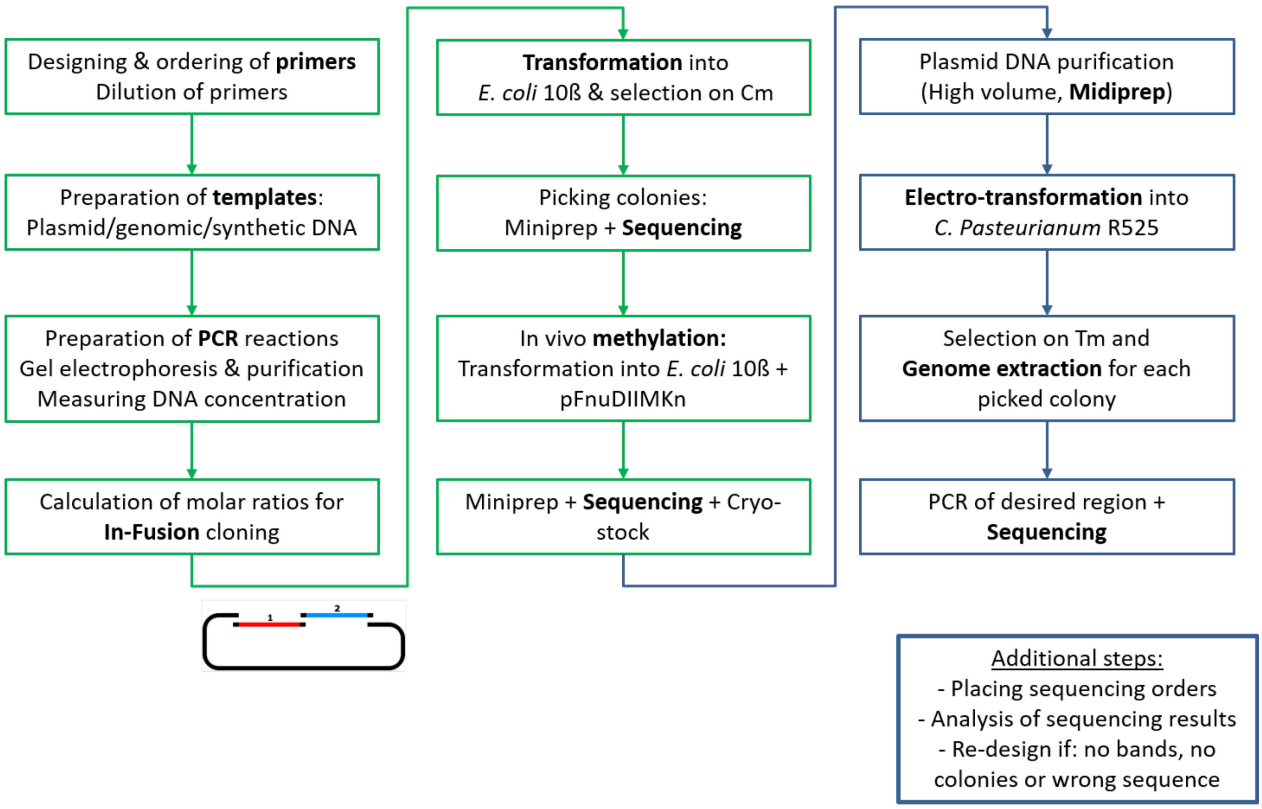

Figure 3-1: Steps for the construction of genome editing plasmids. The boxes with green borders represent the steps for plasmid construction and methylation in *E. coli* 10-beta. The boxes with blue borders represent the steps for the introduction of the plasmid into *C. pasteurianum* R525 and the steps for mutant verification.

3.3.3 EMS-induced random mutagenesis

For random mutagenesis with the mutagen ethyl methanesulfonate (EMS), a cryo-stock of *C. pasteurianum* C8 was inoculated into 50 mL 2xYTG medium and incubated anaerobically at 35°C for 16 h. The grown culture was re-inoculated into fresh 100 mL 2xYTG medium and incubated at 35°C for 8 h to reach exponential growth phase. Subsequently, the culture was exposed to 0.5 or 1% (v/v) EMS for up to 15 min with the goal of selection of a transformable mutant. Higher EMS concentrations were not tried because Lakhssassi et al. (2020) [58] found that EMS concentrations above 140 mM or 1.4% (w/v) are lethal for the treated *C. carboxidivorans* P7 strain in that study. After the exposure to EMS, the mutagenized cells were diluted 1:100 by transferring into fresh 100 mL 2xYTG medium to quench the effects of the mutagen. After incubation at 35°C for 16 h, the culture was used to prepare competent cells for electrotransformation with plasmid

pMTL85141. Solutions containing EMS were inactivated by mixing them with equal volume of inactivating solution which contained 0.1M NaOH and 20% (w/v) $Na_2S_2O_3$ [102].

3.4 Fermentation

3.4.1 Cultivation of *C. pasteurianum* in 1 L DASGIP bioreactor system

After successful isolation of a mutant, pre-cultures were prepared for the inoculation of 1 L media in a DASGIP bioreactor system. The first pre-culture was 2x YTG medium and it was inoculated with 1.8 mL of cryo-stock from the strain to be cultivated. This was then grown at 35°C for 16 h before inoculating 5 mL of it in 100 mL of modified synthetic (MS) medium (40 g L^{-1} glycerol for pre-culture and 80 g L^{-1} for bioreactor medium, 3 g L^{-1} $(NH_4)_2SO_4$, 0.75 g L^{-1} KCL, 2.45 g L^{-1} $NaH_2PO_4*H_2O$, 4.58 g L^{-1} Na_2HPO_4, 0.28 g L^{-1} Na_2SO_4, 0.42 g L^{-1} $C_6H_8O_7*H_2O$, 0.26 g L^{-1}, 0.009 g L^{-1} $CaCl_2*2H_2O$, 1 g L^{-1} Yeast Extract, 2 g L^{-1} $CaCO_3$, 0.2 g L^{-1} resazurin, 2 mL trace element solution [103]) which was then incubated for at least 16 h. The trace element solution contained 70 mg L^{-1} $ZnCl_2$, 100 mg L^{-1} $MnCl_2*4H_2O$, 60 mg L^{-1} H_3BO_3, 200 mg L^{-1} $CoCl_2 * 6H_2O$, 20 mg L^{-1} $CuCl_2*2H_2O$, 20 mg L^{-1} $NiCl_2*6H_2O$, 40 mg L^{-1} $NaMoO_4*2H_2O$ and 1 mL 25% HCl. 10 mg L^{-1} $FeSO_4*7H_2O$ was added to the second pre-culture and 7 µg ml^{-1} of thiamphenicol or 300 µg mL^{-1} erythromycin was added to pre-cultures and fermentation medium of mutant strains.

The bioreactors had a stirrer, a condenser, a gas inlet and probes to measure pH and temperature. Additionally, there was an outlet for sample taking. The bioreactors were placed in a DASGIP Bioblock, which regulated the temperature within the bioreactors. The control system is called DASGIP Parallel Bioreactor System (Eppendorf, Hamburg, Germany) and it documented the measured pH and temperature and controlled also the gas and base inlet (for 5 M KOH), the latter based on the pH measurement. Before inoculation, the pH probes undergo a two-point calibration, using pH values of 7 and 4. After this, the medium was filled into the bioreactor and the probes were screwed in tightly and everything was autoclaved for 20 min at 121°C. Next, the bioreactor was placed in the DASGIP Bioblock and the stirrer and nitrogen gassing were set to 400 rpm and 6 sL h^{-1} and the bioreactor was heated to 35°C. The pH was altered by adding 5% HCl until it reached the desired pH. In case of $FeSO_4 * 7H_2O$ addition (100 mg L^{-1}) for iron excess conditions, it was introduced into the bioreactor shortly before inoculation and the appropriate antibiotic was also added for fermentation with isolated mutants. After 8 h of gassing with nitrogen, the bioreactor

was inoculated with 50 mL of the second pre-culture and the gassing stopped. During cultivation, antifoam was added manually to the bioreactors as soon as a layer of foam covered the surface of the medium.

3.4.2 Sampling and measurement

Samples were taken regularly throughout the cultivations. The first sample was taken directly after inoculation with the second pre-culture. To examine the samples from the experiments carried out, the optical density of the cell suspension was determined by photometric turbidity measurement using a UV/Vis spectrophotometer (VWR, Radnor, PA, USA) at 600 nm. Anaerobic cultivations were diluted at least with a factor of 1:4 with 0.1% HCL to remove the undissolved calcium carbonate in the sample. The rest of the sample was centrifuged for 4 min at 13,000 rpm in a small benchtop centrifuge (Thermo Fisher Scientific, Waltham, MA, USA) and the supernatant was sterile filtered using a filter with a pore size of 0.22 µm (Carl Roth GmbH + Co. KG, Karlsruhe, Germany) as preparation for high performance liquid chromatography (HPLC) measurement. All samples were diluted in a ratio of 1:2 and the samples were stored at -20°C prior to HPLC measurement. The concentrations of glucose, glycerol, ethanol, butanol, PDO, lactate, formate, acetate and butyrate were determined using HPLC (UV and RI detector) [1]. The mobile phase was a 0.1% trifluoroacetic acid (TFA) solution, a flow rate of 0.6 mL min^{-1} was set and the temperature of the column was 60°C.

Certain samples from glucose fermentations were analyzed with gas chromatography coupled with mass spectrometry (GC-MS) by Zentrallabor Chemische Analytik (TUHH). The measurement was carried out with a 7890B GC System with a 5977A mass selective detector (MSD) (Agilent Technologies, Santa Clara, CA, USA), an Agilent HP5ms capillary column (30 m*0.25 mm*0.25 µm) and helium as carrier gas. A programmed temperature vaporizing (PTV) injector (70°C for 0.1 min, increase by 12°C/s to 270°C and 270°C for 1 min) was applied. The temperature of the oven program was set to 100°C for 2 min, increase by 10°C/min to 270°C and 270°C for 7 min. The amount of energy on the ionizing electrons (electron energy) was set to 70 eV and quantification of analytes was conducted using selected ion monitoring (SIM) acquisition mode. 50 µL of sample or calibration standard was derivatized with 100 µL acetonitrile and 50 µL of 1 M phenylboronic acid (PBA) dissolved in 2,2-dimethoxypropane (DMP).

3.5 Construction of plasmids for gene overexpression

3.5.1 Overexpression of *GPD1* and *GPP2*

Plasmid components were amplified by PCR and primer sequences can be found in the appendix in Table 8-1. For overexpression of *GPD1* and *GPP2*, a total of 3 different plasmids were designed to be transformed into *C. pasteurianum* R525 and the plasmid components are summarized in Table 3-5. The Plasmids pGG2 and pGG4 contain a chloramphenicol resistance marker, surrounded by an origin of replication for gram-positive (*C. pasteurianum*) and gram-negative (*E. coli*) microorganisms (Figure 3-2). Right after the gram-negative origin of replication comes the first promoter Csp-fdx [104] (for pGG2), followed by the gene *GPD1*. Next comes the second promoter Csp-fdx, the gene *GPP2* and a Cpa fdx terminator from pMTL85141 [96]. The plasmid pGG4 and pGG8 contain *GPD1* and *GPP2* not as single genes but they are connected by a linker [65], so that both genes become a fusion protein.

Table 3-5: Components of plasmids for the expression of *GPD1* and *GPP2*.

Plasmid	Promoter	Terminator	Genes	Gram+ replicon
pGG2	Csp-fdx (pMTL007C-E2), Csp-fdx (pMTL-85141)	Csp-fdx (pMTL007C-E2)	*GPD1*, *GPP2*	pIM13 (pMTL-85141)
pGG4	Csp-fdx (pMTL007C-E2)	Csp-fdx (pMTL007C-E2)	*GPD1-GPP2*-fusion	
pGG6	Csp-fdx (pMTL007C-E2), Csp-fdx (pMTL-85141)	Csp-fdx (pMTL007C-E2)	*GPD1*, *GPP2*	pCB102 (pMTL007C-E2)
pGG8	Csp-fdx (pMTL007C-E2)	Csp-fdx (pMTL007C-E2)	*GPD1-GPP2*-fusion	

The plasmids pGG6 and pGG8 are constructed in the same way with the only difference that the origin of replication pIM13 from the plasmid pMTL85141 for gram-positive organisms was replaced by pCB102 from the plasmid pMTL007-PC. The plasmid pGG8 originates from pGG2 which was constructed by fusing the backbone for pGG2 (P013, P014, pMTL-GCSY1) with the genes *GPD1* (P004, P015, "phtl_1200-9-9_gpd1" synthetic DNA) and *GPP2* (P005, P016, "pfdx_gpp2_fdx_term" synthetic DNA). The plasmid pGG2 was linearized (P017, P018, pGG2) with primers that were designed to fuse the genes *GPD1* and *GPP2* with the help of a linker from Meynial et al. (2007)[65] in between to create the plasmid pGG4. To form pGG8, the gram-positive

replicon pCB102 of pGG8 (P022, P023, pMTL007-PC) was fused with the backbone and the *GPD1-GPP2* fusion gene (P021, P025, pGG4).

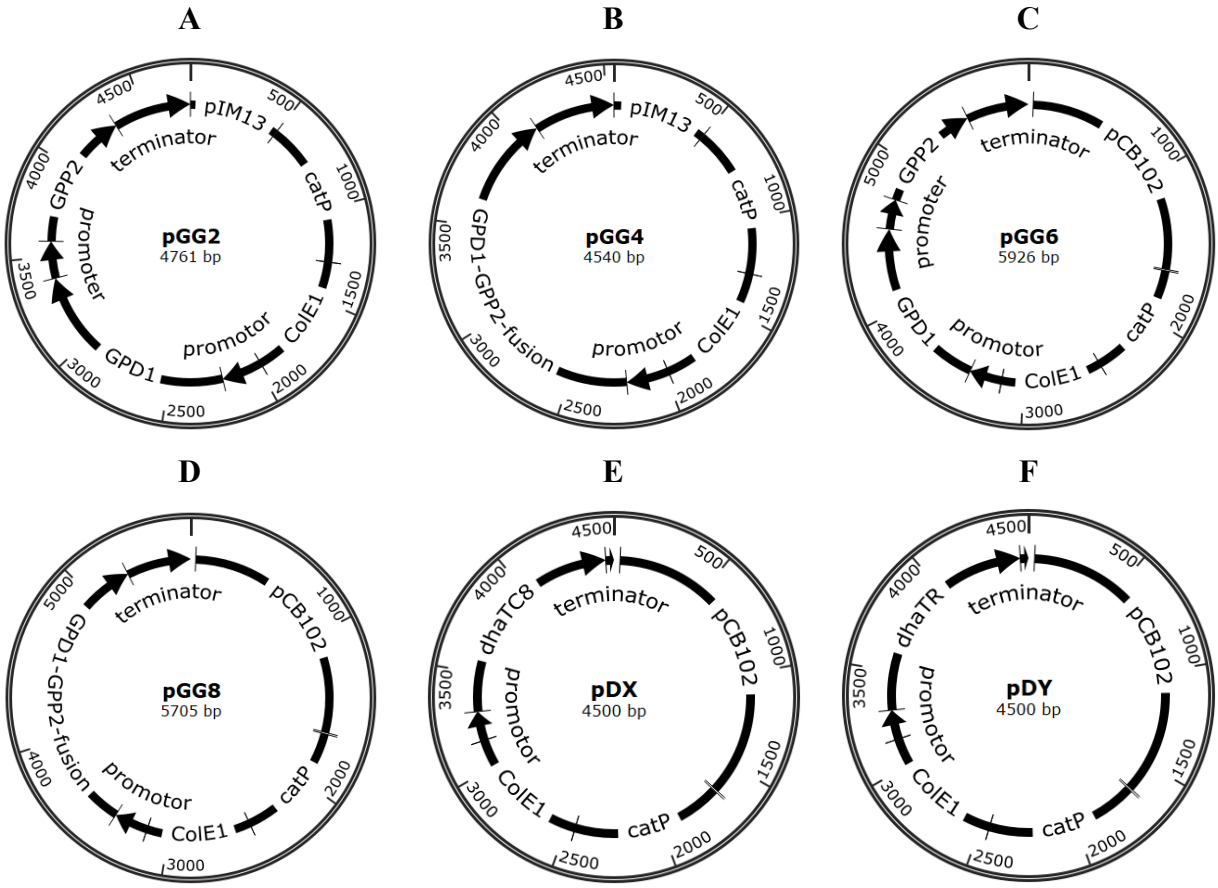

Figure 3-2: Plasmids pGG2, pGG4, pGG6, pGG8, pDX and pDY. A, C: plasmid pGG2 and pGG6 for the overexpression of *GPD1* and *GPP2*, **B, D**: plasmid pGG4 and pGG8 for the overexpression of *GPD1-GPP2*-fusion, **E:** plasmid pDX for the overexpression of *dhaTC8*, **F**: plasmid pDY for the overexpression of *dhaTR*. *GPD1* = glycerol-3-phosphate dehydrogenase, *GPP2*: glycerol-3-phosphate phosphatase, pCB102: gram-positive origin of replication for *C. pasteurianum*, pIM13: gram-positive origin of replication for *C. pasteurianum*, ColE1: gram-negative origin of replication for *E. coli*, *catP*: antibiotic resistance marker for chloramphenicol in *E. coli* and for thiamphenicol in *C. pasteurianum*.

3.5.2 Overexpression of *dhaTR* and *dhaTC8*

In order to find out if the PDO dehydrogenase *dhaTC8* is responsible for higher PDO production in *C. pasteurianum* C8, overexpression of that gene in *C. pasteurianum* R525 was carried out. For this purpose, a plasmid which was named pDX was constructed for the expression of *dhaTC8*

(Figure 3-2). The backbone for plasmid pDX (consisting of pCB102, *catP* and ColE1) was amplified with primers P256 and P257 from plasmid pGG8. The *dhaTC8* gene was amplified with P204 and P205 from a PCR product containing the *dhaTC8* gene from the genome of *C. pasteurianum* C8. For comparison, control fermentations are carried out with the wildtype *C. pasteurianum* R525 but another control was additionally necessary. For this purpose, another plasmid named pDY (Figure 3-2) was constructed for the overexpression of the *dhaTR* gene which is present on the genome of *C. pasteurianum* R525 already. The construction of this plasmids was similar to the construction of pDX. The backbone for the plasmid pDY (consisting of pCB102, *catP* and ColE1) was amplified with primers P256 and P257 from the plasmid pGG8. The *dhaTR* gene was amplified with P303 and P304 from the genome of *C. pasteurianum* R525. Sanger sequencing and colony-PCR was performed with the primers P054 and P037 for both plasmids.

3.6 Construction of genome editing plasmids

3.6.1 Testing and combining antibiotic markers (*tetA*, *ermB*, *aad9*)

In Heap et al. (2009) [96], a total of 28 plasmid components are distributed on several plasmids and they can be combined freely with the use of the restriction enzymes SbfI, AscI, FseI and PmeI as shown in Figure 3-3 for the plasmid pMTL85141. Each plasmid component is flanked with two of these restriction sites and in order to correctly design the plasmids of this work, this was taken into account. Instead of restriction enzymes, specifically designed primers were used for In-Fusion reactions to construct the plasmids and the plasmid components were fused so that they only carried the full restriction site at the 5’ end. The restriction site on the 3’ end was not included because the next plasmid component would already carry that restriction site at the beginning. If *catP* were to be fused into another plasmid, it would contain the restriction site FseI at the 5’ beginning, but not PmeI at the 3’ end. The resistance marker *ermB* was extracted from the plasmid pMTL82254, *aad9* for resistance against spectinomycin from pMTL83353, *tetA* from pTML84422 and KnR from the methylation plasmid pFnuDIIMKn. Different antibiotic markers from the pMTL80000 plasmid series from Heap et al. (2009) [96] (Table 3-2) were fused into shuttle plasmids so that they can be tested for their function in *C. pasteurianum* R525 (Figure 3-3).

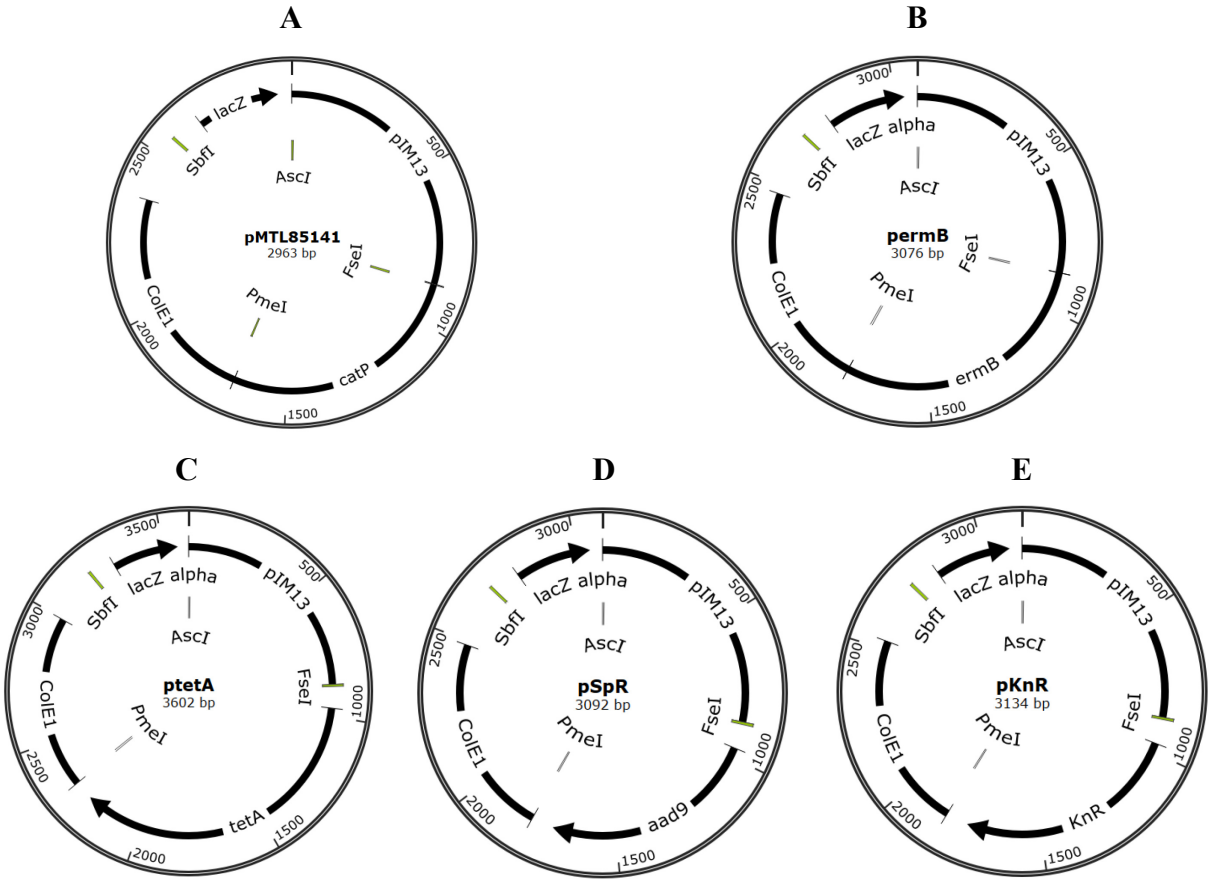

Figure 3-3: Plasmids pMTL85141, permB, ptetA, pSpR and pKnR. The restriction sites SbfI, AscI, PmeI and FSeI according to the modular plasmid series from Heap et al. (2009) [96] are shown on each plasmid. **A**: plasmid pMTL85141 of the pMTL80000 plasmid series [96], **B**: plasmids permB with the *ermB* marker. **C**: plasmid ptetA (3602 bp), **D**: plasmid pSpR (3092 bp), **E**: plasmid pKnR (3134 bp) with the resistance markers against tetracycline, spectinomycin and kanamycin, respectively.

The first antibiotic marker to be tested was *ermB* for resistance against erythromycin and the backbone of the plasmid permB (gram-positive replicon pIM13, ColE1) was amplified with P160 and P161 from the plasmid pMTL85141, while the *ermB* marker was amplified with P162 and P163 from the plasmid pMTL82254 (Table 3-2). The primers were designed so that the full region including the *ermB* gene on the pMTL82254 plasmid was amplified between the restriction sites FseI and PmeI. For the following plasmids, not the full region was amplified but only the gene of the antibiotic marker itself and fused into the plasmid pMTL85141. The backbone of the next plasmid ptetA was amplified P231 and P232 from the plasmid pMTL85141 and the *tetA* gene for resistance against tetracycline was amplified with P233 and P234 from the plasmid pMTL84422

(Table 3-2). The backbone of the plasmid pSpR was amplified P301 and P302 from the plasmid pMTL85141 and the *aad9* gene for resistance against spectinomycin was amplified with P299 and P300 from the plasmid pMTL83353 (Table 3-2). The backbone of the last plasmid pKnR was amplified P293 and P294 from the plasmid pMTL85141 and the KnR gene for resistance against kanamycin was amplified with P291 and P292 from the plasmid pFnuDIIMKn (Table 3-2).

3.6.2 Deletion of *adh2*, *bdhA2* and *bcd1*

The construction of genome editing plasmids of this work are described in the following and respective plasmid components are fused in at least two fusion steps because In-Fusion cloning (Takara Bio) becomes less efficient with increasing number of plasmid components. The mutant BC-III carries three genome modifications which were introduced by the plasmids pAR, pBD and pBC and plasmid constructions are described in detail below. Primer pairs and templates which were used for PCR amplification of plasmid components are mentioned in brackets with the format "(primer 1, primer 2, template)" and primer sequences can be found in Table 8-1. The first genome modification in the mutant BC-III replaces the *adh2* butanol dehydrogenase gene (CLPA_c33950, 1167 bp) with the PDO dehydrogenase gene (*dhaTC8*, 1158 bp) found in *C. pasteurianum* C8. The plasmid for this modification with a total length of 7470 bp was called p-adh2-rpl (pAR) and a two-step fusion process is necessary due to the large number of components on this plasmid. The backbone (P49, P223, pDR) of the first fusion plasmid for pAR (pAR-FI) was fused with part of the *bdhA2* gene (P171, P224, genomic DNA of R525 [28]) and with the respective CRISPR array (P202, P247, adh2_spacer_array). Part of the *bdhA2* gene was included so that the genome editing plasmid pAR can be targeted by the next plasmid pBD (s. below). The whole gene *bdhA2* was not included on plasmid pAR to keep this fragment as short as possible while still containing the necessary spacer sequence (chapter 2.2.3) that is targeted by the next plasmid pBD. The CRISPR array was synthetically generated (Thermo Fisher Scientific, Waltham, MA, USA) with a 36 bp spacer sequence (Figure 3-4A) for targeting the *adh2* gene. In this work, two different spacer sequences were tested for each genome editing plasmid and the spacer sequences are summarized in Table 8-2.

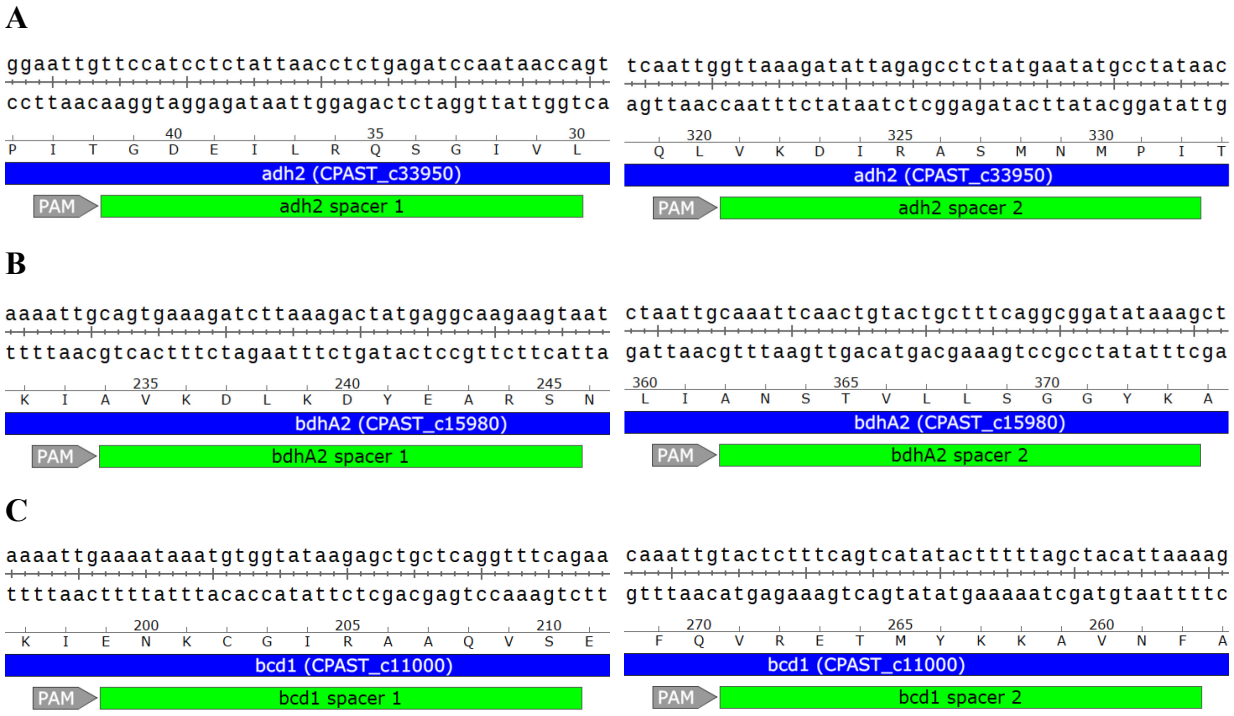

Figure 3-4: Selected spacers for deletion genes *adh2*, *bdhA2* and *bcd1*. A: spacer sequences on butanol dehydrogenase gene *adh2*, **B**: spacer sequences on butanol dehydrogenase gene *bdhA2*, **C**: spacer sequences on butyryl-CoA dehydrogenase *bcd1* gene. The PAM sequence 5'-AATTG-3' and the sequence of the 36 bp long spacer 1 on the left and spacer 2 on the right are shown on the genome of *C. pasteurianum* DSM525.

The backbone (P002, P248, pDR) for the second fusion plasmid (pAR-FII) was fused with homologous region H1 (P220, P250, genomic DNA of R525), H2 (P208, P221, genomic DNA of R525) and the *dhaTC8* gene (P204, P205, C8 genome [16]). H1 and H2 are regions, upstream and downstream of the *adh2* butanol dehydrogenase gene to be replaced. A segment from each of the first (P209, P171, pAR-FI) and second (P208, P252, pAR-FII) fusion plasmids were combined to form the final plasmid pAR. Sanger sequencing was performed with primers P037, P054, P084, P0218 and P245 for the plasmid pAR. Colony-PCR was performed with P054 and P037 to verify the presence of the correct plasmid. When the plasmid for the deletion of the gene *adh2* was introduced into the cells and genome editing works successfully, the PCR product around the *adh2* gene should have a similar length as in the wildtype genome. It is important that PCR primers for verification are designed that are not on the H1 or H2 region because these are also present on the constructed plasmids (Figure 3-5). The plasmid pAR is shown in Figure 3-6 with all plasmid components.

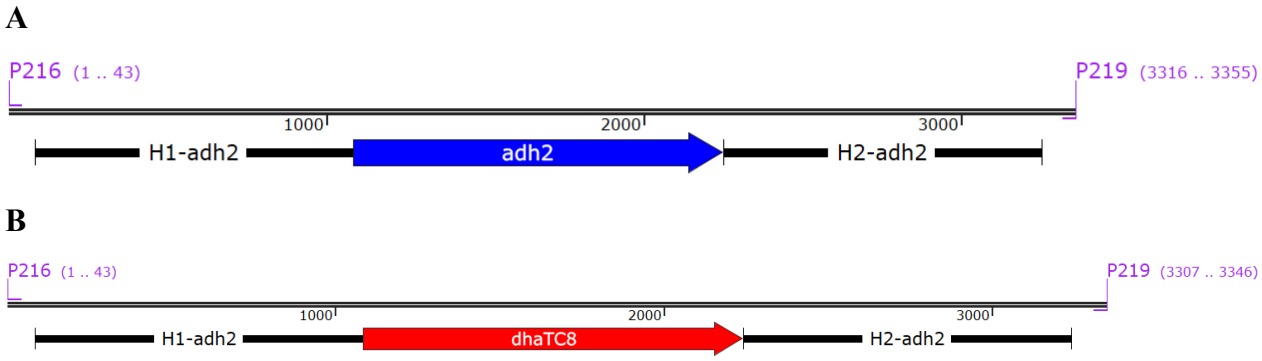

Figure 3-5: *adh2* region on the genome of *C. pasteurianum* R525. A: region around the *adh2* gene on the genome of *C. pasteurianum* R525. **B**: region with deleted *adh2*. The length of the PCR product between primers P216 and P219 would be 3355 bp for the wildtype and shorter when the gene is deleted with 2188 bp for the mutant.

The second genome modification in mutant BC-III was deletion of the *bdhA2* butanol dehydrogenase gene (CLPA_c15980) and the plasmid for this modification with a total length of 7071 bp was called p-bdhA2-del (pBD). The plasmid carries the gram-positive replicon pIM13, combination of antibiotic markers *ermB* and *tetA*, gram-negative replicon ColE1, homologous regions H1 and H2 and the CRISPR array with spacer sequence for deletion of *bdhA2* (Table 8-2). Plasmid pBD additionally carries part of the *bcd1* gene (bcd1r) so that the genome editing plasmid pBD can be targeted by the next plasmid pBC. The whole gene *bcd1* was not included on plasmid pBD to keep this fragment as short as possible while still containing the necessary spacer sequence (chapter 2.2.3) that is targeted by the next plasmid pBC. In order to construct pBD, two other plasmids had to be prepared first. The backbone (P049, P197, pDR) of the first fusion plasmid for plasmid pBD (pBD-FI) was fused with part of the *adh2* gene (P196, P198, genomic DNA of R525), homologous region H1 (P199, P200, genomic DNA of R525), H2 (P130, P201, genomic DNA of R525) and the CRISPR array (P064, P202, bdhA2_spacer_array).

The backbone (P160, P161, pMTL85141) of the second fusion plasmid for plasmid pBD (pBD-FII) was combined with an *ermB* marker (P162, P163, pMTL82254). A segment from each of the first (P242, P315, pBD-FI) and second (P02, P308, pBD-FII) fusion plasmids were combined with a *tetA* marker (P319, P322, pMTL84422) and part of the *bcd1* gene (P210, P316, genomic DNA of R525) to form the final plasmid pBD. Sanger sequencing was performed with the primers P179, P161, P084, P152, P232 and P317 for plasmid pBD. When the plasmid for deletion of the gene

bdhA2 was introduced into the cells and genome editing works successfully, the PCR product around the *bdhA2* gene should be shorter than in the wildtype genome (Figure 3-7). Similar to what is shown in Figure 3-5, PCR primers are designed that are not on the H1 or H2 region.

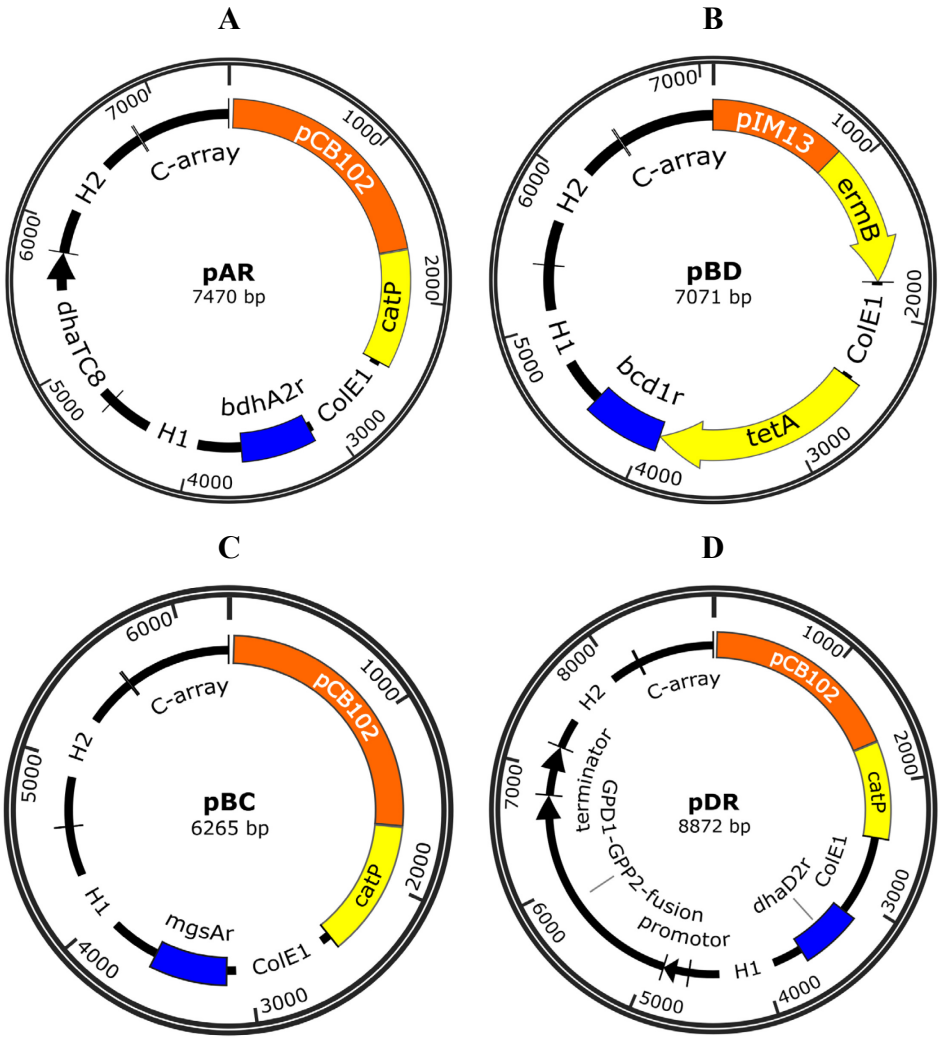

Figure 3-6: Plasmid components of genome editing plasmids pAR, pBD, pBC and pDR. A: plasmid pAR, **B**: plasmid pBD, **C**: plasmid pBC, **D**: plasmid DK. The plasmids are shown for first (pAR), second (pBD) and third (pBC or pDK) genome modification. The orange and yellow colored plasmid components are alternating for each genome modification step, orange: gram-positive replicon (pCB102 or pIM13), yellow: antibiotic markers (*catP* or *ermB* and *tetA*), blue: target region of the next genome editing plasmid. C-array: CRISPR array, ColE1: gram-negative replicon, H1/H2: homologous regions upstream and downstream of the targeted gene, promoter/terminator: Csp fdx promoter and terminator from pMTL007C-E2 [104], bdhA2r, bcd1r, mgsAr and dhaD2r: part of the genes *bdhA2*, *bcd1*, *mgsA* and *dhaD2*, respectively.

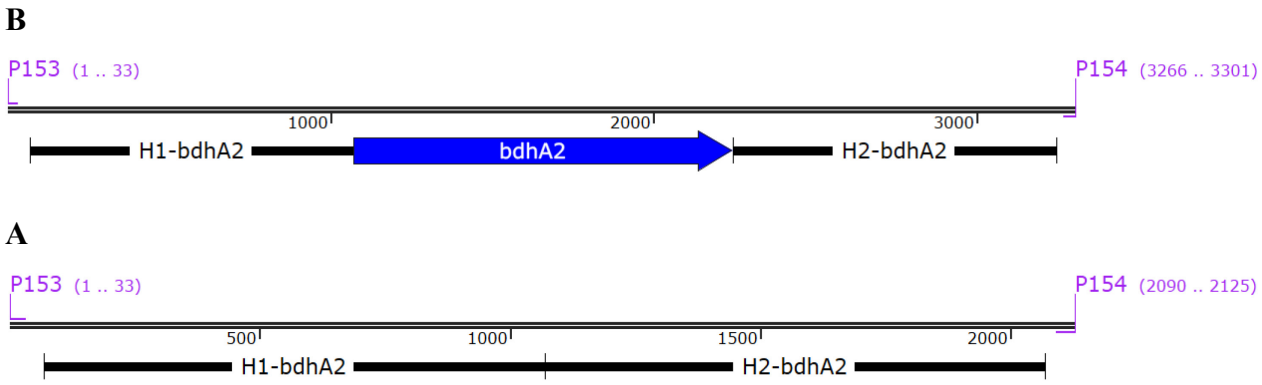

Figure 3-7: *bdhA2* region on the genome of *C. pasteurianum* R525. A: region around the *bdhA2* gene on the genome of *C. pasteurianum* R525. **B**: region with deleted *bdhA2*. The length of the PCR product between primers P153 and P154 would be 3301 bp for the wildtype and shorter when the gene was deleted with 2125 bp for the mutant.

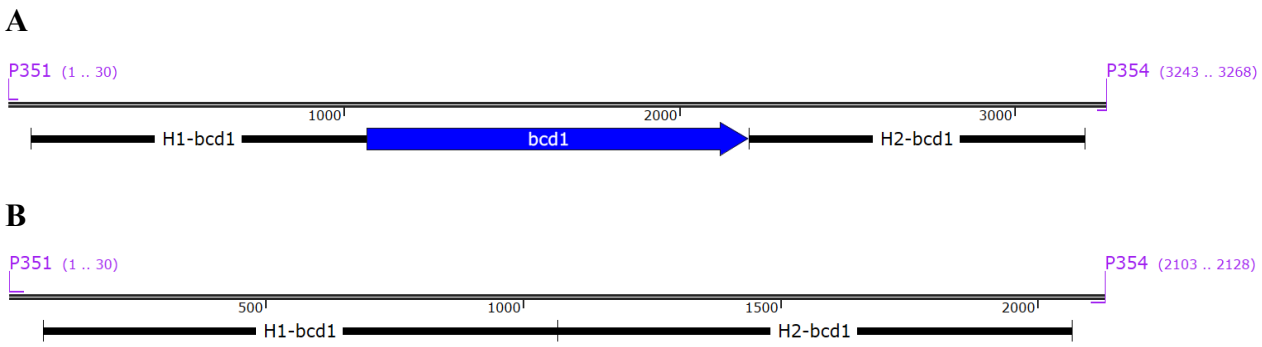

Figure 3-8: *bcd1* region on the genome of *C. pasteurianum* R525. A: region around the *bcd1* gene on the genome of *C. pasteurianum* R525. **B**: region with deleted *bcd1*. The length of the PCR product between primers P351 and P354 would be 3268 bp for the wildtype and shorter when the gene was deleted with 2128 bp for the mutant.

The third deletion in mutant BC-III was butyryl-CoA dehydrogenase gene *bcd1* (CPAST_c11000) which has a length of 1140 bp. The genome editing plasmid with a total length of 6265 bp for deletion of *bcd1* was named p-bcd1-del (pBC). When the plasmids for the deletion of the gene *bcd1* are introduced into the cells and the genome editing works successfully, the PCR product around the *bcd1* gene should be shorter than in the wildtype genome (Figure 3-8). The plasmid pBC contains five plasmid components and a fusion plasmid pBC-FI, which contains only the backbone with the respective CRISPR array, was constructed first. The backbone for pBC-FI (P49, P223, pDR), part of the *bdhA2* gene (P171, P224, genomic DNA of R525) and CRISPR array (P202, P247, bcd1_spacer_array) were fused to form pBC-FI. The backbone for plasmid pBC

(P356, P361, pBC-FI), part of the *mgsA* gene (P115, P355, genomic DNA of R525), homologous region H1 (P357, P358, genomic DNA of R525) and H2 (P359, P360, genomic DNA of R525) were fused to form the final plasmid pBC. Part of the *mgsA* gene was included to delete this gene in the next step, but this was not finished within this work. Sanger sequencing was performed with primers P37, P54, P84 and P353.

3.6.3 Replacement of *dhaD1* and *dhaK* with *GPD1* and *GPP2*

In this work, another third genome modification was introduced which replaces genes *dhaD1* and *dhaK* (CLPA_c12160 and CLPA_c12150) with *GPD1* and *GPP2* on the genome of *C. pasteurianum* R525 and the plasmid for this modification was called pDR. In order to carry out this third genome modification, plasmid pBD had to be modified by replacing part of the *bcd1* gene with part of the *dhaD1* gene.

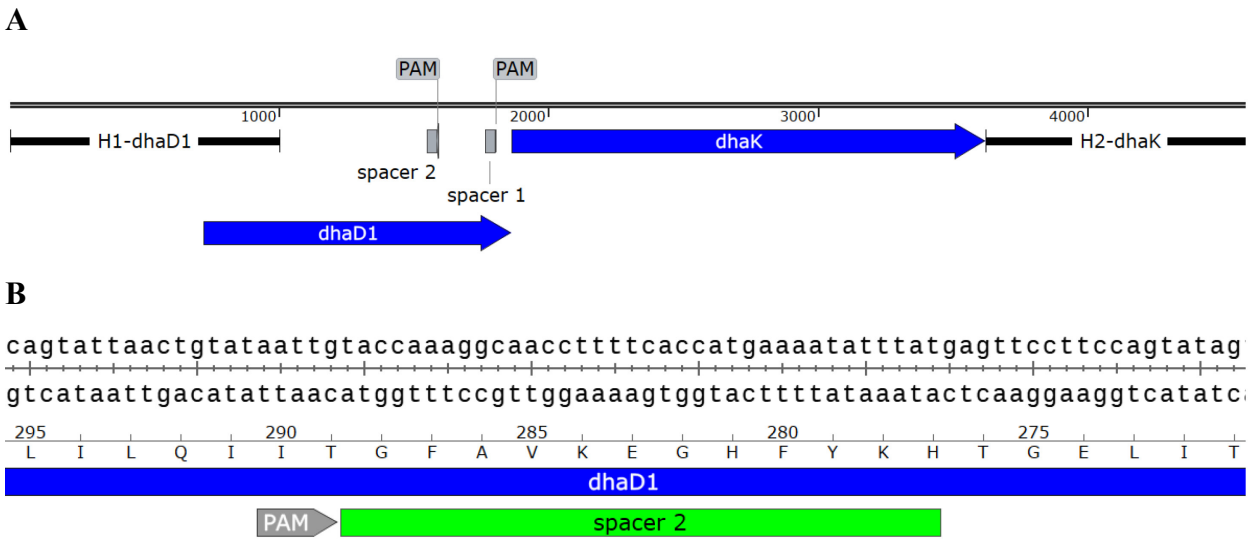

Figure 3-9: Position of spacers on the *dhaD1* gene. A: Region with genes *dhaD1* and *dhaK* on the genome of *C. pasteurianum* R525 with possible spacer regions, **B**: enlarged region of spacer 2 ont the gene *dhaD1*.

In order to construct plasmid pDR, two other plasmids had to be prepared and the first plasmid for pDR was called pGG8. The second plasmid for pDR was called dhaDK-del and the backbone of dhaDK-del (P049, P02, pGG8) was fused with a fragment containing a promoter, the genes *GPD1* and *GPP2* and a terminator (P061-new, P062, PGG8), homologous region H1 (P056-new, P060-new, R525 genome), H2 (P058, P063-new, R525 genome) and the CRISPR array (P064, P065,

synDNA). Finally, the backbone for pDR (P02, P49, dhaDK-del) was fused with homologous regions H1, H2 and the CRISPR array (P202, P331, dhaDK-del) and part of the *dhaD2* gene (P325, P326, R525 genome) to form the complete plasmid pDR. Part of the *dhaD2* gene was already included on the plasmid pDR to delete this gene in the next genome engineering step. Sanger sequencing was performed with the primers P008, P010, P011, P037, P054, P083 and P084 for the plasmid pDR. Various mutants were isolated in this work and an overview of deletions in created mutants is summarized in Table 3-6.

Table 3-6: Overview of gene deletions in isolated mutants. A light blue background indicates presence of a gene and deleted genes are marked as "Δ". Abbreviation for genes: *adh2* and *bdhA2*: butanol dehydrogenases, *bcd1*: butyryl-CoA dehydrogenase, *dhaD1*: glycerol dehydrogenase, *dhaK*: dihydroxyacetone kinase.

Strain	*adh2*	*bdhA2*	*bcd1*	*dhaD1*, *dhaK*
R525				
AR-I	Δ			
BC-I			Δ	
DR-I				Δ
BD-II	Δ	Δ		
BC-III	Δ	Δ	Δ	
DR-III	Δ	Δ		Δ

4 Development of a consecutive genome editing system

With the endogenous CRISPR-Cas method [23], only one genome editing step can be carried out in the same mutant and only gene deletions or replacements are possible so these are important obstacles to overcome. This chapter focuses on developing stable tools for consecutive genome editing of *C. pasteurianum* and *C. pasteurianum* C8 was the initial target strain for the production of PDO from glucose by the introduction of genes glycerol-3-phosphate dehydrogenase (*GPD1*) and glycerol-1-phosphatase (*GPP2*) from *Saccharomyces cerevisiae*. The stable integration of this foreign pathway requires deletion of multiple gene targets of competing pathways, but a transformation procedure for *C. pasteurianum* C8 needed to be tested first, because no genetic engineering was reported for this strain yet. In the first part of this chapter, electrotransformation of *C. pasteurianum* C8 was tested and the first approach was protection of plasmids against restriction modification systems in *C. pasteurianum* C8 by construction of new methylation plasmids. Ethyl methane sulfonate (EMS) treatment of the cells was also carried out for the isolation of a transformable *C. pasteurianum* C8 mutant and in the third approach, plasmids were first introduced into *C. pasteurianum* R525 and then again purified and finally transformed into *C. pasteurianum* C8.

The second part of this chapter describes the construction of plasmids for testing several antibiotic markers to enable consecutive genome editing of *C. pasteurianum*. There are some requirements for consecutive genome editing and one is that the plasmid of the first genome editing step needs to be removed for further metabolic engineering of this strain. However, there is no established method to carry out this crucial step with large genome editing plasmids which contain a CRISPR array. This could be done with the introduction of a second genome editing plasmid which is able to get rid of the first plasmid so that both plasmids should not be able to coexist in the same cell. Simultaneously, another gene can be targeted to create a mutant with two modifications. It is essential to cure the cells from the first plasmid so that the *catP* marker can be used again for the plasmid of a third modification to enable consecutive genome editing. This will be taken as a starting point and the verification of at least two genome-editing steps in the same mutant is the first main goal to achieve. The consecutive method would allow the study of several editing steps on the genome and the resulting influence on metabolic regulations in contrast to preceding studies where only one modification was considered at a time.

4.1 Results

4.1.1 Transformation of *C. pasteurianum* C8

There are reliable methods to transform *C. pasteurianum* R525, but transformation of *C. pasteurianum* C8 was not tested before and therefore, the first step was to carry out the established electrotransformation method [20] with strain R525 [105], strain C8 [2] and also with *C. pasteurianum* K1 (K1) [15] and *C. pasteurianum* G8 (G8) [2] (Figure 4-1).

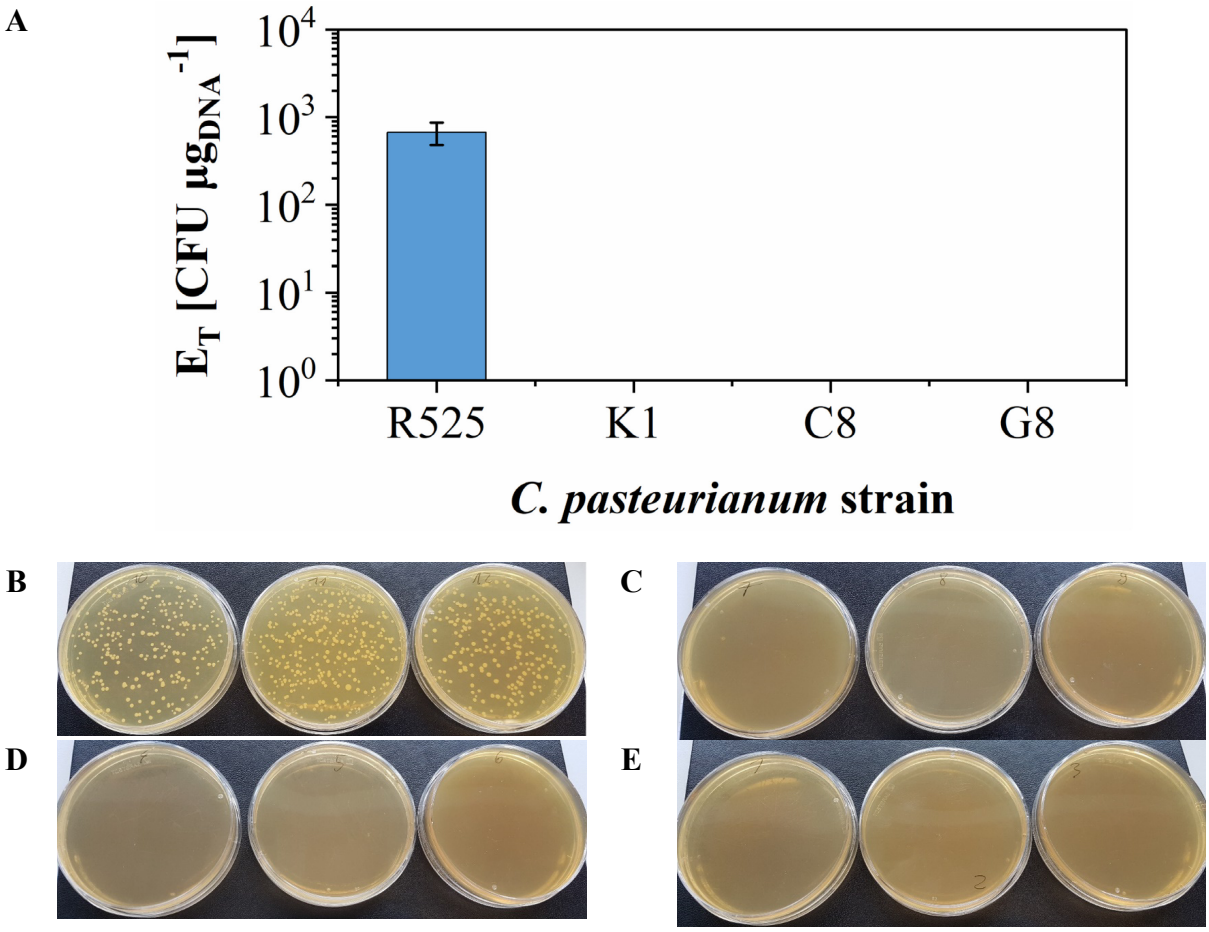

Figure 4-1: Transformation efficiencies with *C. pasteurianum* R525, K1, C8 and G8. A: transformation efficiencies, **B**: *C. pasteurianum* R525, **C**: *C. pasteurianum* K1, **D**: *C. pasteurianum* C8, **E**: *C. pasteurianum* G8. The total volume of the recovery culture, which contained the *C. pasteurianum* cells that were transformed with 5.8 µg plasmid DNA, was 10.631 mL and 1 mL of that volume was plated on 2xYTG + Tm10 agar plates for selection of transformants. For the transformation of R525, 249, 411 and 440 colonies were counted on the three plates from transformation carried out in triplicates and the error bar represents the standard deviation. CFU: colony forming units.

All strains were transformed with plasmid pMTL85141 [96], which is an empty plasmid without heterologous gene expression and it only carries an antibiotic marker *catP* for selection, one replicon for gram-negative and one replicon for gram-positive bacteria. The strain K1 was isolated by Keading et al. (2015) [15] from an active sludge sample, further purification resulted in strain C8 [106] and adaptive laboratory evolution of C8 created the strain G8 [2]. It was found that only strain R525 showed colonies on selective agar plates after the electrotransformation and even after a second attempt there were no colonies for strain C8 or for the other strains. It needs to be noted that for *C. pasteurianum* G8, the cell pellet after the centrifugation step (5000 rpm for 10 min at 4°C) was not as solid compared to the cell pellet of the other strains.

The cell pellet had a slimy texture and did not fully adhere to the wall of the centrifuge tube and some cells were lost when the supernatant was discarded. The transformations were carried out in triplicates for each strain and transformation efficiency of strain R525 was calculated with equation (1) as $6.72 \pm 1.89 \times 10^2$ CFU μg_{DNA}^{-1} (Figure 4-1). This value is two orders of magnitude lower compared to the maximum transformation efficiency of 7.5×10^4 CFU μg_{DNA}^{-1} with the optimized electrotransformation protocol reported by Pyne et al. (2013) [20]. The isolation of a C8 mutant by introducing a plasmid could not be achieved with the established method and approaches to solve this problem are described in the next sections.

4.1.1.1 Construction of methylation plasmids and EMS treatment

It's possible that plasmids were taken up by the cells of the C8 strain, but it was removed by the endogenous restriction modification systems that degrades foreign genetic material. The plasmids for the transformation of strain R525 were protected by in-vivo methylation with the plasmid pFnuDIIMKn and Dam+ methylation and this was found to be essential for successful transformations [20]. Therefore one type III and two type II methyltransferases were chosen from the genome of the G8 strain [16], which originates from the C8 strain (chapter 2.1.2). The methyltransferases were only tested one at a time because it is not secured that all genes are expressed when introduced together. For this reason, type I methyltransferases were not tested since multiple specificity and modification subunits would be necessary. The methyltransferase M.FnuDII on the methylation plasmid pFnuDIIMKn [20] was replaced by the methyltransferases from strain C8 and thus three different methylation plasmids were constructed.

It was tested if one of these methyltransferases is essential for a successful transformation and plasmid pMTL85141 was transformed with one of the new methylation plasmids into *E. coli* SCS110, which is a strain free from methylation. The construction of methylation plasmids was completed, however transformation of *C. pasteurianum* C8 was still not observed. Moreover, random mutagenesis of *C. pasteurianum* C8 with the mutagen ethyl methanesulfonate (EMS) (chapter 3.3.3) was carried out with the goal of selection of a transformable mutant. Small colony-like formations were visible, but re-streaking showed no growth on selective agar plates containing thiamphenicol so the isolation of a mutant which can efficiently take up plasmids was not achieved by this approach.

4.1.1.2 Electrotransformation with plasmids extracted from *C. pasteurianum* R525

The construction of new methylation plasmids or the EMS treatment for the isolation of a transformable C8 mutant didn't lead to the desired outcome so a different approach was tested. For this procedure, the plasmid pMTL85141 was not isolated from *E. coli*, but from the R525 strain as described in chapter 3.2.3. The plasmid purification protocols were carried out and verified by PCR in order to make sure that the plasmid is present. The plasmids were transformed into *C. pasteurianum* C8 and again into *C. pasteurianum* R525 as control and colonies were growing on 2xYTG agar plates with 10 µg mL^{-1} thiamphenicol. Primers pDOD-C8-F and pDOD-C8-R (Table 8-1), which only anneal to the genome of C8 and not to the genome of R525, were used for the verification.

The successful transformation was verified by PCR amplification and Sanger sequencing showed the correction region, indicating transformation of *C. pasteurianum* C8 for the first time. When another plasmid pGG8 for the expression of heterologous genes (chapter 3.5.1) was transformed with this procedure, only a single colony has grown on the agar plates after electrotransformation of *C. pasteurianum* C8. The transformation with a genome editing plasmid pDR (chapter 3.6.3) was also tried, but this didn't result in any colonies. A reason could be the low transformation efficiency of this procedure as the genome editing plasmid pDR (8872 bp) is larger compared to the previously transformed plasmids pMTL85141 (2963 bp) and pGG8 (5705 bp).

4.1.2 Consecutive genome editing

4.1.2.1 Testing of applicable antibiotic markers

It was not possible to introduce large genome editing plasmids into strain C8 with the established method and therefore a consecutive genome editing (CGE) system was developed for the modification of strain R525. A second functioning antibiotic marker is necessary to introduce and select for a second plasmid, but *catP* was the only known marker that functioned for the plasmid construction in the heat-shock transformable *E. coli* 10-beta and applicability was shown in previous works with the strain R525 [21, 22]. In order to determine if there are more antibiotic markers for selection in strain R525, antibiotic markers for resistance against erythromycin (*ermB*), spectinomycin (*aad9*) and tetracycline (*tetA*) were tested (chapter 3.6.1). Their function was tested in several clostridia strains such as *C. acetobutylicum* ATCC 824 or *C. difficile* R2091 in the pMTL80000 plasmid series before [96]. The marker *ermB* was tested first because it was reported to function in *C. pasteurianum* [55, 105], but another *E. coli* ER1821 strain was used in these studies and it requires electroporation for transformation. Plasmid construction and methylation require repeating transformation procedures at each consecutive genome editing step and for that reason, the method should be as simple as possible. Therefore, a functioning antibiotic marker is desired that can be applied with *E. coli* 10-beta, because it doesn't require the more laborious electroporation procedure.

It was found that *E. coli* 10-beta can already grow on all tested erythromycin concentrations up to 300 µg mL^{-1} (Em300) and therefore transformants with the *ermB* containing plasmids can't be selected with that antibiotic. While working with *E. coli* 10-beta and the markers *aad9* and *tetA*, different concentrations were tested and it was found that concentrations of 30 µg mL^{-1} tetracycline (Tc30) and 250 µg mL^{-1} spectinomycin (Sp250) are sufficient for avoiding false-positive colonies. Although *C. pasteurianum* R525 can't grow with spectinomycin or tetracycline supplementation and selection was possible with *E. coli* 10-beta, no colonies were formed on selective agar plates when plasmids with *aad9* and *tetA* markers were transformed into R525 even after repeated attempts of transformations. The testing of the antibiotic markers showed that only the *ermB* marker can be applied for the selection in *C. pasteurianum*, but it would require the strain *E. coli* ER1821 for the plasmid construction. A last attempt was to try the marker Kn for resistance against kanamycin from the methylation plasmid pFnuDIIMKn. For this marker, a new methylation

plasmid with the *tetA* marker was necessary, because the initial methylation plasmid already carried the Kn resistance gene, but the same result occurred with the marker Kn and the findings are summarized in Table 4-1.

Table 4-1: Summary of finding while testing antibiotic markers for *C. pasteurianum* R525.

Antibiotic marker	Resistance against	Applicability in *E. Coli*	Applicability in *C. pasteurianum*
catP	Chloramphenicol	Applicability confirmed [21, 22]	
ermB	Erythromycin	1) *E. coli* 10-beta grows on erythromycin => not applicable 2) *E. coli* ER1821 requires electroporation	Applicability confirmed [55, 105]
aad9	Spectinomycin	Applicable with *E. coli* 10-beta	Not applicable with R525
tetA	Tetracycline		
Kn	Kanamycin	1) Applicable with *E. coli* 10-beta 2) New methylation plasmid with *tetA* marker necessary	

4.1.2.2 Combination of antibiotic markers *tetA* and *ermB* on the same plasmid

At first, a functioning antibiotic marker could not be found because *E. coli* 10-beta was already naturally resistant to erythromycin so that the *ermB* marker can't be used for selection. The plasmid system for a consecutive genome editing system should be as simple and convenient as possible and that is why another approach was tried: the antibiotic markers *tetA* and *ermB* for resistance against tetracycline and erythromycin were combined on the same plasmid.

From the results, it was found that selection with *tetA* works well in the heat-shock transformable *E. coli* 10-beta and with this gained knowledge, plasmid p_bdhA2-del (pBD) was constructed and it contained both antibiotic markers *ermB* and *tetA* (chapter 3.6.2). The plasmid additionally carried a CRISPR array for targeting the butanol dehydrogenase gene bdhA2 and this plasmid was constructed and methylated in *E. coli* 10-beta with selection by *tetA*. The fact that the marker *ermB* was reported to work for *C. pasteurianum* [20] was used as follows: when the plasmid was introduced into the R525 strain, it was not selected on agar plates with tetracycline but with

erythromycin. In order to test if two consecutive genome modifications are possible in the same mutant of *C. pasteurianum* R525, first the plasmid p_adh2-rpl (pAR) was transformed into strain R525 creating the mutant R525+pAR (AR-I). The plasmid pAR contains part of the *bdhA2* gene and it was tested if plasmid pAR can be removed by the introduction of plasmid pBD into the mutant AR-I (Figure 4-2). Cells from the resulting mutant R525+pAR+pBD (BD-II) were re-plated once on 2xYTG+Tm10 agar plates, but colonies were still able to grow on agar medium that contained thiamphenicol.

This should only be possible when the mutant still carries the first plasmid pAR so it was not completely removed at this point. The CRISPR array on the pBD plasmid should target the plasmid pAR and then growth on thiamphenicol should not be possible anymore. Following approach was tested to remove the plasmid pAR: the mutant BD-II was re-plated on 2xYTG+Em300 plates for a total of three times and afterwards, again re-plated on 2xYTG+Tm10 plates to check if the cells can still grow on thiamphenicol after several re-plating steps. When the mutant BD-II was re-plated on 2xYTG+Tm10 after three previous re-plating steps, growth did not occur anymore and this indicates that the plasmid pAR was lost. Therefore, the developed method was used to successfully remove the first plasmid and create a mutant that carries two different gene deletions which was not possible with the available methods before.

This verifies that the combination of the antibiotic markers *tetA* and *ermB* in the same plasmid enabled the selection of *C. pasteurianum* R525 with *ermB* without the need to use the *E. coli* ER1821 strain for plasmid construction which would require the more laborious electroporation for each transformation. The stable method of selection with erythromycin for the work with *C. pasteurianum* R525 constitutes a first step towards the development of a consecutive genome editing plasmid (CGE) system. The purpose of the CGE method is the introduction of multiple genome modifications by utilizing the endogenous CRISPR-Cas method [23] and the main principle is to facilitate plasmid curing which is a crucial requirement for consecutive genome modifications. To enable plasmid curing, each plasmid carries part of the sequence of the next gene target which will be deleted in the subsequent genome engineering step. Therefore, plasmid pAR carries part of the gene *bdhA2* (bdhA2r) (Figure 4-2).

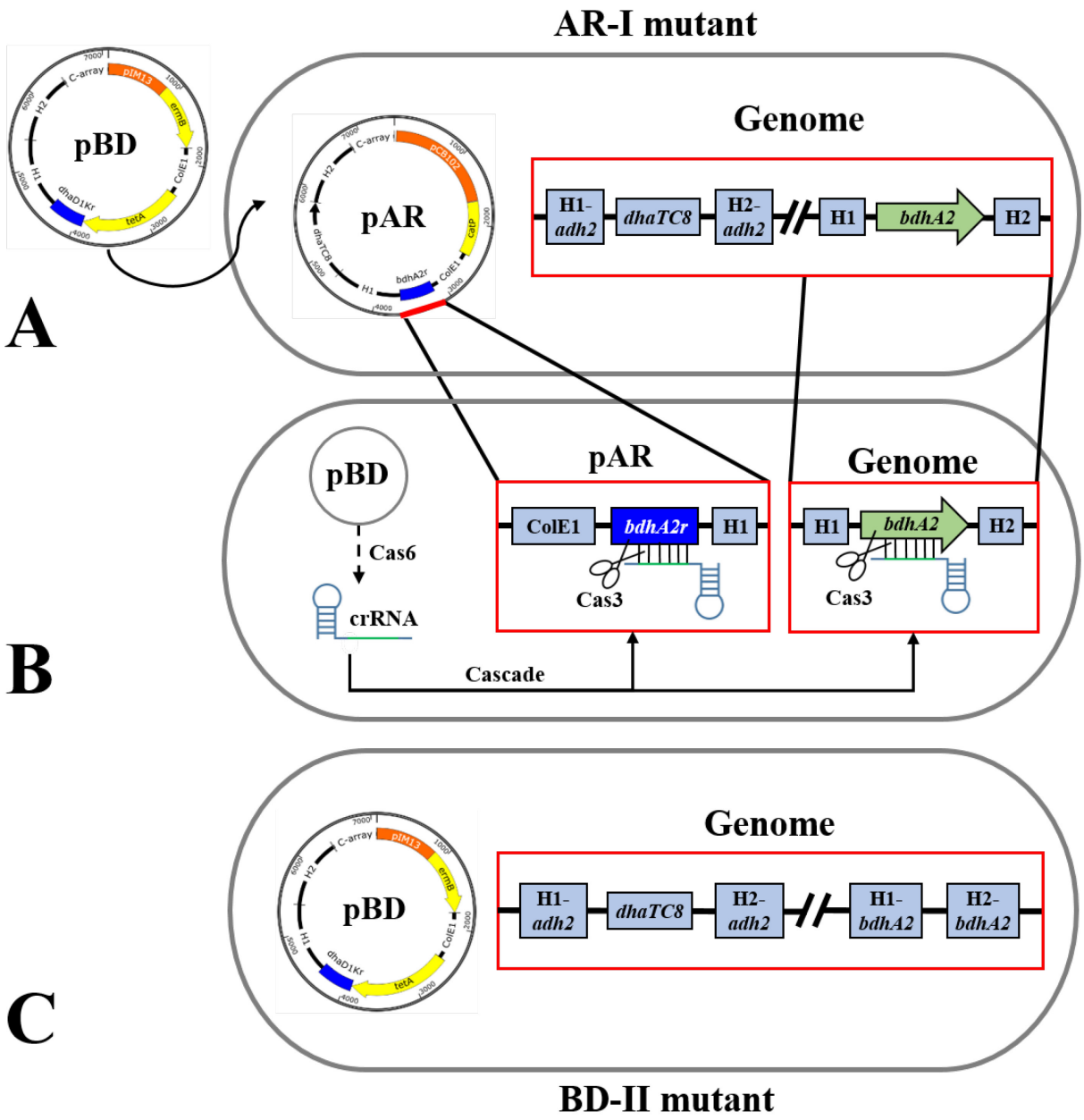

Figure 4-2: Schematic overview of steps for the consecutive genome editing system. The mutant R525+pAR (AR-I) was isolated by selection with thiamphenicol (Tm) after electrotransformation of plasmid pAR into R525. **A**: Gene *adh2* was replaced with gene *dhaTC8* and mutant AR-I was transformed with plasmid pBD. The resulting mutant AR-I+pBD (BD-II) was isolated by selection with erythromycin (Em). **B**: At the same time, transcription of precursor crRNA (CRISPR-RNA) from the CRISPR array of plasmid pBD and subsequent processing by Cas6 endonuclease to mature crRNA fragments occurs [23]. This leads to complementary annealing of mature crRNA to the recognition sequence, starting with a protospacer adjacent motif (PAM), on the gene *bdhA2* within the genome and on plasmid pAR [107, 108]. **C:** Afterwards, the Cas3 endonuclease introduces a DNA nick which ultimately results in survival of cells only with deleted gene *bdhA2* and simultaneously removed plasmid pAR [23, 109]. H1 and H2: homologous regions upstream and downstream of the *adh2* or *bdhA2* gene.

4.1.2.3 Verification of two genome modifications in a single mutant

A *C. pasteurianum* mutant with two genome modifications was created and all modifications were verified by Sanger sequencing, but PCR reactions were also performed to test if the desired gene deletions or replacements are present on the genome. The first genome modification replaced the butanol dehydrogenase gene *adh2* with PDO dehydrogenase gene *dhaTC8* from strain C8 and verification is shown in Figure 4-3. When the plasmid for replacement is introduced into the cells and genome editing works successfully, the PCR product around the *adh2* gene should have around the same length as in the wildtype genome. The length of the inserted *dhaTC8* (1158 bp) is almost as long as the *adh2* gene (1167 bp) and therefore other primer combinations are chosen for the verification. As shown in Figure 4-3B, primers P198 and P246 can only anneal on the *adh2* gene and only PCR products from the wildtype genome should be visible when the replacement of *adh2* with *dhaTC8* was successful (Figure 4-3A, lane 9-10).

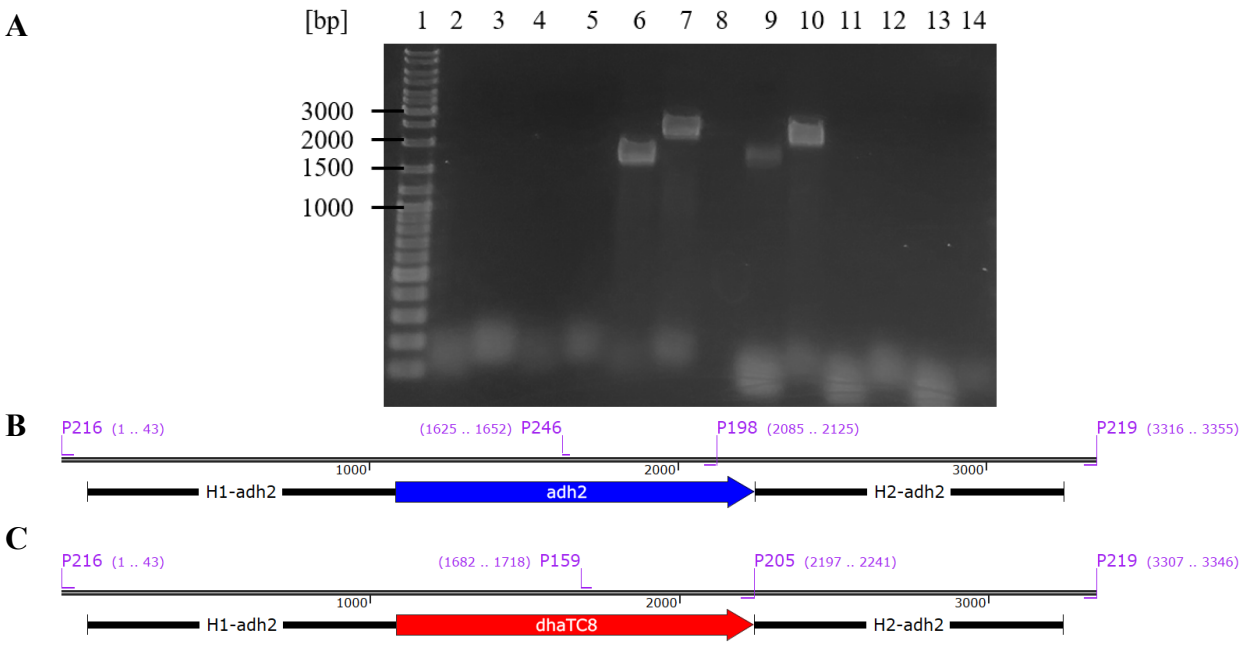

Figure 4-3: Verification of the first genome modification using plasmid pAR. A: Gel picture with PCR products for the verification. Lane 1: GeneRuler DNA Ladder Mix; Lane 2-3: PCR reactions with alternating primer pairs P159 and P219 or P205 and P216 for the wildtype genome; Lane 4-5: for the negative control with water; Lane 6-7: for the genome of the mutant; Lane 8: empty space; Lane 9-10: PCR reactions with alternating primer pairs P246 and P219 or P198 and P216 for the wildtype genome; Lane 11-12: for the negative control with water; Lane 13-14: for the genome of the mutant. **B**: region of the *adh2* gene on the genome of the wildtype, **C**: region of the replaced *adh2* gene with *dhaTC8* on the genome of the mutant.

Similarly in Figure 4-3C, the primers P159 and P205 can only anneal on the *dhaTC8* gene so only PCR products from the genome of the mutant should appear (Figure 4-3A, lane 6-7). It's important for the verification that PCR primers are designed which are not on the H1 or H2 regions because these are also present on the constructed plasmids and all PCR products in lane 6, 7, 9 and 10 in Figure 4-3A show the expected lengths of 1665, 2241, 1731 and 2125 bp, respectively. The second modification deleted a second butanol dehydrogenase gene *bdhA2* (Figure 4-4).

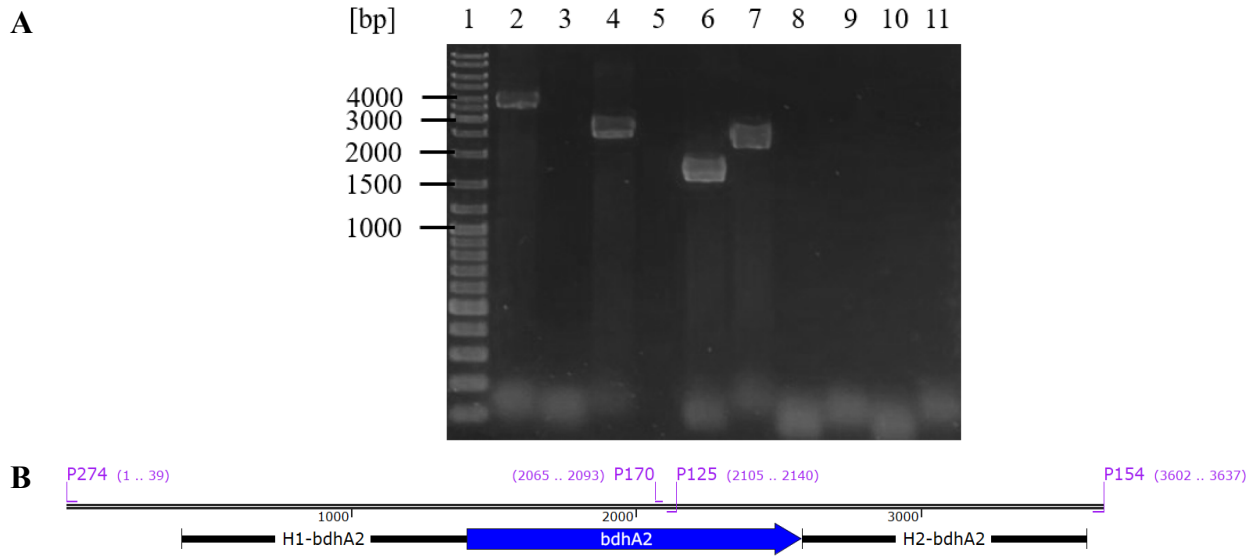

Figure 4-4: Verification of the second genome modification using plasmid pBD. A: Gel picture with PCR products for the verification. Lane 1: GeneRuler DNA Ladder Mix; Lane 2; PCR reaction with primers P154 and P274 for the wildtype genome; Lane 3: for the negative control with water; Lane 4: for the genome of the mutant; Lane 5: empty space; Lane 6-7: PCR reactions with alternating primer pairs P154 and P170 or P125 and P274 for the wildtype genome; Lane 8-9: for the negative control with water; Lane 10-11: for the genome of the mutant. **B**: region of the *bdhA2* gene on the genome of the wildtype.

The PCR products 2 and 4 in Figure 4-4A show that the PCR amplification of the *bdhA2* region with the primers P154 and P274 is shorter (2461 bp) than the same PCR product from the R525 genome (3637 bp) and this means that the *bdhA2* was successfully deleted. As shown in Figure 4-4B, the primers P125 and P170 can only anneal on the *bdhA2* gene and only PCR products from the wildtype genome should be visible when the deletion of *bdhA2* was successful and PCR products in lane 6 and 7 in Figure 4-4A show the expected lengths of 1573 and 2140 bp, respectively.

4.1.3 Characterization of mutants AR-I and BD-II

In order to determine if the mutants show a desired change in metabolic behavior, batch fermentations were carried out in duplicates with the strain R525 with 80 g L^{-1} glycerol and the results are summarized in Figure 4-5 and Figure 4-6 for fermentations under iron excess or iron limited conditions, respectively. The same fermentation conditions were used for fermentations with the mutants AR-I and BD-II and the results are compared with the wildtype in the following.

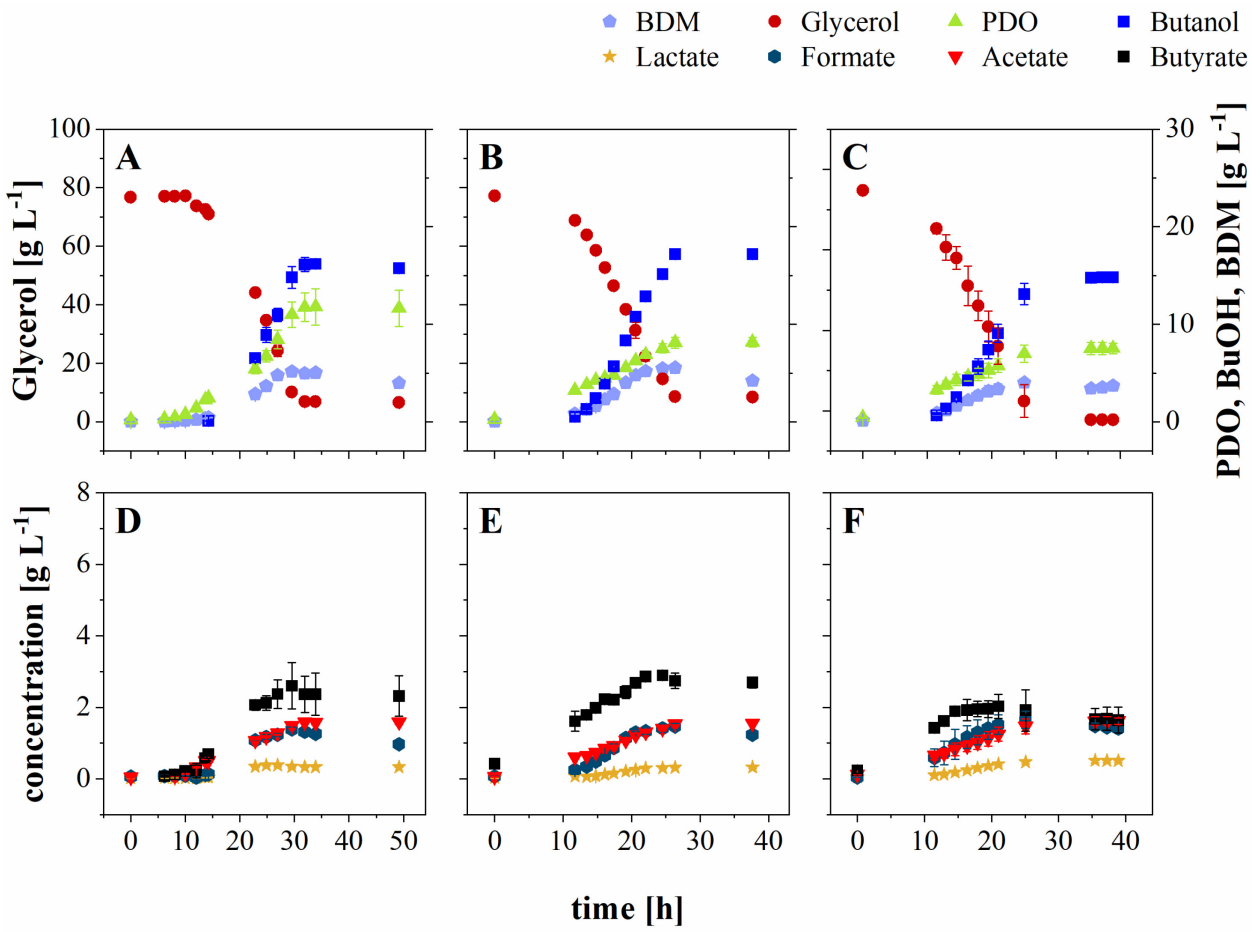

Figure 4-5: Batch fermentation of R525, AR-I and BD-II under iron excess conditions. A, D: wildtype R525; **B, E**: mutant AR-I; **C, F**: mutant BD-II. Fermentations were carried out with addition of 80 g L^{-1} glycerol and 100 mg L^{-1} $FeSO_4$ * $7H_2O$, pH maintained at 6.5, temperature controlled at 35°C and stirrer speed set to 400 rpm. The error bars show the standard deviation from fermentations conducted in duplicates. PDO: 1,3-propanediol, BuOH: butanol, BDM: bio dry mass.

Under iron excess conditions (Figure 4-5), the biomass concentration reached its highest value after 29.5, 26.3 and 25.1 h with growth rates of 0.22 ± 0.01, 0.21 ± 0.01 and 0.14 ± 0.00 h^{-1} for wildtype R525, mutants AR-I and BD-II, respectively. Butanol was the metabolite with the highest yield of up to 0.22 ± 0.01, 0.25 ± 0.00 and 0.25 ± 0.01 g g^{-1} with overall specific production rates of 0.10 ± 0.00, 0.12 ± 0.00, 0.13 ± 0.00 g g^{-1} h^{-1} for wildtype R525 and mutants AR-I and BD-II, respectively. Butanol is followed by the second highest metabolite PDO with yields of 0.16 ± 0.02, 0.11 ± 0.01 and 0.012 ± 0.01 g g^{-1} for wildtype R525 and mutants AR-I and BD-II, respectively.

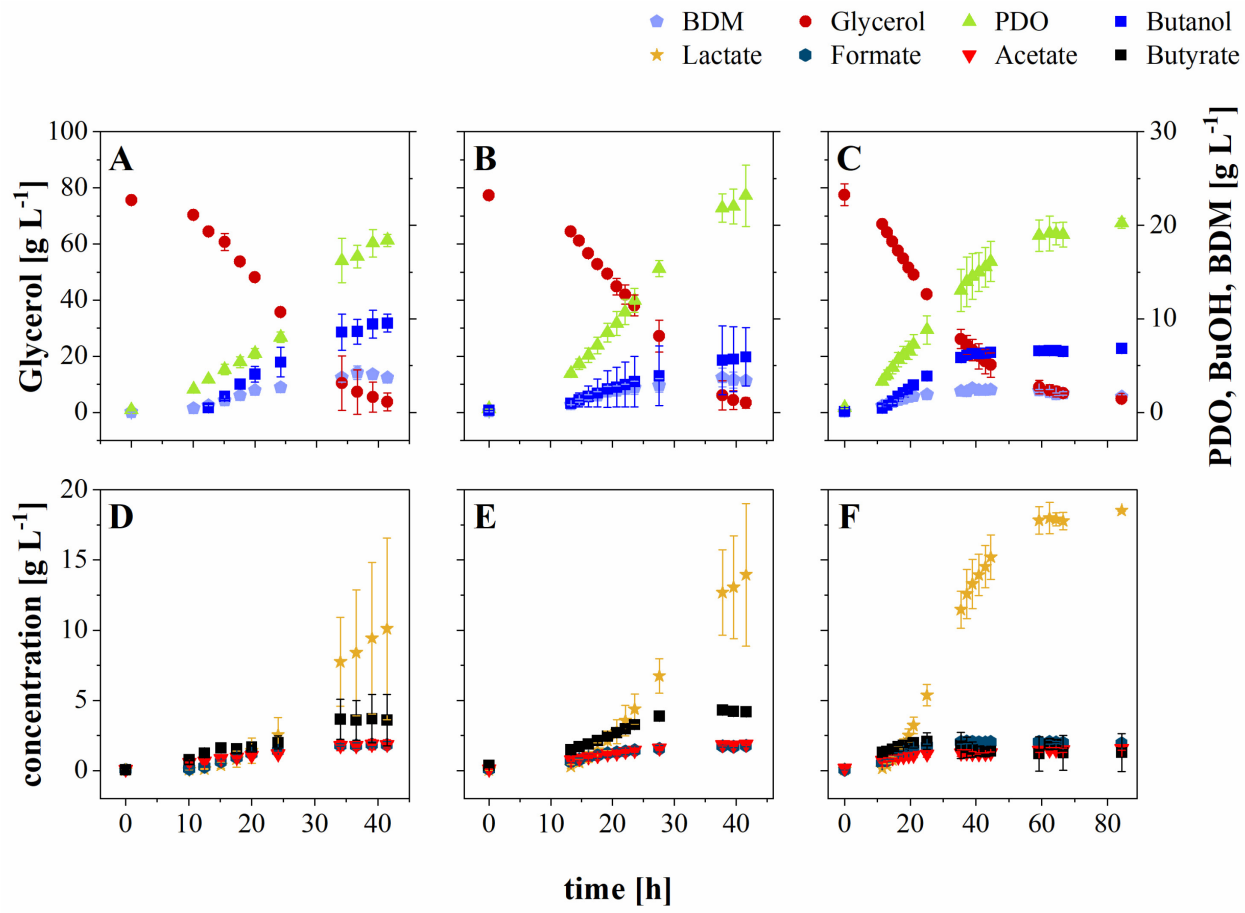

Figure 4-6: Batch fermentation of R525, AR-I and BD-II under iron limited conditions. A, D: wildtype R525; **B, E**: mutant AR-I; **C, F**: mutant BD-II. Fermentations were carried out with addition of 80 g L^{-1} glycerol and 0 mg L^{-1} $FeSO_4$ * $7H_2O$, pH maintained at 6.5, temperature controlled at 35°C and stirrer speed set to 400 rpm. The error bars show the standard deviation from fermentations conducted in duplicates. PDO: 1,3-propanediol, BuOH: butanol, BDM: bio dry mass.

The results show that both mutants produce more butanol and less PDO in comparison to the wildtype and there are no significant differences in the acid production of all strains. Specific glycerol consumption rates of 0.44 ± 0.02, 0.47 ± 0.02 and 0.54 ± 0.00 g g^{-1} h^{-1} for wildtype R525 and mutants AR-I and BD-II, respectively, show that the genome modifications did not inhibit the substrate utilization under iron excess conditions. In the case of iron limited conditions (Figure 4-6), after 36.6, 37.8 and 37.2 h maximum biomass concentrations were reached with growth rates of 0.12 ± 0.01, 0.10 ± 0.02 and 0.10 ± 0.01 h^{-1} for wildtype R525 and mutants AR-I and BD-II, respectively. In contrast to the results in Figure 4-5, highest yields were calculated for PDO with values of up to 0.24 ± 0.01, 0.30 ± 0.05 and 0.25 ± 0.01 g g^{-1} with molar ratios of 1.86 ± 0.15, 5.21 ± 3.84 and 2.21 ± 0.29 mol mol^{-1} for wildtype R525 and mutants AR-I and BD-II, respectively.

The calculated values indicate that more PDO and less butanol was produced by mutant AR-I in comparison to the wildtype. Formate and acetate are produced in similar levels for all strains, but specific lactate production rates of 0.06 ± 0.04, 0.10 ± 0.05 g g^{-1} h^{-1} were reached for wildtype R525 and mutant AR-I, respectively, while mutant BD-II produced the most lactate with 0.14 ± 0.02 g g^{-1} h^{-1}. The carbon distributions of each metabolite (Figure 4-7), calculated with equation (14), also show the increased butanol production and lower PDO production for the mutants under iron excess conditions. Under iron limited conditions, there were larger deviations within duplicate fermentations in comparison to the fermentations under iron excess conditions, but the overall trend shows highest carbon distribution of 38.06 ± 6.10% for PDO with mutant AR-I and highest carbon distribution of 24.78 ± 1.47% for lactate with mutant BD-II. The carbon recoveries (Table 4-2) are slightly higher than 100% under iron excess conditions and below 100% under iron limited conditions, although there are again larger standard deviations.

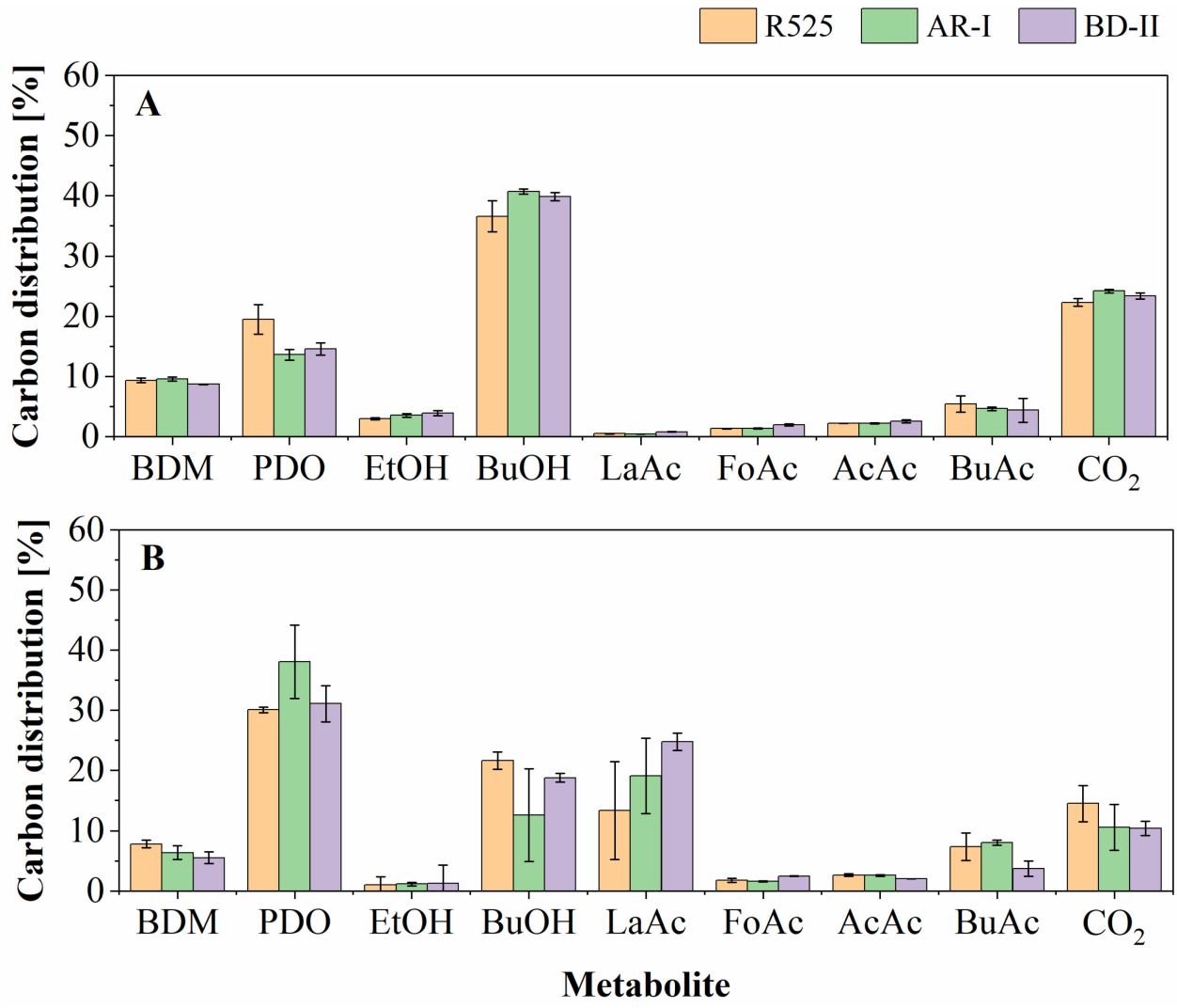

Figure 4-7: Carbon distributions from R525, AR-I and BD-II fermentations. A: Carbon distributions from fermentations with 80 g L^{-1} glycerol under iron excess conditions (100 mg L^{-1} $FeSO_4$ * $7H_2O$), **B**: iron limited conditions (0 mg L^{-1} $FeSO_4$ * $7H_2O$). The molar concentration of each metabolite was multiplied with the respective number of carbons and each carbon distribution represents the ratio of carbon concentrations between a produced metabolite and the sum of all metabolites. The error bars show the standard deviation from fermentations conducted in duplicates. BDM: bio dry mass, EtOH: ethanol, BuOH: butanol, LaAc: Lactate, FoAc: formate, AcAc: acetate, BuAc: butyrate.

Table 4-2: Fermentation parameters of R525, AR-I and BD-II under iron excess and limited conditions.
The standard deviations are given for fermentations carried out in duplicates. AR-I: mutant with *adh2* replaced with *dhaTC8*, BD-II: mutant with *adh2* replaced with dhaTC8 and deleted *bdhA2*. μ: growth rate, $Y_{P/S}$ = substrate specific yield, q_i = specific production rate, C_R: carbon recovery, e_R: electron recovery, BuOH: butanol, LaAc: lactate, PDO: 1,3-propanediol.

Iron excess conditions (100 mg L^{-1} $FeSO_4$ * $7H_2O$)			
Strain:	**R525**	**AR-I**	**BD-II**
μ [h^{-1}]:	0.22 ± 0.01	0.21 ± 0.01	0.14 ± 0.00
$Y_{PDO/Glycerol}$ [g g^{-1}]:	0.16 ± 0.02	0.11 ± 0.01	0.12 ± 0.01
$Y_{BuOH/Glycerol}$ [g g^{-1}]:	0.22 ± 0.01	0.25 ± 0.00	0.25 ± 0.01
q_{PDO} [g g^{-1} h^{-1}]:	0.07 ± 0.01	0.05 ± 0.01	0.07 ± 0.01
q_{BuOH} [g g^{-1} h^{-1}]:	0.10 ± 0.00	0.12 ± 0.00	0.13 ± 0.00
PDO/Butanol [mol mol^{-1}]:	0.71 ± 0.14	0.45 ± 0.03	0.49 ± 0.03
C_R [%]:	100.67 ± 0.40	102.12 ± 0.65	103.93 ± 0.36
e_R [%]:	99.95 ± 0.52	100.69 ± 0.55	102.59 ± 0.85
Iron limited conditions (0 mg L^{-1} $FeSO_4$ * $7H_2O$)			
μ [h^{-1}]:	0.12 ± 0.01	0.10 ± 0.02	0.10 ± 0.01
$Y_{PDO/Glycerol}$ [g g^{-1}]:	0.24 ± 0.01	0.30 ± 0.05	0.25 ± 0.01
$Y_{BuOH/Glycerol}$ [g g^{-1}]:	0.13 ± 0.00	0.07 ± 0.04	0.11 ± 0.01
$Y_{LaAc/Glycerol}$ [g g^{-1}]:	0.13 ± 0.08	0.18 ± 0.06	0.24 ± 0.00
q_{PDO} [g g^{-1} h^{-1}]:	0.11 ± 0.01	0.16 ± 0.06	0.15 ± 0.03
q_{BuOH} [g g^{-1} h^{-1}]:	0.06 ± 0.00	0.04 ± 0.02	0.06 ± 0.00
q_{LaAc} [g g^{-1} h^{-1}]:	0.06 ± 0.04	0.10 ± 0.05	0.14 ± 0.02
PDO/Butanol [mol mol^{-1}]:	1.86 ± 0.15	5.21 ± 3.84	2.21 ± 0.29
C_R [%]:	97.70 ± 2.95	96.38 ± 0.33	98.89 ± 6.76
e_R [%]:	95.34 ± 2.50	95.39 ± 0.32	97.37 ± 6.60

4.2 Discussion

4.2.1 Challenges for the transformation of *C. pasteurianum* C8

There are several challenges to overcome for the efficient transformation of *C. pasteurianum* C8 and the transformation of *C. pasteurianum* C8 was successful only for plasmids that were extracted from *C. pasteurianum* R525. The EMS-induced random mutagenesis of *C. pasteurianum* C8 cultures did not result in transformable mutants, but only two concentrations of 0.5% and 1.0%

(v/v) EMS were tried according to Lemmel (1985) [59] with a dilution by 1:100 after EMS treatment. A systematic exposure to various EMS concentrations and dilution factors after mutagenesis would be necessary to find optimal conditions for EMS treatment of *C. pasteurianum* C8. Methylation of the plasmids by single methyltransferases from *C. pasteurianum* C8 was tried, but with that procedure it was not possible to imitate the whole methylation system. The restriction modification systems are different for both strains, but it is possible that the extracted plasmids from *C. pasteurianum* R525 carry methylations which are very similar to the ones in the strain C8. The in vivo methylation of plasmids by methyltransferases from the genome of the strain R525 would possibly enable the transformation into the strain C8. As an extension of this work, single molecule real-time (SMRT) sequencing of DNA samples extracted from strains R525 and C8 could be carried out to elucidate the differences in methylation patterns of both strains.

The transformation efficiency was not high enough to introduce large genome editing plasmids and the plasmid extraction from *C. pasteurianum* R525 results in lower plasmid concentrations compared to the extraction from *E. coli*. If this could be improved, increased transformation efficiencies are expected, because higher plasmid concentrations were found to be beneficial for the transformation of *C. pasteurianum* R525 [20]. Two methods were combined to isolate *C. pasteurianum* R525 in the past and the first method was the hyper transformable mutant selection [25, 110]. Small plasmids from transformed *C. pasteurianum* DSM525 were cured by repeated re-streaking on non-selective agar plates. Re-transformation was carried out to check if the plasmid-cured strain takes up foreign DNA with higher efficiency, assuming that only rare mutants in the population can be transformed. The *C. pasteurianum* R525 strain was isolated with this procedure with a 50 times higher transformation efficiency compared to DSM525. This mutant selection procedure could also be applied to the strain C8 in order to isolate a strain with higher transformation efficiency.

The second method was the high-level electrotransformation protocol [20] and the treatment of cells prior to transformation with glycine (cell-wall weakening), sucrose (osmoprotection) and ethanol (cell membrane solubilization), variation of electric pulse parameters (optimal at 1.8 kV, ∞ Ω, 25 µF) lead to an even more improved transformation efficiency. The electrotransformation protocol that was optimized for *C. pasteurianum* DSM525 is possibly not adjusted to

C. pasteurianum C8 and this is an additional aspect that can be improved in further studies by optimizing the transformation conditions. In the study of Ortega (2020) [24], successive deletion of genes encoding restriction enzymes created a mutant which was transformable without the need of prior methylation. When efficient transformation of *C. pasteurianum* C8 becomes possible in the future, deletion of such genes encoding restriction enzymes would likely improve the transformation procedures in that strain as well.

4.2.2 Limited number of applicable antibiotic markers for *C. pasteurianum*

The antibiotic marker *catP* for resistance against chloramphenicol or thiamphenicol was the only functioning marker for the plasmid construction in the heat-shock transformable *E. coli* 10-beta in our previous works with the strain R525 [21, 22, 47]. Various antibiotic markers were tested in several clostridia strains such as *C. acetobutylicum* ATCC 824 or *C. difficile* R2091 in the pMTL80000 plasmid series [96] before. Some of the tested strains were already naturally resistant to certain antibiotics and some strains showed that certain resistance markers are not working in these strains. Most of the markers (*ermB*, *tetA*, *aad9*, *KnR*) that were tested in this work for application with *C. pasteurianum* R525 didn't function and thus showing that there are only a limited number of antibiotic markers for the application in *C. pasteurianum*.

The only remaining option was to test the *ermB* marker, but this would require the electrotransformation at each introduction into *E. coli* ER1821 for plasmid propagation and again for the methylation. Additionally, preparation and storage of additional competent cells from *E. coli* ER1821 would be necessary, because *E. coli* 10-beta can't be used for *ermB* selection. These steps would delay the consecutive genome editing as they are required at each cycle of editing. The combination of *tetA* and *ermB* markers on the same plasmid enabled the selection with the *ermB* marker, but only antibiotic markers from Heap et al. (2009) [96] were tried. There might be other markers including clarithromycin or neomycin that can be used in both strains *E. coli* 10-beta and *C. pasteurianum* R525 similarly to the *catP* marker.

The plasmids of the CGE system contain one additional component which is the target region from the CRISPR array of the next plasmid to be introduced. This next plasmid contains a CRISPR array

that would not only target the genome but also the previous plasmid. This would result in survival of cells where the second genome editing can be verified and also the loss of the previous plasmid. In order to develop this tool, critical points were solved e.g., different antibiotic markers that function in *E. coli* and in *C. pasteurianum* for selection of the correct colonies. Furthermore, different replication origins (pCB102, pIm13) were needed because plasmids with the same replicon would compete with each other for the same replication machineries of the cell. Finally, the gene target of the next genome editing plasmid always needs to be known in advance and the respective spacer sequences which are necessary for the CRISPR array need to be tested and verified first so that they can be used for *C. pasteurianum*.

4.2.3 Simultaneous gene deletion and plasmid removal

At the beginning, the order of targets for genomic modifications (first *adh2*, second *bdhA2*) had to be decided and genome modifications were introduced successively with plasmids p_adh2-rpl (pAR) and p_bdhA2-del (pBD). The CRISPR array of the plasmid pBD was designed to target the butanol dehydrogenase gene *bdhA2* on the genome of the strain R525 and degrade the plasmid pAR from the first genome modification at the same time. This was achieved by including a part of the *bdhA2* gene on the first plasmid pAR. Freshly transformed colonies of the mutant BD-II were still able to grow on thiamphenicol so they were re-plated on fresh 2xYTG+Em300 plates for a total of three times to isolate the pure mutant. The initial agar plate was plated with a mixture of cells, some of which have taken up the plasmid and therefore it is possible that cells that don't carry the plasmid were also picked. In theory, mutants are growing without the pressure to replicate the pAR plasmid with each re-plating step and the copy number of the plasmid pAR in each cell should decrease when selection with thiamphenicol is not taking place anymore.

Afterwards, the mutant was re-plated on 2xYTG+Tm10 plates and growth did not occur on agar plates with thiamphenicol anymore. The same colonies were inoculated into liquid 2xYTG+Tm7 medium and no growth was observed, thus indicating that the plasmid pAR was lost. A possible explanation could be that the CRISPR array was designed to target the genome which is present only in one single copy per cell. The exact copy number of plasmid pAR in each cell was not determined so it is possible that it is replicating faster than it can be removed by the CRISPR array.

Small plasmids (e.g. pMTL85141 [96]) can be removed by several re-plating steps without selection pressure, but this was found to be impossible for larger plasmids including genome editing plasmids even after dozens of re-plating steps over several months [93]. This was by-passed by including the CRISPR array, because it targets the *bdhA2* region on the plasmid pAR and decreases the number of that plasmids at each re-plating step. This results in complete loss of the plasmid after sufficient numbers of re-plating steps and the next genome modification cycle can be initiated.

4.2.4 Comparison of the developed method to existing genome editing methods

A comparison will be made between the developed consecutive genome editing method of this work and other existing genome modification methods in *C. pasteurianum*. The overview in Table 2-5 shows that only one of the previous works tried successive modifications by the Allele-coupled exchange (ACE) method on the genome of *C. pasteurianum* and at first, the here developed consecutive genome editing (CGE) method seems to have disadvantages compared to other existing genome editing methods including the need to use multiple selection markers and the requirement to know the planned editing steps in advance. On the other hand, it solves the problem that curing of plasmids with a CRISPR array was not possible even after many re-plating steps of serial transfers onto non-selective medium [93]. Needing to know editing steps in advance is not a major problem, if possible targets for future modifications of *C. pasteurianum* are carefully considered and if the order of targets to be deleted or replaced is determined from the start.

Different characteristics of the two methods, which enabled multiple genome modifications in a single mutant are compared in the following in order to determine further, possible benefits of the CGE method. 5-fluoroorotic acid (FOA) is toxic to cells containing a functional *pyrE* gene and therefore a specific host strain with partial disruption of the *pyrE* gene is necessary for the ACE method so that FOA can be used as a counter-selection marker [95]. This is another difference to the CGE method because CGE has the advantage that it does not have this requirement and can be applied on the wildtype strain. After finishing a genome editing step with ACE, plasmids are cured by re-streaking alone and now this is also possible with the CGE method where plasmids are removed by the plasmid with the CRISPR array of the next gene target.

Although CGE requires the usage of several antibiotic markers, ACE requires the supplementation of FOA and Uracil and the re-streaking of colonies on plates with different media (CBM, Clostridial Basal Media; RCM, Reinforced Clostridial Growth Medium; 2xYTG) to isolate mutants with correct modification and plasmid loss. Both methods require the availability of previously constructed plasmids such as pMTL-KS15, pMTL-AGH12 for ACE and *catP* or *ermB* and *tetA* containing backbones for CGE. The main advantage of the CGE method compared to ACE is the gene deletion or replacement in a single transformation step with selection for a double-crossover event directly after transformation. The ACE needs the selection first, for a single crossover event and then another selection procedure for the double crossover event followed by recovery of the *pyrE* gene to allow the cultivation under wildtype conditions which again requires its own selection procedure [25, 95]. The *pyrE* gene can either be only restored or an additional gene can be simultaneously inserted or inserted and overexpressed [111].

Drawbacks of the endogenous CRISPR-Cas method were addressed with the CGE method. Nevertheless, only two plasmids were successfully cured from mutants in this work (chapter 5 and 6) and it needs to be considered that there could be difficulties in curing other plasmids. On the one hand, different plasmid sizes or plasmid components, e.g. a stronger replication origin, could influence the efficiency of plasmid curing. On the other hand, if the recognition sequence of the targeted gene is already present on essential parts of the plasmid, re-design might not be possible in every case. Apart from that, it's possible that there are genes that can't be deleted due to absent or not recognized target sequences. It's crucial to consider these points in plasmid design for the application of the developed CGE method. In summary, it is the first time that the endogenous CRISPR-Cas method was applied to delete multiple genes in *C. pasteurianum* with the intention to change the metabolism and the developed CGE method opens a broad range of possibilities and provides a new tool for researchers to alter the genome of *C. pasteurianum* for other desired applications.

4.2.5 Impact of genomic modifications on the metabolism (AR-I, BD-II)

The genomic modifications resulted in lower growth rates for both mutants under iron excess and limited conditions, although this observation can also be due to the metabolic burden to replicate a plasmid under selective pressure. Growth inhibitory effects were reported previously with

heterologous expression of the glycine synthase system in the wildtype [22], showing that metabolic changes can negatively affect the growth of *C. pasteurianum*. Characteristic for fermentations of the wildtype under iron excess conditions is a higher butanol production than PDO production and on the other hand, significantly more PDO is produced under iron limited conditions [31].

The genomic modification of the mutant AR-I was expected to decrease butanol production while increasing PDO production and the additional deletion in the mutant BD-II was supposed to enhance this metabolic shift, but the presented data indicated the opposite effect. Under iron excess conditions, PDO yield in fermentations with mutant AR-I (0.11 g g^{-1}) is 31% lower and butanol yield (0.25 g g^{-1}) is 14% higher compared to fermentations with the wildtype. These changes in production levels do not represent improvements toward a high PDO yield of 0.52 g g^{-1} and no butanol production as reported for strain G8 (Table 2-1) [16]. A possible explanation could be that the other two remaining butanol dehydrogenase genes are upregulated in the absence of the deleted genes leading to even more butanol compared to the wildtype. The butanol dehydrogenase gene *adh2* was replaced with the gene encoding PDO dehydrogenase *dhaTC8*, which was introduced with its own promoter, but it's not guaranteed that this introduced gene is correctly expressed.

Under iron limited conditions, a positive effect occurred with mutant AR-I, which showed a 25% higher PDO yield compared to the wildtype, but larger standard deviations were observed and mutant BD-II only produces PDO in comparable levels as the wildtype, even though this mutant carries an additional gene deletion compared to mutant AR-I. The carbon distributions showed that the carbons are directed towards lactate instead and thus indicating that the combination of two deletions of butanol dehydrogenase genes lead unexpected changes in regulation of metabolite productions. In the next chapter, a third gene encoding butyryl-CoA dehydrogenase will be deleted in the mutant BD-II and the effect of three combined modifications will be evaluated.

4.3 Conclusion

Previous synthetic biology works with *Clostridium pasteurianum* mainly created mutants with single genomic modification (chapter 2.2.1), which were already carried out with the utilization of endogenous CRISPR-Cas machineries by using the method reported by Pyne et al. (2016) [23]. The CRISPR array was included on the plasmids to target the genome of unmodified cells and this selection tool allowed to isolate mutants with modifications that were created by homologous recombination events. However, deletion of multiple genes of competing pathways is necessary for stable introduction of novel pathways.

There were critical points to consider for the realization of the presented CGE system, because only one gene can be deleted with the available methods and two genes to be deleted are not always next to each other on the genome. For this purpose, a developed procedure is provided to enable consecutive genome modifications. Findings in this chapter showed that genetic engineering can have an unexpected impact on the metabolism of *C. pasteurianum* and it's the first time that the endogenous CRISPR-Cas method was applied to delete two separate genes in a single mutant. The successfully created mutant BD-II carries two different modifications on the genome of the same mutant which was not possible with the available methods before. The two modifications were verified by PCR and Sanger sequencing in this chapter, but desired changes in production of PDO and butanol were only observed under iron limited conditions. It can be concluded that the deleted genes are likely not the main reason for high PDO production in strain C8 and even the combination of deletions did not contribute to lower butanol levels as reported for the strain C8 [106].

It was necessary to remove the first plasmid pAR because when an additional third genome editing step is desired, another plasmid needs to be introduced which again carries the same antibiotic marker as the first plasmid pAR. Curing of plasmids with a CRISPR array was not possible before and this was solved with the presented method which can be applied on any gene on the genome without the need for a specific host strain. The development of plasmids to create such a mutant and a stable method for the selection with erythromycin enables the realization of a consecutive genome editing system for *C. pasteurianum*. The developed method gives the opportunity to modify the genome of *C. pasteurianum* for desired applications and to improve our knowledge about this microorganism.

5 Consecutive genome editing and analysis of impact on PDO production

The objective of this chapter is to create a *C. pasteurianum* R525 mutant which is similar to *C. pasteurianum* C8 to verify if the differences between these two strains (chapter 2.1.4) could lead to the reported high PDO production from glycerol with *C. pasteurianum* C8. The gained knowledge could be used to improve a mutant for PDO production from glucose. *C. pasteurianum* R525 carries four butanol dehydrogenase genes (*adh1*, *adh2*, *bdhA1*, *bdhA2*) compared to two genes in *C. pasteurianum* C8 (*adh1*, *bdhA1*) and the overexpression by the presence of two additional butanol dehydrogenase genes might be the reason of the high butanol production with *C. pasteurianum* R525 (chapter 2.1.4). Another gene that has a different copy number on the genome of both strains is the 1,3-propanediol dehydrogenase (*dhaT*) and *C. pasteurianum* C8 carries two genes that encode for this enzyme compared to one gene (*dhaTR*) in *C. pasteurianum* R525. The second copy of this gene (*dhaTC8*) may lead to a higher production of PDO with the accompanying NADH consumption through the reductive pathway.

The last difference, which is examined in this chapter, is the butyryl-CoA dehydrogenase gene, which is present twice on the genome of strain R525 (*bcd1*, *bcd2*) and only once on the genome of the strain C8 (*bcd2*). Therefore, targets include the modification of the genome of *C. pasteurianum* R525 using plasmids for deletion of genes encoding for *adh2*, *bdhA2* and *bcd1*. In the previous chapter, a gene encoding butanol dehydrogenase gene *adh2* was replaced with PDO dehydrogenase gene *dhaTC8*, but increased PDO production was not observed. In this chapter, PDO dehydrogenase genes *dhaTC8* and *dhaTR* are overexpressed in strain R525 to determine the impact on PDO production without genome modifications.

In the next step, the work of this chapter was continued with mutant BD-II of the previous chapter and the utilized plasmid pBD carried a part of the *bcd1* gene. This enables the deletion of *bcd1* as the third genome modification in the same mutant. Shuttle vectors were constructed using *E. coli* followed by verification of correct construction by Sanger sequencing before transformation into *C. pasteurianum* R525 using electrotransformation. Batch fermentations were carried out in 1 L DASGIP fermentation setups with different conditions for characterization of the resulting mutants and these were compared with fermentations of the wildtype under the same conditions.

5.1 Results

5.1.1 Isolation of mutants DX, DY, BC-I and BC-III

Different plasmids were constructed in this chapter to create mutants where genes were deleted (BC-I, BC-III) or overexpressed (DX, DY). Target of genome editing plasmid pBC (chapter 3.6.2) was deletion of the butyryl-CoA dehydrogenase gene (*bcd1*) and the objective is to verify if the differences to the *C. pasteurianum* R525 strain could lead to the enhanced PDO production from glycerol in *C. pasteurianum* C8. While constructing the plasmid pDX (chapter 0), sequencing showed that the *dhaTC8* gene, which was amplified from the genome of strain C8, apparently showed many mutations. After analyzing the sequencing result, it became clear that the sequence actually corresponds to the sequence of the *dhaTR* from *C. pasteurianum* R525. This means that the wrong *dhaT* gene was amplified and in this case, it was not possible to design other primers on the same positions at the beginning and at the end of the *dhaTC8* gene because these regions share almost the same sequence in both genes of *dhaT* in *C. pasteurianum* C8. This problem was solved by amplifying a larger PCR product first, which contains the *dhaTC8* gene. The primers were designed so that this PCR product only contains the *dhaTC8* and not the *dhaTR* gene. The *dhaTC8* gene was amplified again from the new PCR product and fused into plasmid pDX. After another sequencing of the plasmid, the correct sequence with the *dhaTC8* gene was verified.

5.1.1.1 Mutants for overexpression of *dhaTC8* and *dhaTR*

The plasmids pDX and pDY (chapter 0) were successfully constructed for the overexpression of genes *dhaTC8* and *dhaTR*, respectively, and transformed into *C. pasteurianum* R525. The transformation efficiencies of $2.34 \pm 0.98 \times 10^1$ and $1.24 \pm 0.90 \times 10^2$ CFU μg_{DNA}^{-1} for transformations with plasmids pDX and pDY, respectively, were calculated with equation (1) and are summarized in Table 5-1. These transformation efficiencies were two to three orders of magnitude lower compared to maximum transformation efficiency of 7.5×10^4 CFU μg_{DNA}^{-1} with the optimized electrotransformation protocol reported by Pyne et al. (2013) [20], but they were sufficient to isolate the mutants for overexpression. These two plasmids are not genome editing plasmids and therefore no PCR amplification of a targeted genome region is required. The isolated mutants were cultivated in a 1 L DASGIP bioreactor system and the 1st pre-culture was prepared in 2xYTG medium which contained 5 g L^{-1} glucose while the 2nd pre-culture was prepared in MS medium with 40 g L^{-1} glycerol prior to the inoculation of the bioreactors.

The quality of the 2nd pre-culture is important for a stable fermentation run, because long lag-phases or no growth can occur with pre-cultures with too low OD_{600}. In the beginning, it was noticed that the quality of the 2nd pre-culture was different each time, sometimes there was barely growth ($OD_{600} < 1$) and other times pre-cultures were growing but the OD_{600} was not sufficiently high ($1 < OD_{600} < 2$). According to Sabra et al. (2014) [29], cell growth stops after glucose limitation when *C. pasteurianum* is grown with glucose and glycerol. This could be a possible reason for low OD_{600} in the 2nd pre-culture with glycerol because it is inoculated with the 1st pre-culture which contains glucose. As soon as the cells start to grow in the 2nd pre-culture and consume the remaining glucose that was taken from the 1st pre-culture, glucose limitation occurs and cell growth stops. In order to verify this assumption, the medium of the 1st pre-culture was changed to 2xYTC3 which contained 10 g L^{-1} glycerol instead of glucose. The growth of the 2nd pre-culture resulted in more reliable and higher OD_{600} ($2 < OD_{600} < 5$) and this change for the 1st pre-culture was carried out for all further fermentations with glycerol as carbon source.

Table 5-1: Pulse parameters and transformation efficiencies from the electrotransformation of *C. pasteurianum* R525 with the plasmids pDX and pDY. CFU: colony forming units, E_T: transformation efficiency.

Strain	Plasmid	Voltage [V]	Time constant [ms]	Colonies [CFU]	E_T [CFU μg_{DNA}^{-1}]	Average E_T [CFU μg_{DNA}^{-1}]
R525	pDX	1789	9.2	6	12.76	23.4 ± 9.75
		1796	18.0	15	31.91	
		1794	14.8	12	25.53	
	pDY	1790	10.5	24	51.14	123.60 ± 89.58
		1791	11.1	45	95.90	
		1791	11.8	105	223.76	

5.1.1.2 Verification of *bcd1* deletion

The genome editing plasmid for deletion of butyryl-CoA dehydrogenase gene *bcd1* was named p_bcd1-del (pBC) and two different 36 bp spacer sequences were tested for the CRISPR array (Table 8-2). First, pBC with spacer 1 (chapter 3.6.2) was transformed into strain R525 and correct deletion was successfully isolated from one of the picked single colonies resulting in the mutant named *C. pasteurianum* R525+pBC (BC-I). In order to create a mutant with three editing targets (*adh2*, *bdhA2 and bcd1*), plasmid pBC with spacer 1 was transformed into mutant BD-II, but no mutant with three modifications could be isolated. It was assumed that spacer 1 of pBC was actually

not functional, because only one of the picked colonies showed correct deletion by chance in mutant BC-I. Therefore, the same transformation was tried with plasmid pBC with spacer 2 and the mutant with all three desired genome modifications was successfully isolated and verified, resulting in the mutant which was called BC-III (Figure 5-1).

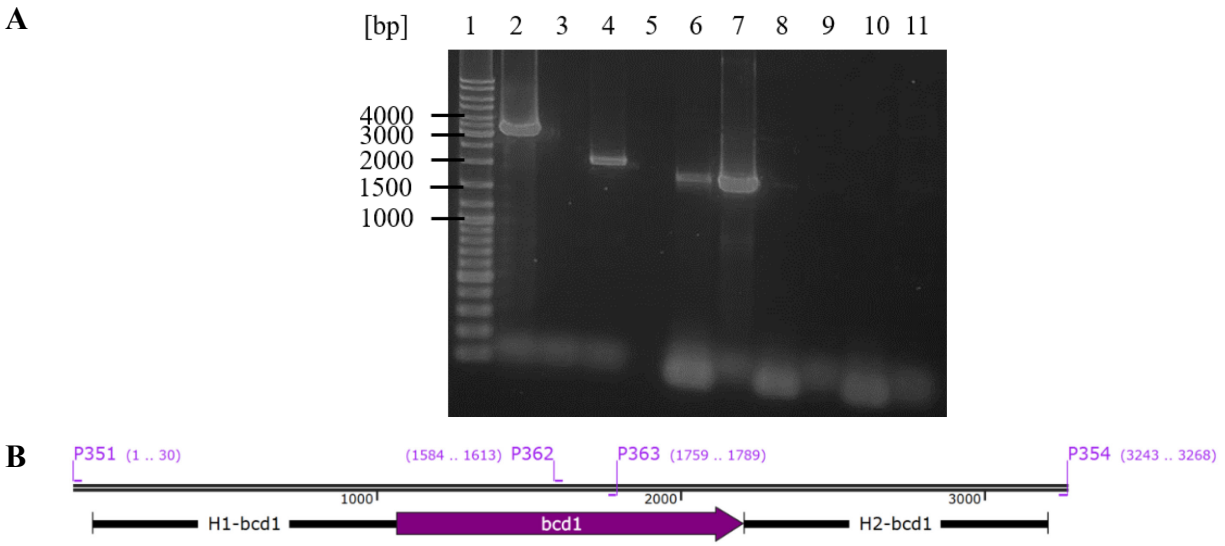

Figure 5-1: Verification of the third genome modification of mutant BC-III. A: Gel picture with PCR products for verification. Lane 1: GeneRuler DNA Ladder Mix; Lane 2; PCR reaction with primers P351 and P354 for wildtype genome; Lane 3: for negative control with water; Lane 4: for genome of the mutant BC-III; Lane 5: empty space; Lane 6-7: PCR reactions with alternating primer pairs P351 and 363 or P354 and P362 for wildtype genome; Lane 8-9: for negative control with water; Lane 10-11: for genome of the mutant BC-III. **B**: region of *bcd1* gene on the genome of the wildtype R525.

Only verification of the third modification is shown, *bcd1* deletion in this case, because first (AR-I) and second (BD-II) modifications resulted in same gel pictures as in Figure 4-3 and Figure 4-4. Lanes 2 and 4 in Figure 5-1A show that PCR amplification of the *bcd1* region with primers P351 and P354 is shorter (2128 bp) than same PCR product from the R525 genome (3268 bp) and this means that *bcd1* gene was successfully deleted. As shown in Figure 5-1B, primers P362 and P363 can only anneal on the *bcd1* gene and only PCR products from the wildtype genome should be visible when deletion of *bcd1* was successful and PCR products in lanes 6 and 7 in Figure 5-1A show the expected lengths of 1789 and 1685 bp, respectively.

5.1.2 Fermentations with glycerol as sole carbon source

5.1.2.1 Characterization of mutants DX and DY

The mutant *C. pasteurianum* R525+pDY (DY) was created as an additional control strain, which carries a plasmid for the overexpression of the PDO dehydrogenase gene from strain R525 (*dhaTR*). This mutant was created to determine if PDO production is enhanced by the overexpression of the native *dhaTR* gene. Batch fermentation results are presented in Figure 5-2 (A, F) and Figure 5-3 (A, F) below for iron excess and limited conditions, respectively. Overall, when comparing the results from different fermentations it can be useful to determine which strain shows the highest yield under the same fermentation conditions. As already observed in fermentations under iron excess conditions in the previous chapter, highest yield of mutant DY was observed for butanol with 0.23 ± 0.00 g g^{-1} followed by PDO with 0.15 ± 0.01 g g^{-1} (Table 5-2). In the case of iron limited conditions, PDO reached the highest yield of 0.29 ± 0.09 g g^{-1} followed by lactate with 0.27 ± 0.02 g g^{-1} and butanol with 0.09 ± 0.00 g g^{-1}. On the one hand, both PDO and butanol yields are similar compared to the yields from fermentations under iron excess conditions with the wildtype (Table 4-2), but on the other hand, PDO yield is 21% higher and butanol is 31% lower under iron limited conditions for mutant DY. Interestingly, overexpression of *dhaTR* led to 108% higher lactate yield under iron limited conditions.

Another mutant *C. pasteurianum* R525+pDX (DX) was created by the introduction of the plasmid pDX which carries the gene *dhaTC8* together with a promoter and terminator for overexpression and batch fermentation results are presented in Figure 5-2 (B, G) and Figure 5-3 (B, G) for iron excess and limited conditions, respectively. Under iron excess conditions, PDO and butanol were produced at similar levels with yields of 0.19 ± 0.01 and 0.18 ± 0.00 g g^{-1} (Table 5-2). In the case of iron limited conditions, PDO reached the highest yield of 0.32 ± 0.05 g g^{-1} followed by lactate with 0.17 ± 0.08 g g^{-1}, while butanol reached 0.05 ± 0.03 g g^{-1}. Therefore, higher substrate specific PDO yield and lower butanol yield were reached in comparison to the wildtype R525 under both iron excess and limited conditions. The largest difference was observed under iron limited conditions with up to 33% higher PDO yield and 62% lower butanol yield. The growth rates from fermentations with mutants DY and DX were lower in all cases with a lowest value of 0.07 ± 0.01 h^{-1} compared to 0.22 ± 0.01 h^{-1} with the wildtype.

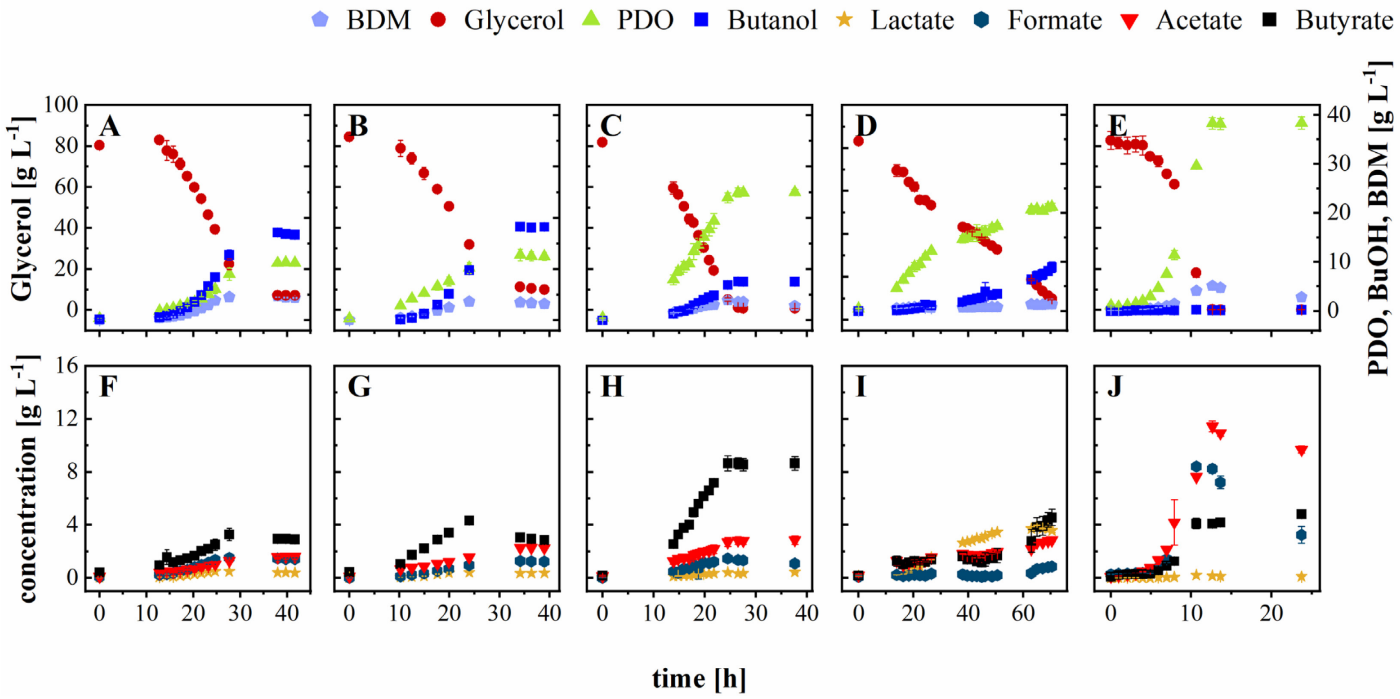

Figure 5-2: Batch fermentations of DY, DX, BC-I, BC-III and C8 with glycerol under iron excess conditions. A, F: *C. pasteurianum* R525+pDY (DY); **B, G**: *C. pasteurianum* R525+pDX (DX), **C, H**: *C. pasteurianum* R525+pBC (BC-I); **D, I**: *C. pasteurianum* R525+pAR+pBD+pBC (BC-III); **E, J**: *C. pasteurianum* C8. Fermentations were carried out with addition 80 g L^{-1} glycerol and 100 mg L^{-1} $FeSO_4$ * $7H_2O$, pH maintained at 6.5, temperature controlled at 35°C and stirrer set to 400 rpm. The error bars show the standard deviation from fermentations conducted in duplicates. PDO: 1,3-propanediol, BuOH: butanol, BDM: bio dry mass.

Fermentation parameters are summarized in Table 5-2 and they were calculated at the time point where maximum biomass concentration was reached. This was the case after 38, 24, 25, 63 and 13 h (iron excess) or 42, 44, 38, 43 and 33 h (iron limited) for mutants DY, DX, BC-I, BC-III and strain C8, respectively. The fermentation parameters were calculated at the time of maximum biomass concentration where maximum product concentration was reached in most fermentations (mutants BC-I, BC-III and strain C8). However, it's important to note that there were fermentations (mutants DY, DX) where product concentrations still increased when biomass concentration decreased. This resulted in different product concentrations at the end of the fermentations, but all fermentation parameters were still determined at the time of maximum biomass concentration for better comparability between all mutants and strains.

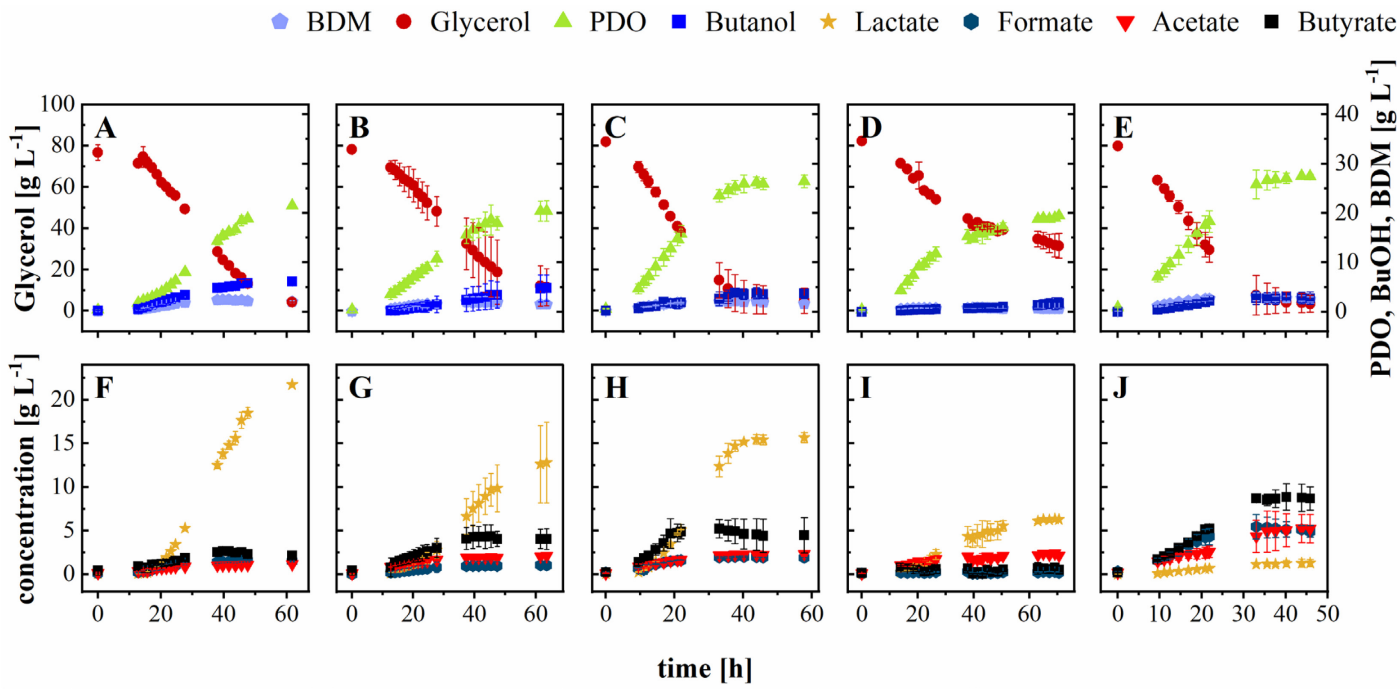

Figure 5-3: Batch fermentations of DY, DX, BC-I, BC-III and C8 with glycerol under iron limited conditions. **A, F**: *C. pasteurianum* R525+pDY (DY); **B, G**: *C. pasteurianum* R525+pDX (DX), **C, H**: *C. pasteurianum* R525+pBC (BC-I); **D, I**: *C. pasteurianum* R525+pAR+pBD+pBC (BC-III); **E, J**: *C. pasteurianum* C8. Fermentations were carried out with addition of 80 g L^{-1} glycerol and 0 mg L^{-1} $FeSO_4$ * $7H_2O$, pH maintained at 6.5, temperature controlled at 35°C and stirrer set to 400 rpm. The error bars show the standard deviation from fermentations conducted in duplicates. PDO: 1,3-propanediol, BuOH: butanol, BDM: bio dry mass.

5.1.2.2 Characterization of mutants BC-I and BC-III

In order to create a mutant with three editing targets (*adh2*, *bdhA2* and *bcd1*), the plasmid pBD was transformed into mutant AR-I resulting in the mutant BD-II (chapter 4.1.2.3). Subsequently, plasmid pBC was transformed into the mutant BD-II resulting in the mutant which was called BC-III. As an additional strain for comparison, plasmid pBC was transformed into strain R525 to create mutant BC-I with a single genome modification. Fermentations with 80 g L^{-1} glycerol were carried out with wildtype R525 as presented previously (Figure 4-5) and with the isolated mutants BC-I and BC-III to determine if the genome modifications had an impact on PDO and butanol production. Additionally, Fermentations with strain C8 were carried out with the conditions reported here for the direct comparison of the fermentation data of the created mutants. The results are shown for iron excess (Figure 5-2) and limited conditions (Figure 5-3).

Under iron excess conditions, glycerol was almost completely consumed during the fermentations with strain C8 and mutant BC-I with overall consumption rates of 6.54 ± 0.34 and 3.13 ± 0.08 g L^{-1} h^{-1}, respectively. In the fermentation with mutant BC-III, a lower glycerol consumption rate of 1.03 ± 0.00 g L^{-1} h^{-1} was reached. PDO yields of 0.45 ± 0.01, 0.31 ± 0.01 and 0.31 ± 0.00 g g^{-1} and butanol yields of 0.00 ± 0.00, 0.09 ± 0.00 and 0.10 ± 0.01 g g^{-1} were reached in the fermentations with strain C8 and mutants BC-I and BC-III, respectively. The results indicate that PDO yield was 94% higher while the butanol yield was 54% (BC-III) or 60% (BC-I) lower compared to the wildtype R525. The produced acid with the highest yield of 0.14 ± 0.00 g g^{-1} was acetate in the C8 fermentation, butyrate in the BC-I fermentation with 0.11 ± 0.01 g g^{-1} and lactate with 0.06 ± 0.00 g g^{-1} in the BC-III fermentation.

The comparison of PDO and butanol yields give a first view on the substrate utilization, but in order to compare the productions of these different strains, biomass specific production rates were calculated. The biomass concentration was significantly lower with mutant BC-III which resulted in similar specific consumption rates with strain C8 and mutants BC-I and BC-III of 1.32 ± 0.04, 0.82 ± 0.05 and 0.81 ± 0.15 g g^{-1} h^{-1}, respectively. In the fermentation with C8, BC-I and BC-III under iron limited conditions, a glycerol consumption rate of 2.19 ± 0.31, 1.95 ± 0.27 and 0.96 ± 0.06 g L^{-1} h^{-1} was reached, respectively, which show lower consumption rates compared to iron excess conditions.

Different amounts of glycerol were consumed in each presented fermentation and the substrate specific yields for PDO and butanol were again calculated. PDO yields of 0.35 ± 0.01, 0.34 ± 0.03 and 0.37 ± 0.07 g g^{-1} and butanol yields of 0.04 ± 0.01, 0.05 ± 0.00 and 0.02 ± 0.00 g g^{-1} were reached in the fermentations with C8, BC-I and BC-III, respectively. The PDO yield for strain C8 was similar to the yield for BC-I, in contrast to what was observed under iron excess conditions, while the results show that mutant BC-III with three modifications reached the highest PDO yield, although not all glycerol was consumed in that BC-III fermentation. Butanol yield was the lowest with mutant BC-III with an 85% lower yield compared to the wildtype R525. Butyrate was the produced acid with the highest yield of 0.12 ± 0.02 g g^{-1} in the C8 fermentation, lactate in the BC-I fermentation with 0.20 ± 0.02 g g^{-1} and again lactate with 0.11 ± 0.04 g gL^{-1} in the BC-III fermentation.

With the amounts of consumed PDO and butanol, the molar PDO/butanol ratios were calculated as 3.31 ± 0.02, 3.07 ± 0.46 and 259.30 ± 33.05 mol mol^{-1} for BC-I, BC-III and C8, respectively, under iron excess conditions (Figure 5-4). The high PDO/butanol ratio for strain C8 results from the highest PDO production and almost no butanol production. All molar ratios are significantly higher compared to the ratio of 0.71 ± 0.14 mol mol^{-1} with wildtype R525. Under iron limited conditions, PDO/butanol ratios were calculated as 6.55 ± 0.39, 18.08 ± 0.70 and 9.57 ± 3.55 mol mol^{-1} for BC-I, BC-III and C8, respectively. These ratios are again higher compared to the value of 1.86 ± 0.15 mol mol^{-1} calculated for the wildtype R525 and the ratio of mutant BC-III is even higher than the ratio of strain C8.

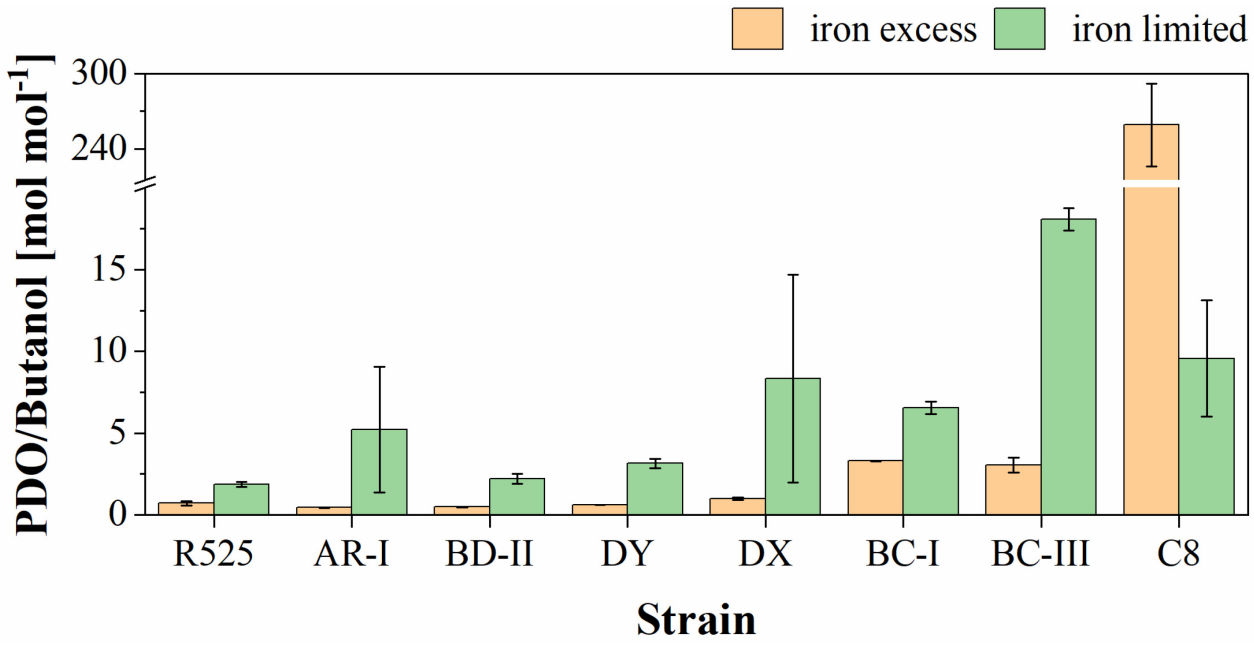

Figure 5-4: Comparison PDO/butanol ratios from fermentations with R525, AR-I, BD-II, DY, DX, BC-I, BC-III and C8. Fermentations were carried out with addition of 100 or 0 mg L^{-1} $FeSO_4$ * $7H_2O$, pH maintained at 6.5, temperature controlled at 35°C and stirrer set to 400 rpm. The error bars show the standard deviation from fermentations conducted in duplicates.

Table 5-2: Fermentation parameters of DY, DX, BC-I, BC-III and C8 under iron excess and limited conditions. The standard deviations are given for fermentations carried out in duplicates. DY: mutant for overexpression of *dhaTR*, DX: mutant for overexpression of *dhaTC8*, BC-I: mutant with deleted *bcd1*, BC-III: mutant with deleted *adh2*, *bdhA2* and *bcd1*. μ: growth rate, $Y_{P/S}$ = substrate specific yield, q_i = specific production rate, C_R: carbon recovery, e_R: electron recovery, BuOH: butanol, LaAc: lactate, PDO: 1,3-propanediol.

Iron excess conditions (100 mg L^{-1} $FeSO_4$ * $7H_2O$)					
Strain:	**DY**	**DX**	**BC-I**	**BC-III**	**C8**
μ [h^{-1}]:	0.12 ± 0.00	0.17 ± 0.00	0.10 ± 0.01	0.05 ± 0.00	0.32 ± 0.00
$Y_{PDO/Glycerol}$ [g g^{-1}]:	0.15 ± 0.01	0.19 ± 0.01	0.31 ± 0.00	0.31 ± 0.01	0.45 ± 0.01
$Y_{BuOH/Glycerol}$ [g g^{-1}]:	0.23 ± 0.00	0.18 ± 0.00	0.09 ± 0.00	0.10 ± 0.01	0.00 ± 0.00
q_{PDO} [g g^{-1} h^{-1}]:	0.06 ± 0.00	0.12 ± 0.01	0.25 ± 0.02	0.25 ± 0.05	0.59 ± 0.00
q_{BuOH} [g g^{-1} h^{-1}]:	0.10 ± 0.00	0.11 ± 0.00	0.07 ± 0.01	0.08 ± 0.01	0.00 ± 0.00
PDO/Butanol [mol mol^{-1}]:	0.62 ± 0.01	0.99 ± 0.06	3.31 ± 0.02	3.07 ± 0.46	259.30 ± 33.05
C_R [%]:	98.70 ± 2.24	102.1 ± 1.20	97.43 ± 0.42	86.60 ± 4.56	94.32 ± 3.91
e_R [%]:	98.16 ± 2.28	100.64 ± 1.27	97.03 ± 0.21	88.27 ± 8.14	93.80 ± 3.74
Iron limited conditions (0 mg L^{-1} $FeSO_4$ * $7H_2O$)					
μ [h^{-1}]:	0.07 ± 0.00	0.07 ± 0.01	0.07 ± 0.02	0.06 ± 0.01	0.09 ± 0.01
$Y_{PDO/Glycerol}$ [g g^{-1}]:	0.29 ± 0.09	0.32 ± 0.04	0.34 ± 0.03	0.37 ± 0.07	0.35 ± 0.01
$Y_{BuOH/Glycerol}$ [g g^{-1}]:	0.09 ± 0.00	0.05 ± 0.03	0.05 ± 0.00	0.02 ± 0.00	0.04 ± 0.01
$Y_{LaAc/\ Glycerol}$ [g g^{-1}]:	0.27 ± 0.02	0.17 ± 0.08	0.20 ± 0.02	0.11 ± 0.04	0.02 ± 0.00
q_{PDO} [g g^{-1} h^{-1}]:	0.16 ± 0.02	0.23 ± 0.10	0.34 ± 0.06	0.52 ± 0.09	0.26 ± 0.04
q_{BuOH} [g g^{-1} h^{-1}]:	0.05 ± 0.00	0.03 ± 0.01	0.05 ± 0.01	0.03 ± 0.00	0.03 ± 0.01
q_{LaAc} [g g^{-1} h^{-1}]:	0.15 ± 0.02	0.13 ± 0.10	0.20 ± 0.04	0.15 ± 0.06	0.01 ± 0.00
PDO/BuOH [mol mol^{-1}]:	3.15 ± 0.29	8.34 ± 6.34	6.55 ± 0.39	18.08 ± 0.70	9.57 ± 3.55
C_R [%]:	102.52 ± 3.16	94.13 ± 0.50	95.57 ± 4.08	71.57 ± 14.85	96.05 ± 8.38
e_R [%]:	100.96 ± 3.25	93.28 ± 0.40	94.92 ± 4.48	74.43 ± 14.52	105.74 ± 22.69

5.1.3 Comparison of carbon distributions

5.1.3.1 Carbon distributions of mutants DX and DY

The results that were observed by the measured metabolite concentrations and calculated yields can also be observed in the carbon distributions (Figure 5-5) and the distributions of wildtype R525 from Figure 4-7 were included as well for a complete comparison. For mutants DX and DY, carbon distributions for metabolites lactate, formate and acetate are in similar ranges without large deviations under iron excess conditions and butyrate shows are larger carbon distribution of 10.10 ± 0.20% for mutant DX in comparison to wildtype R525 (5.41 ± 1.38%). PDO carbon distribution of 22.26 ± 0.93% for mutant DX was higher compared to wildtype R525 (19.46 ± 2.46%) and lower for mutant DY with 18.04 ± 0.29%. The opposite effect was observed for the butanol carbon distribution of 38.75 ± 0.08% for mutant DY which was higher compared to wildtype R525 (36.59 ± 2.61%) and lower for mutant DX with 30.00 ± 0.66%. Overall, carbon distributions of bio dry mass for the mutants are slightly lower under both iron excess and limited conditions.

Under iron limited conditions, PDO carbon distribution was higher for mutant DX with 41.65 ± 4.92% followed by mutant DY with 34.19 ± 0.73% compared to 30.10 ± 0.46% for wildtype R525. Butanol carbon distribution decreased for mutant DX (8.96 ± 6.03%) and mutant DY (14.51 ± 1.03%) compared to 21.64 ± 1.41% for wildtype R525. Butyrate carbon distribution is again increased for mutant DX (10.36 ± 1.15%). Another difference is the carbon distribution for lactate which is higher for mutant DX with 18.81 ± 8.87% and even higher for mutant DY (26.88 ± 0.93%) compared to the wildtype 13.30 ± 8.13%, although standard deviations are relatively large for DX and R525 and therefore only mutant DY showed a statistically higher lactate carbon distribution.

5.1.3.2 Carbon distributions of mutants BC-I, BC-III and strain C8

Under iron excess conditions, carbon distribution of PDO is highest for strain C8 with 57.84 ± 0.72%, followed by 38.00 ± 0.72% and 43.63 ± 3.84% for mutants BC-I and BC-III, respectively. The carbon distribution of butanol is the lowest for the C8 strain with 0.30 ± 0.04%, followed by 15.30 ± 0.39% and 19.05 ± 1.17% for mutants BC-I and BC-III, respectively. In comparison to all strains, carbon distributions of formate and acetate are notably higher for the strain C8 with 6.82 ± 0.20% and 14.87 ± 0.40%, respectively.

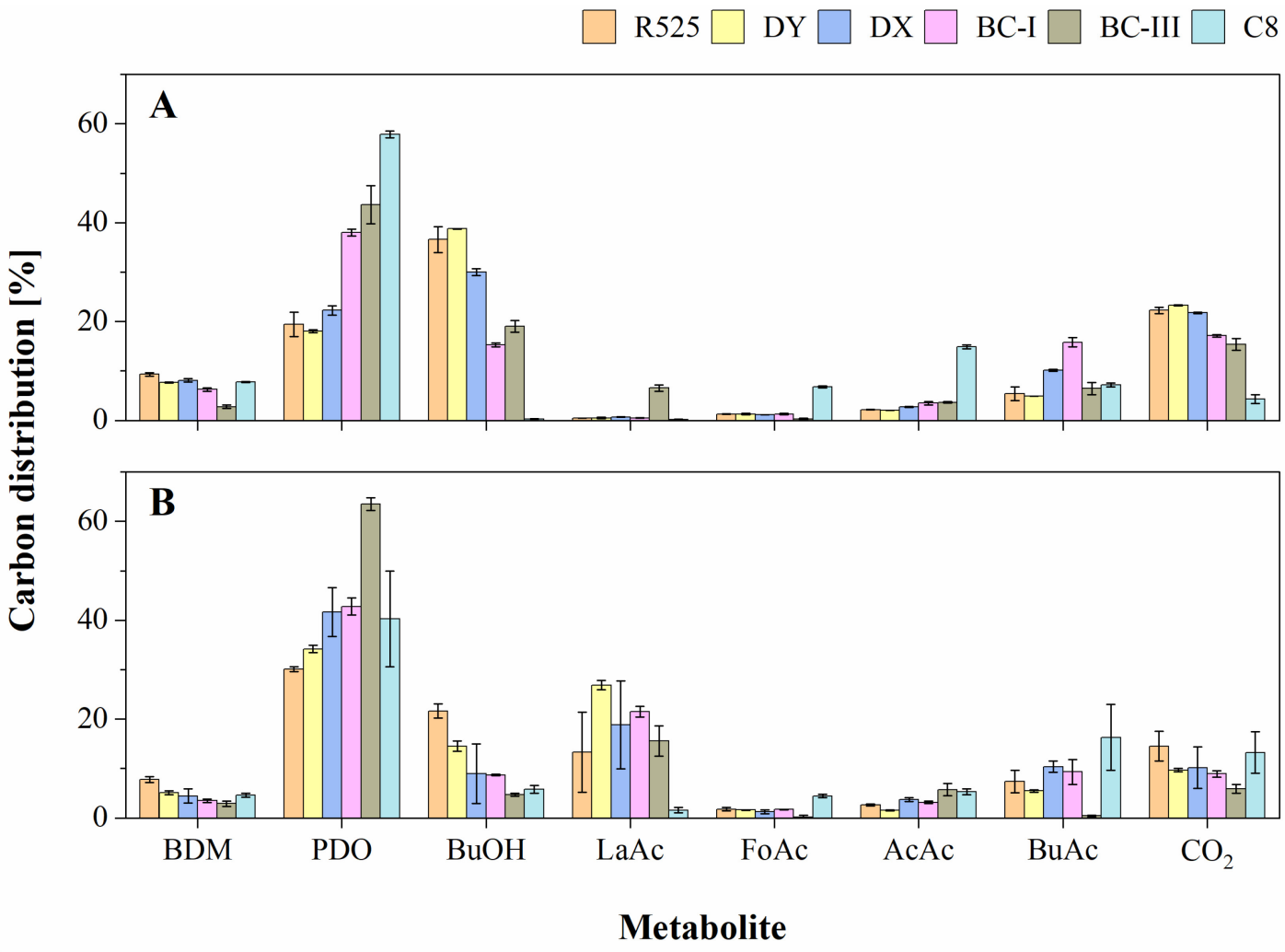

Figure 5-5: Carbon distributions from R525, DY, DX, BC-I, BC-III and C8 fermentations. Fermentations were carried out with addition of 100 mg L^{-1} $FeSO_4$ * $7H_2O$ (**A**) or 0 mg L^{-1} $FeSO_4$ * $7H_2O$ (**B**), pH maintained at 6.5, temperature controlled at 35°C and stirrer set to 400 rpm. The molar concentration of each metabolite was multiplied with the respective number of carbons and each carbon distribution represents the ratio of carbon concentrations between a produced metabolite and the sum of all metabolites. The error bars show the standard deviation from fermentations conducted in duplicates. BDM: bio dry mass, EtOH: ethanol, BuOH: butanol, LaAc: Lactate, FoAc: formate, AcAc: acetate, BuAc: butyrate.

These results show that the PDO and butanol distributions for mutants BC-I and BC-III are closer to the values of the strain C8 under iron excess conditions, but the strain C8 produces even more PDO and less butanol compared to all created mutants. Interestingly, carbon distribution of lactate with mutant BC-III was the highest with 6.57 ± 0.64% compared to the other strains where distributions of only below 1% were reached. Similarly to the mutant DX, carbon distribution of

butyrate with mutant BC-I was highest with 15.79 ± 0.96%. The carbon recoveries (Table 5-2) are slightly below 100% for mutant BC-I and strain C8, but the carbon recovery of 86.60 ± 4.56% for mutant BC-III indicates a significant deviation in comparison to the other fermentations.

Under iron limited conditions, carbon distribution of PDO is highest not for strain C8, but for mutant BC-III with 63.5 ± 1.25%, followed by mutant BC-I mutant and strain C8 with PDO distributions of 42.78 ± 1.74% and 40.28 ± 9.68%, respectively. In contrast to iron excess conditions, PDO carbon distributions are not only closer to the values of strain C8 under iron limited conditions, they are on similar levels for the BC-I mutant or even higher for the BC-III mutant compared to the C8 strain. Carbon distribution for PDO of mutant BC-III was even higher than the highest value under iron excess conditions. Butanol carbon distributions were lower compared to the wildtype R525 (21.64 ± 1.41%) for mutants BC-I and BC-III with values of 8.71 ± 0.16% and 4.69 ± 0.27%, respectively. This time, the difference of butanol distribution of strain C8 (5.76 ± 0.79%) to the other strains is not as high compared to iron excess conditions where no butanol was produced by strain C8. An important change can be observed with the lactate distributions of 21.52 ± 1.09% and 15.6 ± 3.04% for mutants BC-I and BC-III, respectively, which is higher compared to the wildtype under iron limited conditions. Interestingly, barely any carbon distributions of formate and butyrate were observed for mutant BC-III under iron limited conditions.

5.2 Discussion

5.2.1 Overexpression of *dhaTC8* or *dhaTR* and deletion of *bcd1*

5.2.1.1 Impact of *dhaTC8* or *dhaTR* overexpression on PDO and butanol production

In this chapter, overexpression of genes and deletion of single or multiple genes were performed and individual modifications will be examined in the following first. PDO dehydrogenase genes from *C. pasteurianum* R525 (*dhaTR*) and from *C. pasteurianum* C8 (*dhaTC8*) were amplified from the respective genome und cloned on plasmids for the overexpression of these genes. In Zhang et al. (2022) [2] a high production of PDO with a total titer, yield and productivity of 74 g L^{-1}, 0.52 g g^{-1} and 5.3 g L^{-1} h^{-1}, respectively, were reported in a adapted strain *C. pasteurianum* G8 which originates from the strain C8. The intention was to determine, if the additional PDO dehydrogenase gene in strain C8 leads to higher PDO production and redirection of carbons

resulting in less butanol production. The second copy of the PDO dehydrogenase gene may lead to a higher NADH consumption through the reductive pathway for the production of PDO. The presented results from fermentations of mutant DX are proof that overexpression of the *dhatC8* gene from the strain C8 lead to higher substrate specific PDO yields and lower butanol yields in comparison to the wildtype R525 in identical fermentation environments (Figure 5-6). The detection of these differences in the fermentation broth confirms that the overexpression had an effect on the metabolism of the mutant and is different from wildtype *C. pasteurianum* R525. HPLC analysis showed that PDO was also produced in higher amount for the DY mutant, but only under iron limited conditions. Therefore, overexpression of the native *dhaTR* gene did not enhance PDO production in the same way as in the case with *dhaTC8*.

Under iron excess conditions, all four genes encoding butanol dehydrogenases and the PDO dehydrogenase gene are expressed without inhibition. So even if more native PDO dehydrogenase genes are expressed in the cells, the excess amount of butanol dehydrogenase genes dominates the production of metabolites and this could be a reason that no significant change is observed under iron excess conditions for mutant DY. Expression of the gene *dhaTR* already takes place and from the results it's obvious that increased expression of this gene does not improve the overall result. But under iron limited conditions, the pathway towards butanol is partly blocked because of the ferredoxin dependent pathways so that the impact of overexpression of the native PDO dehydrogenase gene is higher in this case and thus increasing the overall PDO production.

When comparing the sequence of the second PDO dehydrogenase gene from *C. pasteurianum* C8 with the gene in *C. pasteurianum* DSM525, they differ by around 9.15% (Table 2-4) [16]. The mutant DY (*dhaTR* overexpression) was created as an additional control to determine if expression of both *dhaTR* and *dhaTC8*, similar as in the strain C8, performs better than only expression of *dhaTR*. The difference in the sequence might be the key for increased PDO production even under iron excess conditions in the mutant DX and further analysis of the activity of both expressed PDO dehydrogenases needs to be examined in future studies. In a next step when inserting the PDO dehydrogenase gene on the genome, the insertion position of the gene *dhaTC8* could play an important role because in *C. pasteurianum* C8, the gene is in the same operon with genes glycerol dehydrogenase (*dhaD*) and dihydroxyacetone kinase (*dhaK*) for the oxidative pathway from

glycerol (Figure 2-2) [16, 106]. The insertion of PDO dehydrogenase gene on the genome was tried for stable expression (data not shown), but not possible without a simultaneous deletion. Therefore, the PDO dehydrogenase gene was overexpressed on a plasmid instead to show the effect of single gene expression.

5.2.1.2 Increased PDO production by deletion of butyryl-CoA dehydrogenase gene

The gene encoding for the butyryl-CoA dehydrogenase *bcd1*, which is involved in the ferredoxin dependent pathway from crotonyl-CoA to butyryl-CoA [21], was deleted in wildtype R525 resulting in the mutant BC-I with a single genomic modification. In addition, *bcd1* was deleted in the mutant BD-II (chapter 4.1.2.3), which already carried two modifications, resulting in the mutant BC-III with three genomic modifications. The increased lactate production with mutants BC-I and BC-III under iron limited conditions indicates that the decrease of butanol production is not fully compensated by higher PDO production. It's partly compensated by the cells by producing more lactate and thus consuming more NADH molecules in the lactate production pathway. An explanation can be given with the pathway map (Figure 2-1) because even if a NADH molecule is consumed for the production of lactate, two NADH molecules are released on the pathways towards lactate. Therefore, formation of lactate results in more NADH molecules in total and is necessary for balance of reducing equivalents while the pathways towards PDO only consume NADH. This observation of competing lactate pathway is limited to mutants originating from strain R525 as large deletions on the lactate dehydrogenase genes in the strain C8 were identified by Zhang et al. 2023 [16] and therefore lactate is barely produced in the strain C8 (chapter 2.1.4).

The results showed that the mutants BC-I and BC-III reached significantly higher PDO yields (0.31 g g^{-1}) compared to the wildtype R525 (0.16 ± 0.02 g g^{-1}), and the yields are closer to the yield of strain C8. However, the yields are still not as high as in the C8 fermentation where an even higher PDO yield of 0.45 ± 0.01 g g^{-1} was reached under iron excess conditions. This PDO yield with strain C8 was achieved in fermentations with the exact same conditions as in the fermentations of the mutants. In fermentations with similar conditions with small differences in medium composition, a PDO yield in a comparable range of 0.50 ± 0.01 g g^{-1} was reached by Zhang et al. (2023) [16]. The PDO yield of mutants BC-I and BC-III is also lower in comparison to reached

yields by other microorganisms in fermentations with pure glycerol (Table 2-1), such as *K. oxytoca* NRCC3006 (0.34 g g^{-1}) [41] and *C. butyricum* AKR102a (0.52 g g^{-1}) [38].

Although the butanol production was decreased for mutants BC-I and BC-III, it was not as low as in the C8 strain where no butanol was produced. In summary, deletion of genes encoding for butanol dehydrogenase and butyryl-CoA dehydrogenase do not completely shut off butanol production in *C. pasteurianum* R525. Although the main differences between strains R525 and C8 were examined in this chapter, there are still other deviations including large deletions in lactate dehydrogenase genes or differences in gene organization of the glycerol uptake operon (Figure 2-2). These can contribute to even more enhanced direction of carbons towards the PDO production pathway resulting in less NADH consumption in the butanol pathway.

5.2.2 Performance of all isolated mutants

5.2.2.1 Comparison of fermentations under iron excess conditions

In order to get an overall overview of all presented data, substrate specific yields for PDO and butanol of isolated mutants DY, DX, BC-I and BC-III are shown in Figure 5-6 (iron excess conditions) together with yields of mutants AR-I and BD-II (chapter 4) and strains R525 and C8. The dashed or dotted lines indicate if the yields are higher or lower compared to the wildtype R525. Under iron excess conditions, only three of the mutants (DX, BC-I, BC-III) show decreased butanol yields and the same mutants show higher PDO yields compared to the wildtype R525. At the same time, deletion of one or two butanol dehydrogenase genes and overexpression of the native PDO dehydrogenase gene *dhaTR* in the remaining mutants (AR-I, BD-II, DY) did not lead to the desired improved performance regarding PDO production. The reason might be the possibility that the remaining butanol dehydrogenase genes are upregulated to compensate for the deleted genes. It can be stated that overexpression of *dhaTC8* in mutant DX had a positive impact on PDO production (increase by 19%), but the effect by deletion of *bcd1* in mutant BC-I and BC-III was much stronger (increase by 94%). Under iron excess conditions, the number of genomic modifications did not play an important role regarding the yield as BC-I and BC-III had very similar PDO and butanol yields.

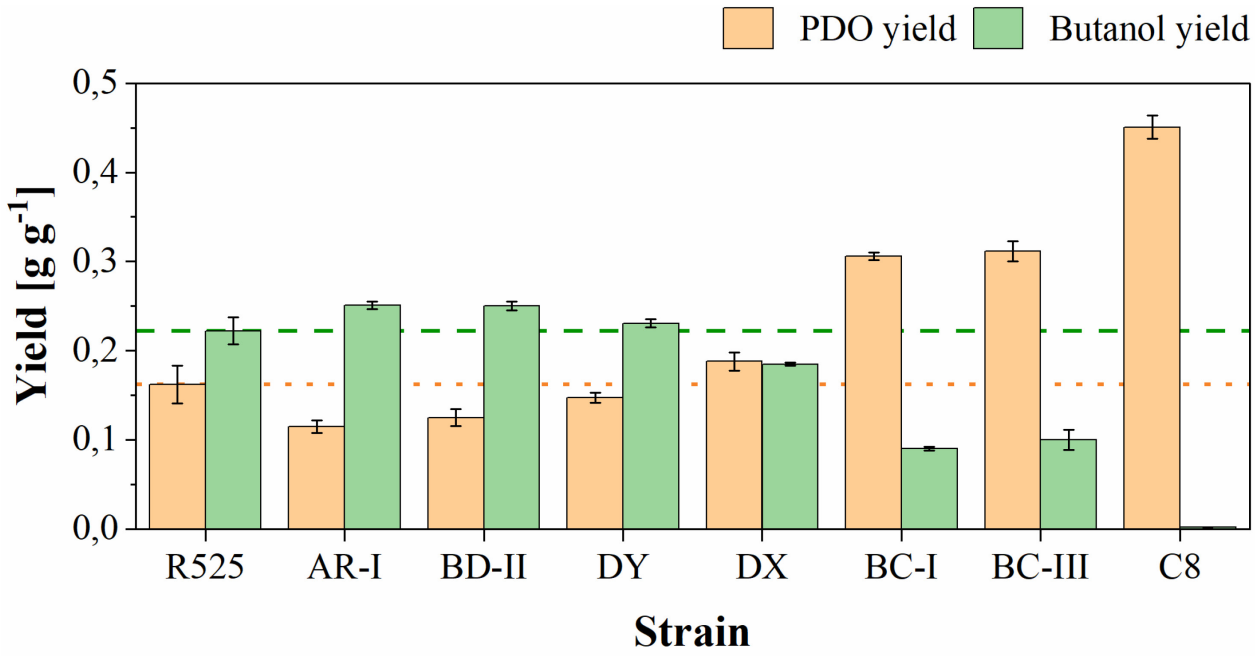

Figure 5-6: Comparison of PDO and butanol yields from fermentations of R525, AR-I, BD-II, DY, DX, BC-I, BC-III and C8 under iron excess conditions. Fermentations were carried out with addition of 100 mg L^{-1} $FeSO_4$ * $7H_2O$, pH maintained at 6.5, temperature controlled at 35°C and stirrer set to 400 rpm. The error bars show the standard deviation from fermentations conducted in duplicates. For comparison purposes, the dashed green line and the dotted orange line show the average butanol and PDO yields of wild type R525, respectively.

However, in the fermentation with BC-III, a glycerol consumption rate of only 1.03 ± 0.00 g L^{-1} h^{-1} was reached, showing a decreased consumption compared to mutant BC-I (3.13 ± 0.08 g L^{-1} h^{-1}) so the higher number of genomic modifications actually had a negative effect. At the same time, biomass concentration was lower with mutant BC-III which resulted in similar specific consumption rates of 0.82 ± 0.05 and 0.81 ± 0.15 g g^{-1} h^{-1} for mutants BC-I and BC-III, respectively. ATP consumption is necessary for biomass formation and it appears that other pathways were favored instead of the biomass growth to keep the intracellular ATP and NADH balances. The carbon recovery of mutant BC-III was only 86.60 ± 4.56% and therefore not complete. It indicates that there were either undetected products from unknown pathways or less substrate was actually consumed than was measured. If the former is the case, these unknown products could be responsible for weakened cell growth and for a previously isolated R525 mutant with deleted glycerol dehydratase large subunit (*dhaB*) [21], it was reported that the genomic modification lead to reduced growth which was also observed in mutants of this work.

The production of PDO and butanol was greatly shifted by metabolic engineering in this work, but there are also other reported ways to influence the molar ratio between these two metabolites. Arbter et al. (2020) [99] exposed the *dhaB*-negativ mutant [21], which didn't produce any PDO and was still able to grow on glycerol, to a cathodic current in a bioelectrochemical system (BES). Electrons from the BES were barely taken up by the cells, but the current resulted in an activation of the butanol pathway by an increase of intracellular NADH/NAD ratio by three to five fold, even though *C. pasteurianum* is not considered to be electroactive. To give a better understanding on the mechanisms that can favor PDO or butanol production in BES cultivations with *C. pasteurianum*, Arbter et al. (2022) [112] developed a system for electrochemical oxidation-reduction potential (ORP) control. This system was able to control the ORP during continuous fermentation and an increase in PDO yield by 57% was observed when the ORP was increased from -462 to -250 mV. Overall, the assumption by Zhang et al. (2023) [16], that butanol production was reduced in *C. pasteurianum* G8 by decreased number of genes encoding butyryl-CoA dehydrogenase, was verified by the presented results in this chapter. Therefore, deletion of the butyryl-CoA dehydrogenase gene led to lower butanol formation because of a weakened bifurcation process catalyzed by the BCdH-ETF complex [16, 36].

5.2.2.2 Comparison of fermentations under iron limited conditions

Under iron limited conditions in Figure 5-7, every single mutant (AR-I, BD-II, DY, DX, BC-I and BC-III) showed higher PDO yield and decreased butanol yield than wildtype R525. Groeger et al. (2017) [31] previously elucidated that iron availability plays a crucial role in fermentations with *C. pasteurianum* and the large differences between fermentations under iron excess and limited conditions of all mutants in this work emphasize these results. The performance regarding PDO production of mutant DX is better compared to mutant AR-I and this means that solely overexpression of *dhaTC8* is sufficient to improve PDO production in *C. pasteurianum* R525 while simultaneous *adh2* deletion is not beneficial, because as mentioned above, the other remaining butanol dehydrogenase genes could potentially be upregulated to compensate for the deleted butanol dehydrogenase gene *adh2*. An unexpected observation was made that deletion of an additional butanol dehydrogenase gene in mutant BD-II apparently showed a worse PDO production compared to mutant AR-I, but there were large standard deviations in the fermentations of mutant AR-I. Thus it cannot be stated with certainty if mutant BD-II produces less or similar

amounts of PDO and when *bcd1* was deleted in mutant BD-II, more PDO and less butanol was produced even in comparison to strain C8.

In contrast to what was observed under iron excess conditions, higher number of genomic modifications in mutant BC-III showed significant improvements with 9% higher PDO and 60% lower butanol yield compared to BC-I. Mutant BC-III carries the modification of mutant AR-I where *dhaTC8* is expressed and this is likely a reason for more PDO and these results suggest that the combination of genomic modifications lead to more improvements in PDO productions under iron limited conditions. However, it needs to be considered that the overall performance depends on the interaction of all single modifications and each modification contributes to changes in metabolic regulations. The latter is particularly important because the combination of three modifications in mutant BC-III inhibited cell growth.

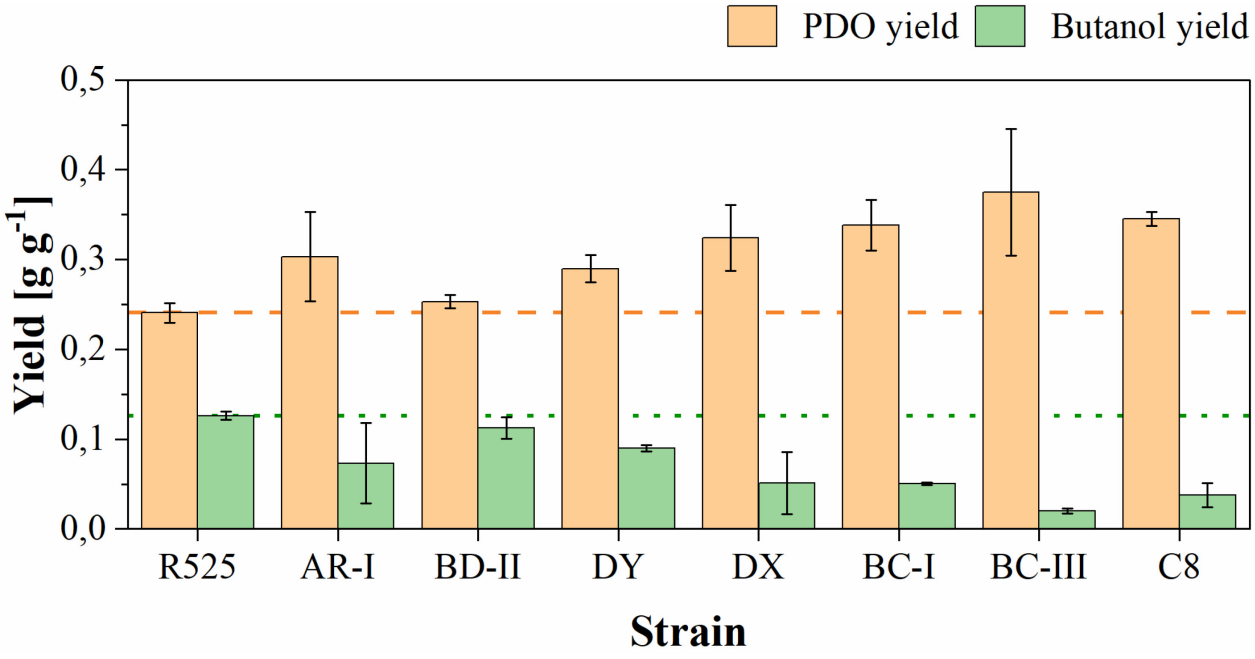

Figure 5-7: Comparison of PDO and butanol yields from fermentations with R525, AR-I, BD-II, DY, DX, BC-I, BC-III and C8 under iron limited conditions. Fermentations were carried out with addition of 0 mg L^{-1} $FeSO_4$ * $7H_2O$, pH maintained at 6.5, temperature controlled at 35°C and stirrer set to 400 rpm. The error bars show the standard deviation from fermentations conducted in duplicates. For comparison purposes, the dashed green line and the dotted orange line show the average butanol and PDO yields of wild type R525, respectively.

5.3 Conclusion

C. pasteurianum C8 was isolated previously and it was found that this strain produces PDO efficiently which was further evolved to metabolize raw glycerol with similar efficiency [2, 15]. The differences of this newly isolated strain showed that it carries two less copies of butanol dehydrogenase genes and an additional PDO dehydrogenase gene (chapter 2.1.4). These findings form the basis for the metabolic engineering work presented in this chapter where experiments were performed to verify if the differences between strain R525 and C8 could be the reason for high PDO production in C8. A newly developed genome editing tool (chapter 4) was applied and it is the first time that up to three genome modifications were carried out with the endogenous CRISPR-Cas method [23] and the impact on the metabolism was examined which revealed various differences to the wildtype for each created mutant.

Overexpression of *dhaTC8* and *bcd1* deletion proved to have the highest impact on enhanced PDO production while deletion of butanol dehydrogenase genes alone was not sufficient under iron excess conditions. However, under iron limited conditions, the pathway towards butanol is weakened and the competition for reducing equivalents in form of NADH is in favor for the pathway towards PDO. The presented results suggest that PDO production can be enhanced by an additional PDO dehydrogenase gene if less butanol is produced under iron limited conditions or if no butanol is produced as in the case with the *C. pasteurianum* C8 strain.

Theoretically, more improvements can be made to produce even more PDO and less butanol. Significant differences were presented between iron excess and limited conditions. This leads to the conclusion that high PDO and low butanol formation under iron limited conditions needs to be combined with great benefits of strong biomass growth under iron excess conditions. Adaptive laboratory evolution (ALE) [2] could be performed to obtain a more stable phenotype and possibly increase biomass formation of mutant BC-III under iron excess conditions. The second goal would be to create an environment which is similar to iron limited conditions by deleting or inhibiting the other ferredoxin dependent pathway which converts pyruvate to acetyl-CoA and CO_2 with the help of enzyme pyruvate ferredoxin oxidoreductase (PFOR) (Figure 2-1). In this case deletion of lactate dehydrogenase genes, similar to large deletions in strain C8, would be necessary so that the metabolism shifts towards PDO and not lactate.

6 Biosynthesis of PDO from glucose in *C. pasteurianum*

Production of PDO from the renewable resource glucose was achieved by development of recombinant *E. coli* strains and was registered in several patents [9, 10, 62–64]. The company DuPont (Wilmington, DE, USA) and the former company Genencor International, Inc. (Palo Alto, CA, USA) established and commercialized the recombinant strains and production processes. However, the introduction of a large set of genes was necessary, because PDO is not natively produced by *E. coli*. Research studies on the characteristic details was prevented due to the broad patenting of the DuPont strains and as a result, other microorganisms such as *Klebsiella pneumoniae* [11, 12] or *Corynebacterium glutamicum* [13] were engineered to produce PDO from glucose (Table 2-1). The objective of this chapter was to initiate a first step toward PDO biosynthesis from glucose in *C. pasteurianum* and study of the introduction of genes glycerol-3-phosphate dehydrogenase (*GPD1*) and glycerol-1-phosphatase (*GPP2*) from *Saccharomyces cerevisiae*, which are not naturally present in *C. pasteurianum*.

Advances in genomic modifications required detailed knowledge about the genome sequence. A draft genome sequence of *C. pasteurianum* was acquired by Rappert et al. (2013) [27] and metabolic engineering was previously performed in this strain by the introduction of a formate consuming pathway [22]. The first part of this chapter describes the construction of plasmids which were used for the overexpression of the genes *GPD1* and *GPP2*. In the second part, the plasmid pDR was constructed for the replacement of genes glycerol dehydrogenase (*dhaD1*) and dihydroxyacetone kinase (*dhaK*) with *GPD1* and *GPP2* on the genome of *C. pasteurianum* R525 resulting in the mutant *C. pasteurianum* R525+pDR (DR-I). The same principle of consecutive genome editing (chapter 4) was used to transform the mutant BD-II, in which butanol dehydrogenase genes *adh2* and *bdhA2* were already deleted, to create the mutant *C. pasteurianum* BD-II+pDR (DR-III). It was not possible to introduce plasmid pDR into mutant BC-III from the previous chapter, because of a different plasmid construction plan and time limitations. Batch fermentations with glucose as carbon source were carried out with different conditions for the characterization of the resulting mutants.

6.1 Results

6.2 Isolation of mutants GG6, GG8, DR-I and DR-III

When constructing the plasmids, a problem often occurred where transposon elements, specifically insertion sequences (IS), were found on the plasmids to be constructed. These are randomly inserted parts from the *E. coli* genome [113], which could be observed by sequencing the plasmid samples leading to undesired plasmids which can't be used for genome engineering without the correct sequence. This problem was addressed by incubating the cells at lower temperatures after the chemical transformation into *E. coli*, using a different medium which contains more nutrients for the cells (SOC instead of LB medium) and selecting only the smallest colonies from the agar plates. These adjustments were made with the assumption that the *E. coli* cells are exposed to increased stress conditions by the introduction of the plasmid and the expression of the genes present on it. Cells that insert transposon elements into the plasmid are able to grow faster because the genes are inactivated and this is favored at the optimum temperature for growth for *E. coli* at 37°C. By lowering the incubation temperature to 30°C, more time to grow is given to cells that carry the new plasmid and by picking the smallest colonies, not the fastest growing cells are picked, but the ones that more likely carry the plasmid.

6.2.1 *C. pasteurianum* mutants for overexpression of *GPD1* and *GPP2*

A total of four different plasmids (pGG2, pGG4, pGG6 and pGG8) were designed to be transformed into *C. pasteurianum* (chapter 3.5.1). The plasmids overexpress *GPD1* and *GPP2* as single genes (pGG2 and pGG6), but also as combined genes (pGG4 and pGG8) which are connected by a linker [65], so that both genes become a fusion protein. The first Sanger sequencing attempts while constructing pGG2 showed that the fragment containing the gene *GPD1* was missing in the plasmid, even after several attempts and modification of the parameters for the cloning procedure (changing primer and template concentrations, specifically increasing the concentration of the *GPD1* fragment). Subsequently, only the small colonies instead of the medium-sized ones were picked and the medium was changed from LB to SOC medium. Each cultivation was strictly observed to harvest the cells as soon as an efficient cell density for plasmid isolation was reached. The assembling of plasmids was successful, but the plasmids pGG2, pGG4, pGG6 and pGG8 were sensitive to missense mutations and IS integration within the gene region

as analyzed by Sanger Sequencing and the Basic Local Alignment Search Tool (BLAST) from the National Centre for Biotechnology Information (NCBI).

Even with the new medium and cell density observation, the construction of plasmid pGG2 and pGG4 failed. The sequence of the IS element was analyzed by NCBI BLAST to be of an IS4 family transposase and the inhibited growth of transformed *E. coli* was also observed during cultivations in liquid medium. All of them needed about 17 h to 40 h to reach an acceptable density for plasmid isolation, which was 3 h to 26 h longer than the growth of untransformed *E. coli*. Constructed plasmids were transformed into *E. coli* and into *E. coli* + pFnuDIIMKn for methylation and colony formation was observed on selective agar plates after successful transformations. The plasmid was taken up by the cells and expresses antibiotic resistance but Sanger sequencing is required in order to make sure that the correct plasmid was assembled. Colony PCR was not used for verification because this method was sufficient to indicate the correct assembly of all needed PCR fragments of a vector but it was not precise enough to indicate the insertion or deletion of bases or fragments. That is why Sanger sequencing was used as the primary verification tool to verify correct plasmid sequence. Correct sequences were only verified for plasmids pGG6 and pGG8 and transformation into *C. pasteurianum* R525 resulted in mutants GG6 and GG8, respectively.

6.2.2 Replacement of *dhaD1* and *dhaK* with *GPD1* and *GPP2*

The initial construction plan of plasmid pDR contained an inducible promoter next to the pCB102 replication origin for testing the so-called conditional replicon which is used for plasmid curing, a required step after each editing step of consecutive genome editing. The basic principle is the interference of plasmid replication by transcription into the pCB102 replication region which would lead to plasmid loss [114]. This effect could be triggered by placing an inducible promoter upstream of the replication origin. Examples are promoters which are inducible by arabinose (*Clostridium acetobutylicum*) [115], xylose (*Clostridium difficile*) [116, 117], lactose (*Clostridium perfringens*) [118, 119], laminaribiose (*Clostridium thermocellum*) [120] and anhydrotetracycline (*Clostridium acetobutylicum*) [121]. Reporter genes such as *mCherryOpt* [117, 122] or the oxygen independent flavin mononucleotide (FMN)–based fluorescent protein (FbFP) [123, 124] were applied in these studies to quantify the induction rates. The latter is especially useful because the common green fluorescent protein is generally limited to aerobic microorganisms.

Different inducible promoters were planned for the construction, but no correctly assembled plasmid could be isolated because in all cases transposon elements were occurring, even with adjustments made. The expression leakage in *E. coli* could be the reason and only cells that introduce transposon elements would survive under the selective pressure. Therefore, the conditional replicon was omitted from the construction of plasmid pDR. Cultures of *C. pasteurianum* R525 which were transformed with plasmid pDR were plated on 2xYTG+Tm10 agar plates and the grown colonies (Figure 6-1) show a clear difference in the number of colonies. When transformed with plasmid pDR (spacer 1), the agar plate was filled with colonies and with pDR (spacer 2) only a few colonies are formed. Colonies were picked after electrotransformation and colony-PCR was carried out, but there were not PCR products on the gel for all picked colonies (Figure 6-1). This phenomenon was already observed in previous experiments when colony-PCR was tested with *C. pasteurianum* R525. In order to make sure that all picked colonies can be tested with PCR amplification, genome extraction was carried out after growing the cells in liquid media with thiamphenicol.

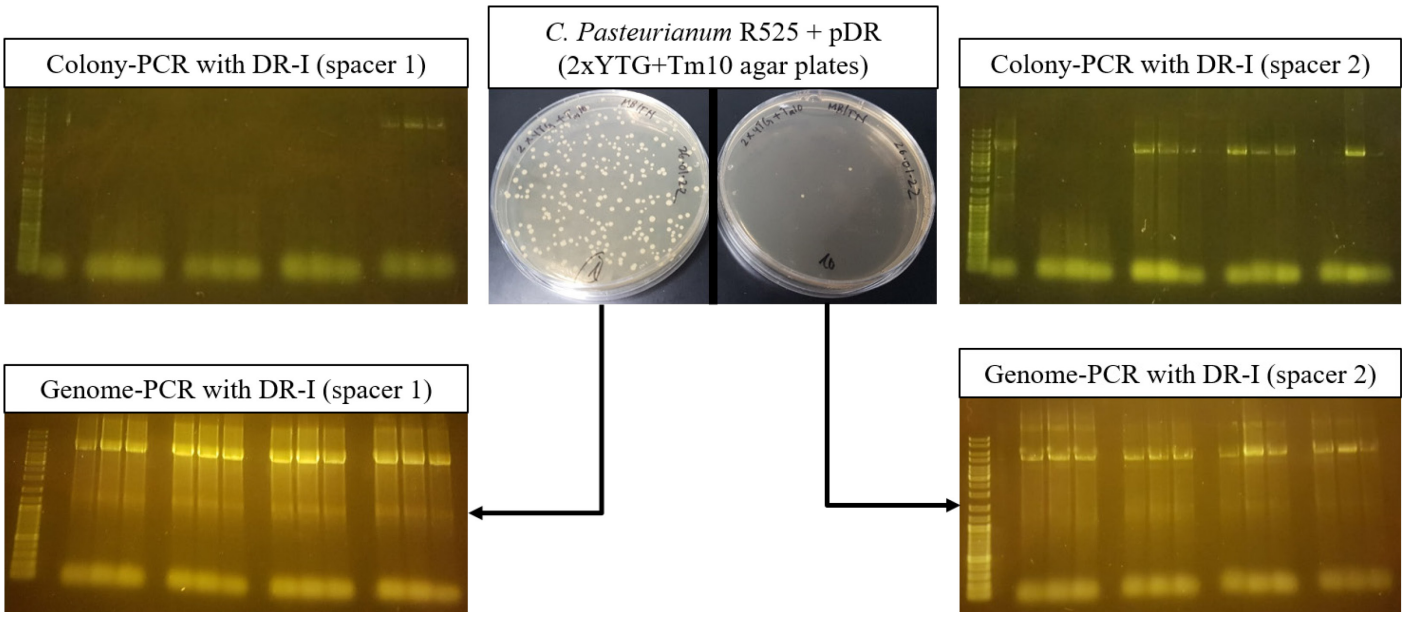

Figure 6-1: Verification of *C. pasteurianum* R525 + pDR (DR-I). 2xYTG+Tm10 agar plates that were plated with cultures containing *C. pasteurianum* R525 transformed with plasmid pDR (spacer 1 or 2) are shown in the middle. Colony-PCR did not show PCR products on the gel for all picked colonies (upper left and right corner). Colonies were then inoculated into liquid 2xYTG+Tm7 medium and PCR was carried out with extracted genomes from grown cultures (lower left and right corner).

PCR amplification worked for all extracted genomes and PCR products were purified and sequenced. Sanger sequencing was carried out for the targeted *dhaD1* and *dhaK* region and only the mutant which was transformed with plasmid pDR with spacer 2 carried the correct gene replacement. Therefore, Figure 6-1 shows that when a functioning spacer sequence is chosen for the CRISPR array, there are only a few colonies. These colonies were only able to survive, because they didn't contain the targeted *dhaD1* gene anymore. In this case high transformation efficiency does not necessarily mean that the genome editing was successful and the sequencing results showed that the genome was altered by introducing the constructed plasmid pDR (with spacer 2) into *C. pasteurianum* R525.

6.2.3 Verification of mutant DR-III

For the third genome modification, mutant BD-II was transformed with the plasmid pDR to create the mutant DR-III. In this mutant, genes encoding glycerol dehydrogenase *dhaD1* and dihydroxyacetone kinase *dhaK* are replaced with the GPD1-GPP2-fusion genes (Figure 6-2). The PCR product around the *dhaD1* and *dhaK* gene should have around the same length as in the wildtype genome, because the length of the inserted *GPD1-GPP2*-fusion gene (2560 bp) is similar compared to the *dhaD1* and *dhaK* genes (2621 bp). Therefore, combinations of alternative primer pairs were used to verify the genome modification. As shown in Figure 6-2B, the primers P155 and P177 can only anneal on the *dhaD1* and *dhaK* genes and only PCR products from the wildtype genome should be visible (Figure 6-2A, lane 9-10).

Similarly in Figure 6-2C, the primers P083 and P008 can only anneal on the *GPD1-GPP2*-fusion gene and this means that only PCR products should appear from the genome of the mutant (Figure 6-2A, lane 6-7). All PCR products in lane 6, 7, 9 and 10 in Figure 6-2A show the expected lengths of 2019, 2720, 3030 and 3668 bp, respectively, and this shows that the third genome modification was successful. The shown PCR products were amplified from the genome of the same mutant R525+pAR+pBD+pDR (DR-III) and the results verify in summary that this mutant carries all three genome modifications. This successfully created mutant was cultivated under different substrate conditions to analyze if PDO is produced from fermentations with glucose only and the impact on glycerol consumption was determined, because genes from the glycerol oxidation pathway were removed.

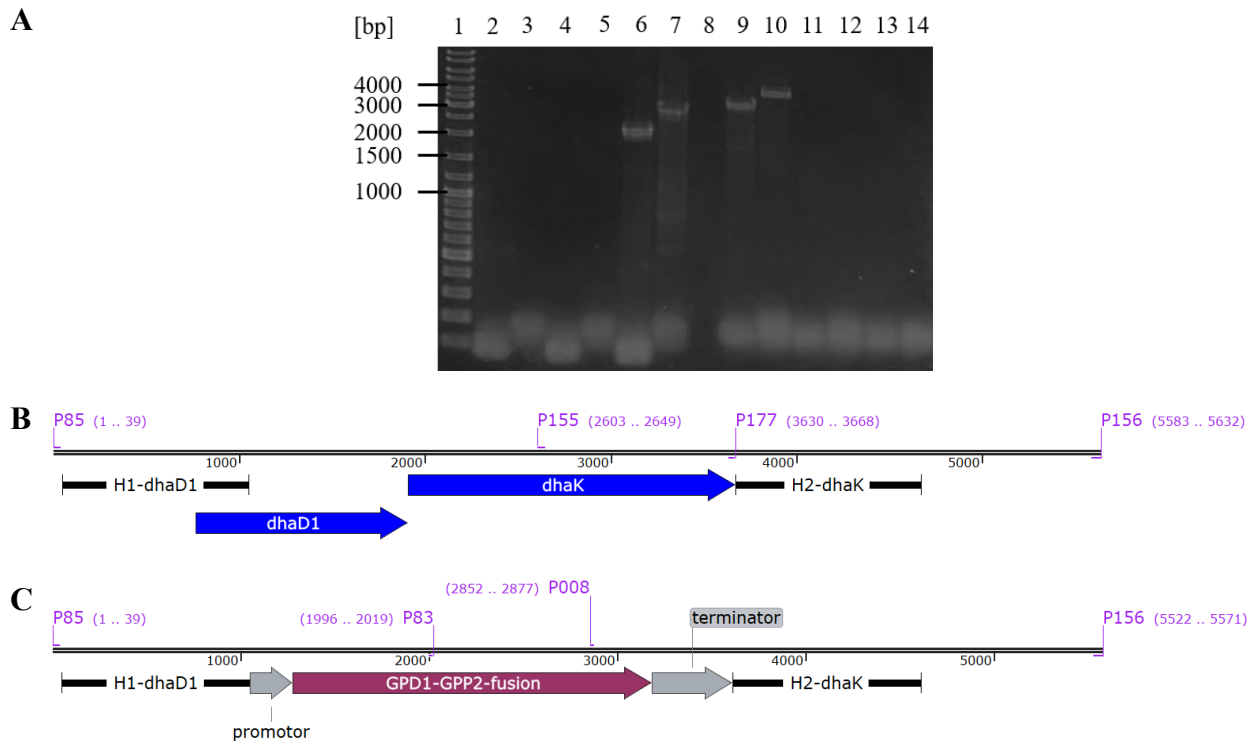

Figure 6-2: Verification of the third genome modification using the plasmid pDR. A: Gel picture with PCR products for the verification. Lane 1: GeneRuler DNA Ladder Mix; Lane 2-3: PCR reactions with alternating primer pairs P85 and P83 or P008 and P156 for the wildtype genome; Lane 4-5: for the negative control with water; Lane 6-7: for the genome of the mutant; Lane 8: empty space; Lane 9-10: PCR reactions with alternating primer pairs P155 and P156 or P85 and P177 for the wildtype genome; Lane 11-12: for the negative control with water; Lane 13-14: for the genome of the mutant. **B**: region of *dhaD1* and *dhaK* genes on the genome of the wildtype, **C**: region of genes replaced with *GPD1*-*GPP2*-fusion on the genome of the mutant DR-III.

6.3 Batch fermentations for the characterization of mutants

6.3.1 Mixed-substrate fermentations with mutants GG6 and GG8

C. pasteurianum R525 was transformed with the plasmids pGG6 and pGG8 and these mutants were named *C. pasteurianum* GG6 and GG8. First, the resulting mutants were cultivated in 1 L DASGIP bioreactors with only glucose, but mixed-substrate fermentations were carried out in the next step, because the target product PDO was not detected from glucose only fermentations (data not shown). From these results it was not clear if the reductive pathway from glycerol to PDO is still active in these new mutants and mixed-substrate fermentations were performed to determine, if PDO production is inhibited by overexpression of genes *GPD1* and *GPP2*. In contrast to other fermentations, no duplicate fermentations were carried out, because the aim was only to

qualitatively find out if PDO production occurs. Batch fermentations with mutants GG6 and GG8 were prepared with the addition of 40 g L^{-1} glucose and glycerol and the measured concentrations during the course of the fermentations are shown in the following Figure 6-3.

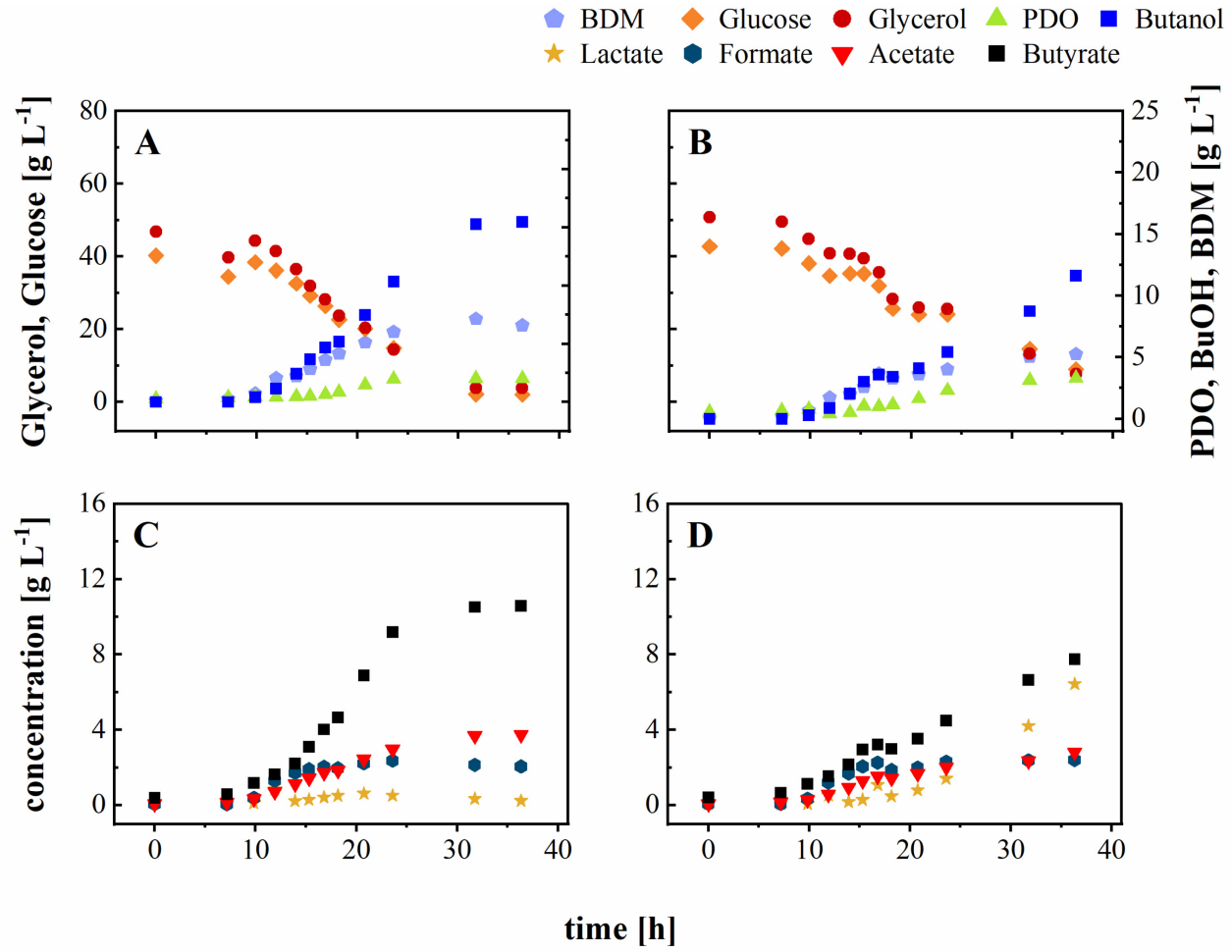

Figure 6-3: Mixed-substrate batch fermentations with mutants GG6 and GG8. A, C: mutant GG6, **B, D**: mutant GG8. Fermentations were carried out with addition of 40 g L^{-1} glycerol, 40 g L^{-1} glucose and 5 mg L^{-1} $FeSO_4$ * $7H_2O$, pH maintained at 6, temperature controlled at 35°C and stirrer set to 400 rpm. PDO: 1,3-propanediol, BuOH: butanol, BDM: bio dry mass. PDO: 1,3-propanediol, BuOH: butanol, BDM: bio dry mass, GG6: *C. pasteurianum* R525+pGG6, GG8: *C. pasteurianum* R525+pGG8.

The main products of the fermentation of mutant GG6 are butanol and butyrate with titers of 15.47 and 10.20 g L^{-1}, respectively, followed by PDO with a titer of 1.76 g L^{-1}. Besides 11.63 g L^{-1} butanol and 7.34 g L^{-1} butyrate, there was also lactate up to 6.38 g L^{-1} in the fermentation of mutant GG8 and PDO titer reached 2.77 g L^{-1}. Therefore, less butanol and butyrate were produced with

mutant GG8 while more lactate and PDO were detected. The fermentation samples that were measured by the HPLC showed a clear peak for the product PDO. From the result is appears that the reductive pathway seems to be active but to make sure if the detected component is really PDO and not 1,2-PDO, it was verified with an additional GC measurement (Table 6-1).

Table 6-1: GC measurement of samples from fermentations of mutants GG6 and GG8. Mixed-substrate fermentations were carried out with addition of 40 g L^{-1} glycerol, 40 g L^{-1} glucose and 5 mg L^{-1} $FeSO_4$ * $7H_2O$, pH maintained at 6, temperature controlled at 35°C and stirrer set to 400 rpm. The last three samples of both fermentations were measured and the concentrations of PDO are shown with the respective standard deviations from duplicate measurements.

Sample No.	Mutant GG6 PDO concentration [g L^{-1}]	Mutant GG8 PDO concentration [g L^{-1}]
10	1,66 ± 0,12	2,09 ± 0,02
11	1,93 ± 0,04	3,20 ± 0,03
12	1,71 ± 0,05	3,26 ± 0,07

As previously mentioned, the plasmids pGG6 and pGG8 contain the genes *GPD1* and *GPP2* as single (pGG6) or as fusion genes (pGG8). The outcome of the fermentations reveals that the reductive pathway from glycerol to PDO is still active after the introduction of these plasmids. In conclusion, overexpression of *GPD1* and *GPP2* was not the reason that PDO was not produced in fermentations with glucose as sole carbon source in these mutants. When glycerol is produced from glucose by the introduction of *GPD1* and *GPP2*, glycerol can be converted into DHA instead of PDO (Figure 2-1). Therefore, the next chapter examines whether PDO can be detected by deleting the oxidative pathway from glycerol to dihydroxyacetone-3-phosphate (DHAP). It's important to note that the fermentation parameters were calculated for the time point at the end of each fermentation. In contrast to the fermentations with glycerol as sole carbon source (chapter 5), cell growth already declined in the glucose fermentations shortly after the lag phase and before the substrate was fully consumed. Product concentrations still increased when biomass concentration decreased so all fermentation parameters were determined when the fermentation was finished for better comparability between mutants and strains from fermentations with glucose.

6.3.2 *C. pasteurianum* R525 + pDR (DR-I)

C. pasteurianum R525 was transformed with plasmid pDR resulting in mutant DR-I and the construction of the genome editing plasmid was described in chapter 3.6.3. Batch fermentations were carried out with 80 g L^{-1} glucose and 20 g L^{-1} glycerol or only with 80 g L^{-1} glucose as a sole carbon source with 5 mg L^{-1} $FeSO_4$ (Figure 6-4). The carbon source glucose was consumed in all bioreactors over the course of the fermentation and in Figure 6-4B, it can be seen that the glycerol consumption is less compared to what was observed for the wildtype in chapter 4.1.3 (almost complete consumption of glycerol) and the glycerol was also not entirely consumed here.

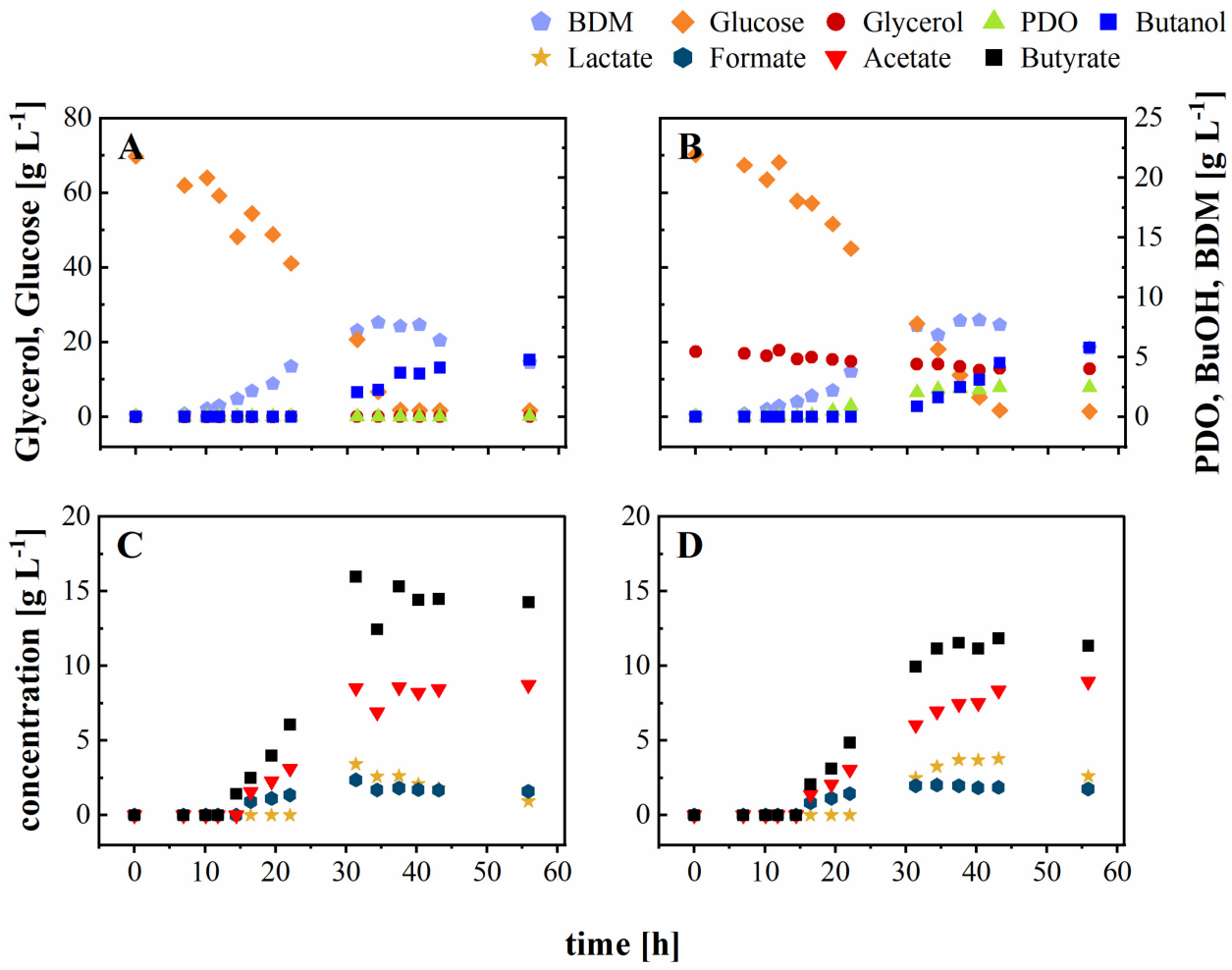

Figure 6-4: Batch fermentations with mutant DR-I. A, C: Addition of 80 g L^{-1} glucose, **B, D**: addition of 80 g L^{-1} glucose, 20 g L^{-1} glycerol. Fermentations were carried out with addition of 5 mg L^{-1} $FeSO_4$ * $7H_2O$, pH maintained at 6, temperature controlled at 35°C and stirrer set to 400 rpm. PDO: 1,3-propanediol, BuOH: butanol, BDM: bio dry mass. PDO: 1,3-propanediol, BuOH: butanol, BDM: bio dry mass, DR-I: *C. pasteurianum* R525+pDR.

This is reflected in the lower specific glycerol consumption rate of 0.01 g g^{-1} h^{-1} compared to 0.44 ± 0.02 g g^{-1} h^{-1} for wildtype R525, although less iron was added in the DR-I fermentation. The main products from fermentations with only glucose (Figure 6-4A) were butyrate, acetate and butanol and glycerol concentration of up to 124 mg L^{-1} and PDO concentrations of up to 40 mg L^{-1} were measured by the HPLC. During fermentations it was first assumed that PDO was produced, since there was a peak at its retention time of 17.6 min in HPLC measurements. The *C. pasteurianum* R525 mutants with plasmids from the pGG6 series also showed a peak for PDO on the HPLC results but they only produced 1,2-propanediol from glucose as a sole carbon source and no PDO. 1,2-propanediol and PDO have similar retention times (17.4 min and 17.6 min, respectively) as well as structural similarities and that is the reason why the last two samples of the fermentation with only glucose were analyzed by GC-MS [125].

A

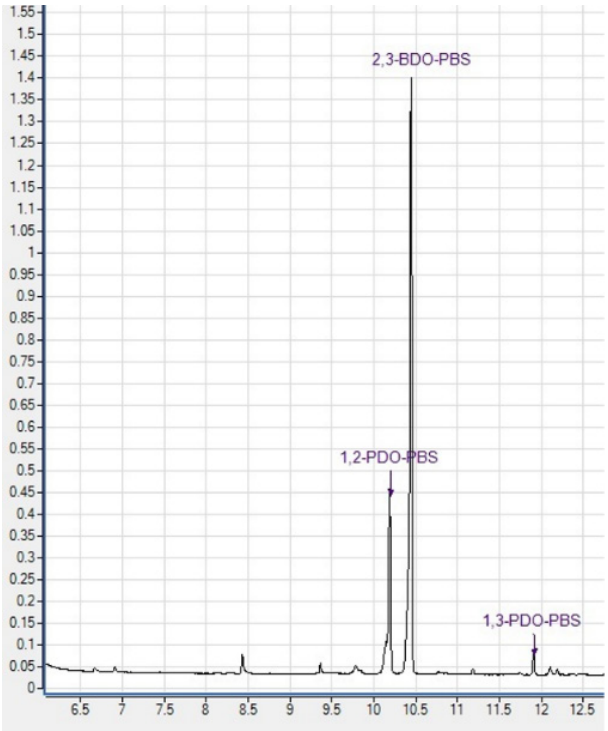

B

Sample	**1,2-propanediol-PBA derivative**	**1,3-propanediol-PBA derivative**
/	[mg L^{-1}]	[mg L^{-1}]
R4-13	31	< 5
R4-14	37	< 5
Milli-Q	<1	< 1

Figure 6-5: GC-MS measurement of fermentation samples. A: measurement with 1,2-PDO, 2,3-BDO and 1,3-PDO peaks, **B**: 1,2-propanediol and 1,3-propanediol quantifications. PBA: phenylboronic acid.

Appropriate calibration standards were prepared and the results are summarized in the following. The detected PDO peak on the HPLC for the last sample R4-14 consists of mainly 37 mg L^{-1} 1,2-PDO, but this time there was also PDO produced with a concentration below 5 mg L^{-1}. Milli-Q water was measured as a negative control and the fermentation samples also showed a large peak for the product 2,3-BDO which was not reported to be a metabolite when fermenting *C. pasteurianum* before (Figure 6-5A). 2,3-BDO has three stereoisomers (D(-), L(+) and meso-form) and it was attempted to determine which stereoisomer was produced. However, the retention times and mass spectra were identical so it was not possible to differentiate the 2,3-BDO stereoisomers at this point.

6.3.3 *C. pasteurianum* mutant DR-III

The third modification of *C. pasteurianum* R525+pAR+pBD+pDR (DR-III) was created by replacing the genes *dhaD1* and *dhaK* from the oxidative pathway, which convert glycerol to DHAP, with the fusion gene *GPD1-GPP2*. It was found that *C. pasteurianum* can be cultivated with mixed substrates which can lead to enhanced growth when a limitation of either substrate is avoided [1, 29]. The ability to metabolize the substrates glycerol and glucose together was used to study the influence of the genome modifications on the metabolism of DR-III and for comparison, fermentations with 80 g L^{-1} glucose and 20 g L^{-1} glycerol were also carried out with the wildtype R525 (Figure 6-6). As shown in Figure 6-6A, B, the glucose was fully consumed over the course of the fermentation of both wildtype and DR-III with specific glucose consumption rates of 0.41 ± 0.02 g g^{-1} h^{-1} (R525) and 0.59 ± 0.04 g g^{-1} h^{-1} (DR-III), respectively, although some glucose was lost due to the autoclaving process.

At the same time, specific glycerol consumption rate of DR-III with 0.08 ± 0.00 g g^{-1} h^{-1} was lower compared to a consumption rate of 0.13 ± 0.01 g g^{-1} h^{-1} of the wildtype. The glycerol was completely consumed after a fermentation time of 34 h in the wildtype, while 12.07 ± 0.42 g L^{-1} glycerol was still remaining after 70 h with mutant DR-III. Therefore, a decrease of the glycerol consumption during the fermentation could be observed for the mutant, similarly to what was observed with mutant DR-I. This shows that the genome modifications had a clear influence on the substrate utilization. Usually, a portion of the glycerol is oxidized to dihydroxyacetone (DHA) by *dhaD1* and phosphorylated by *dhaK* for subsequent transfer to glycolysis (Figure 2-1).

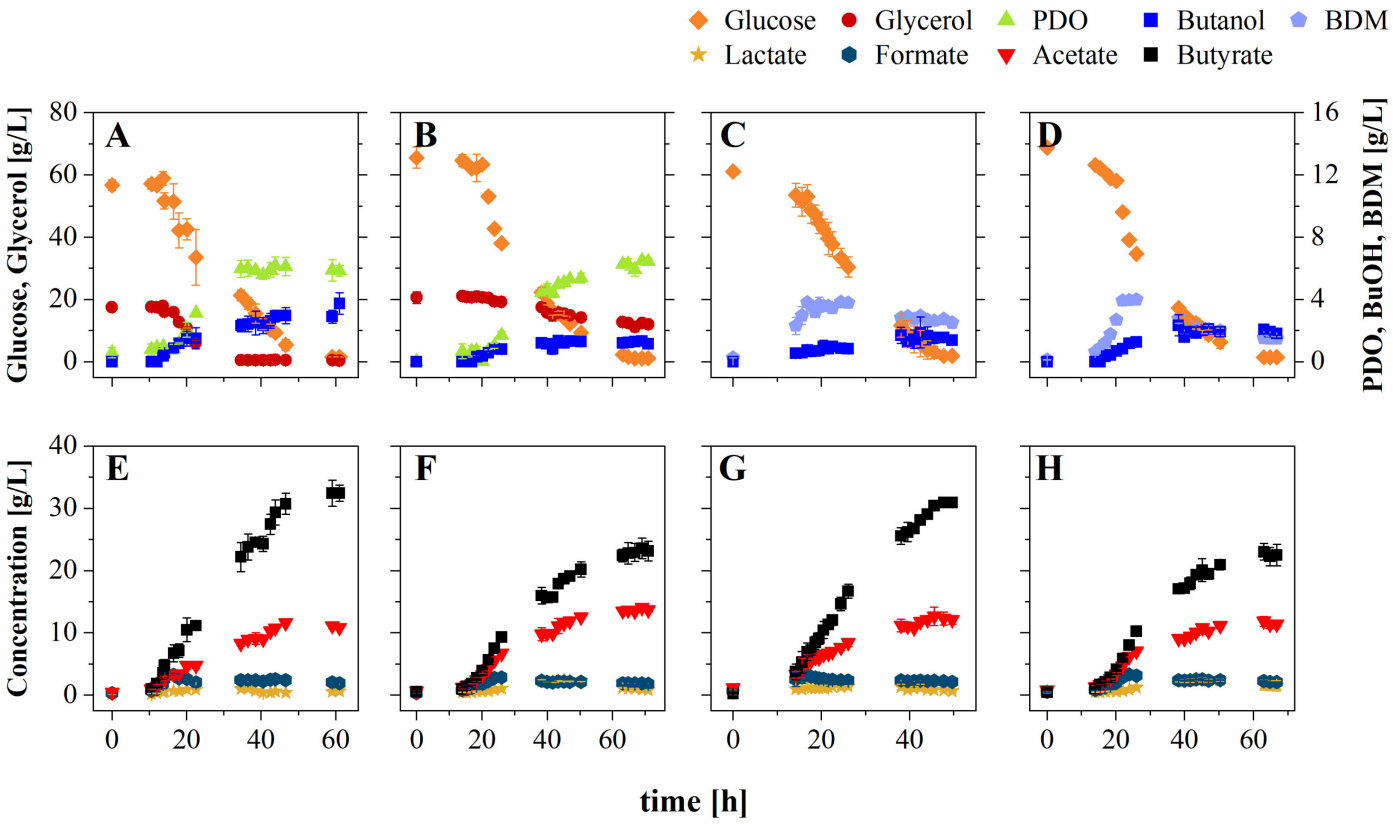

Figure 6-6: Batch fermentation data of R525 and mutant DR-III. A, E: R525 with 80 g L^{-1} glucose and 20 g L^{-1} glycerol; **B, F**: DR-III with 80 g L^{-1} glucose and 20 g L^{-1} glycerol; **C, G**: R525 with 80 g L^{-1} glucose; **D, H**: DR-III with 80 g L^{-1} glucose. Fermentation were carried out with addition of 100 mg L^{-1} $FeSO_4$ * $7H_2O$ under iron excess conditions, pH maintained at 6.5, temperature controlled at 35°C and stirrer set to 400 rpm. The error bars show the standard deviation from mixed substrate fermentations conducted in duplicates. BuOH: Butanol, BDM: Bio dry mass.

The remaining part of the glycerol is first dehydrated to 3-hydroxypropionaldehyde (3-HPA) and next reduced to PDO [4]. In contrast to what was observed for mutant BC-III (chapter 5), glucose consumption rates were not severely inhibited for the mutant DR-III which carries three genomic modifications. This leads to the conclusion that *bcd1* deletion in combination with *adh2* and *bdhA2* deletion was the reason for lower substrate consumption and not necessarily the higher number of genomic modifications. However, when the molar yield for PDO was calculated with the assumption that glycerol was the only substrate for PDO production in the mutant, a value of 0.93 ± 0.19 mol mol^{-1} was obtained. The calculation indicates that a part of the glycerol is still converted into another intermediate and the reason is likely the second glycerol dehydrogenase *dhaD2* so that glycerol could still be consumed to form DHA and therefore *dhaD2* would be a possible future

deletion target. This consideration neglects the fact that glycerol can also be produced from the new pathway by the *GPD1* and *GPP2* genes and thus decreases the overall, calculated glycerol consumption. It is assumed that the produced amount of glycerol is significantly lower compared to the amount of consumed substrate and therefore the observation can be made that a direct change in the substrate consumption was introduced by the modification on the genome level.

Batch fermentations were carried out with 80 g L^{-1} glucose as the sole carbon source under iron excess conditions (100 mg L^{-1} $FeSO_4*7H_2O$). The carbon source glucose is consumed in all fermentations over the course of the cultivation (Figure 6-6C, D) and the main products from glucose fermentations are butyrate and acetate which is displayed in Figure 6-6. The metabolites acetate, lactate and formate reach similar titers for both strains R525 and DR-III with values of 10.59 ± 0.43, 1.03 ± 0.91 and 1.59 ± 0.04 g L^{-1}, respectively. Only butyrate shows a difference by a higher production of 30.65 ± 0.03 g L^{-1} for R525 compared to 22.03 ± 2.13 g L^{-1} for DR-III and this is also reflected in the carbon distributions from glucose fermentations (Figure 6-7A). A higher butanol distribution of 4.44 ± 0.46% with DR-III is shown compared to 2.54 ± 0.26% with R525, but for mixed substrate fermentations (Figure 6-7B), butanol distribution is lower with 2.63 ± 0.32% for DR-III compared to 5.29 ± 0.95% for R525.

The genome modifications, which include the deletion of two butanol dehydrogenase genes, were expected to decrease the butanol production, but this effect was unexpectedly only observed when glycerol was used as a substrate in addition to glucose. In the mixed substrate fermentation, PDO production from glycerol is also possible so that the available reducing equivalents are shifted towards the reductive pathway from glycerol which was enhanced by the introduction of *dhaTC8* in the first genome modification. This improvement in PDO production can also be observed with a higher carbon distribution (Figure 6-7B) of 9.56 ± 0.61% (DR-III) compared to 6.46 ± 0.66% (R525). Similar levels of PDO production were already shown in Figure 6-6A, B for R525 and DR-III, but since the glycerol consumption in the mutant DR-III was lower, glycerol specific yields were calculated as 0.77 ± 0.15 g g^{-1} for DR-III and 0.31 ± 0.05 g g^{-1} for R525 which shows a large increase due to the deletion of the oxidative pathway.

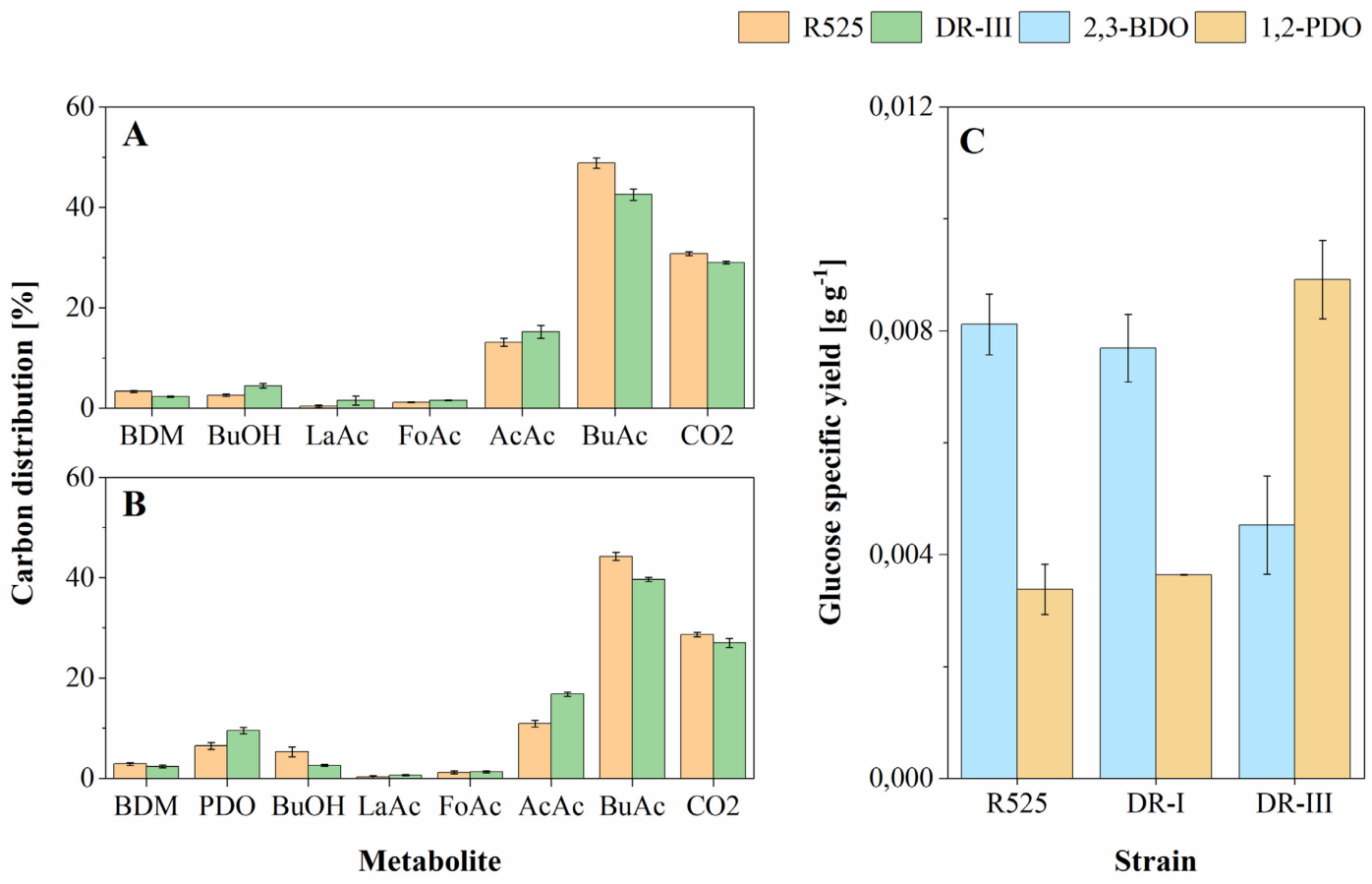

Figure 6-7: Carbon distributions and yields from fermentations with glucose. A: Carbon distributions from fermentations with 80 g L^{-1} glucose, **B**: or 80 g L^{-1} glucose and 20 g L^{-1} glycerol, **C**: Glucose specific yields of 2,3-BDO and 1,2-PDO. The error bars show the standard deviation from duplicate measurements. LaAc: Lactate, FoAc: formate, AcAc: acetate, BuAc: butyrate.

PDO productions of up to 0.97 ± 0.44 g L^{-1} for DR-III were measured by the HPLC in the glucose fermentations, but in order to determine if the detected component corresponds to PDO or another product such as 1,2-PDO, samples were analyzed by GC-MS [125] as it was reported by Pyne et al. (2016) [34] that *C. pasteurianum* is also able to produce 1,2-PDO under certain conditions. The metabolism of *C. pasteurianum* is shown in Figure 2-1 with additionally revealed pathways from previous studies and from findings of this work. The results showed that the detected PDO from the HPLC consists of PDO below a concentration of 10 mg L^{-1} and 600 ± 56.57 mg L^{-1} 1,2-PDO for DR-III. However, also 305 ± 63.64 mg L^{-1} of another unexpected product 2,3-BDO was detected which was not reported to be produced by *C. pasteurianum* before.

For comparison, data from mutant DR-I is included which only carries the third modification of *dhaD1* and *dhaK* replacement with *GPD1* and *GPP2* and the measured values for 1,2-PDO and 2,3-BDO were used to calculate the glucose specific yield (Figure 6-7). The DR-I mutant showed concentrations of 220 ± 0.00 mg L^{-1} 1,2-PDO and 465 ± 35.36 mg L^{-1} 2,3 BDO resulting in a lower 1,2-PDO and higher 2,3-BDO production compared to the DR-III mutant. The difference between these two strains are the first two modifications carried out by the pAR and pBD plasmids, which deleted two butanol dehydrogenase genes with one of them being replaced by *dhaTC8*. During the analysis of the fermentation samples, it was found that 2,3-BDO (480 ± 28.28 mg L^{-1}) is also generally produced in the *C. pasteurianum* wildtype R525 so the formation of 2,3-BDO was not directly triggered by the introduced genome modifications. This metabolite was not reported to be produced by *C. pasteurianum* before so possible pathways are discussed below and the results also show that the production of 2,3-BDO is influenced by the deleted butanol dehydrogenase genes in this work.

Additionally, the results indicate that the first two modifications had a positive impact on 1,2-PDO production but did not increase PDO formation as intended. Surprisingly when measuring samples from R525, traces of PDO were also detected even though there was no pathway for production from glucose in that strain reported. However, frozen cryo-cultures with glycerol were used for all strains and this might explain the PDO that was produced, even in the wildtype fermentation. At this point, several genome modifications were introduced but they didn't result in a sufficient PDO production from glucose compared to the amounts observed with the wildtype. Similar observations of unexpected metabolites inclduing those reported in this work were made in Hong et al. (2020) [22] where the introduction of the glycine synthase system into *C. pasteurianum* lead to the production of 2-oxobutyrate (Figure 2-1). It was reported by Zhang et al. (2023) [16] that the weakened butanol formation pathway in G8, which was developed by adaptive laboratory evolution of C8, might lead to enhanced PDO production from glycerol, but it did not affect the PDO production in this case. The pathway for PDO production was introduced, but the regulation of reducing power and ATP in *C. pasteurianum* can be very sensitive and is a burden for manipulating this strain to produce PDO from glucose. This is an obstacle to overcome, which is discussed in more detail below, in order to shift the carbon flux towards the desired PDO and not to undesired side products.

6.4 Discussion

6.4.1 TCA cycle and NADH generation for PDO production in other bacteria

The results showed that PDO is not produced in sufficient amounts from glucose and a lack of reducing equivalents in the form of NADH could be a possible reason. The pathway map in Figure 2-1 shows that only one NADH molecule is released in the conversion steps from the glycolysis intermediate glyceraldehyde-3-phosphate (GAP) to pyruvate. However, there are two NADH molecules needed for the production of PDO from glucose in the conversion steps of DHAP to glycerol-3-phosphate and from 3-HPA to PDO. Therefore, twice as many NADH molecules are needed and there is always an undersupply so it's plausible that the production pathway from glucose to PDO is not favored by the cells. The supply of reducing equivalents is not a problem for aerobic bacteria such as *E. coli* because the citric acid cycle or tricarboxylic acid cycle (TCA cycle) is active and provides enough NADH for the oxidative phosphorylation and processes that require electron donors [12, 37]. For each pyruvate molecule which is produced from glycolysis, three NADH molecules are released from the citric acid cycle. Hong (2022) [93] proposed an incomplete bifurcated TCA "cycle" in *C. pasteurianum* similar to one present in *C. acetobutylicum* [126], but not all necessary genes are present for the TCA cycle in these obligate anaerobic bacteria [26].

The consequence is a shortage of NADH while facultative anaerobic bacteria including *Corynebacterium glutamicum* [13] and *Klebsiella pneumoniae* [11, 12] were successfully engineered to produce PDO from glucose. Some of the necessary genes for the TCA cycle are already available so one could attempt to engineer a complete cycle in *C. pasteurianum* by adding missing genes such as the 2-oxoglutarate dehydrogenase. This would provide NADH via the conversion of 2-oxoglutarate to succinyl-CoA to generate more NADH, but in order to introduce the full cycle, multiple additional modifications would be needed and that would make it unreasonable to use *C. pasteurianum* as a host strain as other bacteria already carry functioning TCA cycles. Lama et al. (2017 and 2020) demonstrated that the deletion, upregulation or overexpression of a total of 33 genes in *K. pneumoniae* enabled the production of 62 g L^{-1} PDO from glucose in fed-batch culture with a limited supplementation of vitamin B_{12} [11, 12]. The disruption of genes involved in the formation of the five by-products acetate, lactate, ethanol, formate and 2,3-BDO was carried out and this could also be applied in further engineering of *C. pasteurianum* which also produces these metabolites.

Modifications regarding the TCA cycle were also included in other bacteria, but this would not improve the PDO formation without an active TCA cycle in *C. pasteurianum* and the same applies to introduced modifications of genes taking part in the electron transport chain (ETC) where wasteful NADH oxidation through ETC was reduced. Li et al. (2022) reported the metabolic engineering and development of an efficient *C. glutamicum* strain with a titer of 110.4 g L^{-1} PDO from glucose in fed-batch fermentation [13]. Genes involved in the TCA cycle were not directly targeted here, but improved PDO production was achieved by enhancing the regeneration cycle of phosphoenolpyruvate (PEP) because the consumption of PEP was shown to reduce the flux towards PDO [13, 127]. Both strategies for *K. pneumoniae* and *C. glutamicum* required the introduction of a glycerol synthesis pathway as attempted in this report with *C. pasteurianum* and overall, a total of three genome modifications were finished in this work. Although the outcome of thirty more modifications as in the case with *K. pneumoniae* cannot be predicted at this point, the most important changes necessary for *C. pasteurianum* include the modifications which reduce the flux to competing pathways. Furthermore, providing reducing equivalents was crucial for *K. pneumoniae* and *C. glutamicum* and proves to be essential in order to create a promising *C. pasteurianum* host strain for PDO production from glucose.

6.4.2 Possible pathways for formation of 2,3-BDO in *C. pasteurianum*

Other *Clostridia* [128], *Klebsiella* [40, 128, 129] *or Saccharomyces* [130, 131] strains can produce 2,3-BDO, but the detected 2,3-BDO in this work was not reported to be produced by *C. pasteurianum* before and it can be assumed that the 2,3-BDO pathway plays a role in the consumption of excess NADH [132]. Production of 2,3-BDO was reported to be detected by HPLC (0.6 ± 0.29 g L^{-1} after 24 h from 20 g L^{-1} initial glycerol) with *C. pasteurianum* NRRL B-598 (ARS Culture Collection, USA) [128]. But later the complete genome sequence was presented with a single circular chromosome of 6,186,879 bp which is significantly larger than the 4,350,673 bp reported for the complete genome of *C. pasteurianum* DSM525 [28, 133]. A re-classification of *C. pasteurianum* NRRL B-598 to *C. beijerinckii* NRRL B-598 was proposed based on the genome difference and other unexpected traits such as native chloramphenicol/thiamphenicol resistance [134]. Therefore 2,3-BDO production in *C. pasteurianum* is reported for the first time in this work.

Different possible routes exist for the production of 2,3-butanediol in other microorganisms including *Lactococcus lactis* [135] where 2,3-BDO is produced via acetoin which can be produced from α-acetolactic acid or diacetyl in that strain. Song et al. (2019) [136] presents general biological routes for the production of the three isomeric forms of 2,3-BDO and names the necessary key enzymes as α-acetolactate synthase (ALS), α-acetolactate decarboxylase (ALDC) and butanediol dehydrogenase (BDH).

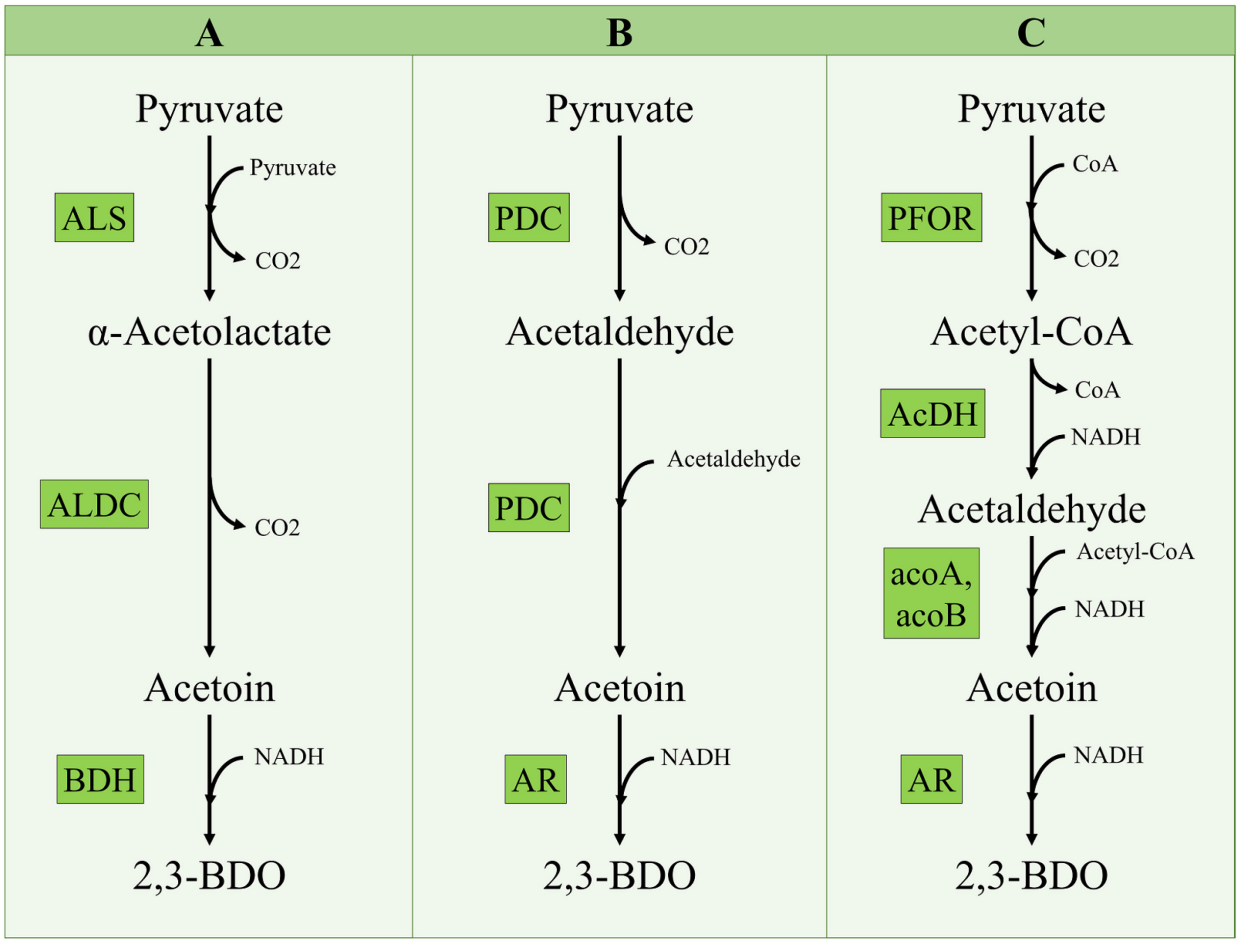

Figure 6-8: Possible pathways for the production of 2,3-BDO from pyruvate. ALS: α-acetolactate synthase, ALDC: α-acetolactate decarboxylase, BDH: 2,3-BDO dehydrogenase, PFOR: pyruvate:ferredoxin oxidoreductase, AcDH: acetaldehyde dehydrogenase, *acoA*, *acoB*: acetoin oxidoreductase.

General production of 2,3-BDO occurs from pyruvate produced from glycolysis and in one of the possible pathways (Figure 6-8A), pyruvate is decarboxylated by the enzyme ALS to form α-

acetolactate, which is further converted in another decarboxylation reaction into acetoin by ALDC. Finally, the acetoin intermediate undergoes a reduction reaction consuming another NADH to produce 2,3-BDO with help of BDH or acetoin reductase (AR) [130]. The genome of *S. cerevisiae* however shows a second possible pathway (Figure 6-8B) for 2,3-BDO production from acetaldehyde due to the absence of ALDC and in this case the pyruvate decarboxylase catalyzes the condensation reaction between two acetaldehyde molecules [130, 137]. In the third possible pathway (Figure 6-8C), acetoin is produced by the condensation of acetaldehyde and acetyl-CoA by acetoin dehydrogenase E1 components (*acoA*, *acoB*) and in order to find out if the necessary genes are present in *C. pasteurianum* for the production of 2,3-BDO, the complete genome [28] was screened.

It was found that the gene for the butanediol dehydrogenase is present as a acetoin reductase (CPAST_c06790) and the components of the acetoin dehydrogenase complex are present as genes that are annotated as "thiamine pyrophosphate-dependent dehydrogenase E1 component subunit alpha" (CPAST_c19650) and „alpha-ketoacid dehydrogenase subunit beta" (CPAST_c19660). The protein IDs were stated as WP_003444341.1 and WP_003444343.1 and the protein research (UniProt accession no. A0A0H3J9W4, A0A0H3J292) proved that these genes are actually the acetoin oxidoreductase subunits alpha and beta (*acoA*, *acoB*). The overexpression of the genes *acoA* and *acoB* from *Bacillus subtilis* in *S. cerevisiae* increased the 2,3-BDO production so based on screening of the *C. pasteurianum* genome, it is likely that *C. pasteurianum* produces 2,3-BDO from acetyl-CoA and acetaldehyde [130]. With the newly developed method, it would be possible to delete both *acoA* and *acoB* in a single mutant in order to verify if these genes are involved in the production of 2,3-BDO in *C. pasteurianum*.

If the prevention of the production of the side product 2,3-BDO is desired, the deletion of the acetoin reductase would be a shorter procedure as only one genome modification would be necessary. To summarize the results of previous studies and results of this work, the introduction of the glycine synthase by Hong et al. (2020) [22] triggered 2-oxobutyrate secretion, the deletion of PDO dehydrogenase gene by Pyne et al. (2016) [34] increased the 1,2-PDO production by 5-fold and the deletion of butanol dehydrogenase genes in this work resulted in decreased 2,3-BDO production while 1,2-PDO formation was increased. The products 2-oxobutyrate, 1,2-PDO and

2,3-BDO are not part of the main metabolites, but their interaction with the central metabolism is summarized in Figure 2-1 and the findings in this work show that genetic engineering can have a significant impact on metabolic regulations in *C. pasteurianum*.

6.4.3 Deletion targets of competing pathways

1,2-PDO can be formed via methylglyoxal which is formed from DHAP by the methylglyoxal synthase *mgsA* [34] and this gene can be a deletion target to block production of undesired 1,2-propanediol. A part of the glycerol was still converted into another intermediate and the reason is likely the second glycerol dehydrogenase gene (*dhaD2*) which would be a possible future deletion target to completely block conversion of glycerol to dihydroxyacetone. Part of the *dhaD2* gene was already included on the plasmid pDR so it is possible to delete this gene in the next genome engineering step. A further deletion target would include the triosephosphate isomerase gene (*tpiA*) to split the metabolism so that half of the carbon can be used in pathways towards pyruvate and the other half can be directed to the desired PDO. PAM sequences (5'-AATTG-3') followed by possible spacer sequences to target the genes *dhaD2* and *tpiA* are included in Table 8-2. The deletion of these targets would show if changes in crucial pathways shift the carbon flux towards the desired product or towards other unexpected products as observed before and it would further improve the understanding about the metabolism of *C. pasteurianum* and other competing pathways. A consecutive genome editing method was successfully developed and it allows the study of several editing steps in contrast to preceding studies where only one modification was considered at a time. It is the first time that the endogenous CRISPR-Cas method was applied to delete multiple genes in *C. pasteurianum* with the developed CGE method. This opens a broad range of possibilities and provides a new tool for researchers to alter the genome of *C. pasteurianum* for desired applications such as deletion of multiple competing pathways.

6.5 Conclusion

In the past, *C. pasteurianum* DSM525 has been cultivated for quite a few purposes by our group and it was found that iron availability plays and important role and can shift the metabolism significantly under iron limited or excess conditions [31]. Glycerol or glucose can be utilized separately as a sole carbon and energy source, but also mixed substrate fermentations were analyzed [1, 29] which were applied in this chapter. In the first part of this chapter, overexpression of *GPD1* and *GPP2* in R525, for introducing a pathway for production of PDO from glucose, didn't result in detectable production levels of PDO, but only of 1,2-PDO. Mixed-substrate fermentations were run with the addition of glycerol and the results show that the reductive pathway for PDO production was not inactivated by overexpression of *GPD1* and *GPP2*.

In the second part of this chapter, the mutant DR-III with three genome modifications was created by introducing the three modifications which are the replacement of the butanol dehydrogenase gene *adh2* with the second PDO dehydrogenase gene *dhaTC8*, deletion of the butanol dehydrogenase gene *bdhA2* and the replacement of the genes *dhaD1* and *dhaK* with *GPD1* and *GPP2*. This mutant showed a difference to R525 in the form of decreased glycerol utilization with a consumption of 8.51 ± 1.43 g L^{-1} (DR-III) compared to 17.06 ± 0.71 g L^{-1} (R525) in mixed-substrate fermentation. The genome modification affected the glycerol oxidation pathway, but when fermentations with only glucose were carried out, only PDO concentrations of below 10 mg L^{-1} were detected so the PDO formation in desired levels from glucose was not observed as intended.

1,2-PDO can be formed via methylglyoxal [34] and 1,2-PDO was detected as another metabolite and additionally 2,3-BDO was detected as an unexpected product which was not reported to be produced by *C. pasteurianum* before. It was concluded that 2,3-BDO is possibly produced via acetyl-CoA and acetaldehyde in *C. pasteurianum*. The products 1,2-PDO and 2,3-BDO are not part of the main metabolites, but their interaction with the central metabolism was summarized in Figure 2-1. The findings in this chapter show that genetic engineering can have a significant impact on metabolic regulations in *C. pasteurianum*, but the regulation of reducing power in *C. pasteurianum* can be very sensitive and is a burden for manipulating this strain to produce PDO from glucose.

7 Summary and Outlook

At the beginning of this work, it was shown that the transformation of *C. pasteurianum* C8 was not possible with the established electrotransformation method developed by Pyne et al. (2013) [20] and applied by Schmitz et al. (2018) [21] and Hong et al. (2020) [22]. Although the transformation of *C. pasteurianum* C8 finally worked by the transformation with a plasmid which was previously isolated from *C. pasteurianum* R525, other attempts including EMS-induced random mutagenesis or methylation by single methyltransferases from strain C8 did not yield successful transformation. Genome editing was not attempted with *C. pasteurianum* C8, because of the low transformation efficiency. High transformation efficiency is required for the transformation of genome editing plasmids which are larger due to the many necessary plasmid components. Further work is necessary to develop an efficient transformation method for *C. pasteurianum* C8 which include protecting the plasmids to be introduced by in-vivo methylation. This might require the protection against several restriction enzymes that cleave different recognition sites and this could be tried with multiple methyltransferases at once or with successive methylations in several steps.

The first step for developing the consecutive genome editing method in this work was testing of antibiotic markers. This was necessary because the *catP* marker was the only marker that functioned reliably with the plasmid construction in *E. coli* 10-beta and selection in *C. pasteurianum* R525. All markers (*ermB*, *tetA*, *aad9*) from the modular system for *Clostridium* shuttle plasmids developed by Heap et al. (2009) [96] were tested and it was found that only combination of *tetA* and *ermB* markers on the same plasmid resulted in successful selection of desired mutants. This finding was used to develop the consecutive genome editing (CGE) system which was applied to create mutants for increased PDO production in fermentations with glycerol. The introduced genome modifications showed a metabolic shift towards PDO production, proving that the absence of the genes *adh2*, *bdhA2* and *bcd1* in *C. pasteurianum* C8 are reasons for high PDO and low butanol production. However, the created mutant could not reach PDO production levels as high as the *C. pasteurianum* C8 strain so further studies are necessary to improve the understanding about the influence of gene organization (chapter 2.1.4) and transcriptional regulation of PDO dehydrogenase on the PDO and butanol production in the C8 strain.

The developed CGE system was also applied to create a mutant for PDO production from glucose, but unexpected metabolites 1,2-PDO and 2,3-BDO were mainly detected. The oxidative pathway from glycerol was deleted and increased PDO production occurred when glycerol was present as a substrate together with glucose. However in contrast to the work from Lama et al. (2020) using a similarly modified strain of *Klebsiella pneumoniae* [11, 12], barely any PDO was produced in fermentations with glucose alone in the created mutant of this work. The results showed that pathways exist that were not reported for *C. pasteurianum* before and they are likely preferred over the pathway towards PDO. It was discussed how these metabolites could possibly be produced in *C. pasteurianum* and the developed CGE method was compared to the ACE method, making clear that certain shortcomings of the ACE methods can be addressed with the developed CGE method. Overall, successive plasmid transformations were verified and they resulted in the desired gene edits, making the CGE system based on endogenous CRISPR-Cas successful.

The application of the developed CGE method requires the usage of several antibiotics so it is not feasible to be transferred to industry because there are problems with antibiotics of different classes in waste streams of wastewater treatment plants (WWTP) which can be hotspots for the spread of antibiotic resistances in the environment. The presence of antibiotics and high diversity of microorganisms in WWTPs can favor the selection of antibiotic-resistance bacteria (ARB) and antibiotic resistance genes (ARG) [138, 139]. The World Health Organization (WHO) has declared that antimicrobial resistances are a major risk for modern medicine and need to be managed urgently [140]. It is also stated that the World Economic Forum identified antibiotic resistances as a global risk that can have significant economic and financial impact in the form of increased health care costs or food production losses, because of resistances against veterinary antimicrobial medicines.

Pazda et al. (2020) showed that ARGs for tetracycline and sulfonamide were enriched after the wastewater treatment process and emphasizes on the significance to implement microbial and antibiotic resistance monitoring [141]. In contrast, the use of several ARGs can be solved by antibiotic-free methods such as the one reported by Brechun et al. (2024) [142]. The essential gene *infA*, encoding for translation initiation factor 1, is controlled by a arabinose-inducible promoter and culture media lacking arabinose induces selection for a plasmid, which carries the endogenous

promoter with the *infA* gene, showing long-term plasmid maintenance. This antibiotic-free selection method could be combined with the consecutive genome editing method to make it less reliable on antibiotic resistance markers, relieved from the metabolic burden coming from expression of ARGs and suitable for industrial application.

An initial goal of this work was to engineer *Clostridium pasteurianum* for the biosynthesis of 1,3-propanediol from glucose, but the results showed that this can't be easily achieved in this microorganism. It was discussed why the desired results did not occur, the lack of free NADH molecules likely inhibited the less favorable PDO production pathway, because the production pathways of ethanol, lactate, 1,2-PDO and 2,3-BDO all require NADH. Deletion of these competing NADH consuming pathways could lead to increased PDO production and additionally, the deletion of the *tpiA* gene could lead to increased flux to PDO production, because the metabolism would be split in half with glyceraldehyde-3-phosphate being converted in the main metabolism, while DHAP could be fully used in the pathway towards PDO. The *dhaD2* gene must also be deleted to prevent glycerol from being converted to metabolites other than PDO. This is possible as the next genome engineering step for mutant DR-III because part of the *dhaD2* gene was already included on the plasmid pDR. The desired engineering of *C. pasteurianum* required the development of a method that can introduce multiple genome modifications in the same mutant which was achieved in the here presented work.

Even the introduction of a single genome modification was very difficult to carry out before this work was initiated, but improvements in sequencing time, multiple sequencing reactions from one single sequencing tube and the storage of sequencing primers at the sequencing facility made the introduction of several modifications in this work possible within a reasonable time. The developed, CGE system was applied to create the mutants of this work and an advantage in comparison to the method used by Ortega (2020) [24] is the gene deletion or replacement in a single transformation step with selection for a double-crossover event directly after transformation. The developed method opens a broad range of possibilities by the introduction of multiple genome modifications which would show the effect of combined changes to the genome. A new tool for researchers is provided to alter the genome of *C. pasteurianum* and is expected to expand the knowledge and understanding of the metabolism in *C. pasteurianum*.

References

1. Sabra W, Wang W, Surandram S et al. (2016) Fermentation of mixed substrates by *Clostridium pasteurianum* and its physiological, metabolic and proteomic characterizations. Microb Cell Fact 15:114. DOI: 10.1186/s12934-016-0497-4
2. Zhang C, Sharma S, Ma C et al. (2022) Strain evolution and novel downstream processing with integrated catalysis enable highly efficient coproduction of 1,3-propanediol and organic acid esters from crude glycerol. Biotechnol Bioeng 119:1450–1466. DOI: 10.1002/bit.28070
3. Biebl H (2001) Fermentation of glycerol by *Clostridium pasteurianum*-batch and continuous culture studies. J Ind Microbiol Biotechnol 27:18–26. DOI: 10.1038/sj.jim.7000155
4. Dabrock B, Bahl H, Gottschalk G (1992) Parameters affecting solvent production by *Clostridium pasteurianum*. Applied and Environmental Microbiology 58:1233–1239. DOI: 10.1128/aem.58.4.1233-1239.1992
5. Biebl H, Marten S, Hippe H et al. (1992) Glycerol conversion to 1, 3-propanediol by newly isolated *clostridia*. Applied Microbiology and Biotechnology 36:592–597. DOI: 10.1007/BF00183234
6. Zeng A-P, Sabra W (2011) Microbial production of diols as platform chemicals: recent progresses. Curr Opin Biotechnol 22:749–757. DOI: 10.1016/j.copbio.2011.05.005
7. Biebl H, Menzel K, Zeng AP et al. (1999) Microbial production of 1,3-propanediol. Applied Microbiology and Biotechnology 52:289–297. DOI: 10.1007/s002530051523.
8. Research and Markets (2024) Global 1,3-propanediol market (PDO) by production (bio-based PDO, petrochemical-based PDO), distribution Channel (offline, online), application - Forecast 2024-2030: https://www.researchandmarkets.com/reports/5968203/global-13-propanediol-market-pdo-production (accessed May 2024).
9. Emptage M, Haynie SL, Laffend LA et al. (2003) Process for the biological production of 1,3-propanediol with high titer. US Patent No. 6,514,733 B1
10. Nakamura CE, Gatenby AA, Hsu AK-H et al. (2000) Method for the production of 1, 3-propanediol by recombinant microorganisms. US Patent No. 6,013,494
11. Lama S, Seol E, Park S (2017) Metabolic engineering of *Klebsiella pneumoniae* J2B for the production of 1,3-propanediol from glucose. Bioresource Technology 245:1542–1550. DOI: 10.1016/j.biortech.2017.05.052

12. Lama S, Seol E, Park S (2020) Development of *Klebsiella pneumoniae* J2B as microbial cell factory for the production of 1,3-propanediol from glucose. Metabolic Engineering 62:116–125. DOI: 10.1016/j.ymben.2020.09.001
13. Li Z, Dong Y, Liu Y et al. (2022) Systems metabolic engineering of *Corynebacterium glutamicum* for high-level production of 1,3-propanediol from glucose and xylose. Metabolic Engineering 70:79–88. DOI: 10.1016/j.ymben.2022.01.006
14. Dietz D, Zeng A-P (2013) Efficient production of 1,3-propanediol from fermentation of crude glycerol with mixed cultures in a simple medium. Bioprocess Biosyst Eng 37:225–233. DOI: 10.1007/s00449-013-0989-0
15. Kaeding T, DaLuz J, Kube J et al. (2015) Integrated study of fermentation and downstream processing in a miniplant significantly improved the microbial 1,3-propanediol production from raw glycerol. Bioprocess Biosyst Eng 38:575–586. DOI: 10.1007/s00449-014-1297-z
16. Zhang C, Traitrongsat P, Zeng A-P (2023) Electrochemically mediated bioconversion and integrated purification greatly enhanced co-production of 1,3-propanediol and organic acids from glycerol in an industrial bioprocess. Bioprocess Biosyst Eng. DOI: 10.1007/s00449-022-02841-6
17. Zhang C, Sharma S, Wang W et al. (2021) A novel downstream process for highly pure 1,3-propanediol from an efficient fed-batch fermentation of raw glycerol by *Clostridium pasteurianum*. Eng Life Sci 21:351–363. DOI: 10.1002/elsc.202100012
18. Albertyn J, Hohmann S, Thevelein JM et al. (1994) *GPD1*, which encodes glycerol-3-phosphate dehydrogenase, is essential for growth under osmotic stress in *Saccharomyces cerevisiae*, and its expression is regulated by the high-osmolarity glycerol response pathway. Mol Cell Biol 14:4135–4144. DOI: 10.1128/mcb.14.6.4135-4144.1994
19. Eriksson P, André L, Ansell R et al. (1995) Cloning and characterization of *GPD2*, a second gene encoding sn-glycerol 3-phosphate dehydrogenase (NAD+) in *Saccharomyces cerevisiae*, and its comparison with *GPD1*. Mol Microbiol 17:95–107. DOI: 10.1111/j.1365-2958.1995.mmi_17010095.x.
20. Pyne ME, Moo-Young M, Chung DA et al. (2013) Development of an electrotransformation protocol for genetic manipulation of *Clostridium pasteurianum*. Biotechnology for Biofuels 6:50. DOI: 10.1186/1754-6834-6-50

21. Schmitz R, Sabra W, Arbter P et al. (2018) Improved electrocompetence and metabolic engineering of *Clostridium pasteurianum* reveals a new regulation pattern of glycerol fermentation. Eng Life Sci 19:412–422. DOI: 10.1002/elsc.201800118
22. Hong Y, Arbter P, Wang W et al. (2020) Introduction of glycine synthase enables uptake of exogenous formate and strongly impacts the metabolism in *Clostridium pasteurianum*. Biotechnol Bioeng 118:1366–1380. DOI: 10.1002/bit.27658
23. Pyne ME, Bruder MR, Moo-Young M et al. (2016) Harnessing heterologous and endogenous CRISPR-Cas machineries for efficient markerless genome editing in *Clostridium*. Scientific Reports 6:25666. DOI: 10.1038/srep25666
24. Ortega D (2020) Synthetic biology & metabolic engineering of *Clostridium pasteurianum*. Doctoral dissertation, University of Nottingham
25. Schwarz KM, Grosse-Honebrink A, Derecka K et al. (2017) Towards improved butanol production through targeted genetic modification of *Clostridium pasteurianum*. Metabolic Engineering 40:124–137. DOI: 10.1016/j.ymben.2017.01.009
26. Pyne ME, Liu X, Moo-Young M et al. (2016) Genome-directed analysis of prophage excision, host defence systems, and central fermentative metabolism in *Clostridium pasteurianum*. Scientific Reports 6:26228. DOI: 10.1038/srep26228
27. Rappert S, Song L, Sabra W et al. (2013) Draft genome sequence of type strain *Clostridium pasteurianum* DSM 525 (ATCC 6013), a promising producer of chemicals and fuels. Genome Announcements 1. DOI: 10.1128/genomeA.00232-12.
28. Poehlein A, Grosse-Honebrink A, Zhang Y et al. (2015) Complete genome sequence of the nitrogen-fixing and solvent-producing *Clostridium pasteurianum* DSM 525. Genome Announcements 3. DOI: 10.1128/genomeA.01591-14.
29. Sabra W, Groeger C, Sharma PN et al. (2014) Improved n-butanol production by a non-acetone producing *Clostridium pasteurianum* DSMZ 525 in mixed substrate fermentation. Applied Microbiology and Biotechnology 98:4267–4276. DOI: 10.1007/s00253-014-5588-8
30. Groeger C, Sabra W, Zeng A-P (2016) Simultaneous production of 1,3-propanediol and n -butanol by *Clostridium pasteurianum* : In situ gas stripping and cellular metabolism. Eng Life Sci 16:664–674. DOI: 10.1002/elsc.201600058

31. Groeger C, Wang W, Sabra W et al. (2017) Metabolic and proteomic analyses of product selectivity and redox regulation in *Clostridium pasteurianum* grown on glycerol under varied iron availability. Microb Cell Fact 16:64. DOI: 10.1186/s12934-017-0678-9
32. Utesch T, Zeng A-P (2018) A novel All-in-One electrolysis electrode and bioreactor enable better study of electrochemical effects and electricity-aided bioprocesses. Eng Life Sci 18:600–610. DOI: 10.1002/elsc.201700198
33. Utesch T, Sabra W, Prescher C et al. (2019) Enhanced electron transfer of different mediators for strictly opposite shifting of metabolism in *Clostridium pasteurianum* grown on glycerol in a new electrochemical bioreactor. Biotechnol Bioeng 116:1627–1643. DOI: 10.1002/bit.26963
34. Pyne ME, Sokolenko S, Liu X et al. (2016) Disruption of the reductive 1,3-propanediol pathway triggers production of 1,2-propanediol for sustained glycerol fermentation by *Clostridium pasteurianum*. Applied and Environmental Microbiology 82:5375–5388. DOI: 10.1128/AEM.01354-16.
35. Dainty RH, Peel JL (1970) Biosynthesis of amino acids in *Clostridium pasteurianum*. Biochemical Journal 117:573–584. DOI: 10.1042/bj1170573
36. Buckel W, Thauer RK (2013) Energy conservation via electron bifurcating ferredoxin reduction and proton/Na(+) translocating ferredoxin oxidation. Biochim Biophys Acta 1827:94–113. DOI: 10.1016/j.bbabio.2012.07.002
37. Nakamura CE, Whited GM (2003) Metabolic engineering for the microbial production of 1,3-propanediol. Curr Opin Biotechnol 14:454–459. DOI: 10.1016/j.copbio.2003.08.005
38. Wilkens E, Ringel AK, Hortig D et al. (2012) High-level production of 1,3-propanediol from crude glycerol by *Clostridium butyricum* AKR102a. Applied Microbiology and Biotechnology 93:1057–1063. DOI: 10.1007/s00253-011-3595-6
39. Chatzifragkou A, Papanikolaou S, Dietz D et al. (2011) Production of 1,3-propanediol by *Clostridium butyricum* growing on biodiesel-derived crude glycerol through a non-sterilized fermentation process. Applied Microbiology and Biotechnology 91:101–112. DOI: 10.1007/s00253-011-3247-x
40. Metsoviti M, Paraskevaidi K, Koutinas A et al. (2012) Production of 1,3-propanediol, 2,3-butanediol and ethanol by a newly isolated *Klebsiella oxytoca* strain growing on biodiesel-

derived glycerol based media. Process Biochemistry 47:1872–1882. DOI: 10.1016/j.procbio.2012.06.011

41. Homann T, Tag C, Biebl H et al. (1990) Fermentation of glycerol to 1, 3-propanediol by *Klebsiella* and *Citrobacter* strains. Applied Microbiology and Biotechnology 33:121–126. DOI: 10.1007/BF00176511
42. Metsoviti M, Zeng A-P, Koutinas AA et al. (2013) Enhanced 1,3-propanediol production by a newly isolated *Citrobacter freundii* strain cultivated on biodiesel-derived waste glycerol through sterile and non-sterile bioprocesses. J Biotechnol 163:408–418. DOI: 10.1016/j.jbiotec.2012.11.018
43. Irmler S, Raboud S, Beisert B et al. (2008) Cloning and characterization of two *Lactobacillus casei* genes encoding a cystathionine lyase. Applied and Environmental Microbiology 74:99–106. DOI: 10.1128/AEM.00745-07
44. Liu Y, Li Y, Wang X (2016) Acetohydroxyacid synthases: evolution, structure, and function. Applied Microbiology and Biotechnology 100:8633–8649. DOI: 10.1007/s00253-016-7809-9
45. Yishai O, Goldbach L, Tenenboim H et al. (2017) Engineered assimilation of exogenous and endogenous formate in *Escherichia coli*. ACS Synthetic Biology 6:1722–1731. DOI: 10.1021/acssynbio.7b00086
46. Wenk S, Rainaldi V, He H et al. (2022) Synthetic carbon fixation via the autocatalytic serine threonine cycle. bioRxiv. DOI: 10.1101/2022.09.28.509898
47. Hong Y, Nguyen T, Arbter P et al. (2021) Phenotype analysis of cultivation processes via unsupervised machine learning: Demonstration for *Clostridium pasteurianum*. Eng Life Sci 22:85–99. DOI: 10.1002/elsc.202100114
48. Bao T, Zhao J, Zhang Q et al. (2019) Development of a shuttle plasmid without host restriction sites for efficient transformation and heterologous gene expression in *Clostridium cellulovorans*. Applied Microbiology and Biotechnology 103:5391–5400. DOI: 10.1007/s00253-019-09882-0
49. Johnston CD, Cotton SL, Rittling SR et al. (2019) Systematic evasion of the restriction-modification barrier in bacteria. Proceedings of the National Academy of Sciences 116:11454. DOI: 10.1073/pnas.1820256116

50. Flusberg BA, Webster DR, Lee JH et al. (2010) Direct detection of DNA methylation during single-molecule, real-time sequencing. Nature methods 7:461–465. DOI: 10.1038/nmeth.1459
51. Riley LA, Ji L, Schmitz RJ et al. (2019) Rational development of transformation in *Clostridium thermocellum* ATCC 27405 via complete methylome analysis and evasion of native restriction–modification systems. J Ind Microbiol Biotechnol 46:1435–1443. DOI: 10.1007/s10295-019-02218-x
52. Yu M, Ji L, Neumann DA et al. (2015) Base-resolution detection of N4-methylcytosine in genomic DNA using 4mC-Tet-assisted-bisulfite- sequencing. Nucleic Acids Res 43:e148. DOI: 10.1093/nar/gkv738
53. Davis BM, Chao MC, Waldor MK (2013) Entering the era of bacterial epigenomics with single molecule real time DNA sequencing. Current opinion in microbiology 16:192–198. DOI: 10.1016/j.mib.2013.01.011
54. Aziz RK, Bartels D, Best AA et al. (2008) The RAST Server: rapid annotations using subsystems technology. BMC genomics 9:1–15. DOI: 10.1186/1471-2164-9-75
55. Pyne ME (2014) Development of genetic tools for metabolic engineering of *Clostridium pasteurianum*. Doctoral dissertation, University of Waterloo
56. Yang X, Xu M, Yang S-T (2016) Restriction modification system analysis and development of in vivo methylation for the transformation of *Clostridium cellulovorans*. Applied Microbiology and Biotechnology 100:2289–2299. DOI: 10.1007/s00253-015-7141-9
57. Mobini-Dehkordi M, Nahvi I, Zarkesh-Esfahani H et al. (2008) Isolation of a novel mutant strain of *Saccharomyces cerevisiae* by an ethyl methane sulfonate-induced mutagenesis approach as a high producer of bioethanol. Journal of Bioscience and Bioengineering 105:403–408. DOI: 10.1263/jbb.105.403
58. Lakhssassi N, Baharlouei A, Meksem J et al. (2020) EMS-Induced Mutagenesis of *Clostridium carboxidivorans* for Increased Atmospheric CO2 Reduction Efficiency and Solvent Production. Microorganisms 8. DOI: 10.3390/microorganisms8081239
59. Lemmel SA (1985) Mutagenesis in *Clostridium acetobutylicum*. Biotechnology Letters 7:711–716. DOI: 10.1007/BF01032281
60. Rogers P, Palosaari N (1987) *Clostridium acetobutylicum* mutants that produce butyraldehyde and altered quantities of solvents. Applied and Environmental Microbiology 53:2761–2766. DOI: 10.1128/aem.53.12.2761-2766.1987

61. Jensen TØ, Kvist T, Mikkelsen MJ et al. (2012) Production of 1,3-PDO and butanol by a mutant strain of *Clostridium pasteurianum* with increased tolerance towards crude glycerol. AMB Express 2:44. DOI: 10.1186/2191-0855-2-44
62. Laffend LA, Nagarajan V, Nakamura CE (1997) Bioconversion of a fermentable carbon souce to 1,3-propanediol by a single microorganism. US Patent No. 5,686,276
63. Diaz-Torres M, Dunn-Coleman N, Chase M et al. (2000) Method for the recombinant production of 1,3-propanediol. US Patent No. 6,136,576
64. Nair RV, Payne MS, Trimbur DE et al. (2006) Method for the production of glycerol by recombinant organisms. US Patent No. US 2006/0177915 A1
65. Meynial Salles I, Forchhammer N, Croux C et al. (2007) Evolution of a *Saccharomyces cerevisiae* metabolic pathway in *Escherichia coli*. Metabolic Engineering 9:152–159. DOI: 10.1016/j.ymben.2006.09.002.
66. Chen X, Zaro JL, Shen W-C (2013) Fusion protein linkers: property, design and functionality. Adv Drug Deliv Rev 65:1357–1369. DOI: 10.1016/j.addr.2012.09.039.
67. Sarma S, Ortega D, Minton NP et al. (2019) Homologous overexpression of hydrogenase and glycerol dehydrogenase in *Clostridium pasteurianum* to enhance hydrogen production from crude glycerol. Bioresource Technology 284:168–177. DOI: 10.1016/j.biortech.2019.03.074
68. Heap JT, Pennington OJ, Cartman ST et al. (2007) The ClosTron: a universal gene knock-out system for the genus *Clostridium*. Journal of Microbiological Methods 70:452–464. DOI: 10.1016/j.mimet.2007.05.021
69. González-Pajuelo M, Meynial-Salles I, Mendes F et al. (2005) Metabolic engineering of *Clostridium acetobutylicum* for the industrial production of 1,3-propanediol from glycerol. Metabolic Engineering 7:329–336. DOI: 10.1016/j.ymben.2005.06.001
70. Dusséaux S, Croux C, Soucaille P et al. (2013) Metabolic engineering of *Clostridium acetobutylicum* ATCC 824 for the high-yield production of a biofuel composed of an isopropanol/butanol/ethanol mixture. Metabolic Engineering 18:1–8. DOI: 10.1016/j.ymben.2013.03.003
71. Bruder MR, Pyne ME, Moo-Young M et al. (2016) Extending CRISPR-Cas9 technology from genome editing to transcriptional engineering in the genus *Clostridium*. Applied and Environmental Microbiology 82:6109–6119. DOI: 10.1128/AEM.02128-16.

72. Pyne ME, Moo-Young M, Chung DA et al. (2014) Expansion of the genetic toolkit for metabolic engineering of *Clostridium pasteurianum*: chromosomal gene disruption of the endogenous *CpaAI* restriction enzyme. Biotechnology for Biofuels 7:163. DOI: 10.1186/s13068-014-0163-1
73. Sandoval NR, Venkataramanan KP, Groth TS et al. (2015) Whole-genome sequence of an evolved *Clostridium pasteurianum* strain reveals *Spo0A* deficiency responsible for increased butanol production and superior growth. Biotechnology for Biofuels 8:227. DOI: 10.1186/s13068-015-0408-7
74. Cañadas IC, Groothuis D, Zygouropoulou M et al. (2019) RiboCas: A universal CRISPR-Based editing tool for *Clostridium*. ACS Synthetic Biology 8:1379–1390. DOI: 10.1021/acssynbio.9b00075
75. Pyne M, Moo-Young M, Chung D et al. (2015) Antisense-RNA-mediated gene downregulation in *Clostridium pasteurianum*. Fermentation 1:113–126. DOI: 10.3390/fermentation1010113
76. Al-Hinai MA, Fast AG, Papoutsakis ET (2012) Novel system for efficient Isolation of *Clostridium* double-crossover allelic exchange mutants enabling markerless chromosomal gene deletions and DNA integration. Applied and Environmental Microbiology 78:8112–8121. DOI: 10.1128/AEM.02214-12
77. Heap JT, Ehsaan M, Cooksley CM et al. (2012) Integration of DNA into bacterial chromosomes from plasmids without a counter-selection marker. Nucleic Acids Res 40:e59-e59. DOI: 10.1093/nar/gkr1321
78. Ng YK, Ehsaan M, Philip S et al. (2013) Expanding the repertoire of gene tools for precise manipulation of the *Clostridium difficile* genome: allelic exchange using *pyrE* alleles. PLOS ONE 8:e56051. DOI: 10.1371/journal.pone.0056051
79. Joseph RC, Sandoval NR (2023) Single and multiplexed gene repression in solventogenic *Clostridium* via Cas12a-based CRISPR interference. Synth Syst Biotechnol 8:148–156. DOI: 10.1016/j.synbio.2022.12.005
80. Adiego-Pérez B, Randazzo P, Daran JM et al. (2019) Multiplex genome editing of microorganisms using CRISPR-Cas. FEMS Microbiol Lett 366. DOI: 10.1093/femsle/fnz086

81. Mojica FJM, Díez-Villaseñor Cs, García-Martínez J et al. (2005) Intervening sequences of regularly spaced prokaryotic repeats derive from foreign genetic elements. Journal of Molecular Evolution 60:174–182. DOI: 10.1007/s00239-004-0046-3
82. Barrangou R, Fremaux C, Deveau H et al. (2007) CRISPR provides acquired resistance against viruses in prokaryotes. Science 315:1709–1712. DOI: 10.1126/science.1138140
83. Brouns SJJ, Jore MM, Lundgren M et al. (2008) Small CRISPR RNAs guide antiviral defense in prokaryotes. Science 321:960–964. DOI: 10.1126/science.1159689
84. Cobb RE, Wang Y, Zhao H (2015) High-efficiency multiplex genome editing of *Streptomyces* species using an engineered CRISPR/Cas system. ACS Synthetic Biology 4:723–728. DOI: 10.1021/sb500351f
85. Jinek M, Chylinski K, Fonfara I et al. (2012) A programmable dual-RNA–guided DNA endonuclease in adaptive bacterial immunity. Science 337:816–821. DOI: 10.1126/science.1225829
86. Mali P, Yang L, Esvelt KM et al. (2013) RNA-guided human genome engineering via Cas9. Science 339:823–826. DOI: 10.1126/science.1232033
87. Zetsche B, Gootenberg JS, Abudayyeh OO et al. (2015) Cpf1 is a single RNA-guided endonuclease of a class 2 CRISPR-Cas system. Cell 163:759–771. DOI: 10.1016/j.cell.2015.09.038
88. Yao X, Wang X, Hu X et al. (2017) Homology-mediated end joining-based targeted integration using CRISPR/Cas9. Cell Research 27:801–814. DOI: 10.1038/cr.2017.76
89. Zetsche B, Heidenreich M, Mohanraju P et al. (2017) Multiplex gene editing by CRISPR-Cpf1 using a single crRNA array. Nature Biotechnology 35:31–34. DOI: 10.1038/nbt.3737
90. Li L, Wei K, Zheng G et al. (2018) CRISPR-Cpf1-assisted multiplex genome editing and transcriptional repression in *Streptomyces*. Applied and Environmental Microbiology 84:e00827-18. DOI: 10.1128/AEM.00827-18
91. Jiang Y, Chen B, Duan C et al. (2015) Multigene editing in the *Escherichia coli* genome via the CRISPR-Cas9 system. Applied and Environmental Microbiology 81:2506–2514. DOI: 10.1128/AEM.04023-14
92. Jiang W, Bikard D, Cox D et al. (2013) RNA-guided editing of bacterial genomes using CRISPR-Cas systems. Nature Biotechnology 31:233–239. DOI: 10.1038/nbt.2508

93. Hong Y (2022) Engineering of *Clostridium pasteurianum* for formate uptake and application of unsupervised learning from fermantation analysis. Doctoral dissertation, Hamburg University of Technology
94. Pyne ME, Bruder M, Moo-Young M et al. (2019) Harnessing Heterologous and endogenous CRISPR-Cas machineries for efficient markerless genome editing in C*lostridium*. US Patent No. US2019/0144846 A1
95. Grosse-Honebrink A (2017) Forward and reverse genetics in industrially important *Clostridia*. Doctoral dissertation, University of Nottingham
96. Heap JT, Pennington OJ, Cartman ST et al. (2009) A modular system for *Clostridium* shuttle plasmids. Journal of Microbiological Methods 78:79–85. DOI: 10.1016/j.mimet.2009.05.004
97. Chmiel H, Takors R, Weuster-Botz D (2018) Bioprozesstechnik, 4th edn. Springer Spektrum, Berlin
98. Bolmanis E, Dubencovs K, Suleiko A et al. (2023) Model Predictive Control—A Stand Out among Competitors for Fed-Batch Fermentation Improvement. Fermentation 9:206. DOI: 10.3390/fermentation9030206
99. Arbter P, Sabra W, Utesch T et al. (2020) Metabolomic and kinetic investigations on the electricity-aided production of butanol by *Clostridium pasteurianum* strains. Eng Life Sci 21:181–195. DOI: 10.1002/elsc.202000035
100. Arbter P (2022) Fluxomic and metabolomic studies on the electro-fermentation of *Rhodosporidium toruloides* and *Clostridium pasteurianum* for improved bioprocesses. Doctoral dissertation, Hamburg University of Technology
101. Zeng A-P (1996) Pathway and kinetic analysis of 1, 3-propanediol production from glycerol fermentation by *Clostridium butyricum*. Bioprocess Engineering 14:169–175. DOI: 10.1007/BF01464731
102. Kodym A, Afza R (2003) Physical and Chemical Mutagenesis. In: Grotewold E (ed) Plant Functional Genomics. Humana Press, Totowa, NJ, 189–203. DOI: 10.1385/1-59259-413-1:189
103. Biebl H, Pfennig N (1981) Isolation of members of the family *Rhodospirillaceae*. In: The prokaryotes: a handbook on habitats, isolation, and identification of bacteria. Springer, 267–273. DOI: 10.1007/978-3-662-13187-9_14

104. Heap JT, Kuehne SA, Ehsaan M et al. (2010) The ClosTron: Mutagenesis in *Clostridium* refined and streamlined. Journal of Microbiological Methods 80:49–55. DOI: 10.1016/j.mimet.2009.10.018
105. Schmitz R (2018) Metabolic engineering von *Clostridium pasteurianum* zur Optimierung der Biobutanolproduktion. Doctoral dissertation, Hamburg University of Technology
106. Zhang C (2022) Process development for co-producing 1,3-propanediol and organic acid esters by adaptively evolved *Clostridium pasteurianum*. Doctoral dissertation, Hamburg University of Technology
107. Xiao Y, Luo M, Dolan AE et al. (2018) Structure basis for RNA-guided DNA degradation by Cascade and Cas3. Science 361. DOI: 10.1126/science.aat0839.
108. Hochstrasser ML, Doudna JA (2015) Cutting it close: CRISPR-associated endoribonuclease structure and function. Trends Biochem Sci 40:58–66. DOI: 10.1016/j.tibs.2014.10.007
109. Westra ER, van Erp PBG, Künne T et al. (2012) CRISPR immunity relies on the consecutive binding and degradation of negatively supercoiled invader DNA by Cascade and Cas3. Mol Cell 46:595–605. DOI: 10.1016/j.molcel.2012.03.018
110. Grosse-Honebrink A, Schwarz KM, Wang H et al. (2017) Improving gene transfer in *Clostridium pasteurianum* through the isolation of rare hypertransformable variants. Anaerobe 48:203–205. DOI: 10.1016/j.anaerobe.2017.09.001
111. Minton NP, Ehsaan M, Humphreys CM et al. (2016) A roadmap for gene system development in *Clostridium*. Anaerobe 41:104–112. DOI: 10.1016/j.anaerobe.2016.05.011
112. Arbter P, Widderich N, Utesch T et al. (2022) Control of redox potential in a novel continuous bioelectrochemical system led to remarkable metabolic and energetic responses of *Clostridium pasteurianum* grown on glycerol. Microb Cell Fact 21:178. DOI: 10.1186/s12934-022-01902-5
113. Fan C, Wu Y-H, Decker CM et al. (2019) Defensive function of transposable elements in bacteria. ACS Synthetic Biology 8:2141–2151. DOI: 10.1021/acssynbio.9b00218
114. Zhang Y, Grosse-Honebrink A, Minton NP (2015) A universal mariner transposon system for forward genetic studies in the genus *Clostridium*. PLOS ONE 10:e0122411. DOI: 10.1371/journal.pone.0122411

115. Zhang J, Liu Y, Cui G et al. (2015) A novel arabinose-inducible genetic operation system developed for *Clostridium cellulolyticum*. Biotechnology for Biofuels 8:36. DOI: 10.1186/s13068-015-0214-2

116. Nariya H, Miyata S, Kuwahara T et al. (2011) Development and characterization of a xylose-inducible gene expression system for *Clostridium perfringens*. Applied and Environmental Microbiology 77:8439–8441. DOI: 10.1128/AEM.05668-11

117. Müh U, Pannullo AG, Weiss DS et al. (2019) A xylose-inducible expression system and a CRISPR interference plasmid for targeted knockdown of gene expression in *Clostridioides difficile*. Journal of Bacteriology 201:e00711-18. DOI: 10.1128/JB.00711-18

118. Hartman AH, Liu H, Melville SB (2011) Construction and characterization of a lactose-inducible promoter system for controlled gene expression in *Clostridium perfringens*. Applied and Environmental Microbiology 77:471–478. DOI: 10.1128/AEM.01536-10

119. Banerjee A, Leang C, Ueki T et al. (2014) Lactose-inducible system for metabolic engineering of *Clostridium ljungdahlii*. Applied and Environmental Microbiology 80:2410–2416. DOI: 10.1128/AEM.03666-13

120. Mearls EB, Olson DG, Herring CD et al. (2015) Development of a regulatable plasmid-based gene expression system for *Clostridium thermocellum*. Applied Microbiology and Biotechnology 99:7589–7599. DOI: 10.1007/s00253-015-6610-5

121. Dong H, Tao W, Zhang Y et al. (2012) Development of an anhydrotetracycline-inducible gene expression system for solvent-producing *Clostridium acetobutylicum*: A useful tool for strain engineering. Metabolic Engineering 14:59–67. DOI: 10.1016/j.ymben.2011.10.004

122. Ransom EM, Ellermeier CD, Weiss DS et al. (2015) Use of mCherry Red Fluorescent Protein for Studies of Protein Localization and Gene Expression in *Clostridium difficile*. Applied and Environmental Microbiology 81:1652–1660. DOI: 10.1128/AEM.03446-14

123. Cui G, Hong W, Zhang J et al. (2012) Targeted gene engineering in *Clostridium cellulolyticum* H10 without methylation. Journal of Microbiological Methods 89:201–208. DOI: 10.1016/j.mimet.2012.02.015

124. Drepper T, Eggert T, Circolone F et al. (2007) Reporter proteins for in vivo fluorescence without oxygen. Nature Biotechnology 25:443–445. DOI: 10.1038/nbt1293

125. Simon A, Stahl A (2019) Qualitative analysis via GC-MS screening: Method M03.022, Version 01. Hamburg: Technische Universität Hamburg, Zentrallabor Chemische Analytik.

126. Nölling J, Breton G, Omelchenko MV et al. (2001) Genome sequence and comparative analysis of the solvent-producing bacterium *Clostridium acetobutylicum*. Journal of Bacteriology 183:4823–4838. DOI: 10.1128/JB.183.16.4823–4838.2001
127. Chen Z, Huang J, Wu Y et al. (2017) Metabolic engineering of *Corynebacterium glutamicum* for the production of 3-hydroxypropionic acid from glucose and xylose. Metabolic Engineering 39:151–158. DOI: 10.1016/j.ymben.2016.11.009
128. Gungormusler M, Gonen C, Ozdemir G et al. (2010) 1,3-Propanediol production potential of *Clostridium saccharobutylicum* NRRL B-643. N Biotechnol 27:782–788. DOI: 10.1016/j.nbt.2010.07.010
129. Wischral D, Zhang J, Cheng C et al. (2016) Production of 1,3-propanediol by *Clostridium beijerinckii* DSM 791 from crude glycerol and corn steep liquor: Process optimization and metabolic engineering. Bioresource Technology 212:100–110. DOI: 10.1016/j.biortech.2016.04.020
130. Kim S-J, Kim J-W, Lee Y-G et al. (2017) Metabolic engineering of *Saccharomyces cerevisiae* for 2,3-butanediol production. Applied Microbiology and Biotechnology 101:2241–2250. DOI: 10.1007/s00253-017-8172-1
131. Remize F, Roustan JL, Sablayrolles J-M et al. (1999) Glycerol overproduction by engineered *Saccharomyces cerevisiae* wine yeast strains leads to substantial changes in by-product formation and to a stimulation of fermentation rate in stationary phase. Applied and Environmental Microbiology 65:143–149. DOI: 10.1128/AEM.65.1.143-149.1999
132. Maina S, Prabhu AA, Vivek N et al. (2022) Prospects on bio-based 2,3-butanediol and acetoin production: Recent progress and advances. Biotechnol Adv 54:107783. DOI: 10.1016/j.biotechadv.2021.107783
133. Sedlar K, Kolek J, Skutkova H et al. (2015) Complete genome sequence of *Clostridium pasteurianum* NRRL B-598, a non-type strain producing butanol. J Biotechnol 214:113–114. DOI: 10.1016/j.jbiotec.2015.09.022
134. Sedlar K, Kolek J, Provaznik I et al. (2017) Reclassification of non-type strain *Clostridium pasteurianum* NRRL B-598 as *Clostridium beijerinckii* NRRL B-598. J Biotechnol 244:1–3. DOI: 10.1016/j.jbiotec.2017.01.003

135. Verhue WM, Tjan FSB (1991) Study of the citrate metabolism of *Lactococcus lactis* subsp. *lactis biovar diacetylactis* by means of 13C nuclear magnetic resonance. Applied and Environmental Microbiology 57:3371–3377. DOI: 10.1128/aem.57.11.3371-3377.1991
136. Song CW, Park JM, Chung SC et al. (2019) Microbial production of 2,3-butanediol for industrial applications. J Ind Microbiol Biotechnol 46:1583–1601. DOI: 10.1007/s10295-019-02231-0
137. González E, Fernández MR, Larroy C et al. (2000) Characterization of a (2R,3R)-2,3-butanediol dehydrogenase as the *Saccharomyces cerevisiae* YAL060W gene product. Disruption and induction of the gene. Journal of Biological Chemistry 275:35876–35885. DOI: 10.1074/jbc.M003035200
138. Pazda M, Kumirska J, Stepnowski P et al. (2019) Antibiotic resistance genes identified in wastewater treatment plant systems - A review. Sci Total Environ 697:134023. DOI: 10.1016/j.scitotenv.2019.134023
139. Langbehn RK, Michels C, Soares HM (2021) Antibiotics in wastewater: From its occurrence to the biological removal by environmentally conscious technologies. Environ Pollut 275:116603. DOI: 10.1016/j.envpol.2021.116603
140. World Health Organization (2015) Global action plan on antimicrobial resistance
141. Pazda M, Rybicka M, Stolte S et al. (2020) Identification of selected antibiotic resistance genes in two different wastewater treatment plant systems in poland: A preliminary study. Molecules 25. DOI: 10.3390/molecules25122851
142. Brechun KE, Förschle M, Schmidt M et al. (2024) Method for plasmid-based antibiotic-free fermentation. Microb Cell Fact 23:18. DOI: 10.1186/s12934-023-02291-z
143. Yang G, Jia D, Jin L et al. (2017) Rapid generation of universal synthetic promoters for controlled gene expression in both gas-fermenting and saccharolytic *Clostridium* species. ACS Synthetic Biology 6:1672–1678. DOI: 10.1021/acssynbio.7b00155

8 Appendix

Table 8-1: Sequences of designed primers for the construction of plasmids and Sanger sequencing.

Primer	Sequence (5'-3')	Size [bp]
P02-colE1-R	TTTCCATAGGCTCCGCCCC	19
P001-pIM13-F	ATGAAAGAAAGATATGGAACAGTCTATAAAGGCTCTC	37
P002-ColE1-R	TTTCCATAGGCTCCGCCCCCCTG	23
P003-Pthl-gpd1-F	CGGAGCCTATGGAAATTTTTAACAAAAAGTATTGAAATTTGGTCTACCCAG	51
P004-Pthl-gpd1-R	CTAATCTTCATGTAGATCTAATTCTTCAATCATGTCCG	41
P005-Pfdx-gpp2-Tfdx-F	CTACATGAAGATTAGGTGTAGTAGCCTGTGAAATAAGTAAGG	52
P006-Pfdx-gpp2-Tfdx-R	ATATCTTTCTTTCATATAAAAATAAGAAGCCTGCAAATGCAGG	43
P007-catP-R	ATACCATCTAAGTTCCCTCTCAAATTCAAGTTTATCG	37
P008-gpp2-F	TGATGTCAAACAGGGTAAGCCTCATC	46
P009-colE1-F	TGAGATACCTACAGCGTGAGCTATGAG	27
P010-gpd1-R	TCTGGGTATCCCTTACAATTTTCGGC	40
P011-gpd1-F	TCAGAGGCGAGGGCAAGG	18
P012-gpp2-F	TCCAGACTTTGCCAATGAAGAGTATG	26
P013-cspfdx-R	AGCTGTTTCCTGTGTGAAATTGTTATG	27
P014-term-F	CTGTTGAAATGGTAAATGTCGAGCACCCGTTCTCG	35
P015-gpd1-F	ACACAGGAAACAGCTATGTCTGCTGCTGCTGATAGATTAAACTTAAC	47
P016-gpp2-R	TTACCATTTCAACAGATCGTCCTTAGC	27
P017-gpd-fusion-R	TTTAGTAGTCAATCCCCATATAACTACAATCATGTCCGGCAGGTTCTTCATTG	53
P018-gpp-fusion-F	GGATTGACTACTAAACCTCTATCTTTGAAAGTTAACGC	38
P019-gpp2-R	ACCATGCGAGACTTGGATAACG	22
P020-gpd1-R	CCATATAACTACAATCATGTCCGGCAGGTTCTTCATTG	38
P021-catP-F	ATGGATTATAAGCGGATTAAGGGCCCGGCCAGTG	34
P022-pCB102-R	CCGCTTATAATCCATAACAATCATCCTTTC	30
P023-pCB102-F	ATGAAAGAAAGATATATCCCCCCACAGATACGGG	34
P024-pCB102-F	AGACCGTAAGGTCGTTGTTTAGG	23
P025-term-R	ATATCTTTCTTTCATTAGATATGACGACAGGAAGAGTTTGTAG	43
P037-ColE1-F	ACGCTTCCCGAAGGGAGAAAG	21
P049-pCB102-F	ATGAAAGAAAGATATATCCCCCCACAGATACG	32
P054-pCB102-R	TCAGCACTGTTATGCCTTTTGACTATCAC	29
P056-new	CGGAGCCTATGGAAATCCAGTGATAGGCAAGATATTAAAGTCACTGAC	48
P058-H2-dhaK-F	TTAGAATGTTTAAAGAAATATTATAATTAAATTAATAATAAACAATTTTAAGATATATG	59
P060-new	ACCTCCACCAAGGCCAATTGTAC	23
P061-new	GGCCTTGGTGGAGGTGTGTAGTAGCCTGTGAAATAAGTAAGGAAAAAAAAGAAG	54
P062-gpd1-gpp2-R	CTTTAAACATTCTAATAGATATGACGACAGGAAGAGTTTGTAGAAACG	48
P063-55D	TCCGAGCTCTGAATGAATTACTCACTAAAATTAGCCACCTTTC	43
P064-array-F	CATTCAGAGCTCGGATGGTTAACAG	25
P065-pCB102	ATATCTTTCTTTCATCCTGATGAGCTCTTCCTGCAAATATTC	42
P083-Seq-fus-R	AGGCAACAACGTTCTTCAAAGCAC	24
P084-Seq-H1H2-R	ACTGTTAACCATCCGAGCTCTGAATG	26
P085-Seq-dhaD-F	AGCAGTTATGGCAGGTCAAGTAAAATTGTC	30
P086-Seq-dhaK-R	ATAAAGACTACCCCAGGCACAAAAGG	26
P124-H1-bdhA2-F	CGGAGCCTATGGAAATTTTAAGTAAAGAACTGTCGTCGGTTGG	43
P125-bdhA2-sp1-R	ATGTTAAGGTTCAACTACTTCTTGCCTCATAGTCTTTAAGATCTTTCACTG	51
P126-H2-bdhA2-F	CGGAGCCTATGGAAATTCATGTGTAGTAGTTATTATGACTGTCAGCGTC	49
P127-H2-bdhA2-R	TCCGAGCTCTGAATGCATCTTCAGTAAGGGTAATCTGTTTATTCCCC	47
P128-bdhA2-sp1-F	AGGATGTATTTAAATCAGTGAAAGATCTTAAAGACTATGAGGCAAGAAGTAG	52
P129-H1-bdhA2-R	ACTACTACACATGAATTTTTCTCCATTCCTGCACATTTTGCG	42
P130-H2-bdhA2-F	TTCATGTGTAGTAGTTATTATGACTGTCAGCGTC	34
P131-Crepeat-R	ATTTAAATACATCCTATGTTAAGGTTCAACTACTTAAAACTAGC	44
P132-bdhA2-sp2-R	ATGTTAAGGTTCAACCTTTATATCCGCCTGAAAGCAGTACAGTTG	45
P133-bdhA2-sp2-F	AGGATGTATTTAAATCAAATTCAACTGTACTGCTTTCAGGCG	42
P145-dhaTC8-R	TACAAATCCTTCCATAGCCCTCTTCCCCTCG	31
P147-dhatC8-R	TCTCCGACTGTTCCTAGCCCTCTTCCCCTCG	31
P151-seq-bdhA2-F	TGCGCAAAATGTGCAGGAATG	21

P152-seq-bdhA2-R	TGACGCTGACAGTCATAATAACTACTACACATG	33
P153-seq-H1-bdhA2-F	ACCTAATAATACAGTATATGCTGGAGTTCCAGC	33
P154-seq-H2-bdhA2-F	TAGCAGTTTTATCTGCCAACTCTATAATCTCCATAG	36
P155-seq-H1-glpF-F	ATTGTCTGAGAGAATTGTAGATTCTATTTTAGAGGATATAAAAATTG	47
P156-seq-H2-glpF-R	TGTAAAAAATACCTTATAATAAACAGAATTTTTCATTGTATCTTCGTTTG	50
P159-seq-dhaTC8-F	ATGCTATAGAAGCATATGTTTCTAAAGATGCAAATCC	37
P160-colE1-F	GTTTAAACTCCTTTTTGATAATCTCATGACCAAAATCCC	39
P161-pIM13-R	CTTAATCGCATTTCATAGATTGACCTCCCAATAACTAC	38
P162-ermB-F	TGAAATGCGATTAAGGGCCGGCCGAAGCAAAC	32
P163-pIM13-R	AAAAGGAGTTTAAACACATTCCCTTTAGTAACGTG	35
P164-pBP1-F	GCTTCTTATTTTTATGGCGCGCCG	24
P165-lacZ-R	ATAAAAATAAGAAGCCTGCAAATGCAGGC	29
P166-tetA-F	TGAAATGCGATTAAGGGCCGGCCACTCTATAATTTAGAGTC	41
P167-tetA-R	AAAAGGAGTTTAAACTGCATCCACGTGTGCTAC	33
P168-tetA-F	TTTATTTACAAATTCGGCCGGCCACTCTATAATTTAG	37
P169-pBP1-R	GAATTTGTAAATAAACCACAAACTATTAAAGTTAAACATAAAAATAACATCG	52
P170-bdhA2SP-F	CGGAGCCTATGGAAAGAGGGACTTCTTCGTTCTATCATCAACAG	44
P171-bdhA2SP-R	GCCGTCTTTAAAATCTCTAAAATTTCTTCCGCTG	34
P176-Crepeat-R	ATTTAAATACATCCTATGTTAAGGTTCAACTAC	33
P179-Seq-ermB-R	TGACGCTCAGTGGAACGAAAACTC	24
P180-Seq-pBp1-R	ACTGCACTATCAACACACTCTTAAGTTTGC	30
P181-Seq-pBP1-F	TGGAGCGTAAGGAAGTTAAGGATATAACTAAAGG	34
P182-Seq-pBP1-F	AATGGCGAATGGCGCTAGC	19
P189-catP-F	GAAGAGCTCATCAGGCCGGCCAGTGGGCAAG	31
P190-cr-R	CCTGATGAGCTCTTCCTGCAAATATTC	27
P192-dhaTC8-R	ATAGATGATATAAAAAGCCCTCTTCCCCTCG	31
P193-pIM13-seq-F	TGAGCAAGAGGCAAATGAAATAGATTGACC	30
P194-tetA-seq-R	TTCTCTTCTTCCGCAATCCAAGCTTC	26
P195-pBP1-seq-R	TGGCCGGCCGAATTTGTAAATAAAC	25
P196-adh2r-F	AATGCTATAGAACACTTAAAATCAGTAAAGGGAAATAAGG	40
P197-colE1-R	TTTAAGTGTTCTATAGCATTTTTCCATAGGCTCCGCCCC	39
P198-adh2r-R	GATTATCCCTGAACTTTTCTTCTGATATACCATATTCTTTC	41
P199-bdhA2-H1-F	AGAAAAGTTCAGGGATAATCTTTTAAGTAAAGAACTGTCGTCGGTTGG	48
P200-bdhA2-H1-R	TAATAACTACTACACATGAATTTTTCTCCATTCCTGCACATTTTGCG	47
P201-bdhA2-H2-R	AACCATCCGAGCTCTGAATGCATCTTCAGTAAGGGTAATCTGTTTATTCCCC	52
P202-pCB102	GGGATATATCTTTCTTTCATCCTGATGAGCTCTTCCTG	38
P203-bdhA2-H1-R	AAAAAATCATACATTCTCATTTTTTCTCCATTCCTGCACATTTTGC	46
P204-dhaTC8-F	ATGAGAATGTATGATTTTTTAGCACCAAGTGTAAATTTTATGG	43
P205-dhaTC8-R	TTAAAATGCTTCTCTAAATATTTTAACTATATCCCTCTCGTTACC	45
P206-bdhA2-H2-F	TATTTAGAGAAGCATTTTAATTCATGTGTAGTAGTTATTATGACTGTCAGCGTC	54
P207-adh2r-seq-F	TGGTTAAAGATATTAGAGCCTCTATGAATATGCCTATAAC	40
P208-H2-adh2-R	CTTATAATTGCCTATCTTCTATTGTTATCCTAGTAATTTTATTAACAGGC	50
P209-array-F	AGAAGATAGGCAATTATAAGCATTCAGAGCTCGGATGGTTAACAG	45
P210-dhaDKr-F	AGTTACACCAGCATTAGAAAATATAATAGAAACAAATATTCTTCTATCTG	50
P211-colE1-R	TTTCTAATGCTGGTGTAACTTTTCCATAGGCTCCGCCCC	39
P213-H1-adh2-F	CACGAGTGATTTCATATTTTTTTGCAGTACAAGG	34
P214-H1-adh2-R	TTTAATTATTTCCCCCTTTTACCAATACCATTTGGC	36
P215-H2-adh2-F	AAAAGGGGGAAATAATTAAAAATTTAAGGGGAGTAAAAACTCCCTCTGTATC	52
P216-seq-H1-adh2-F	TGATAACTCTCTTACAGTAATAACATAATCCATATCACGTATG	43
P217-seq-H1-adh2-F	TGAGAAGCCTATACTAATACTTGTATTAACCATATAAAAATTAATGGC	48
P218-seq-H2-adh2-R	AGCCATTTAAGCCGCCAATTAACAAAG	27
P219-seq-H2-adh2-R	TCTGGTGATAAATCGAACATGGTAGTATTCATATTGTTAG	40
P220-H1-adh2-R	AAAAAATCATACATTCTCATTTTAATTATTTCCCCCTTTTACCAATACCATTTGGC	56
P221-H2-adh2-F	TATTTAGAGAAGCATTTTAAAATTTAAGGGGAGTAAAAACTCCCTCTGTATC	52
P222-seq-dhaDKr-F	AGTAATGGAGATGTGTAATGGCATAGCC	28
P223-colE1-R	ATAGAACGAAGAAGTCCCTCTTTCCATAGGCTCCGCCCC	39
P224-bdhA2r-F	GAGGGACTTCTTCGTTCTATCATCAACAG	29
P229-dhaTC8-R	TCACTTACAAATCCTTCCATAGCCCTCTTCCCCTCG	36
P231-pIM13-R	AAGTTTATTAACCATCTAAGTTCCCTCTCAAATTCAAGTTTATC	44
P232-ColE1-F	GAAGAAAATAATTAACTTCAGGTTTGTCTGTAACTAAAAACAAGTATTTAAGC	53

P233-tetA-F	ATGGTTAATAAACTTTCAGCATATAAAACTTATTTATTATTTTCAGCTATTACAG	55
P234-tetA-R	TTAATTATTTTCTTCATAATCAATACCTCCAACTCTATCATCCAC	45
P235-H1-bdhA2-F	ATGTGTAATGGCATAGCCATTTTTAAGTAAAGAACTGTCGTCGGTTGG	48
P236-dhaDKr-R	ATGGCTATGCCATTACACATCTCCATTAC	29
P237-array-F	AGAAAAGTTCAGGGATAATCCATTCAGAGCTCGGATGGTTAACAG	45
P238-catP-F	GATTACCCTTACTGAAGATGCCGGCCAGTGGGCAAG	36
P239-catP-F	CCGGCCAGTGGGCAAG	16
P240-H2-bdhA2-R	CATCTTCAGTAAGGGTAATCTGTTTATTCCCC	32
P241-H2-bdhA2-R	TCAACTTGCCCACTGGCCGGCATCTTCAGTAAGGGTAATCTGTTTATTCCCC	52
P242-H1-bdhA2-F	TTTTAAGTAAAGAACTGTCGTCGGTTGG	28
P243-H1-bdhA2-F	GGGGGCGGAGCCTATGGAAATTTTAAGTAAAGAACTGTCGTCGGTTGG	48
P244-colE1-R	CGACAGTTCTTTACTTAAAATTTCCATAGGCTCCGCCCC	39
P245-dhaTC8-R	ATCTCTAACATTGGTATCCTTAGGATTAGGCTC	33
P246-adh2r-F	TGCCTAAAGCACTAATTGCTAACACTGG	28
P247-array-F	TTAGAGATTTTAAAGACGGCCATTCAGAGCTCGGATGGTTAACAG	45
P248-catP-F	AGAAGATAGGCAATTATAAGCCGGCCAGTGGGCAAG	36
P249-colE1-R	AAAATATGAAATCACTCGTGTTTCCATAGGCTCCGCCCC	39
P250-H1-adh2-F	GGGGGCGGAGCCTATGGAAACACGAGTGATTTCATATTTTTTTGCAGTACAAGG	54
P251-bdhA2SP-R	AAAATATGAAATCACTCGTGGCCGTCTTTAAAATCTCTAAAATTTCTTCCGCTG	54
P252-H1-adh2-F	TTAGAGATTTTAAAGACGGCCACGAGTGATTTCATATTTTTTTGCAGTACAAGG	54
P253-H1-adh2-F	TGGTAATCCTTTGAACCAGTTCTGAAGC	28
P254-bdhA2SP-R	AACCATCCGAGCTCTGAATGGCCGTCTTTAAAATCTCTAAAATTTCTTCCGCTG	54
P255-pCB102	GGGATATATCTTTCTTTCATCCTGATGAGCTCTTCCTGCAAATATTCATAATC	53
P256-pGG8-R	AAAAAATCATACATTCTCATGGATCCTAACCTCCTAAATTTTGATACGGG	50
P257-pGG8-F	TATTTAGAGAAGCATTTTAACATAAAAATAAGAAGCCTGCATTTGCAGG	49
P258-pGG8-R	AAAAAATCATACATTCTCATAGCTGTTTCCTGTGTGAAATTGTTATGAG	49
P259-pGG8-F	TATTTAGAGAAGCATTTTAAATGTCGAGCACCCGTTCTCG	40
P260-TASP1-R	ATGTTAAGGTTCAACTAATTCTACGATGTTTTTACCATCTTCCTTTAAGATAGATAC	57
P261-TASP1-F	AGGATGTATTTAAATATCTTAAAGGAAGATGGTAAAAACATCGTAGAATTAGTTG	55
P262-TASP2-R	ATGTTAAGGTTCAACCACGACTTTTTCATAAGTTGGGTTTGCC	43
P263-TASP2-F	AGGATGTATTTAAATGGAATTATGGCAAACCCAACTTATGAAAAAG	46
P264-AASP4-R	ATGTTAAGGTTCAACCACAATATGCAGATACAGAAATCGCCTTTG	45
P265-AASP4-F	AGGATGTATTTAAATATTGTGCAAAGGCGATTTCTGTATCTG	42
P266-TASP3-R	ATGTTAAGGTTCAACCCAGTAACGTGTCCAAGCATCAC	38
P267-TASP3-F	AGGATGTATTTAAATGCATATTGTGAAGGTGATGCTTGGAC	41
P268-TTSP1-R	ATGTTAAGGTTCAACTTTAGGTAATGTGAATGTATATTCTGGATTCAATATTG	53
P269-TTSP1-F	AGGATGTATTTAAATATATTGAATCCAGAATATACATTCACATTACCTAAAGTTGAAC	58
P270-TTSP2-R	ATGTTAAGGTTCAACTAAAATTTCTTCCGCTGTCAAAGCTTTATATCCG	49
P271-TTSP2-F	AGGATGTATTTAAATGGCGGATATAAAGCTTTGACAGCG	39
P272-BD-F	ACATTTCTATTAGCACAATAATTGTTTGTTCAACAAAGTG	40
P273-BD-R	ATACCAGCTCCATTTGATACAAAATAAGTAGCAC	34
P274-BD-F	TGATAGTAAACTTGATAGCTCTGTACAAGTATTAACACC	39
P275-BD-R	TCTATCCTCGTAAGGAAGCTTCATCGAATC	30
P276-BD-F	TCACCCACTAGATTATAAAAATAGACGTGGTGTTATTC	38
P277-BD-R	ACCGGTTCTACTAATAGTCCAATATCAACCAG	32
P278-BD-H1-F	TCTACAAAGGGTATCAGTCCCTCTTTGTC	29
P279-BD-H2-R	ACACCAGATACCACAGTGGCATTTG	25
P280-dhaTC8-F	AGGAGGTTAGGATCCATGAGAATGTATGATTTTTTAGCACCAAGTGTAAATTTTATGG	58
P281-dhaTC8-R	CTTCTTATTTTTATGTTAAAATGCTTCTCTAAATATTTTAACTATATCCCTCTCGTTAC C	60
P282-term-F	CATAAAAATAAGAAGCCTGCATTTGCAGG	29
P283-prom-R	GGATCCTAACCTCCTAAATTTTGATACGGG	30
P284-dhaTC8-F	CGGAGCCTATGGAAAATGAGAATGTATGATTTTTTAGCACCAAGTGTAAATTTTATGG	58
P285-colE1-R	ATCATACATTCTCATTTTCCATAGGCTCCGCCCC	34
P286-dhaTC8-R	ACTACTACACATGAATTAAAATGCTTCTCTAAATATTTTAACTATATCCCTCTCGTTAC C	60
P287-H2-bdhA2-R	ATATCTTTCTTTCATCATCTTCAGTAAGGGTAATCTGTTTATTCCCC	47
P288-pCB102-F	CCCTTACTGAAGATGATGAAAGAAAGATATATCCCCCCACAGATACG	47
P289-M-R	AAGTTTATTAACCATGCGAAACGATCCTCATCCTGTC	37
P290-M-F	GAAGAAAATAATTAAGCGGGACTCTGGGGTTC	32

P291-KnR-F	ATGATTGAACAAGATGGATTGCACGC	26
P292-KnR-R	TCAGAAGAACTCGTCAAGAAGGCGATAG	28
P293-pIM13-R	ATCTTGTTCAATCATCTAAGTTCCCTCTCAAATTCAAGTTTATCGCTC	48
P294-ColE1-F	GACGAGTTCTTCTGACTTCAGGTTTGTCTGTAACTAAAAACAAGTATTTAAGC	53
P295-pIM13-R	CTAAGTTCCCTCTCAAATTCAAGTTTATCGCTC	33
P296-ColE1-F	CTTCAGGTTTGTCTGTAACTAAAAACAAGTATTTAAGC	38
P297-KnR-F	TGAGAGGGAACTTAGATGATTGAACAAGATGGATTGCACGC	41
P298-KnR-R	CAGACAAACCTGAAGTCAGAAGAACTCGTCAAGAAGGCGATAG	43
P299-aad9-F	TTGAATACATACGAACAAATTAATAAAGTGAAAAAAATAC	40
P300-aad9-R	TTATAATTTTTTTAATCTGTTATTTAAATAGTTTATAGTTAAATTTACATTTTC	54
P301-pIM13-R	TTCGTATGTATTCAACTAAGTTCCCTCTCAAATTCAAGTTTATCGCTC	48
P302-ColE1-F	TTAAAAAAATTATAACTTCAGGTTTGTCTGTAACTAAAAACAAGTATTTAAGC	53
P303-dhaTR-F	ATGAGAATGTATGATTTTTTAGCACCAAATGTAAACTTTATGG	43
P304-dhaTR-R	TTAAAATGCTTCTCTAAATATTTTAACTATATCTTTTTCATTACCTTTTCTTGG	54
P305-dhaTR-F	ATGAGAATGTATGATTTTTTAGCACCAAATGTAAAC	36
P306-dhaTR-R	TTAAAATGCTTCTCTAAATATTTTAACTATATCTTTTTCATTACC	45
P307-dhaTR-F	ATAGAGTCCTATGTTTCTAAAGATGCAAACCC	32
P308-pIM13-F	GGCGCGCCGCATTCAC	16
P309-pIM13-F	TGCAGGAAGAGCTCATCAGGGGCGCGCCGCATTC	34
P310-ermB-R	ACATTCCCTTTAGTAACGTGTAACTTTCCAAATTTAC	37
P311-colE1-F	CACGTTACTAAAGGGAATGTGTTTAAACTCCTTTTTGATAATCTCATGACCAAAATCCC	59
P312-dhaTC8-R	ATAAAAATAAGAAGCCTGCAAATGCAGGC	29
P313-dhaTC8-R	CGACAGTTCTTTACTTAAAAATAAAAATAAGAAGCCTGCAAATGCAGGC	49
P314-H1-BD-F	TGCAGGCTTCTTATTTTTATTTTTAAGTAAAGAACTGTCGTCGGTTGG	48
P315-cr-R	AGAAGTGAATGCGGCGCGCCCCTGATGAGCTCTTCCTGCAAATATTC	47
P316-dhaDKr-R	CGACAGTTCTTTACTTAAAAATGGCTATGCCATTACACATCTCCATTAC	49
P317-seq-pIM13-R	AGAACAAACAAATTCCTTATAAACCTTATCATCTCAACC	39
P318-seq-pIM13-F	AGCCGAAGGGTAGCATTTACGTTAG	25
P319-tetA-F	GGGGGCGGAGCCTATGGAAAGGCCGGCCAGTGGG	34
P320-tetA-R	TTAGGGTAACAAAAAACACCGTATTTCTACGATG	34
P321-pIM13-F	GGTGTTTTTTGTTACCCTAAGGCGCGCCGCATTC	34
P322-tetA-R	TTTCTAATGCTGGTGTAACTTTAGGGTAACAAAAAACACCGTATTTCTACGATG	54
P323-tetA-R	TCAATACTTTTTGTTAAAAATTAGGGTAACAAAAAACACCGTATTTCTACGATG	54
P324-dhaTC8-F	TTTTTAACAAAAAGTATTGAAATTTGGTCTACCCAGG	37
P325-dhaD2r-F	TAGCAAAGGCATCTCCCATACCAG	24
P326-dhaD2r-R	AAGAAAGTATGTACAAGGTTCAGGTGTACTTAC	33
P327-colE1-R	TATGGGAGATGCCTTTGCTATTTCCATAGGCTCCGCCCC	39
P328-dhaD2r-F	GGGGGCGGAGCCTATGGAAATAGCAAAGGCATCTCCCATACCAG	44
P329-dhaD2r-R	ATATCTTGCCTATCACTGGAAAGAAAGTATGTACAAGGTTCAGGTGTACTTAC	53
P330-H1-dhaD-F	TCCAGTGATAGGCAAGATATTAAAGTCACTGAC	33
P331-H1-dhaD-F	AACCTTGTACATACTTTCTTTCCAGTGATAGGCAAGATATTAAAGTCACTGAC	53
P332-H1-dhaD2-F	GGGGGCGGAGCCTATGGAAATATCTGTATAATACAAAAGAAGACGTGG	48
P333-H1-dhaD2-R	CAATCACTGATAAAAAAATAAACTTTCCCTCCACTTTTTATAATTTTATATATTG	55
P334-H2-dhaD2-F	TATTTTTTTATCAGTGATTGTTACATATTAGACAAATATGTTATAAGTCAAACAATG	57
P335-H2-dhaD2-R	AACCATCCGAGCTCTGAATGTTTGGCTTCATAACAATTATCATAATAATTGCCTCCTC	58
P336-H1-mgsA-F	GGGGGCGGAGCCTATGGAAAGTTGTCAGTGATTAAATCATAATAGTGG	48
P337-H1-mgsA-R	TCTCTTTAAATTTATTATATATTAATCCCCCTCGATGTAATC	42
P338-H2-mgsA-F	ATATAATAAATTTAAAGAGACTGATATTATTGATAAAACTATCAATAATATCAGTCTG	58
P339-H2-mgsA-R	AACCATCCGAGCTCTGAATGTACTTCACAACAATGTAATAAATCCAGTGAATATAGC	57
P340-H1-tpiA-F	GGGGGCGGAGCCTATGGAAACTCAAAAGAATTAGCTTCACTTGCTG	46
P341-H2-tpiA-F	AAAATTGGAGCGTGAATTATAGGTAAGTTAAAGAAAAAAATAGATTTATGATATGTAATC	60
P342-H2-tpiA-R	AACCATCCGAGCTCTGAATGGCAGTTTCTCCCTGGCC	37
P343-bcd1r-F	GGTGTTTTTTGTTACCCTAACTCTTTTGGACTTACAGAGCCAAATGCAG	49
P344-bcd1r-R	GTTCTGCCATTTTAAAAGCCAAATATTGATTTTTAAATAGTGG	43
P345-H1-dhaD2-F	GGCTTTTAAAATGGCAGAACTATCTGTATAATACAAAAGAAGACGTGG	48
P346-H1-dhaD2-F	TGTGCCCACCCGCTTATGAAATATATG	27
P347-H2-dhaD2-R	ACCTAATATACAGTATTTATCACCAAAATCTGTATGAACTATTAGTCC	48
P348-Seq-dhaD2-F	TGCATATACTTTTTGCTGATGCTAAAATTAACTTGTAATAC	41
P349-Seq-dhaD2-R	TTGTCTAATTTATAACAGCATTGTTTGACTTATAACATATTTGTC	45

P350-H1-bdhA2-F	GGCTTTTAAAATGGCAGAACTTTTAAGTAAAGAACTGTCGTCGGTTGG	48
P351-H1-bcd1-F	TATAAGGGGAAGTTTTGCAGATGAGAATGG	30
P352-Seq-bcd1-F	ACTTATGGATGAACGTATTTTTTATGATAAACCTATGGG	39
P353-Seq-bcd1-R	TCAATAAAACTATCCCAAAAATTAAGTTAAGAAAGAAAGGTGTAC	45
P354-H2-bcd1-R	AGAATATTTGGTACAGTGGGGCTTGC	26
P355-mgsAr-F	ATGAGTATAGATAAATTAGAAAAACAAAAGAAAATTGCACTTGTTG	46
P356-ColE1-R	TCTAATTTATCTATACTCATTTTCCATAGGCTCCGCCCC	39
P357-H1-bcd1-F	TAAGGAAAAACAATTTTTAGAGCTACTTCCATGGCCCAGG	40
P358-H1-bcd1-R	ATTATATTCCTCCAAAAATTATATTTATTTTTAGTTATTATTTTTTAATCCCATAGG	57
P359-H2-bcd1-F	AATTTTTGGAGGAATATAATAACAAAATTTTATTAAGTTTAAACTGTGACCAATAAAAG	59
P360-H2-bcd1-R	TACTCAATATTCTACTAATTTAGATATAATATTAAGACTAGTAGTAGC	48
P361-array-F	AATTAGTAGAATATTGAGTACATTCAGAGCTCGGATGGTTAACAG	45
P362-bcd1-F	ATAGAAGTAAAGGTGCTAAGGGACTCTCTG	30
P363-bcd1-R	TCCATCAAGAGTACTAAGTGCCATTCCTAAC	31
P364-tpiAr-F	TAGTGAATCTTTAAAATTAATTGAAGAACTAAAACCACTTG	41
P365-tetA-R	TTAATTTTAAAGATTCACTATTAGGGTAACAAAAAACACCGTATTTCTACGATG	54
P366-tpiAr-R	CTAGAAATTAACAATAGCTGCAAAATCAGAAGC	33
P367-H1-mgsA-F	CAGCTATTGTTAATTTCTAGGTTGTCAGTGATTAAATCATAATAGTGGGAAAG	53
P368-H1-mgsA-F	GTTGTCAGTGATTAAATCATAATAGTGGGAAAG	33
P369-tpiAr-R	ATGATTTAATCACTGACAACCTAGAAATTAACAATAGCTGCAAAATCAGAAGC	53
P370-tpiAr-F	GGTGTTTTTTGTTACCCTAATAGTGAATCTTTAAAATTAATTGAAGAACTAAAACCAC	58
P371-H1-mgsA-R	TCTCTTTAAATTTATTATATATTAATCCCCCTCGATGTAATCTTTTTTATAAAATTATATC	61
P372-H2-mgsA-R	TACTTCACAACAATGTAATAAATCCAGTGAATATAGC	37
P373-array-F	TATTACATTGTTGTGAAGTACATTCAGAGCTCGGATGGTTAACAG	45
P374-dhaD2-F	AGCCGGTATCAGTAATGAATGCAGTAG	27
P375-dhaD2-R	AAAAGCTCAAAGTTCTGCATATTTCTAGCTCC	32
P376-dhaD2-F	TTTCTTGTAGTAGCAGATCCTTTTGTTCTTGAAG	34
P377-dhaD2-R	TAATCCTGAGCTTTCAGCACCAACTC	26
P378-H2-mgsA-F	ATATAATAAATTTAAAGAGACTGATATTATTGATAAAAC	39
P379-H2-mgsA-R	TACTTCACAACAATGTAATAAATCCAG	27
P380-H2-mgsA-R	AACCATCCGAGCTCTGAATGTACTTCACAACAATGTAATAAATCCAG	47
P381-H1-tpiA-F	CTCAAAAGAATTAGCTTCACTTGCTGATGTATATG	35
P382-H1-tpiA-F	GGTGTTTTTTGTTACCCTAACTCAAAAGAATTAGCTTCACTTGCTGATGTATATG	55
P383-tetA-R	GTGAAGCTAATTCTTTTGAGTTAGGGTAACAAAAAACACCGTATTTCTACGATG	54
P384-tpiA-F	AGGTGTGGAATATGTAATACTTGGACACAG	30
P385-tpiA-R	TTCGTAAGCTATTACAACTTTAGCAGCTTCATC	33
P386-Seq-tpiA-F	TTTGCAGCAGATGATACTGTTGTAGGAG	28
P387 (blunt 60, TD)	TTTTCTATTAAAATTTACGTAAGACTAAAAATAGCTGGTAAAATTTTTGC	50
P388 (blunt 56, ND)	TTTTCTATTAAAATTTACGTAAGACTAAAAATAGCTGG	38
P389 (sticky 56, OD)	TACATAAGGCTTATAGGTGTTTTTCTATTAAAATTTACG	39
P392 (sticky 60 ND)	ATTCTTAATAACATTTAATAACTCTGTTCTATCCGTAATAAAATCGC	47
P393 (sticky 55 ND)	ATTCTTAATAACATTTAATAACTCTGTTCTATCCG	35
P394 (blunt - 56, ND)	CTCAAAAGAATTAGCTTCACTTGCTG	26
P395 (sticky - 56, ND)	GGTGTTTTTTGTTACCCTAACTCAAAAGAATTAGCTTCACTTGCTG	46
P396 (blunt 59, OD)	ACACCTATAAGCCTTATGTATAAGTACTTCATAGGTATC	39
P399 (sticky 56, ND)	ACGTAAATTTTAATAGAAAAACACCTATAAGCC	33
P400 (blunt 60 ND)	TATTAAATGTTATTAAGAATGGAGAAAATTCATATATAGAATTCAAAGAAGAAGC	55
P404 (sticky 60 ND)	GTGAAGCTAATTCTTTTGAGTTTCCATAGGCTC	33

Table 8-2: Spacer sequences for CRISPR arrays used in the genome editing plasmids.

Spacer name	PAM and 36 bp spacer sequence (5' – 3')
adh2_spacer1	AATTG TTCCATCCTCTATTAACCTCTGAGATCCAATAACCA
adh2_spacer2	AATTG GTTAAAGATATTAGAGCCTCTATGAATATGCCTATA
bdhA2_spacer1	AATTG CAGTGAAAGATCTTAAAGACTATGAGGCAAGAAGTA
bdhA2_spacer2	AATTG CAAATTCAACTGTACTGCTTTCAGGCGGATATAAAG
bcd1_spacer1	AATTG AAAATAAATGTGGTATAAGAGCTGCTCAGGTTTCAG
bcd1_spacer2	AATTG TACTCTTTCAGTCATATACTTTTTAGCTACATTAAA
dhaD1_spacer1	AATTG CTGCTGCTACTGCTTCAACAGTTATTGGGAATGGCA
dhaD1_spacer2	AATTG TACCAAAGGCAACCTTTTCACCATGAAAATATTTAT
mgsA_spacer1	AATTG CACTTGTTGCTCACGACAATAGAAAAGAGGCTTTAA
mgsA_spacer2	AATTG TTTTTCCTTATTTTATTGTAATAATCTATCACATGT
tpiA_spacer1	AATTG GAACAGGTAAAACAGCTACAGATGAGCAAGCCAATG
tpiA_spacer2	AATTG ATGGAGCACTAGTTGGAGGAGCAAGTTTAAAAGCTT
dhaD2_spacer1	AATTG CAAAAGTAAAGAAAAGTGATGCAGTAATTGCCATAG
dhaD2_spacer2	AATTG GAAAGATATGTAGGGAGTTTGGGAAACTCTTTTCTT

Table 8-3: Molar masses and degrees of reduction of substrates and products.

Substrate or metabolite	Abbreviation	Molar mass (M_i)	Chemical formula	Number of carbons ($N_{C,i}$)	Degree of reduction (γ_i)
[-]	[-]	[g mol^{-1}]	[-]	[mol mol^{-1}]	[mol mol^{-1}]
Biomass	BDM	101.1	$C_4H_7O_2N$ [3]	4	16
Glucose	Glu	180.2	$C_6H_{12}O_6$	6	24
Glycerol	Gly	92.1	$C_3H_8O_3$	3	14
1,3-propanediol	PDO	76.1	$C_3H_8O_2$	3	16
Ethanol	EtOH	46.1	C_2H_6O	2	12
Butanol	BuOH	74.1	$C_4H_{10}O$	4	24
Lactate	LaAc	90.1	$C_3H_6O_3$	3	12
Formate	FoAc	46.0	CH_2O_2	1	2
Acetate	AcAc	60.1	$C_2H_4O_2$	2	8
Butyrate	BuAc	88.1	$C_4H_8O_2$	4	20
Carbon dioxide	CO_2	44.0	CO_2	1	0
Hydrogen	H_2	2.0	H_2	0	2

Appendix

Sequences of synthetic DNA "Pthl_1200-9-9_gpd1" and "Pfdx_gpp2_fdx_term":

Pthl_1200-9-9_gpd1 (Pthl_1200-9-9 promoter [143] and *GPD1* (YDL022W) gene from *S. cerevisiae* ATCC 204508, strain designation: S288c)

TTTTTAACAAAAAGTATTGAAATTTGGTCTACCCAGGTATTATAATGTGGTTGTTAGAGAAAACGTATAAATTAGGGATAAA
CTATGGAACTTATGAAATAGATTGAAATGGTTTATCTGTTACCCCGTATCAAAATTTAGGAGGTTAGGATCCATGTCTGCTG
CTGCTGATAGATTAAACTTAACTTCCGGCCACTTGAATGCTGGTAGAAAGAGAAGTTCCTCTTCTGTTTCTTTGAAGGCTGC
CGAAAAGCCTTTCAAGGTTACTGTGATTGGATCTGGTAACTGGGGTACTACTATTGCCAAGGTGGTTGCCGAAAATTGTAAG
GGATACCCAGAAGTTTTCGCTCCAATAGTACAAATGTGGGTGTTCGAAGAAGAGATCAATGGTGAAAAATTGACTGAAATCA
TAAATACTAGACATCAAAACGTGAAATACTTGCCTGGCATCACTCTACCCGACAATTTGGTTGCTAATCCAGACTTGATTGA
TTCAGTCAAGGATGTCGACATCATCGTTTTCAACATTCCACATCAATTTTTGCCCCGTATCTGTAGCCAATTGAAAGGTCAT
GTTGATTCACACGTCAGAGCTATCTCCTGTCTAAAGGGTTTTGAAGTTGGTGCTAAAGGTGTCCAATTGCTATCCTCTTACA
TCACTGAGGAACTAGGTATTCAATGTGGTGCTCTATCTGGTGCTAACATTGCCACCGAAGTCGCTCAAGAACACTGGTCTGA
AACAACAGTTGCTTACCACATTCCAAAGGATTTCAGAGGCGAGGGCAAGGACGTCGACCATAAGGTTCTAAAGGCCTTGTTC
CACAGACCTTACTTCCACGTTAGTGTCATCGAAGATGTTGCTGGTATCTCCATCTGTGGTGCTTTGAAGAACGTTGTTGCCT
TAGGTTGTGGTTTCGTCGAAGGTCTAGGCTGGGGTAACAACGCTTCTGCTGCCATCCAAAGAGTCGGTTTGGGTGAGATCAT
CAGATTCGGTCAAATGTTTTTCCCAGAATCTAGAGAAGAAACATACTACCAAGAGTCTGCTGGTGTTGCTGATTTGATCACC
ACCTGCGCTGGTGGTAGAAACGTCAAGGTTGCTAGGCTAATGGCTACTTCTGGTAAGGACGCCTGGGAATGTGAAAAGGAGT
TGTTGAATGGCCAATCCGCTCAAGGTTTAATTACCTGCAAAGAAGTTCACGAATGGTTGGAAACATGTGGCTCTGTCGAAGA
CTTCCCATTATTTGAAGCCGTATACCAAATCGTTTACAACAACTACCCAATGAAGAACCTGCCGGACATGATTGAAGAATTA
GATCTACATGAAGATTAG

Pfdx_gpp2_fdx_term (Csp fdx promoter from pMTL007C-E2 [104], *GPP2* (YER062C) gene from *S. cerevisiae* ATCC 204508, strain designation: S288c, Cpa fdx terminator from pMTL85141 [96])

GTGTAGTAGCCTGTGAAATAAGTAAGGAAAAAAAAGAAGTAAGTGTTATATATGATGATTATTTTGTAGATGTAGATAGGAT
AATAGAATCCATAGAAAATATAGGTTATACAGTTATATAAAAATTACTTTAAAAATTAATAAAAACATGGTAAAATATAAAT
CGTATAAAGTTGTGTAATTTTTAAGGAGGTGTGTTACATATGGGATTGACTACTAAACCTCTATCTTTGAAAGTTAACGCCG
CTTTGTTCGACGTCGACGGTACCATTATCATCTCTCAACCAGCCATTGCTGCATTCTGGAGGGATTTCGGTAAGGACAAACC
TTATTTCGATGCTGAACACGTTATCCAAGTCTCGCATGGTTGGAGAACGTTTGATGCCATTGCTAAGTTCGCTCCAGACTTT
GCCAATGAAGAGTATGTTAACAAATTAGAAGCTGAAATTCCGGTCAAGTACGGTGAAAAATCCATTGAAGTCCCAGGTGCAG
TTAAGCTGTGCAACGCTTTGAACGCTCTACCAAAAGAGAAATGGGCTGTGGCAACTTCCGGTACCCGTGATATGGCACAAAA
ATGGTTCGAGCATCTGGGAATCAGGAGACCAAAGTACTTCATTACCGCTAATGATGTCAAACAGGGTAAGCCTCATCCAGAA
CCATATCTGAAGGGCAGGAATGGCTTAGGATATCCGATCAATGAGCAAGACCCTTCCAAATCTAAGGTAGTAGTATTTGAAG
ACGCTCCAGCAGGTATTGCCGCCGGAAAAGCCGCCGGTTGTAAGATCATTGGTATTGCCACTACTTTCGACTTGGACTTCCT
AAAGGAAAAAGGCTGTGACATCATTGTCAAAAACCACGAATCCATCAGAGTTGGCGGCTACAATGCCGAAACAGACGAAGTT
GAATTCATTTTTGACGACTACTTATATGCTAAGGACGATCTGTTGAAATGGTAACATAAAAATAAGAAGCCTGCATTTGCAG
GCTTCTTATTTTTAT